NBS TECHNICAL NOTE 1196

U.S. DEPARTMENT OF COMMERCE/National Bureau of Standards

NBS Solar Collector Durability/Reliability Test Program: Final Report

The National Bureau of Standards[1] was established by an act of Congress on March 3, 1901. The Bureau's overall goal is to strengthen and advance the nation's science and technology and facilitate their effective application for public benefit. To this end, the Bureau conducts research and provides: (1) a basis for the nation's physical measurement system, (2) scientific and technological services for industry and government, (3) a technical basis for equity in trade, and (4) technical services to promote public safety. The Bureau's technical work is performed by the National Measurement Laboratory, the National Engineering Laboratory, the Institute for Computer Sciences and Technology, and the Center for Materials Science.

The National Measurement Laboratory

Provides the national system of physical and chemical measurement; coordinates the system with measurement systems of other nations and furnishes essential services leading to accurate and uniform physical and chemical measurement throughout the Nation's scientific community, industry, and commerce; provides advisory and research services to other Government agencies; conducts physical and chemical research; develops, produces, and distributes Standard Reference Materials; and provides calibration services. The Laboratory consists of the following centers:

- Basic Standards[2]
- Radiation Research
- Chemical Physics
- Analytical Chemistry

The National Engineering Laboratory

Provides technology and technical services to the public and private sectors to address national needs and to solve national problems; conducts research in engineering and applied science in support of these efforts; builds and maintains competence in the necessary disciplines required to carry out this research and technical service; develops engineering data and measurement capabilities; provides engineering measurement traceability services; develops test methods and proposes engineering standards and code changes; develops and proposes new engineering practices; and develops and improves mechanisms to transfer results of its research to the ultimate user. The Laboratory consists of the following centers:

- Applied Mathematics
- Electronics and Electrical Engineering[2]
- Manufacturing Engineering
- Building Technology
- Fire Research
- Chemical Engineering[2]

The Institute for Computer Sciences and Technology

Conducts research and provides scientific and technical services to aid Federal agencies in the selection, acquisition, application, and use of computer technology to improve effectiveness and economy in Government operations in accordance with Public Law 89-306 (40 U.S.C. 759), relevant Executive Orders, and other directives; carries out this mission by managing the Federal Information Processing Standards Program, developing Federal ADP standards guidelines, and managing Federal participation in ADP voluntary standardization activities; provides scientific and technological advisory services and assistance to Federal agencies; and provides the technical foundation for computer-related policies of the Federal Government. The Institute consists of the following centers:

- Programming Science and Technology
- Computer Systems Engineering

The Center for Materials Science

Conducts research and provides measurements, data, standards, reference materials, quantitative understanding and other technical information fundamental to the processing, structure, properties and performance of materials; addresses the scientific basis for new advanced materials technologies; plans research around cross-country scientific themes such as nondestructive evaluation and phase diagram development; oversees Bureau-wide technical programs in nuclear reactor radiation research and nondestructive evaluation; and broadly disseminates generic technical information resulting from its programs. The Center consists of the following Divisions:

- Inorganic Materials
- Fracture and Deformation[3]
- Polymers
- Metallurgy
- Reactor Radiation

[1]Headquarters and Laboratories at Gaithersburg, MD, unless otherwise noted; mailing address Gaithersburg, MD 20899.
[2]Some divisions within the center are located at Boulder, CO 80303.
[3]Located at Boulder, CO, with some elements at Gaithersburg, MD.

NBS Solar Collector Durability/Reliability Test Program: Final Report

David Waksman

Center for Building Technology
National Engineering Laboratory
National Bureau of Standards
Gaithersburg, MD 20899

William C. Thomas

Department of Mechanical Engineering
Virginia Polytechnic Institute and State University
Blacksburg, VA 24061

Elmer R. Streed[1]

Center for Building Technology
National Engineering Laboratory
National Bureau of Standards
Gaithersburg, MD 20899

[1]Now retired.

Prepared for:
Office of Solar Heat Technologies
U.S. Department of Energy
Washington, DC 20585

NBS Technical Note

. DEPARTMENT OF COMMERCE, Malcolm Baldrige, Secretary
IONAL BUREAU OF STANDARDS, Ernest Ambler, Director

Issued September 1984

National Bureau of Standards Technical Note 1196
Natl. Bur. Stand. (U.S.), Tech. Note 1196, 148 pages (Sept. 1984)
CODEN: NBTNAE

U.S. GOVERNMENT PRINTING OFFICE
WASHINGTON: 1984

ABSTRACT

Efforts in the development of reliability/durability tests for solar collectors and their materials have been hampered by the lack of real time and accelerated degradation data that can be correlated with in use conditions. The focus of this report is on research undertaken at the National Bureau of Standards (NBS) to help generate the data required to develop methods for predicting the long term durability and reliability of flat-plate solar collectors and their materials.

In this research, eight different types of flat-plate solar collectors were exposed outdoors at four sites located in different climatic regions. Small scale cover and absorber materials coupon specimens consisting of samples taken from a collector of each of the eight types used and a number of additional materials were exposed concurrently with the full-size collectors. Periodic measurements were made of collector and materials performance as a function of outdoor exposure time. Indoor laboratory aging tests were conducted concurrently on specimens of the same materials to provide a basis for comparison with the outdoor exposure tests.

This report presents the results obtained in this test program. Recommendations are made regarding the use and limitations of performance measurements and environmental exposure tests for assessing the durability of solar collectors and absorber and cover materials.

Key words: absorber materials; accelerated aging; cover materials; durability; environmental exposure; solar collectors; solar materials; stagnation testing; thermal performance.

ACKNOWLEDGEMENTS

The work discussed in this publication was funded by the Office of Solar Heat Technologies of the United States Department of Energy. Outdoor thermal performance testing and exposure of solar collectors and materials were carried out by DSET Laboratories (DSET), the Florida Solar Energy Center (FSEC), the Lockheed Research Laboratory (LMSC), and the National Bureau of Standards (NBS). Indoor solar simulator tests were performed at the Kent Space Center of the Boeing Company and by Wyle Laboratories. The cover and absorber optical property data reported were measured by DSET, LMSC, and NBS. Assistance in data analysis and evaluation was provided by the Department of Mechanical Engineering of the Virginia Polytechnic Institute and State University (VPI&SU). Optical and scanning electron microscope studies and PMMA molecular weight measurements were performed at NBS.

Personnel from the above mentioned organizations who participated in the test program are listed below. Apologies are expressed by the authors for any omissions.

Test Site Managers

DSET: Richard D. Whitaker
FSEC: James C. Huggins and Ross McCluny
LMSC: Roger K. Wedel
Boeing: Al R. Lunde
Wyle: Wallace R. Youngblood

Collector Exposure and Thermal Performance Testing

DSET: William J. Putnam
FSEC: James C. Huggins and James D. Rowland
LMSC: Ronald Dammann
NBS: John R. Jenkins and Donn F. Ebberts (of NBS),
Ken Shih and Mark Rallas (of Wyle)
Boeing: Al R. Lunde
Wyle: Wallace W. Youngblood

Outdoor Exposure of Materials

DSET: Thomas E. Anderson
FSEC: James C. Huggins and James D. Rowland
LMSC: Ronald Dammann
NBS: James F. Seiler

Cover and Absorber Optical Property Measurements

DSET: Thomas E. Anderson
LMSC: Roger K. Wedel
NBS: Willard E. Roberts and Catharine D. Kelly

Data Analysis and Evaluation

VPI & SU: Aaron G. Dawson,III, Donald S. Culkin,
Daniel E. Douro, and Mark A. Monroe

Optical and Scanning Electron Microscopy

NBS: W. Eric Byrd

PMMA Molecular Weight Measurements

NBS: Brian Dickens and Sharyl J. Santema

SI CONVERSION UNITS

The metric SI system of units is used throughout this report. This table is included to assist in converting from SI metric units to common U.S. units which are presently used by the building industry in the United States.

LENGTH

1 in = 0.0254 meter (exactly)

1 ft = 0.3048 meter (exactly)

AREA

1 in^2 = 6.45 x 10^{-4} $meter^2$

1 ft^2 = 0.09290 $meter^2$

VOLUME

1 in^3 = 1.639 x 10^{-5} $meter^3$

1 gal (U.S. liquid) = 3.75 x 10^{-3} $meter^3$

MASS

1 ounce-mass (avoirdupois) = 2.835 x 10^{-2} kilogram

1 pound-mass (avoirdupois) = 0.4536 kilogram

PRESSURE OR STRESS (Force/Area)

1 inch of mercury (60°F) = 3.377 x 10^3 pascal

1 pound-force/$inch^2$ (psi) = 6.895 x 10^3 pascal

1 pound-force/$foot^2$ (psf) = 47.88 pascal

ENERGY

1 foot-pound-force (ft-lbf) = 1.356 joule

1 Btu (International Table) = 1.055 x 10^3 joule

POWER

1 Watt = 1 x 10^7 erg/second

1 Btu/hr = 0.2931 Watt

TEMPERATURE

t°C = 5/9 (t°F - 32)

HEAT

1 Btu/in/hr•ft^2•°F = 1.442 x 10^{-1} W/m•K (thermal conductivity)

1 Btu/lbm•°F = 4.187 x 10^3 J/kg•K (specific heat)

1 langley = 4.184 x 10^4 J/m^2 = 1 cal/cm^2 = 3.69 Btu/ft^2

TABLE OF CONTENTS

TABLE OF CONTENTS (Continued)

LIST OF TABLES

LIST OF TABLES (Continued)

LIST OF FIGURES

LIST OF FIGURES (Continued)

1. INTRODUCTION

Public Law 93-409, the "Solar Heating and Cooling Demonstration Act of 1974" [1]* and Public Law 93-473, the "Solar Energy Research, Development and Demonstration Act" [2] authorized a vigorous Federal program of research, development, and demonstration to help establish solar energy as a viable energy resource for the nation. The primary goal of the program, as stated in the National Program for Solar Heating and Cooling of Buildings (ERDA 76-6) [3], is to work with industry in the development and early introduction of economically competitive and environmentally acceptable solar energy systems to help meet national energy requirements.

The National Bureau of Standards (NBS) and other Federal agencies are cooperating with various private sector organizations in the development of consensus methods for the installation, performance, and testing of solar equipment. This effort has resulted in the publication of several procedures that can be used to assess the thermal performance and durability of solar energy systems and the components and materials used in their construction. The American Society of Heating, Refrigerating, and Air-Conditioning Engineers (ASHRAE) Standards 95-1981 [4], 94-77 [5], and 93-77 [6] for testing the thermal performance of residential hot water systems, thermal storage devices, and solar collectors, respectively, were based to a considerable extent on technical data generated by NBS. Similarly, the American Society for Testing and Materials (ASTM) has developed several standards concerned with the reliability and durability of solar collectors [7], cover plate materials [8, 9, 10, 11], absorptive materials [12, 13], rubber hoses and seals [14, 15, 16, 17, 18], metal-heat transfer fluid compatibility [19, 20], and polymeric containment material-heat transfer fluid compatibility [21].

In 1977, a program was initiated by NBS to help provide an experimental basis for the development of consensus standards for assessing the reliability and durability of solar collectors and their materials. In this program, eight different types of flat-plate solar collectors and small-scale cover and absorber materials specimens, representative of those in use at that time, were exposed outdoors at four sites located in different climatic regions. Periodic measurements were made of their performance as a function of exposure time. Laboratory aging tests were conducted concurrently on specimens of the same materials to provide a basis for comparison with the outdoor exposure tests.

This report presents and discusses the results obtained for these outdoor and laboratory aging tests. Several additional publications resulted from this program. These include:

- an overall program test plan [22, 23];
- an analysis of thermal performance data uncertainty for liquid-heating flat-plate solar collectors [24, 25];
- a discussion of the determination of incident angle modifiers for flat-plate solar collectors [26, 27];
- a comparison of outdoor and solar simulator solar collector thermal performance tests [28];
- a discussion of preliminary test program results [29];
- an evaluation of the use of absorber stagnation temperature as a parameter for determining changes in flat-plate solar collector performance [30, 31]; and
- an analysis of an integrated day-long stagnation temperature technique for detecting changes in solar collector performance [32].

Key research findings contained in these publications are discussed in section 4.1 of this report.

This work is intended to be complementary to other collector materials test methods development projects underway at NBS and elsewhere by providing a basis for comparing the results of small-scale materials level tests with changes taking place in full-size commercially available solar collectors.

Throughout this report, reference is made to days of outdoor exposure. Unless otherwise specified, the term "days" refers to days with solar radiation levels of 17,000 kJ/m^2 (1500 Btu/ft^2) or greater measured in the plane of the test specimen. These 17,000 kJ/m^2 days were used for accounting purposes rather than calendar days in an attempt to make the solar radiation exposure at the various outdoor exposure test sites more comparable.

---

* Numbers in brackets indicate references given in section 6 of this report.

2. TEST PROGRAM OVERVIEW

The tests and exposure procedures described herein are intended to determine the influence of environmental exposure parameters that could affect the degradation of solar collectors and their materials. They are also intended, to the extent possible, to provide a correlation between changes that occur at the materials and the collector component levels.

A more complete description of the test procedures summarized in this section is given in NBS Technical Note 1136 [22].

2.1 SOLAR COLLECTOR TESTS

2.1.1 Outdoor Exposure Conditions

The four different collector test series selected for use in the program and the purpose of each test series are summarized in table 2.1.1.

Series 1 and 2 were intended to evaluate the effects of "normal" stagnation conditions. The collectors in series 1 were allowed to stagnate dry, whereas the collectors in series 2 were filled, allowed to stagnate under filled conditions with a pressure relief valve set to the maximum allowable collector pressure, and subjected to thermal shock/cold fill and thermal shock/water spray tests at specified time intervals. The purpose of exposing filled collectors to stagnation conditions was to evaluate the combined effects of the temperatures and pressures that would occur under stagnation conditions.

Series 3 was intended to determine whether or not changes in collector performance will occur under the reduced absorber plate temperatures characteristic of operational conditions. Augmentation reflectors were used to amplify the solar radiation to which stagnating collectors were exposed in series 4. This series was intended to determine the effects that such reflectors would have when they are used in actual systems and to determine whether or not reflectors are a practical way of accelerating the degradation of stagnating collectors.

These exposure conditions were intended to subject the solar collectors and their materials to different thermal stress levels at each outdoor exposure site. The thermal stress level that would occur in normal use most likely lies between the series 1 and 2 and the series 3 test conditions, with some stagnation being a normal occurrence.

The stagnation testing of solar collectors is often considered to be an accelerated test in that it exposes solar collectors to temperatures that would not occur with the heat transfer fluid flowing. However, solar collectors may frequently be exposed to stagnation conditions in normal service. This can occur either when the collectors are initially installed, before system start-up, or when the system is shut down for maintenance or for seasonal considerations. In commercial buildings, time periods of up to a year between the installation and start-up of equipment have been experienced. Thus, only that portion of stagnation exposure time which would not be attributed to normal service can be considered to represent accelerated aging.

Four outdoor exposure test sites were selected which represent both the median and extreme United States climatological conditions. These test sites can be briefly described as follows:

Climatological Extremes

Site 1. hot, dry
high solar radiation
(high UV radiation would accompany these conditions)

The hot, dry condition can be found in southwestern states (i.e., Arizona, Nevada, and New Mexico). DSET Laboratories, Inc., located in Phoenix, Arizona was selected as this test site.

Site 2. hot, humid
high solar radiation
(low to moderate UV radiation would accompany these conditions)

The hot, humid condition can be found either in Florida or along the Gulf Coast in the states of Alabama, Mississippi, Louisiana or Texas. The Florida Solar Energy Center, located in Cape Canaveral, Florida was selected as this test site.

Table 2.1.1 Summary Description of Field Test Series for Solar Collectors

Test Series	Collector Performance Measurement	Conditions for Weathering Exposure	Purpose of Test Series**
Series 1 "dry stagnation"	Initial measurement in accordance with ASHRAE 93-77 except delete 3 day pre-exposure and measurement of time constant Performance retest after 3, 15, 30, 60, 120, 240 and 480 day exposures.*	Each collector preconditioned for each weathering exposure by purging with dry air to remove the remaining heat transfer fluid. Successive weathering exposure between performance retests provide cumulative exposures of 3, 15, 30, 60, 120, 240, and 480 days.*	1. Observation of effects of dry stagnation collector performance and other characteristics for various weathering times. 2. Provide data for comparing initial performance without 3 day pre-exposure per ASHRAE 93-77.
Series 2 "no-flow stagnation"	Initial measurement in accordance with ASHRAE 93-77 after 3 day pre-exposure. Delete measurement of time constant. Performance retests same as in series 1.	Collectors preconditioned for weathering exposure by filling per NBSIR 78-1305A [33], capping and allowing to boil dry. Weathering exposures same as in series 1 except that Thermal Shock Tests per NBSIR 78-1305A will be performed during first 30 day exposure on series 2 test collectors only.	1. Observation of effects of no-flow stagnation on collector performance and other characteristics. 2. Observation of effects of Thermal Shock Tests representing: (a) filling a hot collector with cool heat transfer medium, and (b) rain on a hot collector. 3. Observation of static pressure leakage after 30 and 120 days of exposure
Series 3 "controlled flow"	Performance of test collectors measured in accordance with ASHRAE 93-77, taking only 3 points. Delete 3 day pre-exposure and time constant measurement. Performance retests up to 240 days, same as series 1.	During weathering exposure, heat transfer flow rate maintained at 25% of operational flow rate for liquid.	1. Observation of effects of normal operation on collector performance and other characteristics.
Series 4*** "dry stagnation with augmentation reflectors"	Initial measurement same as in series 1. Performance retests same as in series 1.	Preconditioning and weathering exposures same as in series 1, except that a reflector was used on each collector during each day of weathering exposure.* Solar radiation measurements required both with and without reflector.	1. Observation of effects of dry stagnation on collector performance and other characteristics with solar radiation amplified by a reflector. 2. Obtaining temperature history within collectors for most severe exposure conditions.

* Individual days with solar radiation of 17,000 $kJ/m^2 \cdot day$ or greater as measured in the plane of the collector aperture without the influence of a reflector.

** All series include provision of data for comparisons between test series, test sites (climatic regions), collector designs, etc.

*** This series was terminated prematurely after 60 days* due to a serious lack of uniformity in radiation caused by the augmentation reflectors.

Median Climatological Conditions

Site 3. moderate temperature
dry
high solar radiation
moderate UV radiation

The moderate, dry condition can be found primarily in parts of California. The Lockheed Research Laboratory, located in Palo Alto, California was selected as this test site.

Site 4. moderate temperature
humid
moderate solar radiation
moderate to low UV radiation

The moderate, humid condition can be found in the Pacific Northwest, Midatlantic and Midsouth regions of the United States. The NBS test facility, located in Gaithersburg, Maryland served as this test site.

All four test series, each having a sample of the eight collector types described in section 2.1.2, were conducted at sites 1 and 2. Only series 1 and 2 were conducted at sites 3 and 4.

2.1.2 Collector Description

Eight types of liquid-heating flat-plate type solar collectors were selected for use in the test program. The designs chosen were representative of commonly used materials and types of construction. All collectors from each manufacturer were from the same production lot. The collector cover and absorber materials, their pertinent optical properties, and average collector areas (gross and aperture) are listed in table 2.1.2. The absorber material optical property data are based upon measurements of at least ten samples taken from an actual absorber of each collector type prior to aging. The solar transmittance of the glass materials was obtained using the full cover and a pyranometer (ASTM Standard E 424, Method B [34]). The solar transmittance of nonglass cover materials and the solar absorptance values were obtained from spectral measurements with an integrating sphere (ASTM Standard E 424, Method A [34]). Emittance was measured using a portable-type instrument employing a thermopile and infrared reflectance technique, in accordance with ASTM Standard E 408, Method A [35].

Detailed descriptions of each collector's construction dimensions and pertinent material properties useful for thermal analytical modeling are listed in Appendix B of NBS Technical Note 1140 [25]. Type T thermocouples were attached to the center of the underside of the collector absorber plates for the measurement of stagnation temperatures.

Collectors were identified by a coding scheme which will be used in later sections of this report in conjunction with test data. In this scheme, a letter identifying the collector type (A through H) is followed by a number identifying the test site (1 to 4), which in turn is followed by another number identifying the test series (1 to 4). For example, G14 represents collector type G exposed at test site 1 to the series 4 exposure conditions.

2.1.3 Measurements and Observations

Thermal performance measurements were made on the collectors in each test series in accordance with the schedule summarized in table 2.1.1. The ASHRAE Standard 93-77 thermal performance test procedure [6] was used in this program both as a full test (four temperatures, four data points at each temperature) and as a three-point performance retest (three temperatures, four data points at each temperature). The retest was conducted to demonstrate the magnitude of changes in the intercept and slope of the efficiency curve as a function of environmental exposure time. The measurements were required to be spread over the range of 0.02 to 0.07°C·m^2/W. The term "performance retest" will be used throughout this document when the three-point test is specified.

Data collected in addition to collector thermal performance included the following:

- Key environmental parameters; high and low daily ambient temperature, total and diffuse solar radiation, peak hourly solar radiation, wind velocity, precipitation, and visual sky and weather conditions, on a daily basis.

Table 2.1.2 Test Collector Specimen Description

Collector Code	Cover Material			Absorber Material			Average Areas*	
	Outer	Inner	Solar Transmittance	Material	Solar Absorptance	Emittance	Gross (m^2)	Aperture (m^2)
A	Water White Glass	---	0.90	Black Nickel	0.87	0.13	2.150	1.831
B	Low Iron Glass	Low Iron Glass	0.88 (ea)	Black Velvet Paint	0.97	0.96	1.732	1.602
C	Plate Glass	Thin Film Heat Trap	0.86	Black Velvet Paint	0.98	0.92	2.589	1.924
D	Etched Glass	Etched Glass	0.96 (ea)	Black Chrome	0.97	0.07	1.655	1.402
E	FRP** (Type I)	---	0.85	Lacquer Primer	0.95	0.87	1.892	1.720
F	Water White Glass	---	0.90	Copper Oxide	0.96	0.75	1.922	1.769
G	FRP** (Type II)	FEP*** Film	0.84 ** 0.96 ***	Porcelain Enamel	0.93	0.86	2.563	2.188
H	PET**** Film	FEP*** Film	0.85 **** 0.96 ***	Siliconized Polyester Paint	0.95	0.89	2.916	2.641

* Average of values reported by the four test sites.

** Glass fiber reinforced plastic

*** Fluorinated (ethylene propylene) copoylmer.

**** Poly(ethylene terephthalate)

- Maximum daily collector absorber plate temperature (for all collectors).

- Daily profiles of absorber plate temperature (for collectors D and H), ambient temperature, irradiance, and wind velocity at all four outdoor exposure sites for a period of one year.

- Visual observations of changes in collector appearance during outdoor exposure and of disassembled collectors following the completion of outdoor exposure and thermal performance testing.

- Optical property measurements on coupon samples of polymeric cover materials and absorber materials taken from disassembled exposed and unexposed collectors and microstructural studies on specimens showing degradation.

2.2 COLLECTOR MATERIALS TESTS

2.2.1 Exposure Conditions

Coupon specimens of cover plate and absorber materials were subjected to several different types of laboratory and outdoor environmental exposure tests. These specimens consisted of samples taken from the eight types of full-size collectors used in the test program and of several additional materials of interest. Changes in the optical properties of these materials were measured as a function of exposure time. Microstructural studies were conducted on materials showing visible degradation.

Outdoor exposure conditions at the materials coupon specimen level included "real time" exposure in simulated collectors and exposure to concentrated radiation in machines, described in ASTM E 838 [36]. Indoor laboratory tests conducted included exposure to: (1) temperature, (2) combined temperature and humidity, (3) combined temperature and radiation, and (4) thermal cycling (absorber materials only). Additional materials level exposure tests were conducted in xenon arc and tungsten lamp solar simulators.

The outdoor "real time" materials level exposures were conducted concurrently with those on full-scale collectors at the four outdoor exposure test sites discussed in section 2.1.1.

The exposure conditions used for the cover and absorber materials are summarized in tables 2.2.1 and 2.2.2, respectively. The exposure conditions summarized in these tables are intended to simulate a broad range of environmental stress conditions. Primary emphasis was placed on exposure to temperature, solar radiation, and moisture. Other degradation factors such as hail, pollutants, and dust are localized in nature and were assessed via their occurrence at the "real time" outdoor exposure test sites participating in the program.

2.2.2 Test Specimens

Materials level tests were conducted on the cover and absorber materials listed in tables 2.2.3 and 2.2.4. Materials specimens having code letters "A" through "H" were cut from solar collectors of the same type and batch as those exposed outdoors as full-size collectors. Figures 2.2.1 through 2.2.5 depict the apparatus in which test specimens were mounted for outdoor exposure.

2.2.3 Measurements and Observations

Data collected included:

- Integrated solar transmittance and absorptance per ASTM E 424, Method A.

- Emittance per ASTM E 408, Method A.

- Normal and hemispherical spectral transmittance curves measured on spectrophotometers with and without integrating spheres.

- Visual observation of changes.

- Microscopic evaluations using both optical and scanning electron microscopes.

- Key environmental parameters, as for solar collector exposure.

- Test apparatus exposure temperatures on a daily basis.

Table 2.2.1 Exposure Tests for Cover Materials

Exposure Condition	Value or Range	Exposure Time
Temperature (indoor)	a) 70°C b) 90°C c) 125°C	500, 1,000, and 2,000 h
Temperature and Humidity (indoor)	a) 70°C and 95% RH b) 90°C and 95% RH	500, 1,000, and 2,000 h
Temperature and Radiation (indoor)	Xenon arc weathering machine a) 70°C b) 90°C	500, 1,000, and 2,000 h
Solar Simulator	a) Tungsten b) Xenon simulators with irradiance of ~ 950 W/m^2 and ~ 70°C	30, 60, and 120 cycles*
"Real Time" Outdoor	1 sun at ~ 60°C	80, 160, 240, and 480 days**
Accelerated Outdoor	~ 6 suns at ~ 70°C	6, 12, and 24 equivalent months***

* Each cycle consists of 5 h irradiation and 1 h cooling

** Days having a minimum radiant exposure of 17,000 kJ/m^2.

*** One equivalent month equals 6.625×10^8 J/m^2 (15,835 Langleys).

Table 2.2.2 Exposure Tests for Absorber Materials

Exposure Condition	Value or Range	Exposure Time
Temperature (indoor)	a) 150°C b) 175°C	1,000 and 2,000 h
Temperature and Humidity (indoor)	90°C and 95% RH	1,000, and 2,000 h
Thermal Cycling (indoor)	-10°C to 175°C	5, 15, and 30 cycles
Temperature and Radiation (indoor)	Xenon arc weathering machine at 90°C	1,000 and 2,000 h
Solar Simulator	a) Tungsten b) Xenon simulators with irradiance of ~ 950 W/m^2 and ~ 130°C	30, 60, and 120 cycles*
"Real Time" Outdoor	1 sun at ~ 140°C and ~ 160°C	80, 160, 240, and 480 days**
Accelerated Outdoor	~ 6 suns at ~ 150°C	6, 12, and 24 equivalent months***

* Each cycle consists of 5 h irradiation and 1 h cooling

** Days having a minimum radiant exposure of 17,000 kJ/m^2.

*** One equivalent month equals 6.625×10^8 J/m^2 (15,835 Langleys).

Table 2.2.3 Cover Test Materials

Code[1]	Cover Material	Solar Transmittance[3] (Controls)
E	FRP[4] Type Ia	0.85
G	FRP[4] Type II	0.84
H[2]	PET[5] / FEP[6] (outer) / (inner)	0.85/0.96
J	Polycarbonate	0.88
K	Poly(vinyl fluoride)	0.89
L	FRP[4] Type Ib	0.84
M	FRP[4] Type III	0.78
N	Poly(methyl methacrylate)	0.90
O [2]	Glass[7] / Poly(vinyl fluoride) (outer) / (inner)	0.86/0.89

[1] Code letters E, G, and H indicate materials coupon specimens cut from solar collectors E, G, and H. Codes, J, K, L, M, N, and O tested at the materials level only.

[2] Materials exposed as a combination in the cover mini-boxes and in the accelerated exposure cover mini-boxes. Materials exposed individually in all other tests. Glass and FEP materials were not exposed individually.

[3] These properties are dependent on the formulation and manufacturing processes used. Other products within a generic class of materials may have significantly different properties.

[4] Glass fiber reinforced plastic.

[5] Poly(ethylene terephthalate).

[6] Fluorinated (ethylene propylene) copolymer.

[7] Ordinary plate glass.

Table 2.2.4 Absorber Test Materials

Code[1]	Absorber Material		Optical Properties[2]	
	Coating	Substrate	Solar Absorptance[3]	Emittance[3]
A	Black Nickel	Steel	0.87	0.13
C	Black Velvet Paint	Copper	0.98	0.92
D	Black Chrome	Steel (nickel flashed)	0.97	0.07
E	Black Lacquer Primer	Copper	0.95	0.87
F	Copper Oxide	Copper	0.96	0.75
G	Black Porcelain Enamel	Steel	0.93	0.86
H	Black Siliconized Polyester Paint	Aluminum	0.95	0.89
I	Black Chrome	Stainless Steel	0.88	0.19
J	Black Chrome	Aluminum	0.98	0.14
L	Lead Oxide	Copper	0.99	0.29
M	Oxide Anodized	Aluminum	0.94	0.10
N	Oxide Conversion Coating	Aluminum	0.93	0.51
P	Black Chrome	Copper (nickel flashed)	0.96	0.08

[1] Code letters A through H indicate materials coupon specimens cut from solar collectors A through H. Codes I through P tested at the materials level only.

[2] These properties are dependent on the formulations and manufacturing processes used. Other products within a generic class of materials may have significantly different properties.

[3] Average values based on a minimum of ten test specimens.

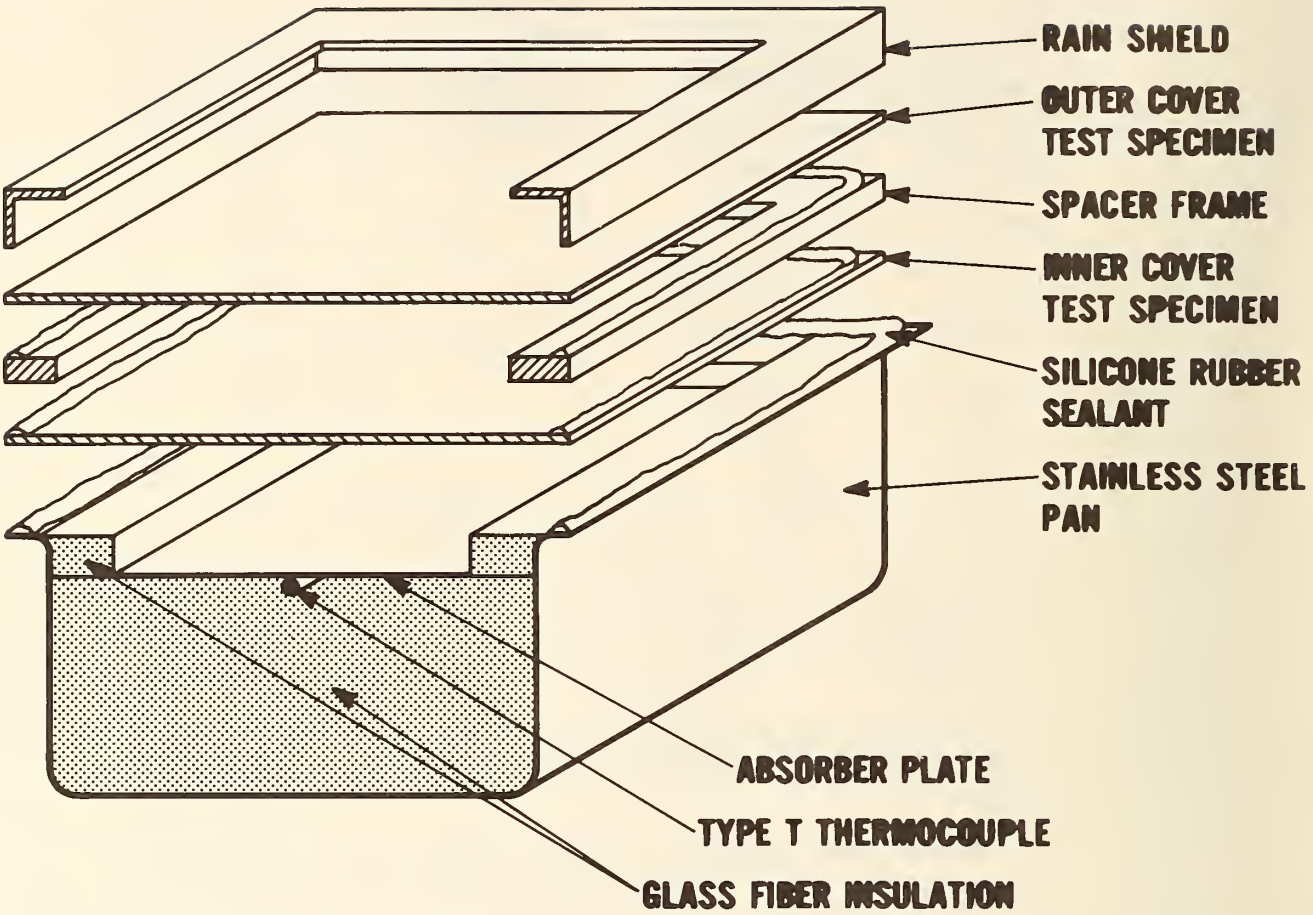

Notes:

Stainless Steel Pan: 22 x 12 x 10 cm without rim
Glass Fiber Insulation: 64 kg/m^3 density
Bottom thickness 10 cm
Edge thickness 2.5 cm wide x 2.5 cm thick
Baked out at 230°C for 24 hours
Absorber Plate: Black chrome on copper
Silicone Rubber Sealant: Between covers and pan, and covers and spacer
Cover Test Specimens: 26 x 16 cm
Rain Shield: 16 ga stainless steel, clamped to pan
Spacer Frame: 6 mm thick aluminum

Figure 2.2.1 Cover exposure mini-box

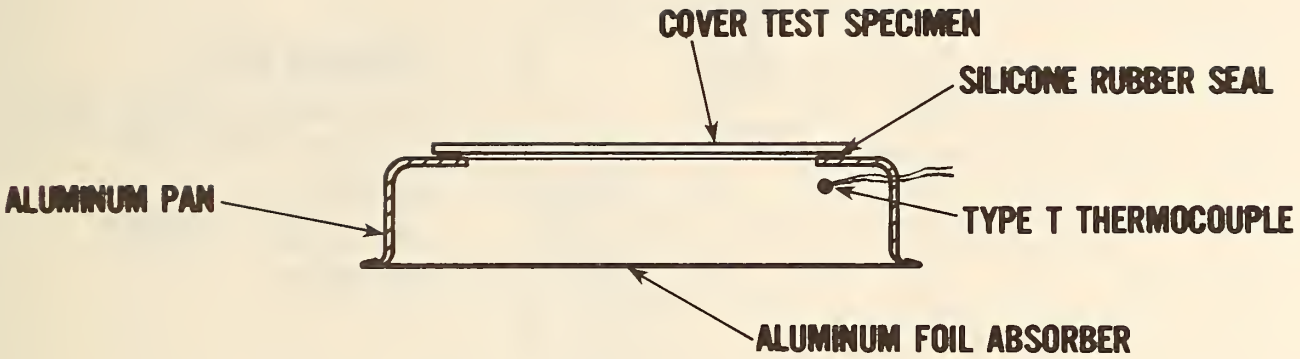

Notes:

Cover Size: 7.6 x 5.1 cm
Aluminum Pan: 11.5 x 6.5 x 2 cm
Aluminum foil painted black and baked at 230°C for 24 hours

Figure 2.2.2 Accelerated exposure cover mini-box

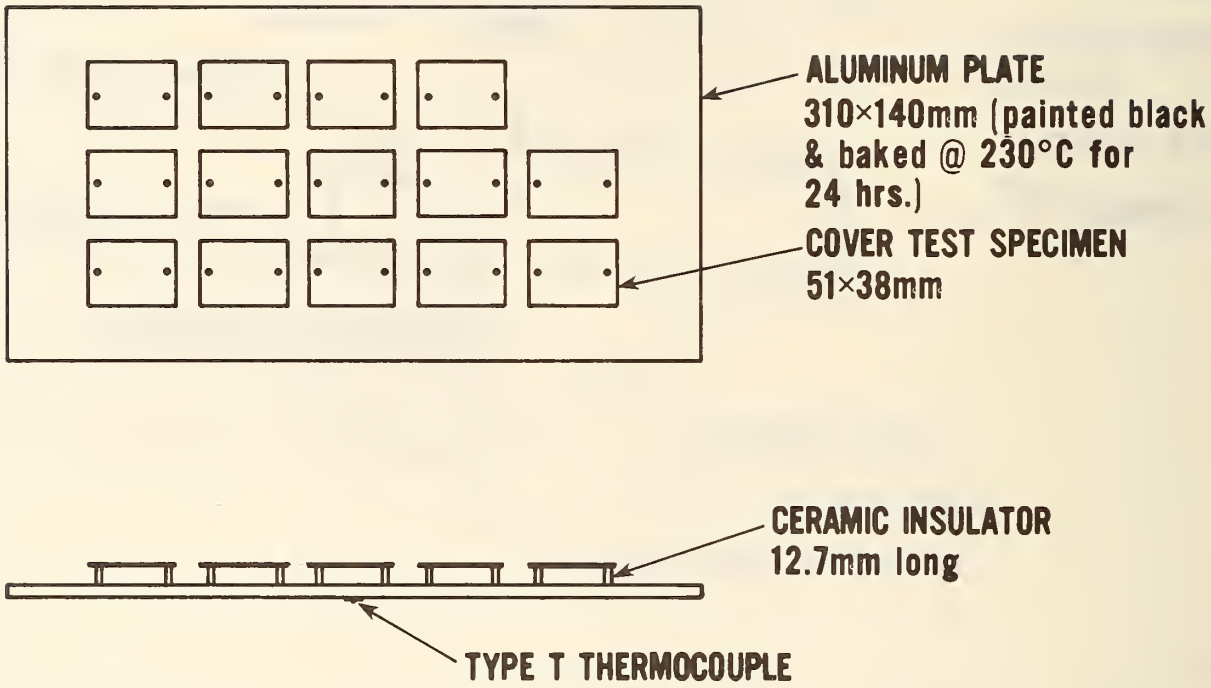

Figure 2.2.3 Accelerated exposure test plate

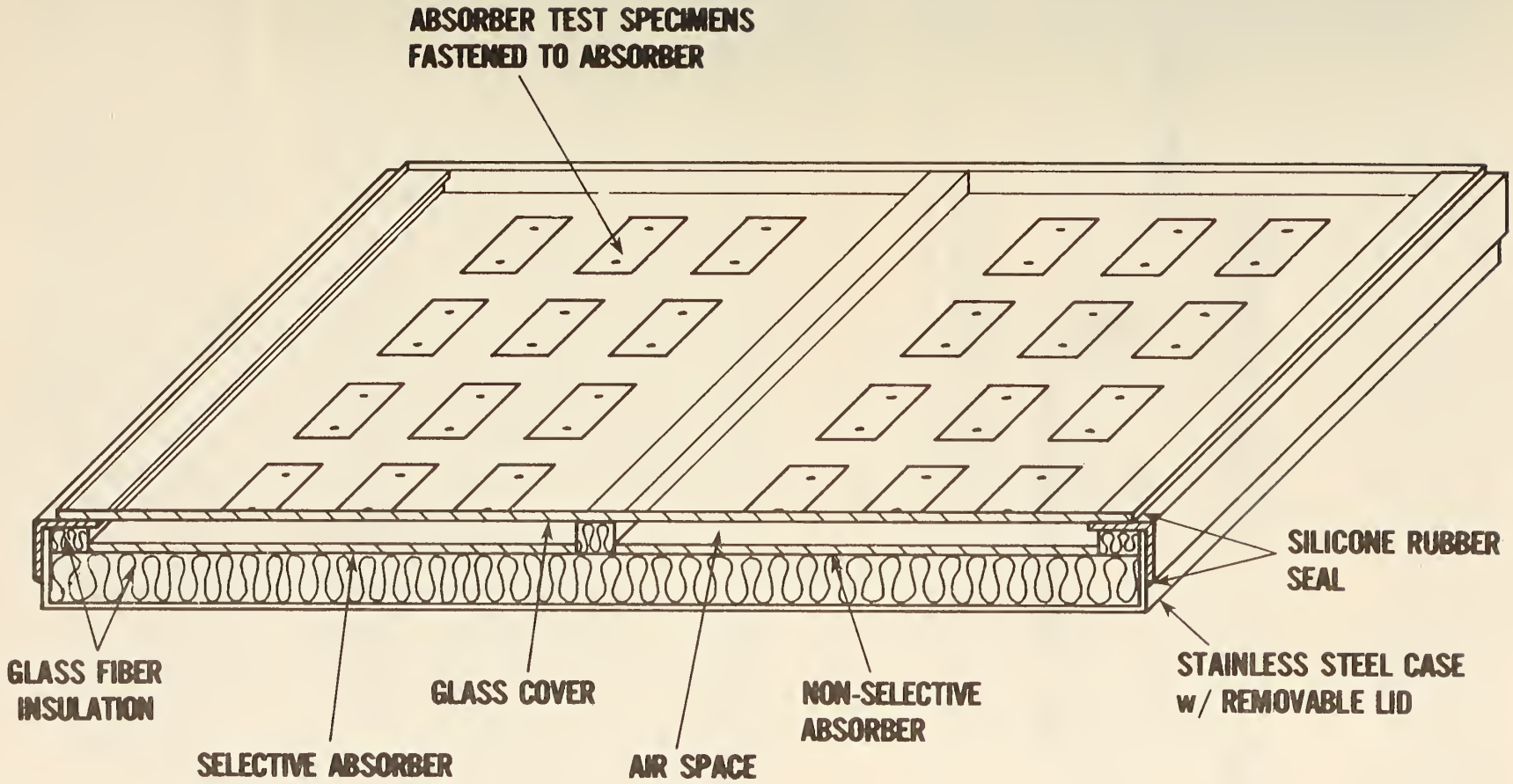

Notes:

Absorber Test Specimens: 7.6 x 5.1 cm
Stainless Steel Case: ≈190 x 84 x 9 cm
Glass Fiber Insulation: 64 kg/m^3 density
Baked out at 230°C for 24 hours
Edges and center 1.3 cm thick
Bottom 10 cm thick
Air Space: 1.3 cm
Cover: Water white glass
Absorber: Selective side - Black chrome on copper
Non-selective side - Black porcelain enamel on steel
Type T thermocouples attached to center of each absorber

Figure 2.2.4 Outdoor absorber exposure box

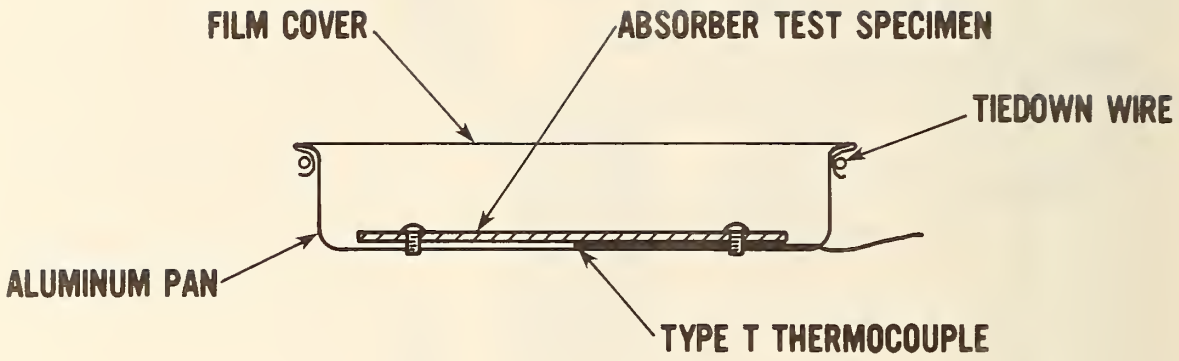

Notes:

Film Cover: Polytetrafluoroethylene
Absorber Test Specimen: 7.5 x 5.1 cm
Aluminum Pan: 11.5 x 6.5 x 2 cm
Interior painted black and baked at 230°C for 24 hours

Figure 2.2.5 Accelerated exposure absorber mini-box

3. RESULTS AND DISCUSSION: MATERIALS EXPOSURE STUDIES

The sections which follow present results obtained through the outdoor and indoor laboratory testing of solar collector cover and absorber materials. Additional materials-related observations made during the disassembly of full-size solar collectors following outdoor exposure testing are also presented. The properties of materials discussed in this section are dependent on the formulations and manufacturing processes used. Other products within a generic class of materials may have significantly different properties.

3.1 COVER MATERIALS TESTING

In this section, the results of outdoor and indoor laboratory exposure testing of cover materials are presented and the extent to which accelerated outdoor and indoor laboratory tests simulate "real time" outdoor exposure is discussed. Materials used for these comparisons included: poly(ethylene terephthalate) - material code H, polycarbonate - material J, poly(vinyl fluoride) - material K, poly(methyl methacrylate) - material N, and several types of glass fiber reinforced plastics - materials E, G, L, and M. Materials E and L were essentially the same, with the exception of specimen thickness. Fluorinated (ethylene propylene) copolymer film was also investigated as an inner glazing, however, it is not discussed in detail in this section since there were no obvious changes observed in any of the exposure tests performed. The same is true for glass materials used as an outer glazing. In addition to the small-scale tests which were performed on all materials, samples of cover materials E, G, and H were cut from full-size solar collectors having the same code letter designations and evaluated following the completion of collector exposure testing as described in section 2 of this publication. The types of small-scale outdoor and indoor laboratory tests performed on cover materials are also summarized in section 2. The reader should note that visual observations of yellowing in materials E and L are somewhat biased towards the low side since these materials contained a blue additive which could conceal a considerable amount of yellowing on visual inspection.

Both hemispherical and normal spectral transmittance measurements were made in the UV-visible range using spectrophotometers with and without integrating spheres, respectively . The integrating sphere data are representative of the amount of radiation that would reach a flat-plate solar collector absorber surface. The normal measurements made without an integrating sphere are a more sensitive indicator of changes in scattering, especially in materials which do not contain reinforcing fibers. Integrated solar transmittance values given in the tables contained in this section were calculated in accordance with ASTM E 424, method A using the air mass 2 solar spectrum.

3.1.1 Full-Size Collector Stagnation Testing

Visual Inspection: Cover material E showed a slight amount of yellowing after "real time" exposure for 480 exposure days at all four outdoor exposure sites. There was also evidence of minor surface dulling at the Cape Canaveral and Palo Alto sites. A moderate amount of yellowing was observed for material G after 480 days at all four sites. In addition, the exposed surfaces of this glazing became quite dull and readily absorbed liquids such as ink and there was some resin erosion which exposed glass fibers. Cover material H showed a considerable amount of top surface dulling after "real time" exposure for 480 days at all four outdoor exposure sites. The material also became quite brittle as a result of this exposure and snapped readily when it was bent so that the exposed surface was in tension. It was much more resistant to breaking when the bottom (unexposed) surface was in tension on flexing. The covers on several of the H collectors tore from the stresses imposed when the collectors were moved from exposure racks to test stands for periodic thermal performance measurements and had to be patched. In addition, the covers of all of the H collectors on exposure at the Phoenix test site were punctured in several places when exposed to impact from 1.2 cm maximum diameter hailstones. Testing previously conducted at NBS on unaged material indicated that this unaged material was capable of withstanding impact by 2.5 cm hailstones without puncture.

Microscopic Examination: Examination of the exposed surfaces of materials G and H with optical and scanning electron microscopes revealed that the surface dulling was primarily due to the formation of micro-cracks (see figure 3.1.1). The microcracking was more extensive at the Cape Canaveral and Palo Alto sites than at the Phoenix and Gaithersburg sites for both materials. There was evidence of directional stresses in the microcrack patterns observed for material H. A minor amount of surface pitting was observed optically on those material E specimens which showed surface dulling. The same type of microcracking observed in this program for material H was also observed by the authors in samples of the same type of material taken from solar collectors that were installed on a building in Colorado for about 5 years.

(a) Material H - Phoenix

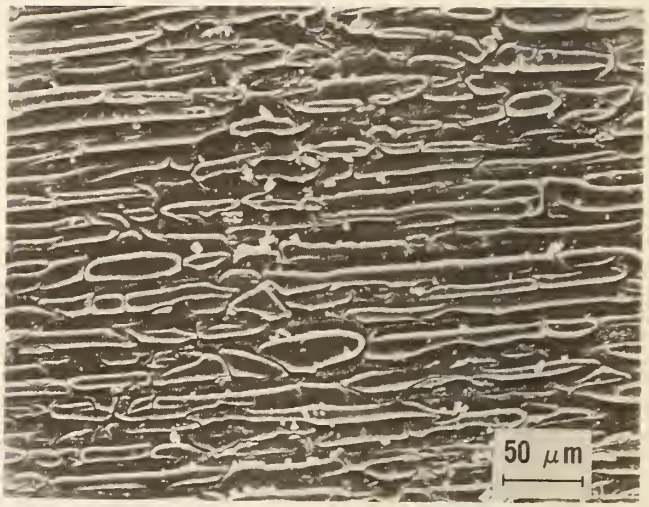

(b) Material H - Cape Canaveral

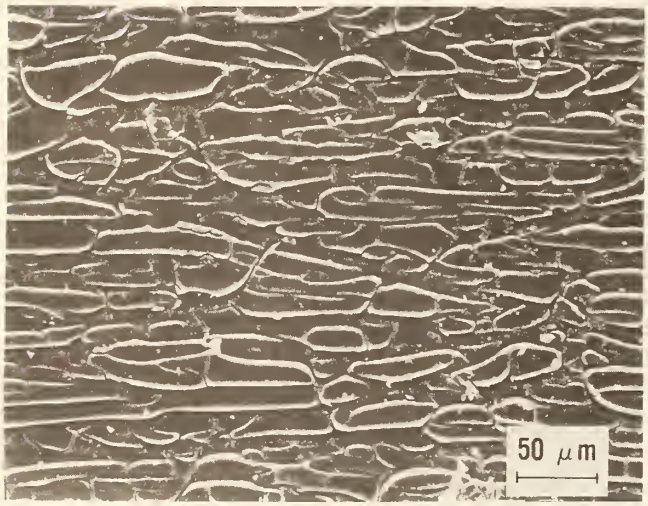

(c) Material H - Palo Alto

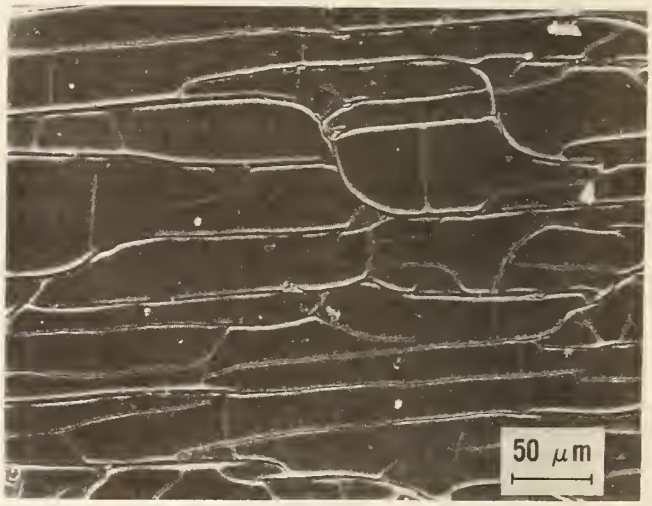

(d) Material H - Gaithersburg

Figure 3.1.1 Microcracking of cover samples from full-size collectors after 480 exposure days (≥17,000 kJ/sq-m-day)

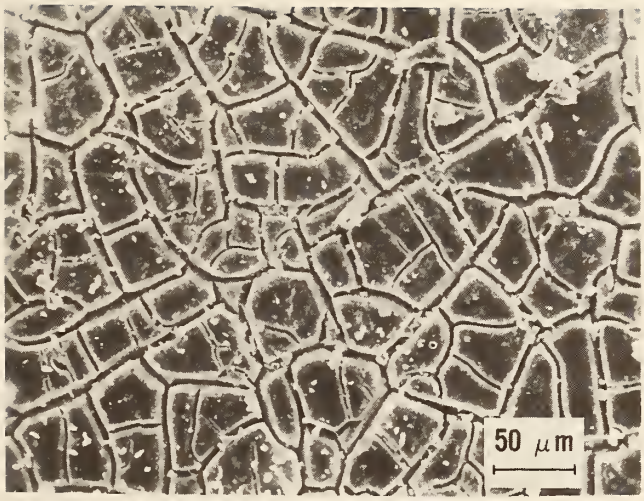

(e) Material G - Cape Canaveral

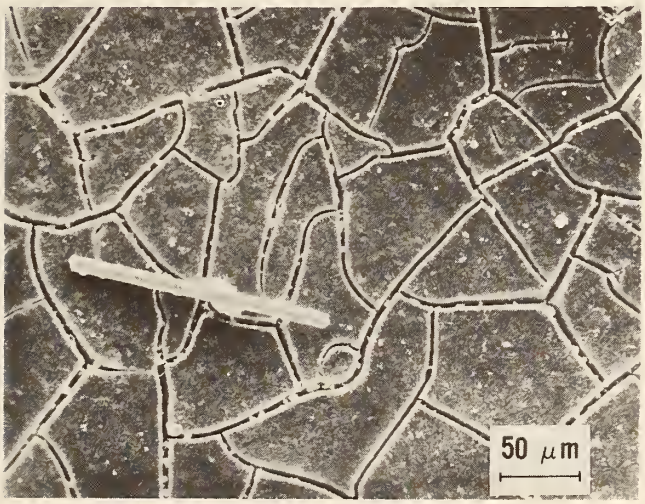

(f) Material G - Gaithersburg

Figure 3.1.1 continued

Optical Measurements: Integrated solar transmittance values are given in table 3.1.1 for cover samples cut from full-size collectors E, G, and H following exposure for 480 days at the four test sites. Material E had minor changes that are probably due to variations in sample homogeneity. Material G showed a substantial amount of change, with the greatest changes occurring at the Cape Canaveral site and the least at the Phoenix site. Transmittance curves for samples of materials G and H cut from the series 2 collectors at all four sites are shown in figure 3.1.2. The changes shown in the curves for material G are most likely due to a combination of yellowing (evidenced by the shift in the absorption edge* of the curve to longer wavelengths) and the extent of microcracking, which was greater at the Cape Canaveral site than at the Phoenix and Gaithersburg sites. Material H showed the greatest changes at the Cape Canaveral and Palo Alto sites. Examination of the transmittance curves for samples of material H taken from series 2 collectors exposed at all four sites and scanning electron microscope photos (see figure 3.1.1) shows that these changes were most likely due to the extent of microcracking, which was greatest at the Cape Canaveral and Palo Alto sites.

3.1.2 "Real Time" Outdoor Mini-Box Testing

Visual Inspection: Outdoor "real time" exposure of materials E and L on cover mini-boxes caused slight yellowing after 480 days at the Cape Canaveral and Palo Alto sites with no visual signs of degradation after 480 days at the Phoenix or Gaithersburg sites or at shorter exposure times at any of the sites. A slight to moderate amount of yellowing and exposed surface dulling was observed for material G after 480 days at all four sites with the most severe changes at the Cape Canaveral and Palo Alto sites. Exposure for 160 and 240 days caused slight yellowing at the Cape Canaveral, Phoenix, and Palo Alto sites, but no visual evidence of surface dulling. A slight increase in yellowing and a minor loss in surface gloss was also observed for material M after 480 days. Exposure of material H caused top surface dulling and embrittlement after 480 days at all four sites, but not after shorter exposure times. In addition, the same hail damage noted in the previous section for full-size collectors also occurred for the material H mini-box specimens at Phoenix. Very slight yellowing was observed in material J after 80 days at all four sites which progressed to slight to moderate after 480 days. In addition, surface dulling was observed after 240 and 480 days at all four sites. Exposure at the Palo Alto and Cape Canaveral sites caused noticeably more severe changes. With the exception of embrittlement after 480 days at the Phoenix site, there were no other visible signs of degradation of material K. Outdoor "real time" exposure of material N caused a minor amount of yellowing and a noticeable increase in embrittlement on breaking in flexure after 480 days at all sites. This yellowing could only be observed in material N by viewing the edge of the test specimens.

Microscopic Examination: Examination of the exposed surfaces of materials G, H, and J with optical and scanning electron microscopes revealed that the surface dulling observed visually, without magnification, was primarily due to the formation of microcracks (see figure 3.1.3). In general, the microcracking was more extensive at the Cape Canaveral and Palo Alto sites than at the other sites and had more open crack structure. In addition to the microcracking, the samples of material H exposed at the Palo Alto site and of material J at the Palo Alto and Cape Canaveral sites had evidence of surface etching. The microcracks observed for material J were not as open and extensive as those in materials G and H.

Optical Measurements: Integrated solar transmittance values are given in table 3.1.2 for cover samples exposed on collector mini-boxes for up to 480 days at all four outdoor exposure sites. With the exception of material G at all of the outdoor sites, material H at Cape Canaveral, and material M at the Gaithersburg site, the changes measured for integrated transmittance were not substantial. Examination of the spectral transmittance curves for materials G, H, J, K, and N revealed the changes shown in figure 3.1.4. The hemispherical transmittance curves for material G at both the Cape Canaveral and Phoenix sites were virtually identical for up to 240 days. After 480 days of exposure, the transmittance curves dropped substantially with the greatest change occurring at the Cape Canaveral site. This most likely is related to the extend of microcracking occurring with these two materials. Examination of the curves obtained for material H using an integrating sphere showed no changes after 480 days at Phoenix or for up to 240 days at Cape Canaveral. After 480 days of exposure at Cape Canaveral, there was a drop in the transmittance curve for material H. Once again, this is most likely related to the size and extent of microcracking. There also was a slight shift in the

---

* The term "absorption edge" as used in this report refers to the long wavelength side of the intense absorption band typically occurring in the 300 to 400 nm wavelength region in the spectral transmission curves shown in this report.

Table 3.1.1. Transmittance of Full-Size Collector Cover Material after Exposure.

Collector	Series	Control	Exposure Days**	Site: Phoenix	Cape Canaveral	Palo Alto	Gaithersburg
E	1	0.85	480	0.78	0.81	0.81	0.80
	2		480	0.80	0.78	0.82	0.81
	3		240	0.83	0.77	--	--
	4		60	0.79	0.82	--	--
G*	1	0.84	480	0.71	0.76	0.77	0.75
	2		480	0.67	0.54	0.63	0.80
	3		240	0.60	0.67	--	--
	4		60	0.74	0.66	--	--
H*	1	0.85	480	0.85	0.79	0.80	0.84
	2		480	0.86	0.81	0.80	0.84

* Outer Cover

** Days with a Minimum Solar Radiation Level of 17,000 kJ/sq m

Table 3.1.2. Effect of 'Real Time' Outdoor Exposure on Cover Sample Transmittance

Sample	Control	Phoenix Days Exposure*				Cape Canaveral Days Exposure				Palo Alto Days Exposure				Gaithersburg Days Exposure			
		80	160	240	480	80	160	240	480	80	160	240	480	80	160	240	480
E	0.85	0.83	0.83	0.80	0.84	0.84	0.81	0.81	0.83	0.85	0.82	0.80	0.77	0.82	0.81	0.80	0.81
G	0.84	0.80	0.80	0.83	0.68	0.81	0.79	0.79	0.63	0.81	0.80	0.80	0.73	0.82	0.80	0.80	0.75
H	0.85	0.85	0.85	0.85	0.85	0.84	0.85	0.85	0.79	0.84	0.85	0.83	0.84	0.84	0.86	0.87	0.85
J	0.88	0.87	0.86	0.86	0.85	0.85	0.85	0.84	0.84	0.84	0.85	0.83	0.83	0.86	0.86	0.85	0.84
K	0.89	0.89	0.90	0.90	0.90	0.90	0.90	0.84	0.90	0.90	0.89	0.91	0.89	0.90	0.90	0.90	0.90
L	0.84	0.83	0.83	0.83	0.84	--	--	--	--	0.84	0.84	0.85	0.85	0.84	0.84	0.82	0.80
M	0.78	0.80	0.74	0.78	0.78	0.78	0.77	0.73	0.75	0.80	0.81	0.74	0.80	0.74	0.75	0.76	0.70
N	0.90	0.89	0.88	0.89	0.89	0.88	0.88	0.88	0.90	0.89	0.89	0.88	0.89	0.89	0.89	0.89	0.88
O	0.89	0.89	--	--	0.89	--	--	--	0.89	--	--	--	--	--	--	--	--

* 17000 kJ/sq-m (1500 Btu/sq-ft) Minimum Days

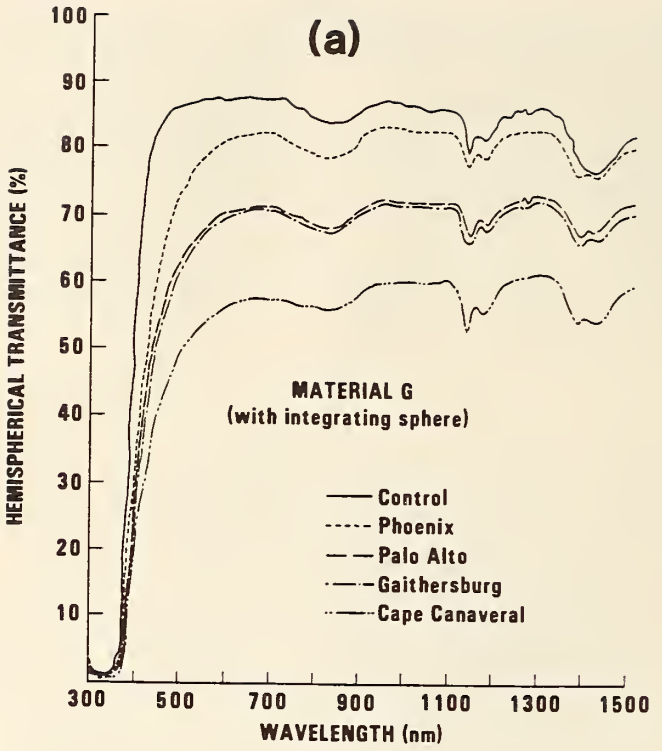

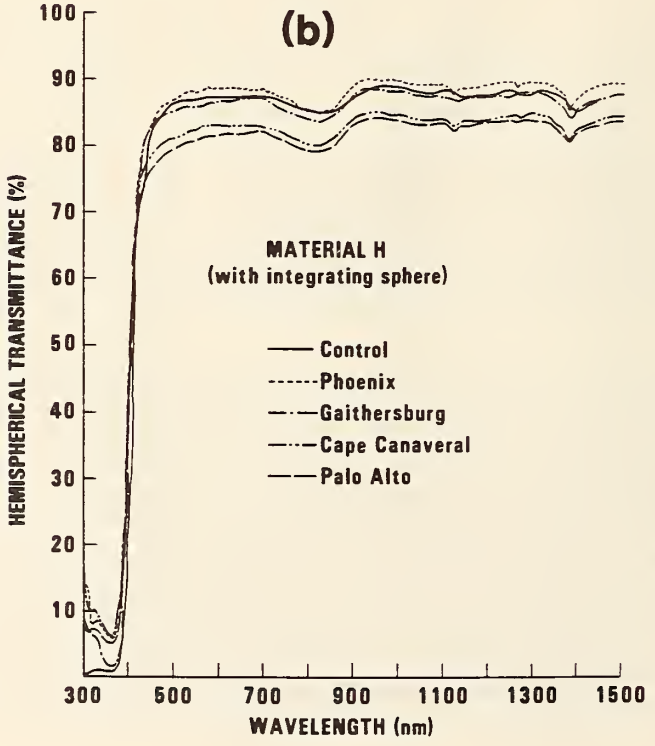

Figure 3.1.2 Spectral transmittance curves for cover samples from full-size collectors after 480 exposure days (≥17,000 kJ/sq-m-day)

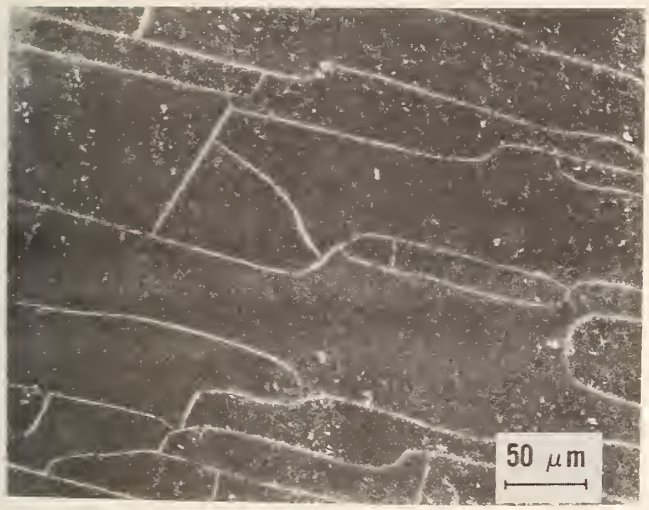

(a) Material H - Phoenix

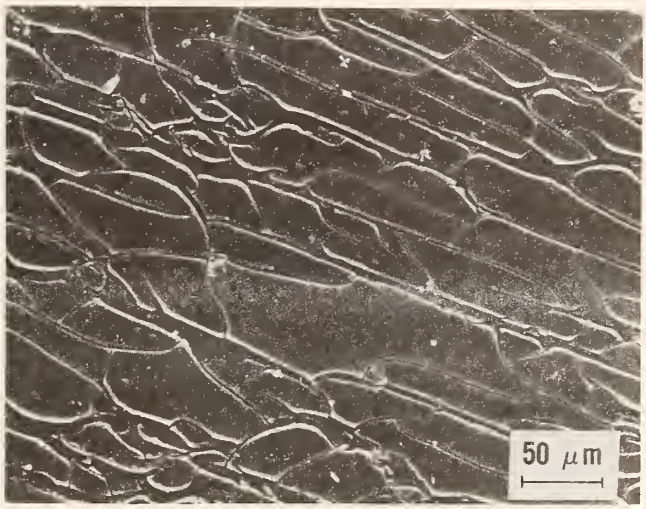

(b) Material H - Cape Canaveral

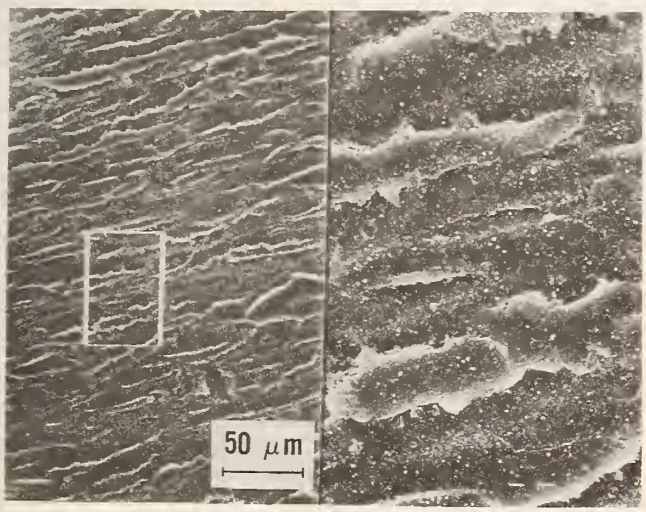

(c) Material H - Palo Alto

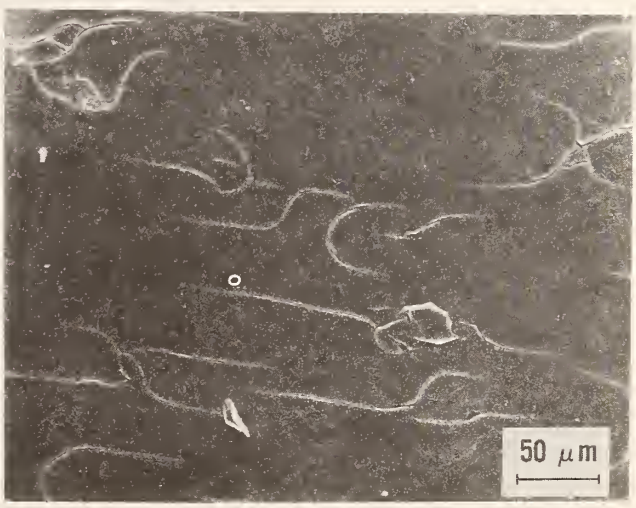

(d) Material H - Gaithersburg

Figure 3.1.3 Microcracking of cover samples after "real time" exposure on mini-boxes for 480 exposure days (≥17,000 kJ/sq-m-day)

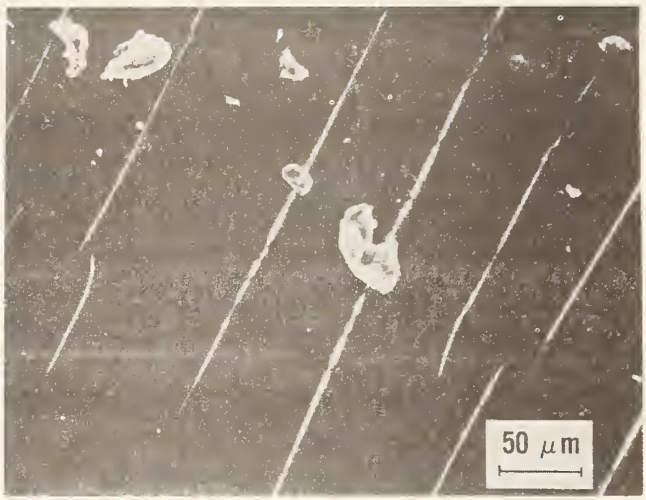

(e) Material J - Phoenix

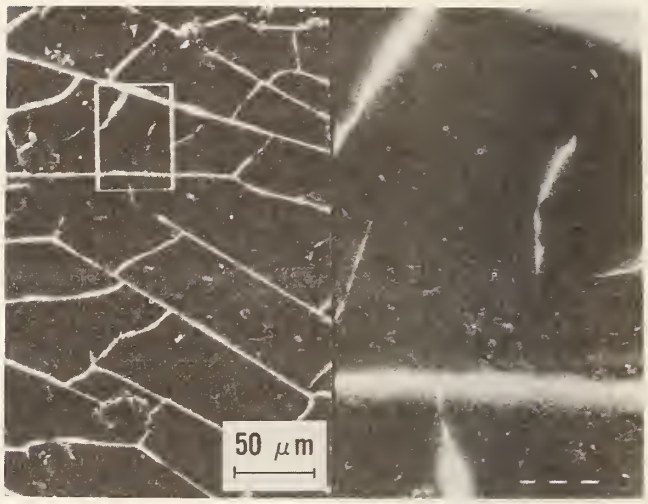

(f) Material J - Cape Canaveral

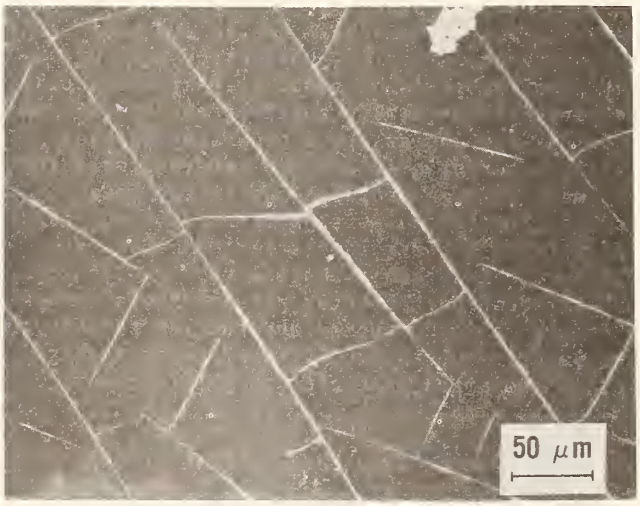

(g) Material J - Palo Alto

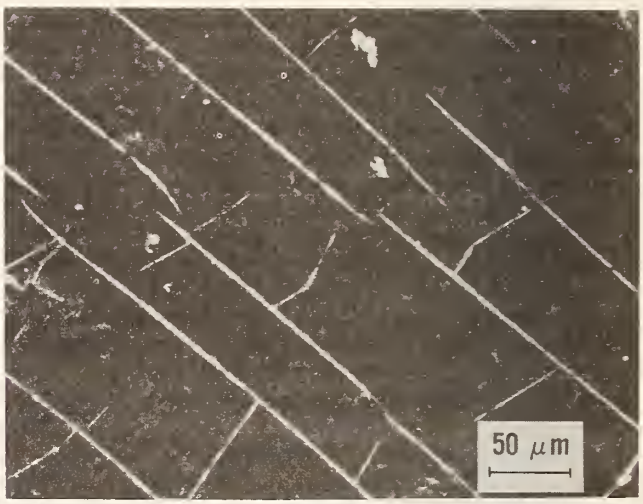

(h) Material J - Gaithersburg

Figure 3.1.3 continued

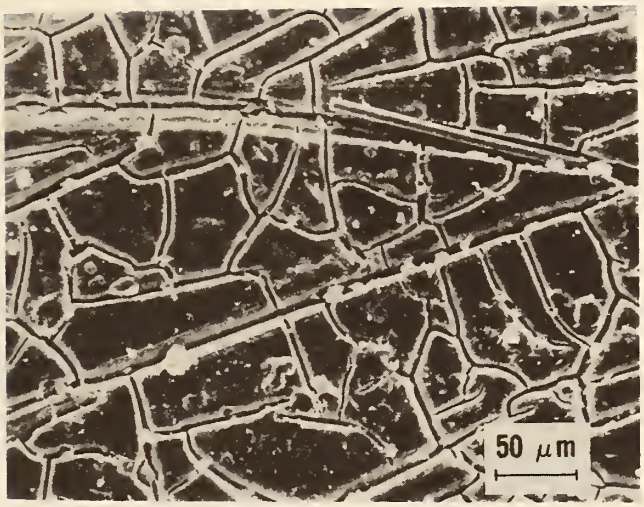

(i) Material G - Cape Canaveral

Figure 3.1.3 continued

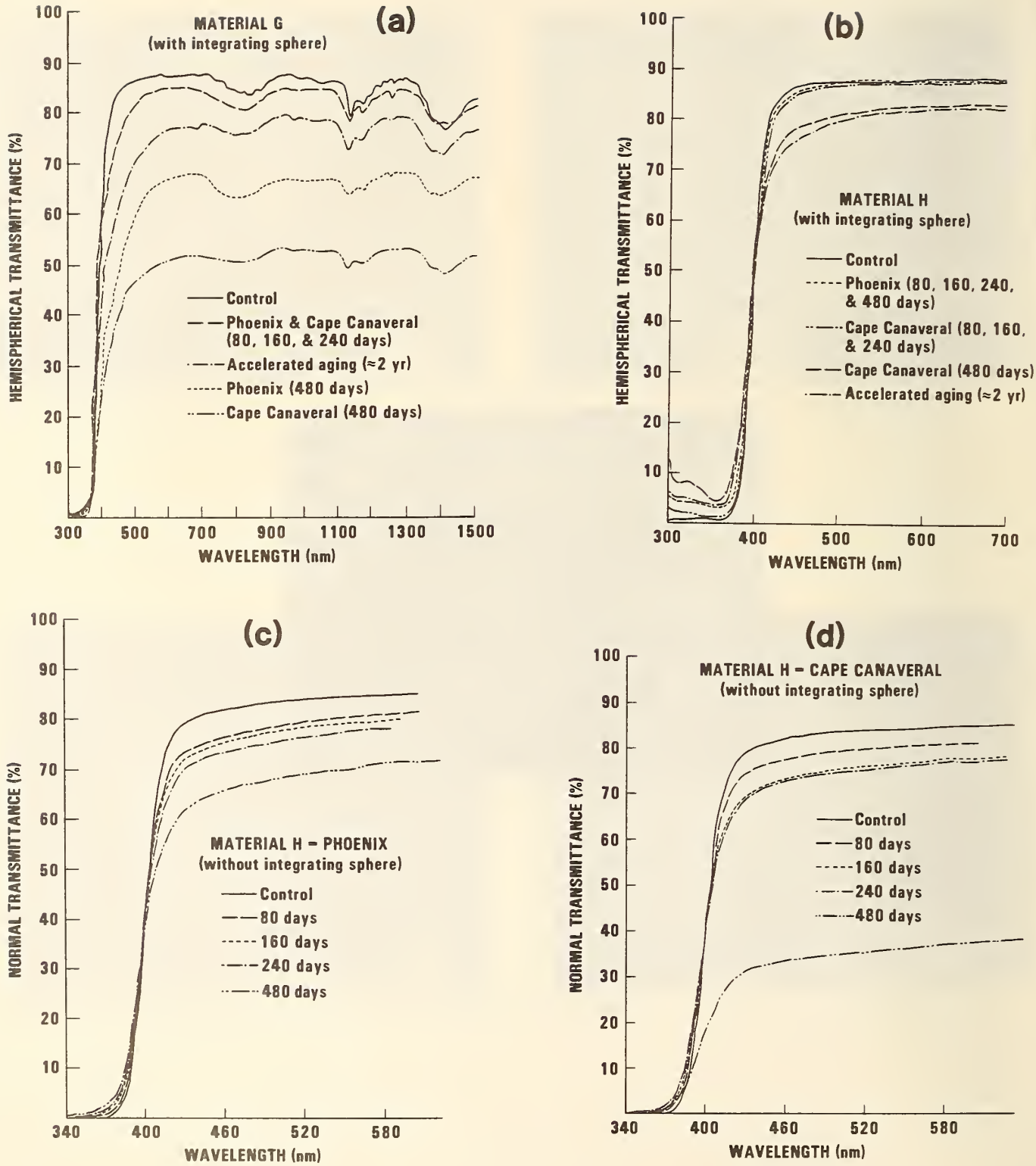

Figure 3.1.4 Spectral transmittance curves for cover samples exposed to "real time" and accelerated outdoor exposure on mini-boxes

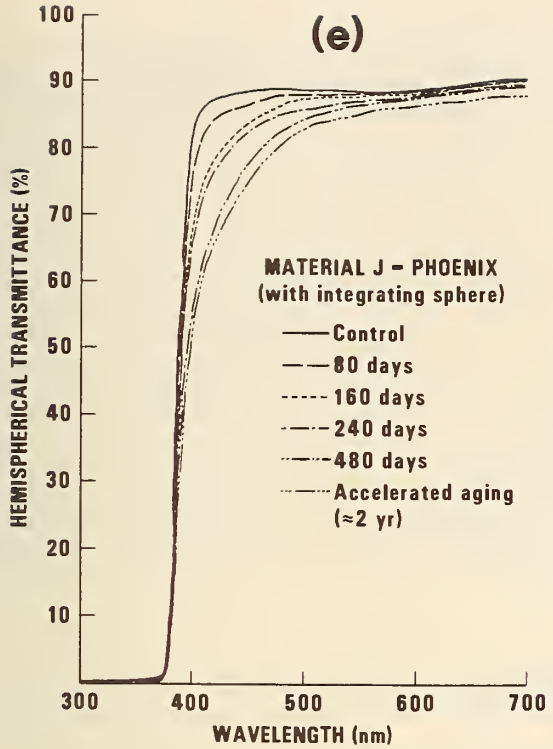

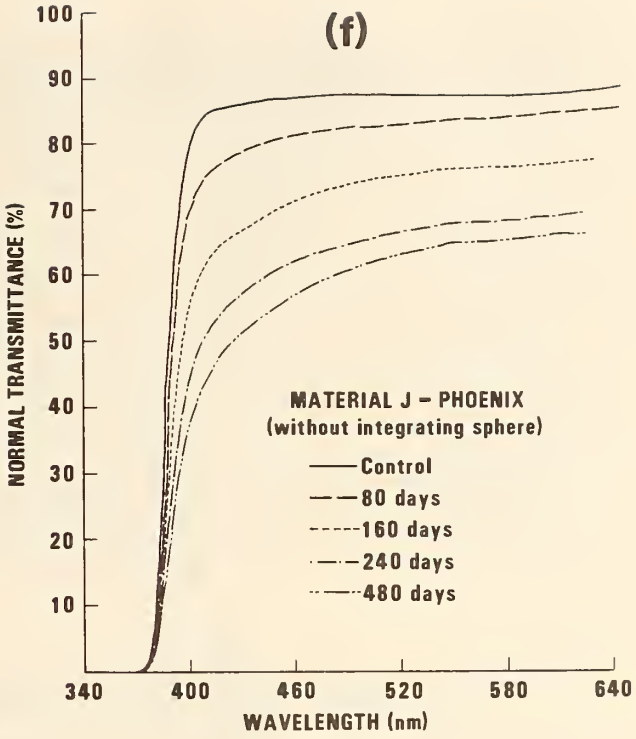

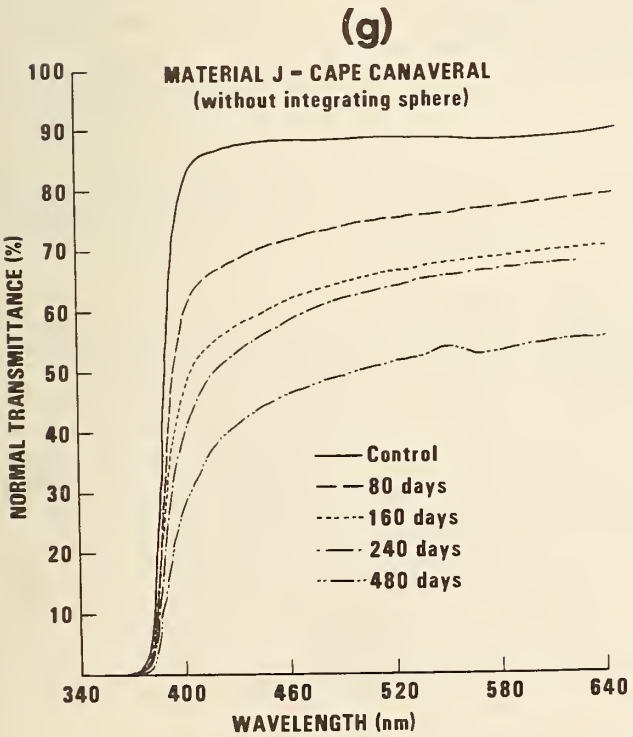

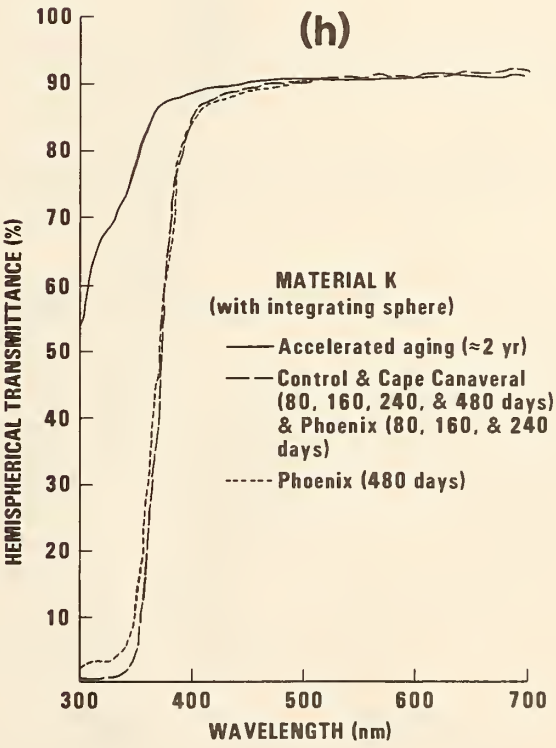

Figure 3.1.4 Continued

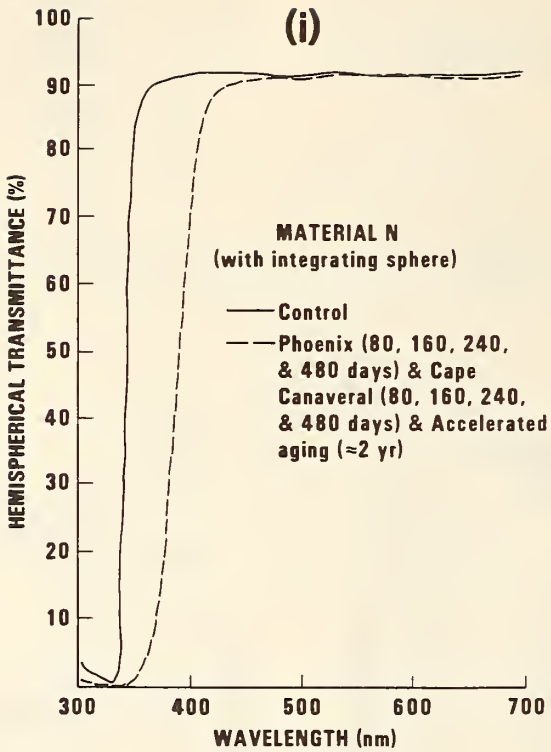

Figure 3.1.4 Continued

absorption edge towards shorter wavelengths which may be due to loss of UV inhibitor. Normal spectral transmittance measurements showed systematic changes in the transmittance of material H at both the Phoenix and Cape Canaveral sites with the greatest changes occurring at the Cape Canaveral site where the microcracking was more extensive. Hemispherical spectral transmittance curves measured for samples of material J exposed at Phoenix and Cape Canaveral showed identical shifts in the absorption edge to longer wavelengths as a function of exposure time (see figure 3.1.4e.). The similarity of these two curves is probably due to the fact that the microcracking in material J was not as open or extensive as that observed with materials G and H. Normal spectral transmittance curves showed greater changes for material J as a function of exposure time at Cape Canaveral than at Phoenix. With the exception of a slight shift in the absorption edge of material K to shorter wavelengths after 480 days of exposure at the Phoenix site, outdoor "real time" exposure of material K at the Phoenix and Cape Canaveral sites did not cause significant changes in the hemispherical transmittance. Measurements made without an integrating sphere on specimens from the two sites showed small decreases in transmittance as a function of exposure time and the same slight shift in the absorption edge towards shorter wavelengths for the 480 day Phoenix specimen. The significance of this shift in absorption edge will be discussed in section 3.1.3. A shift in the absorption edge of material N towards longer wavelengths was observed with spectral measurements made both with and without integrating spheres. In addition, a slight increase in scattering as a function of exposure time in Cape Canaveral was detected using the spectrophotometer without an integrating sphere. The shift in the absorption edge of material N to longer wavelengths is most likely due to photodegradation of the UV inhibitor as reported by Newland and Tamblyn [37].

3.1.3 Accelerated Outdoor Testing

Only the results obtained for cover samples mounted in mini-boxes will be discussed here because of peeling problems experienced with the absorber paint used in the board mount configuration.

Visual Inspection: Accelerated outdoor exposure of material E for a period equivalent to 2 years "real time" gave rise to slight yellowing. Similar exposure of material G caused slight to moderate yellowing and evidence of exposed surface dulling. Material M had a slight increase in yellowing and a minor loss in surface gloss when exposed to these conditions. Accelerated outdoor exposure equivalent to 2 years "real time" caused noticeable top surface dulling and embrittlement of material H and a slight amount of yellowing and loss in gloss of the exposed surface in material J. Exposure under these conditions also caused a very slight amount of yellowing in material N which could only be observed by viewing the edge of the specimen and did not cause any visible changes in material K.

Microscopic Examination: Examination of the exposed surfaces of materials G, H, and J revealed the presence of microcracking (see figure 3.1.5). The microcracks observed with accelerated outdoor aging generally appeared to be finer and less open than those observed with outdoor "real time" aging.

Optical Measurements: Integrated solar transmittance values are given in table 3.1.3 for cover samples exposed outdoors on an accelerated weathering machine for a period of time equivalent to 2 years "real time." Materials G, H, and M were the only materials which showed substantive changes in their transmittance in this time period. Examination of hemispherical spectral transmittance curves measured on materials G, H, J, K, and N revealed a number of changes resulting from this accelerated exposure (see figures 3.1.4a, b, e, h, and i). The transmittance curve for material G was somewhat higher than those measured on "real time" samples exposed at Phoenix and Cape Canaveral for 480 days; however, it was lower than the curves of the 240 day samples. This is probably due to the less developed microcrack pattern that occurred on the samples of material G exposed to accelerated aging. The curve for material H was very similar to that obtained for the 480 day Cape Canaveral sample. Both of these samples had a well developed microcrack structure. The slight shift of the absorption edge towards shorter wavelengths that occurred with "real time" exposure of material H also occurred with the accelerated aging sample. As a result of the accelerated aging, the absorption edge of material K showed a large shift towards shorter wavelengths. This was probably due to the loss of UV inhibitor which permitted the material to transmit further into the ultraviolet.

The same shift of the absorption edge of material N towards longer wavelengths observed with "real time" exposure also occurred with accelerated exposure. As was previously mentioned, this is probably due to photodegradation of the UV inhibitor into products which absorb at longer wavelengths.

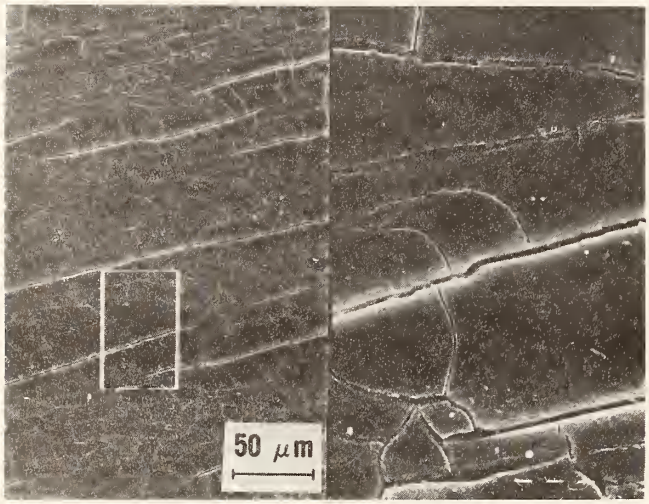

(a) Material H - Sample 1

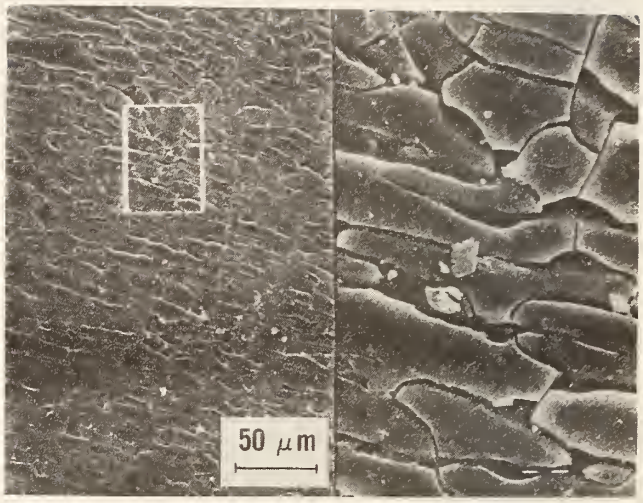

(b) Material H - Sample 2

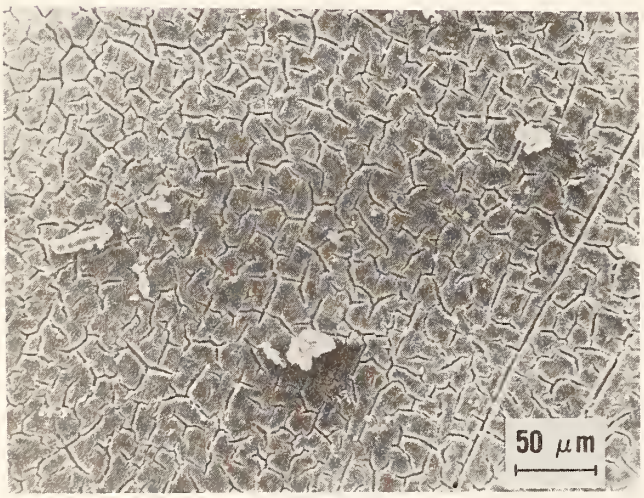

(c) Material G

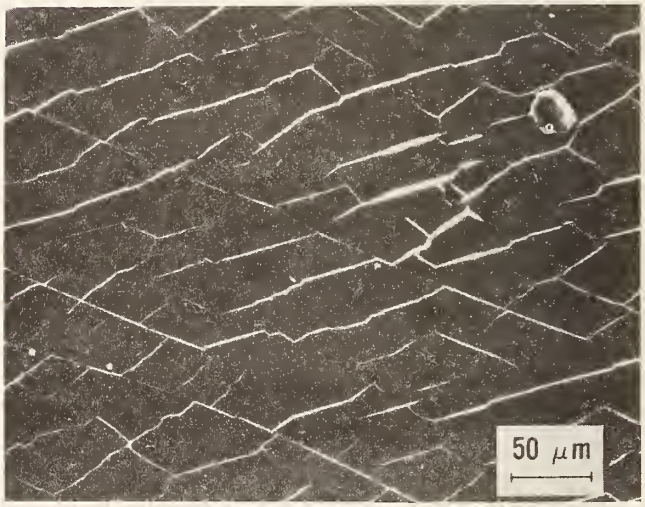

(d) Material J

Figure 3.1.5 Microcracking of cover samples after accelerated exposure on mini-boxes equivalent to ≈ 2 years "real time"

Table 3.1.3. Effect of Accelerated Outdoor Tests on Cover Sample Transmittance

		Sample 1,Mini-box Days Exposure*			Sample 2,Mini-box Days Exposure		
Sample	Control	30	60	120	30	60	120
E	0.83	0.83	0.84	0.83	0.83	0.83	0.83
G	0.84	0.83	0.83	0.78	0.81	0.82	0.74
H	0.85	0.84	0.85	0.81	0.84	0.85	0.81
J	0.87	0.86	0.86	0.84	0.84	0.86	0.85
K	0.90	0.93	0.92	0.92	0.92	0.92	0.91
L	--	--	--	--	--	--	--
M	0.82	0.77	0.79	0.76	0.81	0.79	0.80
N	0.91	0.89	0.89	0.89	0.89	0.89	0.89

* Equivalent Days; 5 Equivalent Days = 1 Month Real Time
= 6.625E+5 kJ/sq m

Table 3.1.4. Effect of Temperature Exposure on Cover Sample Transmittance

Temperature:		70 C			90 C			125 C		
		Hours Exposure			Hours Exposure			Hours Exposure		
Sample	Control	500	1000	2000	500	1000	2000	500	1000	2000
E	0.85	0.83	0.85	0.81	0.84	0.84	0.82	0.82	0.81	0.79
G	0.84	0.82	0.80	0.79	0.73	0.73	0.78	0.70	0.66	0.64
H	0.85	0.84	0.85	0.84	0.84	0.84	0.85	0.85	0.85	0.84
J	0.88	0.87	0.87	0.87	0.87	0.87	0.87	0.87	0.87	0.86
K	0.89	0.91	0.91	0.91	0.90	0.91	0.91	0.89	0.87	0.85
L	0.84	0.83	0.81	0.83	0.83	0.80	0.83	0.81	0.80	0.80
M	0.78	0.81	0.79	0.80	0.75	0.64	0.66	0.68	0.63	0.55
N	0.90	0.89	0.90	0.90	0.90	0.90	0.89	0.89	0.90	0.91

3.1.4 Temperature Testing

Visual Inspection: Laboratory exposure of materials E and L to temperature caused a slight amount of yellowing after 2000 h at 70°C and after 500, 1000, and 2000 h at 90°C. At 125°C, slight yellowing was observed after 500 h which became progressively deeper after 1000 h and 2000 h of exposure. Exposure to a temperature of 70°C caused very slight yellowing of material G after 1000 h which became slightly deeper at 2000 h. A moderate amount of yellowing occurred in this material at 90°C after 500, 1000, and 2000 h of exposure. At 125°C, this material had very severe yellowing after 500 h which became progressively worse at 1000 and 2000 h. Laboratory exposure of material M to a temperature of 70°C caused a slight increase in yellowing after 500 h that increased slightly after 2000 h of exposure. A slight to moderate amount of yellowing occurred at 90°C after 500 h, which deepened to moderate at 2000 h. At 125°C, material M had severe yellowing after 500 h which became progressively worse at 1000 h and 2000 h. The top surface also exhibited a wrinkled pattern. Laboratory exposure of material H to temperatures of 70°C, 90°C, and 125°C did not cause any visible changes with the exception of possible very slight yellowing after 2000 h at 125°C. Material J showed no visible changes after exposure for up to 2000 h at 70°C and 90°C and 125°C. Laboratory exposure of material K to temperatures of 70°C and 90°C did not cause any visible changes in 2000 h. At 125°C, there was moderate yellowing after 500 h which became progressively more severe with exposures up to 2000 h; however, the film still remained flexible. Similarly, laboratory exposure of material N for up to 2000 h at 70°C and 90°C did not cause any visible changes. After 1000 h at 125°C, there was noticeable sagging and warping and a minor amount of yellowing that could only be seen by looking at the edge of the specimen.

Microscopic Examination: Examination of the surface of a specimen of material H, heated for 2000 h at 125°C, with a scanning electron microscope revealed a considerable number of small surface blisters (see figure 3.1.6). Changes were not observed for any of the other cover materials exposed to temperature in this program.

Optical Measurements: Integrated solar transmittance values are given in table 3.1.4 for cover samples exposed for up to 2000 h at temperatures of 70°C, 90°C, and 125°C. Material G was the only material to show a change at 70°C. At 90°C, materials G and M had substantial changes. At 125°C, materials G and M had greater changes than those observed at lower temperatures and materials E, K, and L showed slight changes. Spectral transmittance curves are shown for materials G, H, J, and K as a function of exposure temperature and exposure time in figure 3.1.7. The absorption edge of material G, measured on a spectrophotometer with an integrating sphere, shifts to longer wavelengths as temperature and exposure time increase. This accounts for the changes in yellowing observed visually. The absorption edge of material H had a substantial shift to shorter wavelengths at 125°C. As was previously mentioned, this shift is most likely due to loss of UV inhibitor. Material J shows a slight rounding off of the top of the absorption edge as a function of exposure temperature and time. This is probably indicative of the onset of degradation. Measurements made on material K using an integrating sphere show an initial shift in the absorption edge to shorter wavelengths followed by a gradual shift back towards longer wavelengths. Measurements made on material K on a spectrophotometer without an integrating sphere show that this shift back towards longer wavelengths, following the loss of the UV inhibitor at temperatures as low as 70°C may be at least partially due to either an increase in scattering or film shrinkage. The spectral curves measured for material N using an integrating sphere did not show any signs of change after 2000 h at 125°C.

3.1.5 Temperature and Humidity Testing

Visual Inspection: Exposure to combined moisture and temperature caused moderate whitening of materials E and L at 70°C and a combination of severe whitening, blister formation, and yellowing at 90°C which became progressively worse with exposure time (500 h to 2000 h). Exposure of material G to combined moisture and temperature caused severe whitening after 500 h at 70°C which became more severe at longer times. At 90°C with moisture, there was a combination of very severe whitening and yellowing which progressed from moderate to very severe as the exposure time increased from 500 h to 2000 h. The surfaces remained glossy but changed in appearance from the unexposed specimens. Exposure of material M to combined moisture and temperature caused severe whitening after 500 h at 70°C and evidence of large blisters on the bottom surface. The top surface became very sticky after this exposure. At 90°C with moisture, there was a combination of severe whitening and yellowing which progressed from moderate after 500 h to a deep tan after 2000 h. There was also a noticeable change in top surface texture and evidence of large blisters on the bottom surface. Exposure of material H to combined moisture and temperature caused a slight amount of yellowing after 1000 at 70°C; however, the material remained flexible. At 90°C with moisture, there was slight yellowing and material H became brittle after 500 h of exposure; after 1000 h, there was moderate yellowing and some clouding of the material in addition to the embrittlement and after 2000 h the material broke into small pieces. Exposure of material J to combined moisture and temperature caused no visual changes at

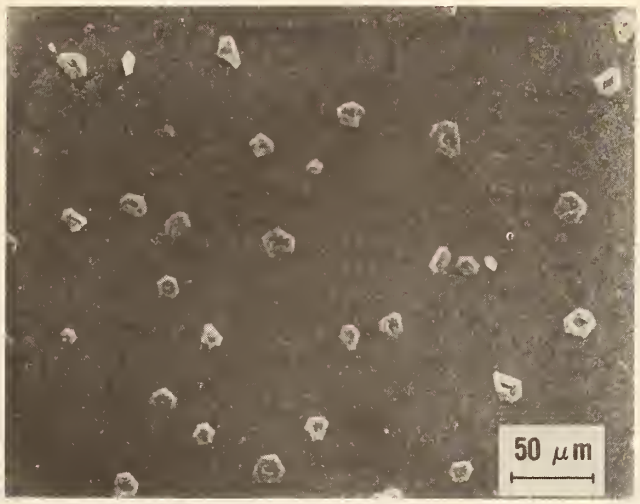

Figure 3.1.6 Blistering of cover material H after 2000 h at 125°C

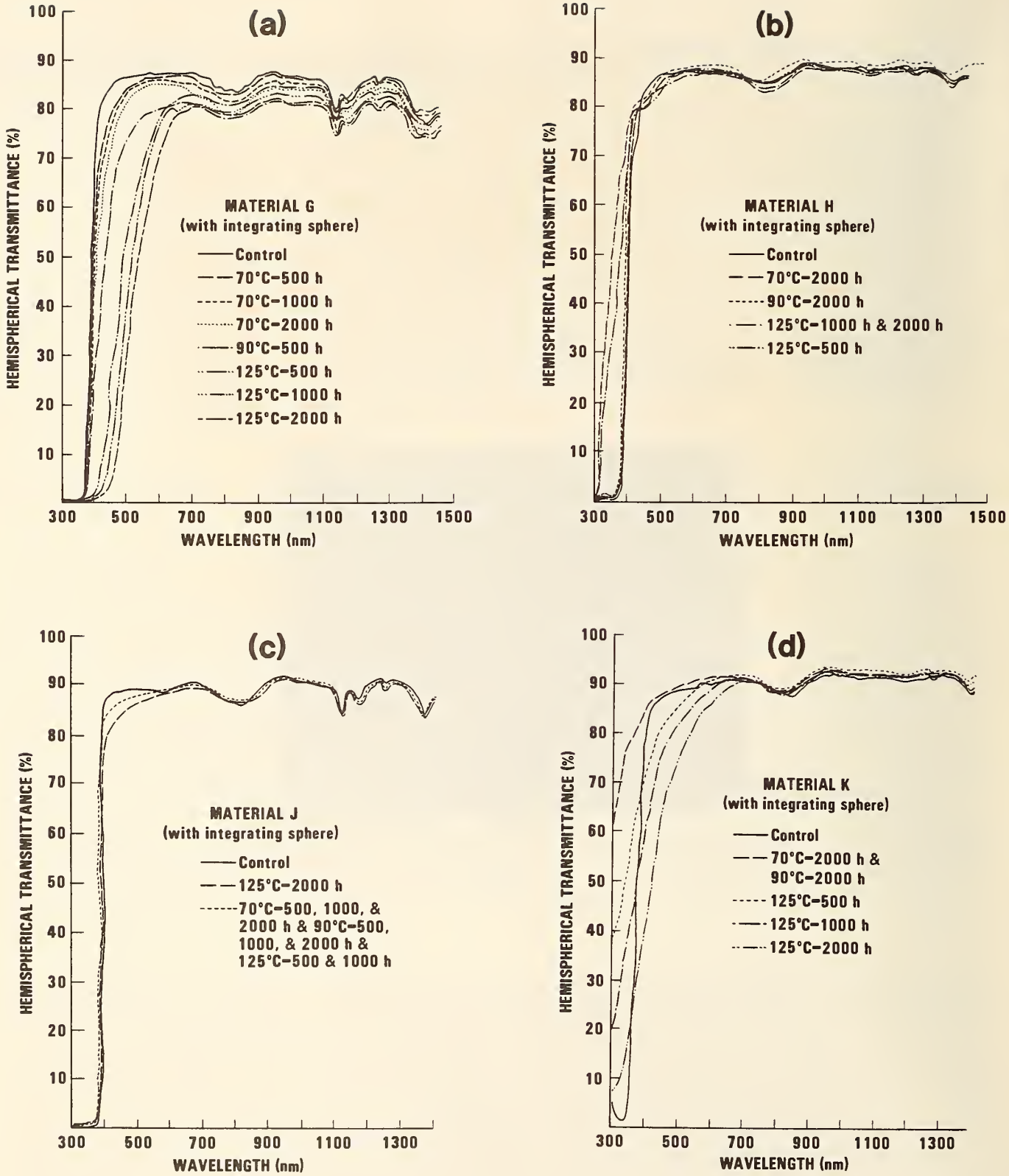

Figure 3.1.7 Spectral transmittance curves of cover samples after temperature aging

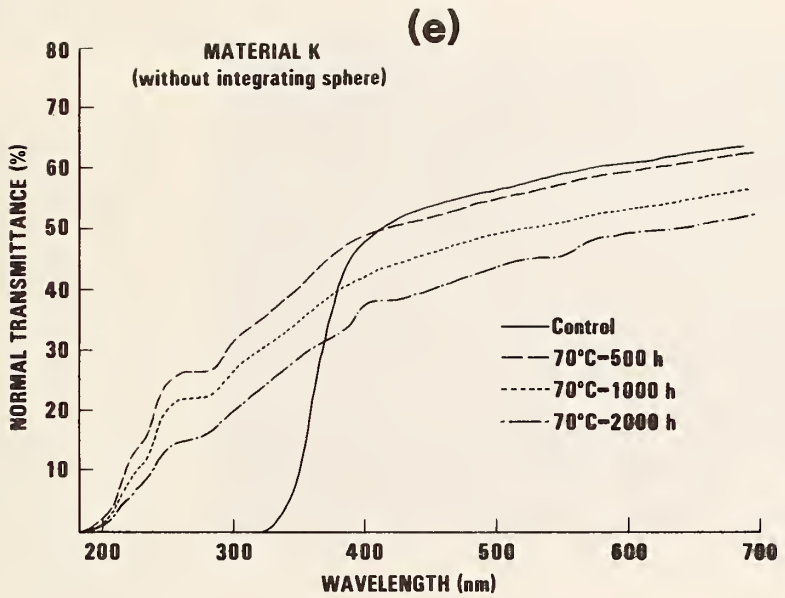

Figure 3.1.7 Continued

70°C. At 90°C with moisture, the material started to whiten after 1000 h, and was considerably whiter after 2000 h. The material also became progressively more brittle as a result of this exposure; however, its surfaces remained glossy. Exposure of material K to moisture at temperatures of 70°C and 90°C for up to 2000 h caused no visible changes. Material N showed no visible signs of change after exposure to moisture at 70°C. After 500 h of exposure to moisture at 90°C, the material started to take on a cloudy white appearance, which became progressively more severe at longer exposure times. The cloudy white appearance was accompanied by a noticeable increase in embrittlement when specimens were broken in flexure; however, the specimen surfaces remained glossy indicating that surface microcracking was probably not the cause of this whitening.

Microscopic Examination: Examination of materials E, G, L, and M with an optical microscope revealed that the whitening of these materials, when exposed to temperature in combination with moisture, was probably due to delamination between the glass fibers and the resin in the bulk of the material. This type of resin-glass fiber separation was not observed with specimens exposed outdoors to either "real time" or accelerated conditions or in any other type of laboratory exposure used. Surface microcracking was observed in specimens of material G after 500 h of exposure to moisture at 90°C; but not at 70°C with moisture. The change in surface texture observed visually for material M at 90°C with moisture was also found to be due to the formation of surface microcracks. Examination with a scanning electron microscope of specimens of material H, exposed to moisture at 90°C, indicated a considerable amount of moisture etching; but no microcracking (see figure 3.1.8). Similar moisture etching was also observed on the Palo Alto "real time" exposure test specimen after 480 days. Examination of the surfaces of materials J, K, and N after exposure to combined moisture and temperature showed no noticeable changes.

Optical Measurements: Integrated solar transmittance values are given in table 3.1.5 for cover samples exposed for up to 2000 h at temperatures of 70°C and 90°C with a relative humidity of approximately 95 percent. With the exception of the sample of material H which disintegrated after 2000 h at 90°C and could not be measured, all of the materials showed very large changes in their transmittance at this temperature. After 1000 h at 70°C, materials H, K, and N did not show changes in integrated transmittance. The remainder of the materials showed substantial changes which were somewhat less than those which occurred at 90°C with humidity. Spectral transmittance curves are shown for materials G, H, J, K, and N in figure 3.1.9. Material G showed a drastic decrease in spectral transmittance as a result of exposure to temperature and humidity. The other glass fiber reinforced plastics performed somewhat better, but also showed substantial decreases in performance. Measurements of material H using an integrating sphere showed a slight shift in the absorption edge to shorter wavelengths at 90°C. The curves measured for this material without an integrating sphere, which are shown in figure 3.1.9b, show a substantial decrease in transmittance, probably due to scattering, after 1000 h of exposure to humidity at 90°C; the 2000 h samples broke into small flakes. Materials J and N showed similar changes in their spectra, both with and without an integrating sphere. These changes, which were much greater without an integrating sphere, are most likely due to scattering which would account for the cloudy white appearance observed visually for these materials. Material K showed the same loss in UV inhibitor observed for exposure to temperature without humidity with a shift of the absorption edge towards shorter wavelengths.

3.1.6 Temperature and Xenon Arc Radiation Testing

Visual Inspection: Temperature and xenon arc radiation exposure for up to 2000 h at 70°C caused no visual signs of degradation in materials E and L. After 500 h at 90°C with xenon arc radiation, a slight amount of yellowing was observed in these materials which became progressively more severe with exposure time. Similarly, material G showed no visible signs of degradation with xenon arc radiation at 70°C; however, at 90°C there was severe yellowing after 500 h of radiation exposure which became progressively more severe with exposure time. Temperature and xenon arc exposure of material M for 500 h at 70°C caused a slight increase in yellowing after 500 h which became slightly more intense with exposure time. At 90°C with xenon arc radiation, there was slight yellowing after 500 h which progressed to severe yellowing after 2000 h. No visible signs of degradation occurred in material H after exposure to temperature and xenon arc radiation for 2000 h at 70°C and after 1000 h at 90°C; after 2000 h of exposure at 90°C, there was a slight amount of yellowing and the material became quite brittle. In the case of material J, temperature and xenon arc radiation caused a moderate amount of yellowing after 500 h at both 70°C and 90°C. This yellowing appeared to remain fairly constant for exposure times up to 2000 h. Material K showed no visible signs of degradation after radiation exposure for 2000 h at 70°C and 500 h at 90°C. After 1000 h at 90°C, there was a slight amount of yellowing and after 2000 h of xenon arc radiation exposure at 90°C, material K became moderately yellow and brittle. Exposure of material N to temperature and xenon arc radiation caused no visible signs of degradation after 2000 h at 70°C. After 500 h of radiation exposure at 90°C, a slight amount of yellowing could be seen on viewing the edge of the test specimen. Specimens

(a) 500 hours

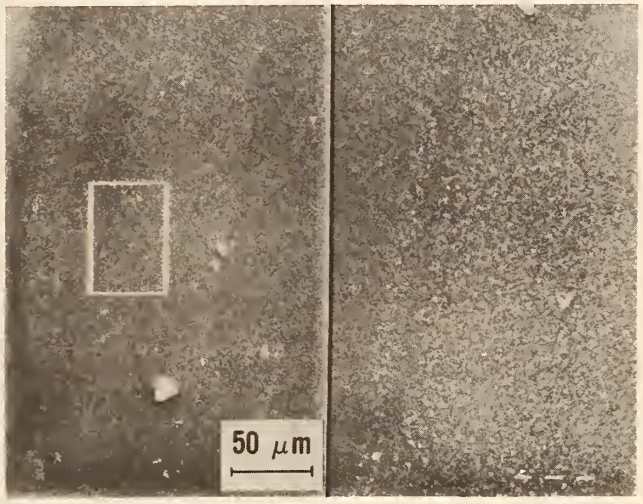

(b) 1000 hours

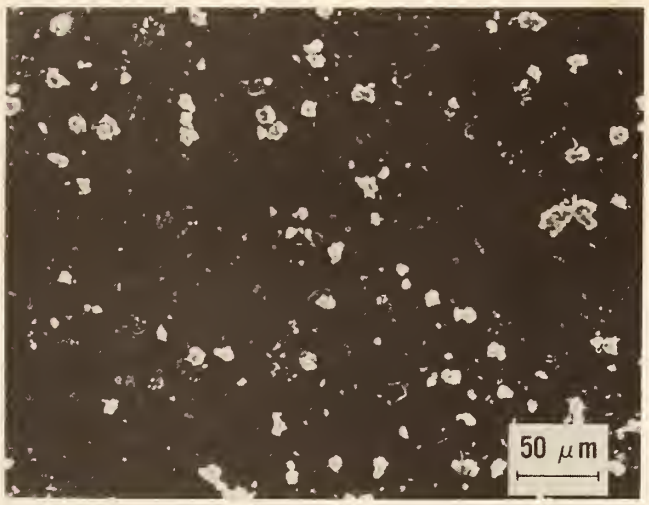

(c) 2000 hours

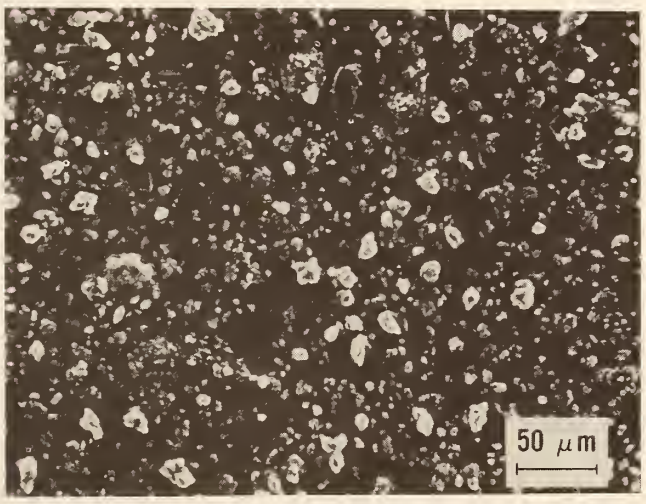

Figure 3.1.8 Surface changes in cover material H after 500, 1000, and 2000 h at 90°C and 95% RH

Table 3.1.5. Effect of Temperature & Humidity on Cover Sample Transmittance

		70 C and 95% RH Hours Exposure			90 C and 95% RH Hours Exposure		
Sample	Control	500	1000	2000	500	1000	2000
E	0.85	0.72	0.64	--	0.50	0.46	0.30
G	0.84	0.15	0.13	--	0.10	0.08	0.07
H	0.85	0.85	0.85	--	0.84	0.83	--
J	0.88	0.87	0.87	--	0.86	0.84	0.74
K	0.89	0.90	0.91	--	0.91	0.91	0.87
L	0.84	0.54	0.51	--	0.31	0.25	0.21
M	0.78	0.35	0.31	--	0.24	0.23	0.18
N	0.90	0.88	0.89	--	0.76	0.82	0.64

Table 3.1.6. Effect of Temperature & Xenon Arc Radiation on Cover Sample Transmittance

		70 C and Xenon Arc Hours of Exposure			90 C and Xenon Arc Hours of Exposure		
Sample	Control	500	1000	2000	500	1000	2000
E	0.85	0.85	0.85	0.84	0.78	0.79	0.77
G	0.84	0.80	0.78	0.81	0.78	0.78	0.74
H	0.85	0.85	0.85	0.85	0.86	0.86	0.85
J	0.88	0.86	0.86	0.86	0.85	0.85	0.84
K	0.89	0.92	0.93	0.92	0.91	0.89	--
L	0.84	0.82	0.84	0.83	0.83	0.83	0.80
M	0.78	0.79	0.78	0.80	0.74	0.73	0.70
N	0.90	0.89	0.89	0.90	0.89	0.88	0.88

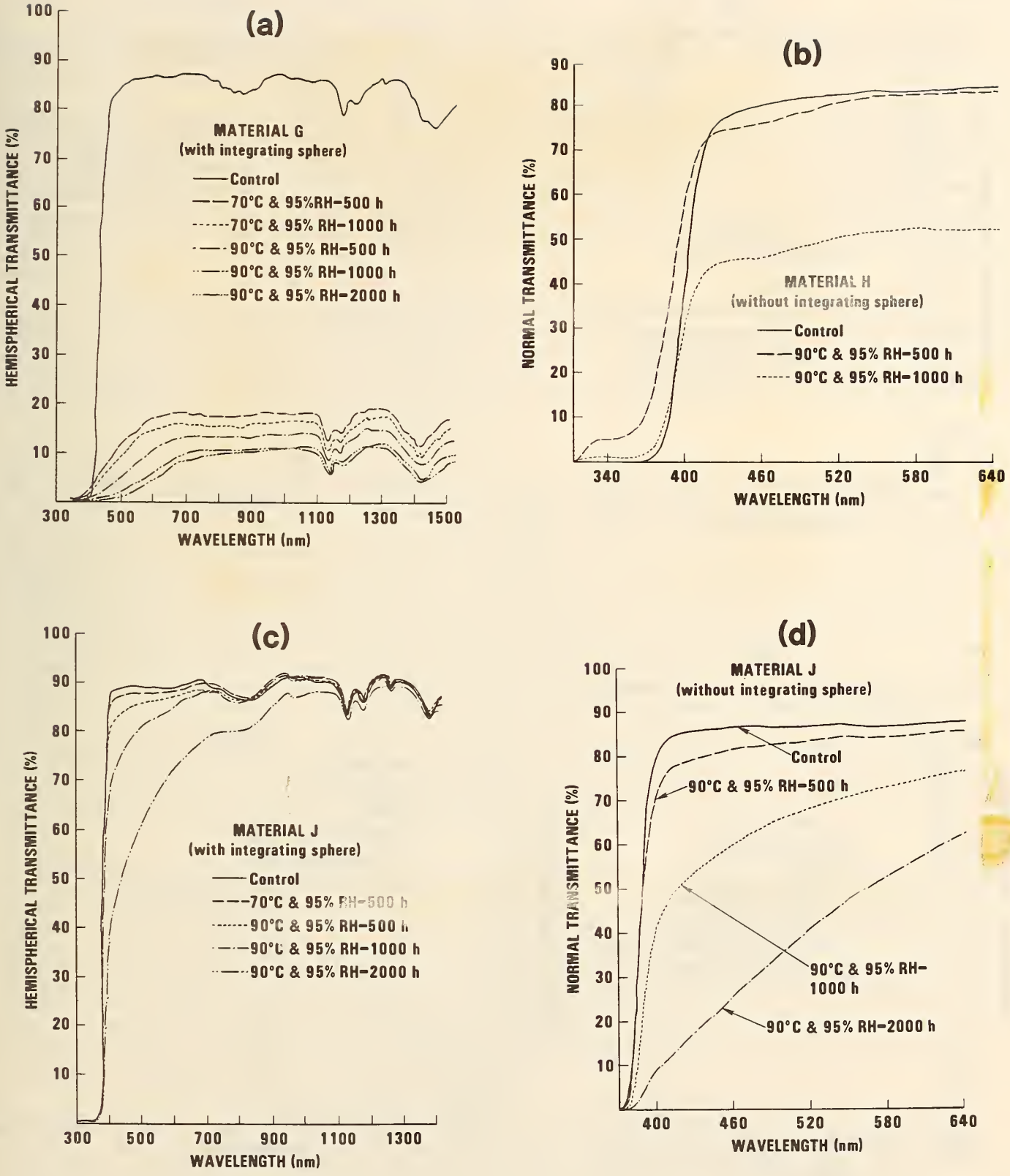

Figure 3.1.9 Spectral transmittance curves of cover samples after temperature and humidity aging

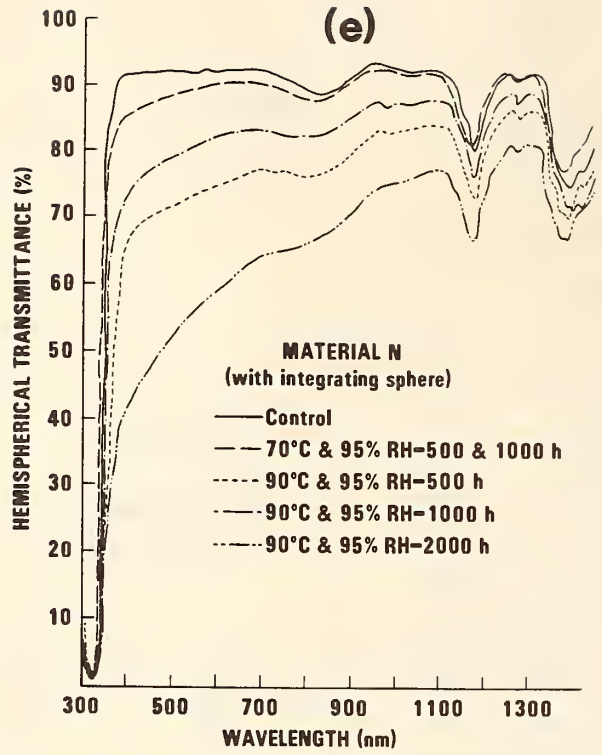

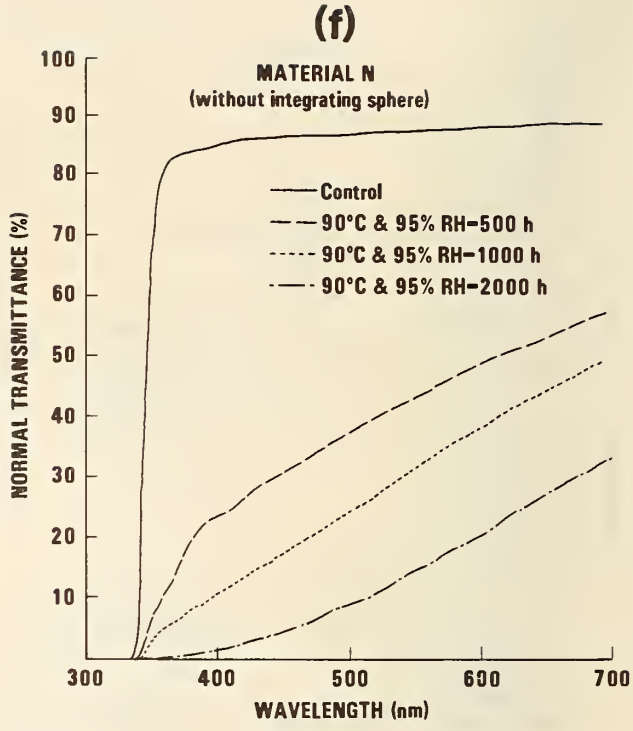

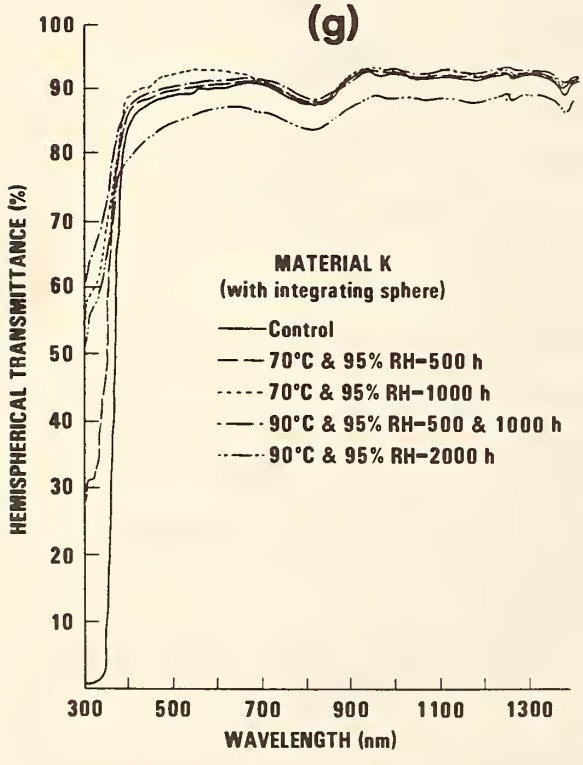

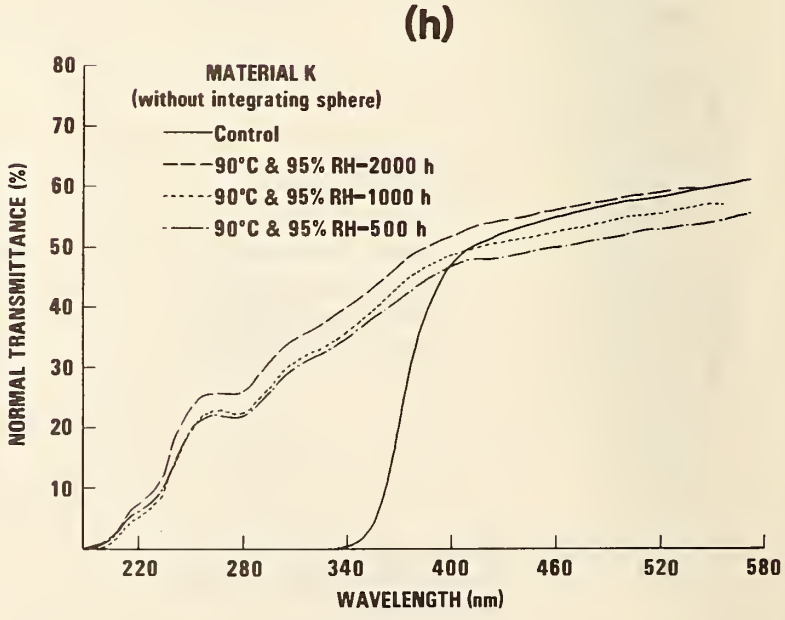

Figure 3.1.9 Continued

exposed for 1000 h and 2000 h under these conditions became noticeably more brittle on breaking in flexure in addition to showing this slight yellowing.

Microscopic Examination: Surface microcracking was observed in the specimen of material J exposed to xenon arc radiation at 90°C for 2000 h. No other changes were observed for test specimens exposed to xenon arc radiation in conjunction with temperature.

Optical Measurements: Integrated solar transmittance values are given in table 3.1.6 for cover samples exposed to xenon arc radiation for up to 2000 h at temperatures of 70°C and 90°C. Material G was the only material which showed a change at 70°C. At 90°C, materials E, G, J, L, and M showed significant changes in their integrated transmittance. Examination of spectral curves obtained for material G showed shifts in the absorption edge to longer wavelengths as a function of exposure time and temperature (see figure 3.1.10a). This shift probably accounts for the yellowing observed visually for this material. Material H showed a slight shift in its absorption edge towards shorter wavelengths similar to that observed with the exposure tests discussed in preceding sections of this report.

Changes in the absorption edge of material K, similar to those previously found for exposure to temperature and temperature and humidity, were also found after exposure to temperature and xenon arc radiation. Material N exhibited the same spectral shift in its absorption edge observed previously in outdoor exposure (see figure 3.1.4i). Material J showed a slight shift in its absorption edge which increased with the exposure time and temperature (see figure 3.1.10b). This probably accounts for the yellowing observed visually for this material.

3.1.7 Comparison and Assessment of Test Procedures

The "real time" outdoor mini-box testing and accelerated outdoor testing both appear to be good ways of duplicating the types of changes observed with full-size collectors. However, outdoor "real time" exposure of 480 days having a minimum solar radiation level of 17,000 $kJ/m^2/day$ is required with the cover mini-boxes to make many of the changes observed at shorter times with full-size stagnating collectors evident. The accelerated outdoor test appears to be capable of doing this in 120 actual exposure days. This is most likely because the temperatures of cover samples mounted on the mini-boxes were typical of those measured on operating solar collectors, whereas those of samples in the accelerated test apparatus were typical of those measured on the covers of stagnating collectors. The changes used for comparative purposes included spectral changes, microcracking, embrittlement on bending, visual yellowing, and in the case of PMMA, molecular weight measurements (see table 3.1.7). The amount and extent of microcracking observed in outdoor "real time" exposure appeared to be closely related to the amount of moisture and condensation present at the exposure site with the greatest changes observed at sites with high prevailing humidity, i.e., Cape Canaveral rather than Phoenix. The cumulative amounts of solar radiation received at all four sites were roughly comparable (see Appendix A). The microcrack patterns observed with accelerated outdoor testing appeared to be finer and less open than those observed with outdoor "real time" exposure. This is probably due to the higher stress levels and loading rates caused by exposure to concentrated solar radiation in conjunction with an intermittent water spray.

The indoor laboratory tests were able to duplicate some but not all of the changes observed outdoors. The temperature and xenon arc radiation tests appeared to be reasonable methods for determining changes due to these parameters. However, the indoor temperature and humidity testing produced changes that were not observed in outdoor exposure under conditions representative of those occurring in actual solar collectors. The primary value of this type of long-term test would be for glazings for trickle down collectors and polymeric water storage tanks where continuous exposure to moisture at elevated temperatures is likely. None of the indoor laboratory tests duplicated the extensive microcracking observed outdoors. Some of the glass fiber reinforced plastics produced microcracking as a result of temperature and moisture exposure; however, as mentioned above, the exposure conditions used in this study for humidity testing are believed to be too severe, i.e., there was extensive delamination between the glass fiber reinforcement and the resin in all of the glass fiber reinforced plastics subjected to this test.

With regard to optical property measurements, emphasis in current ASTM methods concerned with the durability of cover materials [8, 9, 11] has been placed on the use of integrated spectral transmittance values. These integrated values are not sensitive to spectral changes that occur in a limited part of the solar spectrum, i.e., at short wavelengths in many polymers. Since little or no energy is found in the solar spectrum in this short wavelength region, integrated solar spectral transmittance values are of little value in detecting these changes which are sensitive indicators of degradation in many polymers. More emphasis should be placed on the analysis of normal and hemispherical spectral transmittance curves.

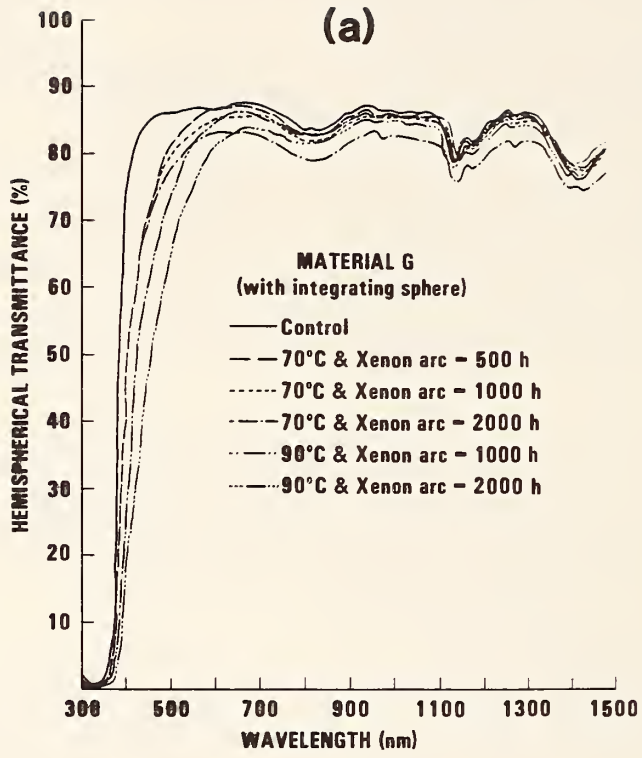

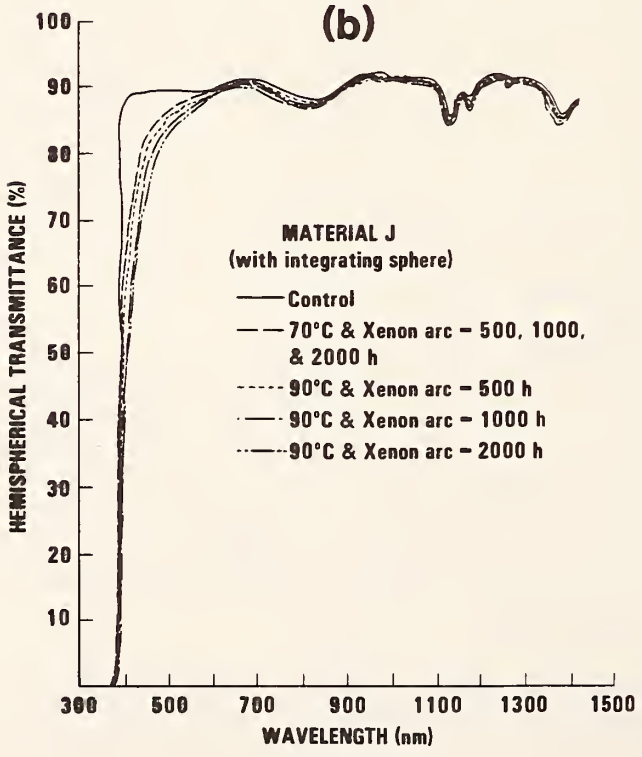

Figure 3.1.10 Spectral transmittance curves of cover samples after temperature and xenon arc radiation aging

Table 3.1.7 Effect of Environmental Exposure on the Molecular Weight of Poly (methyl methacrylate)

Exposure Condition	Exposure Time	Mw	Mn
Unexposed	------	9.1 E5	4.7 E5
	------	8.9 E5	4.6 E5
Outdoor-Phoenix	80 days*	7.0 E5	3.6 E5
	160 days*	6.7 E5	3.4 E5
	240 days*	5.9 E5	3.0 E5
	480 days*	5.0 E5	2.5 E5
Outdoor-Cape Canaveral	80 days*	7.0 E5	3.6 E5
	160 days*	6.8 E5	3.4 E5
	240 days*	6.5 E5	3.3 E5
	480 days*	5.2 E5	2.7 E5
Outdoor-Palo Alto	80 days*	7.9 E5	4.0 E5
	160 days*	6.8 E5	3.5 E5
	240 days*	-----	-----
	480 days*	5.3 E5	2.7 E5
Outdoor-Gaithersburg	80 days*	7.5 E5	4.0 E5
	160 days*	7.1 E5	3.6 E5
	240 days*	7.6 E5	3.4 E5
	480 days*	5.7 E5	3.0 E5
Accelerated Outdoor-Phoenix	120 days**	6.2 E5	2.8 E5
	120 days**	6.0 E5	2.8 E5

Indoor Laboratory Exposure Condition	Exposure Time	Mw	Mn
70°C	500 h	7.8 E5	4.2 E5
	1000 h	7.1 E5	3.8 E5
	2000 h	5.7 E5	3.2 E5
90°C	500 h	6.7 E5	3.5 E5
	1000 h	6.0 E5	3.1 E5
	2000 h	4.8 E5	2.7 E5
70°C and xenon arc	500 h	6.5 E5	3.5 E5
	1000 h	6.6 E5	3.3 E5
	2000 h	6.5 E5	3.3 E5
90°C and xenon arc	500 h	5.1 E5	2.5 E5
	1000 h	4.7 E5	2.3 E5
	2000 h	3.4 E5	1.8 E5
70°C and 95% RH	500 h	8.2 E5	4.4 E5
	1000 h	8.0 E5	4.2 E5
	2000 h	----	----
90°C and 95% RH	500 h	8.3 E5	4.1 E5
	1000 h	7.9 E5	3.9 E5
	2000 h	7.3 E5	3.8 E5

* 17,000 kJ/m^2 minimum days
** Equivalent days; 5 equivalent days ≈ 1 month "real time".

3.2 ABSORBER MATERIALS TESTING

In this section, the results of outdoor and indoor laboratory exposure testing of absorber materials are presented and the extent to which accelerated outdoor and indoor laboratory tests simulate "real time" outdoor exposure tests are discussed. A complete listing of materials used for these comparisons and their code letters are presented in table 2.2.4 of this publication. These materials were selected as being representative of the broad variety of absorber materials being used in flat-plate solar collectors when this test program was initiated. In addition to the small-scale tests which were performed on all materials, samples of those absorber materials having code letters A through H were cut from full-size solar collectors and evaluated following the completion of collector exposure testing as described in section 2 of this publication. The types of small-scale outdoor and indoor laboratory tests performed on absorber materials are also summarized in section 2.

3.2.1 Full-Size Collector Stagnation Testing

Visual Inspection: Whitish areas appeared on the absorptive coatings of several of the type A collectors within the first few months of outdoor exposure (see figure 3.2.1). There were no obvious environmental trends with regard to the occurrence of this whitening, i.e., one of the two type A collectors exposed at the Palo Alto site had extensive whitening and the other showed no evidence of this phenomenon. The source of this whitening has been identified by Moore as a crystalline zinc salt [38]. Large dark gray irregular areas appeared on the absorptive coatings of most of the type C collectors exposed outdoors. These collectors had considerable evidence of water leakage and condensation which may have been the source of the problem. Pitting and, in some cases, extensive corrosion occurred on the absorbers of most of the type D collectors (see figure 3.2.2). Once again, there was no consistent trend that could be observed with regard to outdoor exposure site location and the degree of pitting and corrosion may have been caused by water leakage which could vary with the construction and assembly of individual collectors. The absorbers of collector types E, F, G, and H showed no visual signs of deterioration.

Optical Measurements: Tables 3.2.1 and 3.2.2 present values for absorptance and emittance, respectively, measured on samples taken from the absorber plates of full-size collectors A through H following the completion of outdoor exposure and thermal performance testing. The nonselective coatings did not show any significant changes in optical performance as a result of exposure for 480 days. The absorptance of coating A changed from an original value of 0.87 to as low as 0.79 and the emittance from 0.13 to as high as 0.30 for the series 1 and series 2 collectors. These changes in emittance appeared to be associated with the whitish deposits observed visually, with the largest change occurring in the series 2 collector exposed in Palo Alto. The series 4, Type A, collector exposed to stagnation conditions with radiation augmentation reflectors in Phoenix had a larger change in emittance to 0.43; however, the whitish deposits on this sample did not visually appear to be as extensive as those on the Palo Alto Series 2 collector. Changes in emittance for coating A were minimal at the Gaithersburg site, which correlated with the lack of visual signs of change for samples exposed there. Moore [38] measured values in emittance of 0.18 in the whitish areas of absorber samples taken from type A collectors used in an operational system for 2 years. As observed by Moore, variations in the color of absorptive coating A from tan to bluish-purple did not affect the optical properties of this material. Such colors were observed on both exposed and unexposed materials in this program. Increases in the emittance of absorber material D from 0.06 to as much as 0.17 are related to the amount of corrosion that occurred. Significant changes in absorptance were not observed for this material. The emittance of material F improved from 0.75 to as low as 0.50. Accompanying this improvement in emittance was a decrease in absorptance from 0.96 to as low as 0.88. Samples of absorber material P, which were taken from collectors used in a solar energy system in Gaithersburg, Maryland, showed no significant changes in optical properties. These collectors had been in use for 5 years with a little more than a year of that time consisting of stagnation exposure.

3.2.2 "Real Time" Coupon Specimen Testing

Visual Inspection: The only materials which showed visual evidence of changes were material N, which changed in color from dark brown to tan within 80 days of exposure at all four sites, and material H, which showed large gray areas lighter than the original coating after 480 days of exposure at the Palo Alto site. All of the paints used as absorptive coatings gave off condensible outgassing products. This resulted in the appearance of cloudy areas on the glazing of the absorber exposure box directly above the paint coupon specimens. There were no visible signs of the whitening and corrosion observed for full-size collectors.

Optical Measurements: Tables 3.2.3 and 3.2.4 present values for absorptance and emittance, respectively, measured as a function of exposure time for coupon specimens exposed on the selective

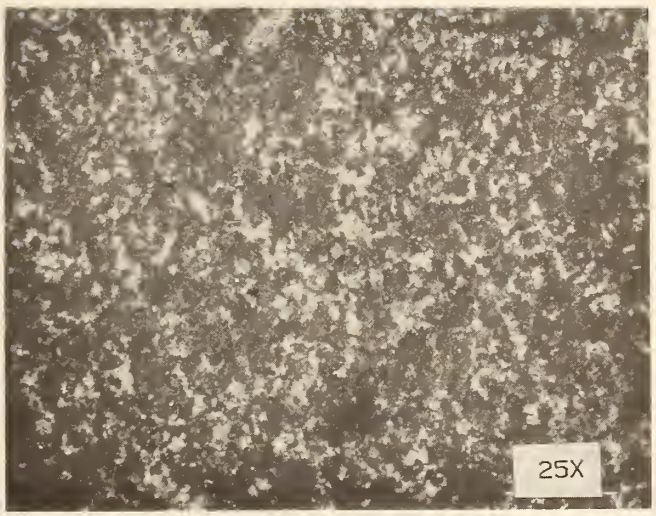

Figure 3.2.1 Whitish deposits on absorber material A sample from a full-size collector after 480 exposure days (≥17,000 kJ/sq-m-day)

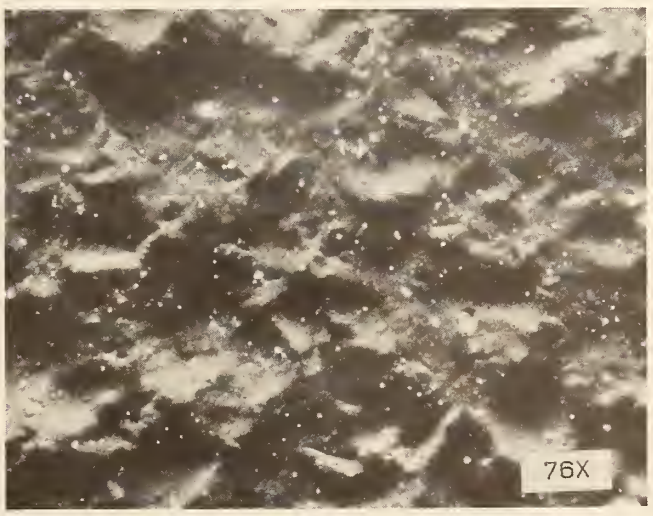

Figure 3.2.2 Corrosion of absorber material D sample from a full-size collector after 480 exposure days (≥17,000 kJ/sq-m-day)

Table 3.2.1. Absorptance of Full-Size Collector Absorber Coatings after Exposure.

Collector	Series	Control	Exposure Days**	Site: Phoenix	Cape Canaveral	Palo Alto	Gaithersburg
A	1	0.87	480	0.79	0.83	0.86	0.84
	2	0.87	480	0.83	0.82	0.82	0.84
	3	0.87	240	0.86	0.84	--	--
	4	0.87	60	0.88	0.83	--	--
B	1	0.98	480	0.98	0.97	0.97	0.97
	2	0.98	480	0.98	0.97	0.97	0.97
	3	0.98	240	0.97	0.96	--	--
	4	0.98	60	0.98	0.97	--	--
C	1	0.98	480	0.96	0.96	0.95	0.97
	2	0.98	480	0.96	0.96	0.96	0.97
	3	0.98	240	0.96	0.96	--	--
	4	0.98	60	0.97	0.97	--	--
D	1	0.97	480	0.95	0.95	0.95	0.95
	2	0.97	480	0.95	0.95	0.96	0.96
	3	0.97	240	0.95	--	--	--
	4	0.97	60	--	--	--	--
E	1	0.95	480	0.96	0.95	0.96	0.96
	2	0.95	480	0.96	0.95	0.96	0.95
	3	0.95	240	0.95	0.94	--	--
	4	0.95	60	0.96	0.95	--	--
F	1	0.96	480	0.91	0.90	0.90	0.88
	2	0.96	480	0.90	0.91	0.89	0.89
	3	0.96	240	0.94	0.93	--	--
	4	0.96	60	0.91	0.90	--	--
H	1	0.95	480	0.95	0.95	0.95	0.95
	2	0.95	480	0.95	0.95	0.95	0.95
	3	0.95	240	0.95	0.95	--	--
	4	0.95	60	0.95	0.95	--	--
P1	-	0.96	*				0.93
P2	-	0.96	*				0.96

* Samples from NBS Townhouse Collectors after Approximately 5 Years Exposure.

** Days with a Minimum Solar Radiation level of 17,000 kJ/sq m

Table 3.2.2 Emittance of Full-Sized Collector Absorber Coatings after Exposure.

Collector	Series	Control	Exposure Days**	Site: Phoenix	Site: Cape Canaveral	Site: Palo Alto	Site: Gaithersburg
A	1	0.13	480	0.12	0.15	0.18	0.14
	2	0.13	480	0.17	0.13	0.31	0.12
	3	0.13	240	0.12	0.13	--	--
	4	0.13	60	0.43	0.13	--	--
B	1	0.91	480	0.91	0.91	0.91	0.91
	2	0.91	480	0.91	0.91	0.91	0.91
	3	0.91	240	0.91	0.91	--	--
	4	0.91	60	0.91	0.91	--	--
C	1	0.92	480	0.90	0.91	0.90	0.90
	2	0.92	480	0.90	0.91	0.91	0.91
	3	0.92	240	0.91	0.91	--	--
	4	0.92	60	0.91	0.90	--	--
D	1	0.07	480	0.06	0.06	0.06	0.14
	2	0.07	480	0.06	0.10	0.06	0.06
	3	0.07	240	0.06	--	--	--
	4	0.07	60	--	--	--	--
E	1	0.87	480	0.88	0.87	0.88	0.87
	2	0.87	480	0.89	0.88	0.88	0.87
	3	0.87	240	0.86	0.86	--	--
	4	0.87	60	0.87	0.87	--	--
F	1	0.75	480	0.56	0.55	0.50	0.53
	2	0.75	480	0.60	0.58	0.57	0.53
	3	0.75	240	0.63	0.54	--	--
	4	0.75	60	0.55	0.50	--	--
H	1	0.89	480	0.89	0.88	0.89	0.88
	2	0.89	480	0.89	0.89	0.89	0.88
	3	0.89	240	0.88	0.89	--	--
	4	0.89	60	0.89	0.88	--	--
P1	-	0.08	*				0.07
P2	-	0.08	*				0.08

* Samples from NBS Townhouse Collectors after Approximately 5 Years Exposure.

** Days with a Minimum Solar Radiation Level of 17,000 kJ/sq m.

Table 3.2.3. Effect of Outdoor Exposure on Absorber Coating Absorptance - Selective Side

		Phoenix				Cape Canaveral				Palo Alto				Gaithersburg			
		Days Exposure*				Days Exposure				Days Exposure				Days Exposure			
Sample	Control	80	160	240	480	80	160	240	480	80	160	240	480	80	160	240	480
A	0.87	0.87	0.86	0.88	--	0.88	0.85	0.86	0.86	0.88	0.86	0.87	0.88	0.87	--	0.87	0.87
C	0.98	0.97	0.97	0.97	0.97	0.97	0.98	0.98	0.97	0.97	0.97	0.98	0.97	0.97	0.97	0.97	0.97
D	0.97	0.96	0.95	0.94	0.94	0.95	0.96	0.96	0.94	0.96	0.96	0.96	0.95	0.96	0.96	0.96	0.94
E	0.95	0.96	0.96	0.96	0.96	0.96	0.96	0.96	0.96	0.96	0.96	0.96	0.96	0.96	0.96	0.96	0.96
F	0.96	0.92	0.92	0.90	0.89	0.93	0.91	0.91	0.89	0.93	0.90	0.90	0.89	0.93	0.92	0.91	0.89
G	0.93	0.92	0.90	0.92	0.93	0.93	0.93	0.93	--	0.93	0.93	0.93	--	0.93	0.93	0.93	--
H	0.95	0.96	0.95	0.96	0.94	0.95	0.96	0.96	0.95	0.95	0.96	--	0.95	0.95	0.96	0.96	0.95
I	0.88	--	--	0.87	--	--	--	0.88	0.87	--	--	0.88	0.86	--	--	0.87	0.87
J	0.98	0.97	0.97	0.97	0.96	0.97	0.97	0.98	0.97	0.97	0.97	0.91	0.90	0.97	0.98	0.97	0.97
L	0.99	0.98	0.97	0.97	0.96	0.98	0.98	0.99	0.97	0.99	0.99	--	0.98	0.99	0.98	--	0.97
M	0.94	0.94	0.92	0.91	--	0.96	0.93	0.96	0.95	0.91	0.96	0.92	0.92	0.94	--	0.93	0.93
N	0.93	0.76	--	0.77	--	0.74	--	0.74	0.73	0.76	--	0.78	0.76	0.77	--	0.77	0.76
P	0.96	0.95	0.95	0.94	0.94	0.95	0.95	0.95	0.94	0.95	0.94	0.95	0.95	0.95	0.95	0.95	0.94

* 17000 kJ/sq-m (1500 Btu/sq-ft) Minimum Days

Table 3.2.4. Effect of Outdoor Exposure on Absorber Coating Emittance - Selective Side

		Phoenix				Cape Canaveral				Palo Alto				Caithersburg			
		Days Exposure*				Days Exposure				Days Exposure				Days Exposure			
Sample	Control	80	160	240	480	80	160	240	480	80	160	240	480	80	160	240	480
A	0.13	0.10	0.11	0.18	0.22	0.10	0.12	0.11	0.17	0.11	0.13	0.14	0.18	0.14	0.11	0.11	0.11
C	0.92	0.91	0.92	--	0.91	0.91	0.91	0.91	0.91	0.91	0.91	0.91	0.91	0.91	0.91	0.91	0.91
D	0.07	0.05	0.10	--	0.07	0.06	0.09	0.06	0.06	0.05	0.07	0.08	0.07	0.06	0.06	0.06	0.06
E	0.87	0.89	0.85	--	0.90	0.89	0.90	0.90	0.90	0.88	0.89	0.89	0.90	0.88	0.89	0.89	0.90
F	0.75	0.65	0.61	--	0.64	0.66	0.66	0.62	0.63	0.67	0.63	0.62	0.62	0.68	0.65	0.63	0.64
G	0.86	0.86	0.86	--	0.85	0.85	0.85	0.85	0.85	0.85	0.85	0.85	0.85	0.85	0.85	0.85	0.85
H	0.89	0.87	--	--	0.86	0.88	0.85	0.86	0.86	0.88	0.89	0.86	0.86	0.88	0.88	0.87	0.86
I	0.19	--	--	0.17	0.16	--	--	0.18	0.17	--	--	0.18	0.18	--	--	0.17	0.19
J	0.14	0.13	0.15	--	0.11	0.10	0.11	0.11	0.12	0.12	0.12	0.10	0.09	0.12	0.11	0.13	0.12
L	0.29	0.39	--	--	0.44	0.39	0.42	0.36	0.44	0.27	0.35	0.30	0.31	0.29	0.35	--	0.34
M	0.10	0.11	0.08	0.08	0.07	0.12	0.10	0.13	0.13	0.08	0.13	0.11	0.09	0.09	--	0.09	0.09
N	0.51	0.48	--	0.49	0.50	0.45	--	0.47	0.47	0.47	--	0.47	0.48	0.46	--	0.48	0.48
P	0.08	0.07	0.10	--	0.09	0.07	0.07	0.07	0.07	0.08	0.08	0.09	0.07	0.07	0.08	0.06	0.07

* 17000 kJ/sq-m (1500 Btu/sq-ft) Minimum Days

side of the absorber box described in section 2. Values for specimens exposed on the nonselective side are given in tables 3.2.5 and 3.2.6. With the exception of absorber material H, which had a slight, but consistent, improvement in emittance from 0.88 to 0.86 after 480 days on the selective side of the absorber box, there were no changes in the optical properties of the nonselective absorber coupon specimens studied. Material A increased in emittance from about 0.13 to values of 0.22, 0.17, and 0.18 after 480 days of selective side exposure at the Phoenix, Cape Canaveral, and Palo Alto sites, respectively. No significant changes were observed for this material when exposed on the selective side at the Gaithersburg site or for the nonselective side at any of the outdoor exposure sites. Material D had a slight tendency towards lower absorptance values, decreasing from 0.97 to 0.94. Material F had decreases in absorptance from 0.96 to 0.89 (selective side) and about 0.91 (nonselective side) and improvements in emittance from 0.75 to approximately 0.63 (selective side) and 0.66 (nonselective side). The major portion of the changes occurred within 80 days of exposure. Material J decreased in absorptance from 0.97 to 0.90 and improved in emittance from 0.12 to 0.09 when exposed on the selective side of the absorber box at Palo Alto for 480 days. Similar changes were not observed at the other exposure sites. Material L increased substantially in emittance from 0.29 to as much as 0.51 with a slight decrease in absorptance. The changes were greatest at the Cape Canaveral site and the least at the Palo Alto and Gaithersburg sites. Material N decreased in absorptance from 0.93 to as low as 0.73 and improved slightly in emittance from 0.51 to as low as 0.45 within 80 days of outdoor exposure and then showed no further changes. Changes in the optical properties of materials, I, M, and P were not obvious from examination of the absorptance and emittance data.

3.2.3 Accelerated Outdoor Testing

Visual Inspection: One of the two samples of absorptive coating material D after exposure equivalent to 2 years "real time" had several small spots which, on microscopic evaluation, were found to be pits due to corrosion. After the same exposure, one of two samples of material J exhibited several small surface spots, one of two samples of material L showed considerable lightening and a light gray mottled appearance, and both specimens of material N changed from dark brown to tan. No other changes were observed.

Optical Measurements: Table 3.2.7 presents values for absorptance and emittance for absorber materials exposed outdoors in accelerated weathering machines with temperatures simulating stagnation conditions. Material C was the only nonselective absorber material exposed since prior "real time" outdoor exposure did not cause significant optical property changes in this class of materials. Changes similar to those which occurred in the "real time" outdoor exposure occurred for materials D, F, L, N, and one of two samples of material A. The optical property changes in material J, which were observed for "real time" exposure of coupon specimens only at the Palo Alto site (and not at the other three "real time" outdoor exposure sites), were not observed following accelerated outdoor exposure.

3.2.4 Temperature Testing

Visual Observations: With the exception of material N, which changed from dark brown to light tan within 1000 h of exposure at 150°C, none of the other materials showed visual signs of degradation after exposure for up to 2000 h at this temperature. Material A darkened considerably after 1000 h at 175°C and became a darker brown after 2000 h at this temperature. After 2000 h at 175°C, material L had a slight lightening in color and material G took on a slight purplish tinge. Material N changed from dark brown to tan within 1000 h of exposure at this temperature. No other visual changes were observed.

Optical Measurements: Table 3.2.8 presents values for absorptance and emittance for absorber materials exposed in the laboratory for up to 2000 h at temperatures of 150°C and 175°C. Absorber coating materials F, L, and N were the only materials which showed substantial changes within 2000 h of exposure at 150°C. These changes were consistent with those reported for the outdoor exposure tests and occurred prior to the 1000 h time period at which samples were removed for measurement. After 2000 h at 175°C, material A had a substantial increase in emittance from 0.13 to 0.52. Materials F, L, and N also showed substantial changes at this temperature. A slight change in emittance was observed for material G after 2000 h.

3.2.5 Temperature and Humidity Testing

Visual Observations: After 1000 h at 90°C and 95 percent RH, the absorptive coating on material A had disintegrated, exposing the galvanized substrate beneath it. There was also some corrosion through the galvanized layer; after 2000 h, there was severe corrosion. Material C had no visual signs of degradation after 2000 h of exposure. After 1000 h, a considerable amount of the black

Table 3.2.5. Effect of Outdoor Exposure on Absorber Coating Absorptance - Nonselective Side

		Phoenix				Cape Canaveral				Palo Alto				Gaithersburg			
		Days Exposure*				Days Exposure				Days Exposure				Days Exposure			
Sample	Control	80	160	240	480	80	160	240	480	80	160	240	480	80	160	240	480
A	0.87	0.87	0.87	0.87	--	0.87	0.87	0.88	0.87	0.87	0.86	0.87	0.87	0.88	0.87	0.86	0.86
C	0.98	0.97	0.97	0.98	--	0.97	0.97	0.97	--	0.97	0.97	0.97	--	0.97	0.97	0.97	--
D	0.97	0.96	0.96	0.96	--	0.96	0.95	0.96	0.94	0.96	0.96	0.96	0.95	0.96	0.96	0.94	0.94
E	0.95	0.96	0.96	0.96	--	0.96	0.96	0.96	--	0.96	0.96	0.96	--	0.96	0.96	0.96	--
F	0.96	0.93	0.93	0.93	--	0.93	0.92	0.93	0.91	0.93	0.92	0.93	0.92	0.94	0.93	0.93	0.91
G	0.93	0.92	0.93	0.92	--	0.93	0.93	0.93	--	0.93	0.93	0.93	--	0.93	0.93	0.93	--
H	0.95	0.95	0.95	0.96	--	0.95	0.95	0.96	0.95	0.95	0.95	--	0.95	0.95	0.95	0.95	0.95
I	0.88	--	--	--	--	--	--	--	--	--	--	--	--	--	--	--	--
J	0.98	--	--	--	--	--	--	--	--	--	--	--	--	--	--	--	--
L	0.99	0.99	0.99	0.99	--	0.98	0.97	0.97	0.96	0.99	0.98	--	0.98	0.98	0.98	0.98	0.97
M	0.94	0.91	0.95	0.95	--	0.94	0.91	0.92	0.92	0.96	0.94	0.94	0.94	0.95	0.95	0.94	0.93
N	0.93	--	--	0.77	--	--	--	0.75	0.74	--	--	0.78	0.78	--	--	0.78	0.77
P	0.96	0.95	0.95	0.95	--	0.95	0.95	0.96	0.94	0.96	0.95	0.95	0.95	0.95	0.95	0.95	0.94

* 17000 kJ/sq-m (1500 Btu/sq-ft) Minimum Days

Table 3.2.6. Effect of Outdoor Exposure on Absorber Coating Emittance - Nonselective Side

		Phoenix				Cape Canaveral				Palo Alto				Gaithersburg			
		Days Exposure*				Days Exposure				Days Exposure				Days Exposure			
Sample	Control	80	160	240	480	80	160	240	480	80	160	240	480	80	160	240	480
A	0.13	0.14	0.11	0.11	0.12	0.14	0.10	0.13	0.13	0.14	0.14	0.15	0.13	0.11	0.11	0.10	0.10
B	0.92	0.91	0.91	0.91	0.91	0.91	0.91	0.91	0.91	0.91	0.91	0.90	0.91	0.91	0.91	0.91	0.91
D	0.07	0.09	0.07	0.06	0.06	0.07	0.05	0.06	0.06	0.07	0.06	0.08	0.06	0.06	0.06	0.06	0.06
E	0.87	0.88	0.89	0.89	0.90	0.87	0.89	0.89	0.90	0.87	0.89	0.89	0.90	0.87	0.89	0.89	0.89
F	0.75	0.66	0.66	0.66	0.65	0.66	0.65	0.66	0.66	0.67	0.66	0.67	0.68	0.68	0.67	0.67	0.66
G	0.86	0.85	0.85	0.85	0.85	0.85	0.85	0.85	0.85	0.85	0.85	0.85	0.85	0.85	0.85	0.85	0.85
H	0.89	0.88	0.88	0.88	0.87	0.88	0.88	0.88	0.87	0.88	0.88	0.88	0.87	0.88	0.88	0.88	0.87
I	0.19	--	--	--	--	--	--	--	--	--	--	--	--	--	--	--	--
J	0.14	--	--	--	--	--	--	--	--	--	--	--	--	--	--	--	--
L	0.29	0.29	0.32	0.31	0.37	0.44	0.42	0.46	0.51	0.33	0.38	0.34	0.32	0.32	0.30	0.30	0.31
M	0.10	0.08	0.11	0.10	0.10	0.10	0.08	0.09	0.10	0.13	0.12	0.11	0.10	0.11	0.10	0.09	0.10
N	0.51	--	--	0.49	0.50	--	--	0.46	0.47	--	--	0.48	0.49	--	--	0.47	0.46
P	0.08	0.07	0.07	0.07	0.07	0.07	0.08	0.07	0.08	0.07	0.07	0.09	0.08	0.07	0.07	0.07	0.07

* 17000 kJ/sq-m (1500 Btu/sq-ft) Minimum Days

Table 3.2.7. Effect of Accelerated Outdoor Exposure on Absorber Coatings

Coating	Absorptance Control	Sample 1 36*	Sample 1 60	Sample 1 120	Sample 2 36	Sample 2 60	Sample 2 120	Emittance Control	Sample 1 36	Sample 1 60	Sample 1 120	Sample 2 36	Sample 2 60	Sample 2 120
A	0.87	0.87	0.87	0.88	0.87	0.87	0.86	0.13	--	--	0.18	--	--	0.12
C	0.97	0.96	0.97	0.97	0.97	0.98	0.97	0.92	--	--	0.91	--	--	0.91
D	0.96	0.96	0.97	0.93	0.95	0.95	0.94	0.07	--	--	0.07	--	--	0.07
E	--	--	--	--	--	--	--	--	--	--	--	--	--	--
F	0.94	0.95	0.92	0.88	0.91	0.91	0.91	0.75	--	--	0.64	--	--	0.66
G	--	--	--	--	--	--	--	--	--	--	--	--	--	--
H	--	--	--	--	--	--	--	--	--	--	--	--	--	--
I	--	--	--	--	--	--	--	--	--	--	--	--	--	--
J	0.97	0.97	0.97	0.96	0.97	0.97	0.96	0.14	--	--	0.14	--	--	0.12
L	0.97	0.97	0.97	0.95	0.97	0.97	0.96	0.29	--	--	0.47	--	--	0.36
M	0.94	0.93	0.94	0.93	0.94	0.94	0.93	0.10	--	--	0.11	--	--	0.10
N	0.91	0.78	0.77	0.73	0.78	0.76	0.74	0.51	--	--	0.43	--	--	0.42
P	0.94	0.95	0.95	0.94	0.94	0.94	0.94	0.08	--	--	0.08	--	--	0.07

* Equivalent Days; 5 Equivalent Days = 1 Month 'Real Time' = 6.625E+5 kJ/sq m

Table 3.2.8. Effect of Temperature on Absorber Coatings

Temperature:	150 C						175 C			
	Absorptance			Emittance			Absorptance		Emittance	
Sample	Control	1000*	2000	Control	1000	2000	1000	2000	1000	2000
A	0.87	0.86	0.86	0.13	0.09	0.13	0.87	0.91	0.13	0.52
C	0.96	0.97	0.97	0.92	0.91	0.92	0.97	0.97	0.91	0.91
D	0.97	0.96	0.96	0.07	0.06	0.06	0.95	0.96	0.07	0.07
E	0.95	0.96	0.96	0.87	0.86	0.87	0.96	0.96	0.89	0.89
F	0.96	0.91	0.90	0.75	0.66	0.65	0.89	0.89	0.67	0.70
G	0.93	0.93	0.93	0.86	0.85	0.85	0.94	0.95	0.86	0.82
H	0.95	0.96	0.96	0.89	0.88	0.88	0.95	0.95	0.88	0.87
I	0.88	--	--	0.19	0.19	--	0.87	--	0.18	--
J	0.98	0.98	0.98	0.14	0.12	0.12	0.97	0.97	0.13	0.13
L	0.99	0.99	0.99	0.29	0.37	0.35	0.98	0.99	0.41	0.38
M	0.94	0.95	0.91	0.10	0.12	0.08	0.93	0.92	0.12	0.12
N	0.93	0.85	--	0.51	0.49	--	0.80	--	0.50	--
P	0.96	0.95	0.95	0.08	0.07	0.06	0.95	0.95	0.08	0.10

* Hours Exposure

chrome absorptive coating had flaked off absorber material D, exposing the nickel layer beneath it, and there was some pitting and corrosion of the steel substrate through the nickel layer in the areas where the flaking occurred. This pitting and corrosion became more severe after 2000 h; however, it did not have the same appearance as that which occurred on the absorbers of full-size collectors. Coating E lightened to mid-gray after 1000 h at 90°C and 95 percent RH and remained the same color after 2000 h. Several small mid-gray specks appeared on the coating of material F after 1000 h of exposure which became somewhat larger after 2000 h. There was severe surface etching of the porcelain enamel coating of material G after 1000 h and some rust spots; this remained about the same after 2000 h of exposure. Extensive broken paint blisters were observed in coating H after 1000 h and 2000 h of exposure. Coating I had no visual signs of degradation after 1000 h of exposure. A considerable amount of light gray specks and streaking was observed in coating J after 1000 h and 2000 h of exposure. Material L was severely corroded and took on a white, mottled gray appearance after 1000 h and 2000 h at 90°C and 95 percent RH. The absorptive coatings of materials M and N were removed, exposing the bare metal substrate after 1000 h of temperature and moisture exposure. There were large gray mottled areas on the coating of material P after 1000 h of exposure and the coating appeared to be washed away.

Optical Measurements: Table 3.2.9 presents values for absorptance and emittance for absorber materials exposed in the laboratory for up to 2000 h at 90°C and 95 percent RH. The nonselective absorber materials (C, E, G, and H) were not significantly affected by this exposure. With the exception of material I, which was only exposed to these conditions for 1000 h and material F, all of the selective absorber materials (A, D, J, L, M, N and P) had substantial (>0.03) changes in their optical properties.

3.2.6 Temperature and Xenon Arc Radiation Testing

Visual Observations: Absorber coating materials A, C, D, E, H, I, J, M, and P had no visual signs of change after exposure to xenon arc radiation at 90°C for up to 2000 h. Material F changed from black to dark gray after 2000 h of exposure. There was a dull gray surface film on material G, after 1000 h and 2000 h of exposure, which could be wiped off. Material L lightened to a medium gray from a dark gray after 1000 h and 2000 h of exposure and material N changed from dark brown to tan.

Optical Measurements: Table 3.2.9 presents values for absorptance and emittance for absorber materials exposed in the laboratory for up to 2000 h in conjunction with xenon arc radiation simulating the solar spectrum. Materials F, I, L, N, and P showed substantial changes in their optical properties as a result of this exposure.

3.2.7 Thermal Cycling

Visual Observations: White spots, similar in appearance to those observed on full-size collectors, were observed on absorber coating material A after 15 cycles from -10°C to 175°C. This whitening became progressively more severe after 30 cycles. After thermal cycling, material D had small spots which looked like the early stages of corrosion observed on full-size collectors. Light specks appeared on the surface of the material J after 15 and 30 cycles. Material L had a mottled light to medium gray appearance after 15 cycles and the surface of material N changed from dark brown to tan after 15 cycles. Visual changes were not observed for materials C, E, F, G, H, I, M, and P.

Optical Measurements: Table 3.2.10 presents values for absorptance and emittance for absorber materials exposed in the laboratory for up to 30 cycles from -10°C to 175°C. Materials A, F, L, M. and N had significant changes in their optical properties.

3.2.8 Comparison and Assessment of Test Procedures

The test boxes used for the outdoor "real time" exposure of absorber coupon specimens appear to be a good way of exposing a large number of samples to determine their thermal stability under stagnation conditions. However, the boxes, which were carefully constructed and designed to be watertight, did not have the moisture and condensation problems that were observed for virtually all of the full-size collectors. The problem of how to determine the proper test conditions for assessing the moisture stability of absorber materials is very complex, i.e., the presence of moisture on the inner surface of the glazing of a collector that is stagnating on a clear day does not mean that the relative humidity in the vicinity of the absorber is anywhere near as high as that in the vicinity of the glazing since absorber temperatures are much higher than cover temperatures. In addition, the presence of porosity in many absorptive coatings means that moisture can condense in these pores at humidities lower than 100 percent RH. It is more likely that moisture would condense out on the absorber at night, when it is cool, rather than in the daytime. The thermal cycling test was the test

Table 3.2.9. Effect of Temperature & Humidity and Temperature & Xenon Arc Radiation on Absorber Coatings

	Temperature & Humidity, 90 C & 95% RH						Temperature & Radiation, 90 C & Xenon Lamp			
	Absorptance			Emittance			Absorptance		Emittance	
Sample	Control	1000*	2000	Control	1000	2000	1000	2000	1000	2000
A	0.87	0.73	0.84	0.13	0.70	0.53	0.86	0.87	0.10	0.11
C	0.98	0.97	0.97	0.92	0.91	0.91	0.97	0.98	0.91	0.91
D	0.97	0.95	0.95	0.07	0.13	0.19	0.96	0.96	0.06	0.06
E	0.95	0.92	0.92	0.87	0.88	0.89	0.96	0.97	0.89	0.89
F	0.96	0.93	0.93	0.75	0.76	0.77	0.90	0.89	0.73	0.71
G	0.93	0.93	0.94	0.86	0.89	0.87	0.94	0.94	0.86	0.86
H	0.95	0.94	0.94	0.89	0.90	0.90	0.95	0.96	0.87	0.87
I	0.88	0.88	--	0.19	0.17	--	0.85	--	0.15	--
J	0.98	0.96	0.96	0.14	0.22	0.26	0.98	0.98	0.12	0.11
L	0.99	0.85	0.81	0.29	0.81	0.85	0.98	0.90	0.37	0.39
M	0.94	0.59	0.54	0.10	0.62	0.65	0.94	0.95	0.10	0.11
N	0.93	0.50	--	0.51	0.81	--	0.79	--	0.45	--
P	0.96	0.95	0.95	0.08	0.12	0.14	0.95	0.96	0.11	0.32

* Hours Exposure

Table 3.2.10. Effect of Thermal Cycling on Absorber Coatings

	Absorptance				Emittance			
	Thermal Cycling (Simulated Daily Cycles) *							
Sample	Control	5	15	30	Control	5	15	30
A	0.87	--	0.87	0.87	0.13	--	0.16	0.25
C	0.98	--	0.97	0.97	0.92	--	0.91	0.91
D	0.97	--	0.95	0.96	0.07	--	0.06	0.06
E	0.95	--	0.96	0.96	0.87	--	0.86	0.85
F	0.96	--	0.91	0.91	0.75	--	0.64	0.65
G	0.93	--	0.92	0.93	0.86	--	0.85	0.85
H	0.95	--	0.95	0.95	0.89	--	0.88	0.88
I	0.88	--	0.88	--	0.19	--	0.17	--
J	0.98	--	0.97	0.97	0.14	--	0.16	0.12
L	0.99	--	0.95	0.94	0.29	--	0.45	0.43
M	0.94	--	--	0.94	0.10	--	--	0.14
N	0.93	--	0.85	--	0.51	--	0.53	--
P	0.96	--	0.95	0.95	0.08	--	0.09	0.09

* -10 C to 175 C

which most closely simulated the types of corrosion and other changes that were observed in full-size collectors. In this test, coupon specimens were removed from a chamber at -10°C and allowed to equilibrate at room temperature prior to being placed in an oven at 177°C. During this equilibration process, moisture condensed on the test specimen surfaces; this most likely led to the corrosion observed. The accelerated outdoor test, in which test specimens were exposed to concentrated solar radiation and stagnation temperatures, appeared to provide results compariable to the "real time" coupon specimen exposure; but it was not obvious that the concentrated solar radiation accelerated the photolytic degradation of absorber materials. Laboratory testing at stagnation temperatures brought out a number of thermal stability problems; however, these problems and a number of additional ones were also brought out by the thermal cycling test. The temperature and humidity testing caused corrosion problems different from those observed in "real time" exposure and is believed to be unduly severe. Exposure to temperature and xenon arc radiation made evident some appearance changes not observed with other tests. The importance of this test will be determined to a large extent by the spectral transmittance of the collector glazing used in conjunction with the absorber.

3.3 ADDITIONAL COLLECTOR-LEVEL OBSERVATIONS

During the outdoor exposure of the full-size collectors, visual observations were made to identify potential problems. Condensed moisture on the inner surfaces of glazing materials was a common occurrence, especially after periods of rainfall. In several cases, there were obvious openings in the collector cases. The corners of the cases of several of the collectors used in the test program were found to be unsealed on disassembly following outdoor exposure and testing. In addition, several of the glazing gasket designs used would allow ponding of water between the glazing and the gasket on the lower part of the collector during a rainstorm. It is unlikely that the water condensation observed is due only to normal collector breathing and cooling down at night in view of differences observed in the corrosion of duplicate collectors exposed outdoors at the same exposure sites. All of the exposed collectors had visible evidence of the buildup of outgassing products on their glazings; however, these products did not appear to substantially affect the collector thermal performance as will be discussed in section 4. As discussed in section 3.2.2, all of the paints used as absorptive coatings gave off condensible outgassing products when exposed in the absorber test box as coupon specimens. Another probable source of outgassing is the insulation used in several of the collectors as will be discussed later in this section. Outgassing was especially obvious in collector H where the buildup of condensible material on the inner glazing resulted in a change in transmittance from an original value of 0.96 to as low as 0.79. The amount of change measured varied from collector to collector and depended on the location within the collector from which the sample was taken. The fluorinated (ethylene propylene) copolymer film used as an inner glazing in collector H and as a heat trap in collector C tended to sag and touch the absorber plates when the collectors were heated by the sun. Support wires were used in collector G to prevent this from happening. The film did not appear to be affected by a few years of contact with the absorbers of the Type C collectors, which reached temperatures as high as 160°C under stagnation conditions. Absorber plate buckling was also observed in several collector types; however, it did not appear to be serious enough to cause failure. There was also evidence of cracking in the rubber grommets used to seal the absorber plate inlet and outlet tubes.

Disassembly of the solar collectors following the completion of outdoor stagnation exposure for 480 days revealed a number of problems. The paper facing material used on mineral wool insulation in collector A charred badly on the side in contact with the absorber plate. There was a considerable amount of browning and shrinkage of the foam insulation used in collector C, despite the fact that there was a 2.5 cm layer of glass fiber insulation between the absorber plate and the foam material. The binder in the top layer of glass fiber insulation turned from yellow to tan. The binder in the glass fiber insulation used in collector B turned from yellow to brown in the layer closest to the absorber plate. The binder was completely burned out of the glass fiber insulation used in collector D to a depth of about 2.5 cm on the side closest to the absorber plate. Absorber plate stagnation temperatures of 220°C were measured for this collector on clear days. The foil-faced foam insulation board used in collectors E, G, and H, and in collector F with a top layer of glass fiber insulation 2.5 cm thick showed little evidence of change.

4. RESULTS AND DISCUSSION: COLLECTOR THERMAL PERFORMANCE AND EXPOSURE STUDIES

The sections which follow: 1) summarize previously published research findings resulting from this test program, 2) present the collector thermal efficiency test results obtained during the test program and analyze possible sources of the scatter observed in these measurements, and 3) analyze the sensitivity of collector thermal efficiency and absorber plate stagnation temperature measurements to changes in collector materials performance.

4.1 SUMMARY OF PREVIOUSLY REPORTED RESEARCH FINDINGS OF THIS PROGRAM

The research findings summarized in the following sections are discussed in detail in the publications referenced.

4.1.1 Collector Thermal Performance Test Data Uncertainty

Statistical analyses of the thermal performance data sets obtained on eight liquid-heating, flat-plate solar collectors at four test sites broadly dispersed in the U.S. have confirmed that the total experimental uncertainty is about the same as the probable estimate of random error predicted for the use of ASHRAE Standard 93-77 [24, 25]. Measurement error is believed to be the major contributor to the "within" test site variability (repeatibility), and environmental effects a significant additional factor influencing the slope (loss coefficient) data obtained "between" test sites (reproducibility). No evidence of product variability was discerned for the various collector types.

On the basis of first-order curve fits of the data points, an average "within" test site coefficient of variation, percent $\overline{cv}_r$, of 2.1 percent and "between" test site coefficient of variation, percent cv_R, of 2.4 percent was calculated for the intercept $[F_R(\tau\alpha)_e]$.

Similar data for the overall heat loss coefficient, F_RU_L, indicated a "within" (percent $\overline{cv}_r$) coefficient of variation value of 5.93 percent and a "between" (percent cv_R) of 8.37 percent. A coefficient of variation (percent cv_R) for incident angle modifier (IAM) data of 34 percent was found based upon measurements at three test sites.

The data uncertainties, when used in appropriate analytical models, resulted in the following application uncertainties:

- Material degradation equivalent to about a 0.10 change in cover transmittance or absorber solar absorptance and emittance
- Variations in collector all-day thermal output of from ± 17 to ± 68 percent for specific winter operating conditions resulting in significant ranking changes
- Variations in residential annual heating and domestic hot water solar fraction of ± 6 to 7 percent.

4.1.2 Analysis of Measurement and Calculation Procedures for Incident Angle Modifiers for Flat-Plate Solar Collectors

The test procedure used to determine incident angle modifiers (IAM) for flat-plate collectors was shown to give an IAM curve with a large uncertainty [26, 27]. The problem results from measuring collector efficiency at non-normal incident angles where the measurement uncertainty is of the same order as the efficiency reduction attributable to these off-normal angles. The effects of side and end shading of the absorber are of the same order of importance as the effects of non-normal angles on the optical properties of the cover assembly. Consequently, even flat-plate collectors can have a significant bidirectional angular response.

Comparing the advantages and limitations of analytical versus experimental procedures for determining incident angle modifiers for flat plate collectors of simple geometry, analytical methods are considered to be as adequate as current experimental procedures and considerably less expensive. A simplified analytical procedure for calculating the IAM for these type collectors is described. Further consideration is needed, however, for collectors with additional directional characteristics, such as convex covers, honeycomb grid convection suppressors, and nontracking radiation concentration features.

4.1.3 Evaluation of Absorber Stagnation Temperature as an Indicator of Changes in Solar Collector Materials Performance

Results obtained from nearly steady-state measurements (actually, time-average results for a relatively short duration) showed that the technique based on measuring the absorber stagnation temperature rise above ambient resulting from a given solar irradiance is at least as, and possibly more, sensitive than thermal efficiency measurements for detecting small changes in material properties with a much simpler test apparatus and experimental procedure [30, 31]. While the measured results using the new method appear reliable and less expensive to obtain, problems were identified which can be attributed to the strong effects on measured absorber temperature of transients resulting from changes in solar irradiance and environmental conditions. Short term transients in the solar irradiance profile, such as would be caused by intermittent cloud cover, and in other environmental parameters can reduce the reproducibility of the data significantly. A solar irradiance simulator could solve the problems arising from such transients and nonrepeating environmental conditions. A limitation associated with simulators, however, is the possible sensitivity of material properties to the spectral distribution of the irradiance simulator.

A subsequent investigation [32] showed that an all-day integration method is a viable approach for outdoor experimental determination of degradation in the thermal performance of solar collector materials. This method is at least as accurate as the energy output method, provided that appropriate limits are placed on variations in environmental conditions (primarily wind), and much simpler to perform experimentally. The all-day integration technique resolves problems associated with the method based on steady-state temperatures such as short-term transients in solar irradiance and wind speed, which are serious limitations. The graphical presentation of data resolves the difficulties of comparing results obtained on days with different levels in solar irradiation.

4.1.4 Comparison of Solar Simulator and Outdoor ASHRAE Standard 93 Thermal Performance Tests

Standard test methods for determination of solar collector thermal performance permit the use of solar simulators. An evaluation of available outdoor and solar simulator data [28] showed that the thermal efficiency of flat-plate solar collectors can be substantially higher when measured in a solar simulator. The data and analytical studies indicated that heated optics and a relatively large view factor can cause excessive infrared radiation exchange with the collector cover and result in higher efficiencies for some collectors. Modifications to the simulator to change the spectral distribution, incident angle and direct/diffuse ratio are possible but careful monitoring of the uniformity, spectral distributions, and effective environmental radiance temperature is necessary to maintain consistent test conditions.

A more extensive experimental and analytical evaluation of solar simulator characteristics was recommended to determine the minimum requirements of adequate simulation and to provide a better understanding of the effect of individual environmental parameters experienced in outdoor testing.

4.2 OUTDOOR SLOPE AND INTERCEPT DATA

In this section, collector thermal performance results are presented and compared. The bases of comparison are the intercept and (negative) slope of the linearized curves which correlate measured efficiency values.

The most commonly used method of characterizing collector performance is in terms of the thermal efficiency curve. The useful energy gain may be determined from a Hottel-Whillier-Bliss analysis for collectors of the type used in the present study. Based on this theory, the thermal efficiency may be expressed as

$$\eta = F_R(\tau\alpha) - F_R U_L \, [t_i - t_a]/G \qquad (4.2.1)$$

If the parameters $F_R(\tau\alpha)$ and $F_R U_L$ are assumed constant, the efficiency is a linear function of the parameter $[t_i - t_a]/G$ where $F_R(\tau\alpha)$ is the intercept and $-F_R U_L$ is the slope of the efficiency curve.

The assumptions of constant $F_R(\tau\alpha)$ and $F_R U_L$ are reasonable for correlating efficiency test results. The transmittance-absorptance product, $(\tau\alpha)$, is a measure of collector optical characteristics and is relatively insensitive to the test environment. The overall loss coefficient U_L depends more strongly on environmental factors such as wind speed, ambient and sky temperature, and mean absorber plate temperature. The heat removal factor F_R is a weak function of U_L and, consequently, depends somewhat on collector temperature. Previous investigations [26, 39, 40] have shown, however, that any errors inherent in assuming constant $F_R(\tau\alpha)$ and constant $F_R U_L$ are generally overshadowed by experimental error and variations caused by different test environments. In a later section the suitability of linearized efficiency curves for comparing results is further validated.

The values reported for the intercept and slope of the efficiency curves for all tests conducted in the program are presented in table 4.2.1. The collector type, test site, and test series, respectively, are designated by the codes in the first column. The other eight column pairs from left to right show the performance parameters for the initial (0- or 3-day) through final tests. This tabulation of measured results is the data base used for all investigations of possible thermal degradation in the collectors. In order to investigate possible trends more clearly, the values of the parameters $F_R(\tau\alpha)$ and $F_R U_L$ are presented in bar graph type plots for each retest. These results are shown in figures 4.2.1 through 4.2.24. The parameters are normalized with initial (0-day) test values for test series 1, 3, and 4. For the series 2 tests, the results are normalized with initial values which were obtained after 3 days of exposure.

Several observations follow from an examination of the slope and intercept data. Few, if any, general conclusive statements can be made with regard to long-term degradation trends. The figures show an apparent random scatter in results of about the same order of magnitude as any general change in performance. While the plots of $F_R U_L$ vs exposure exhibit far more scatter than the corresponding plots for $F_R(\tau\alpha)$, even the latter show significant and inconsistent variations within and between test sites, collectors, and retests.

A greater scatter in the $F_R U_L$ plots is expected because this parameter is affected more strongly by environmental and test conditions than is $F_R(\tau\alpha)$. Additionally, visual inspection reports from the participating laboratories suggest that the insulation in some collectors might experience a curing process which would affect $F_R U_L$. On the other hand, visual inspections suggested some insulations were degraded by the presence of moisture within the collector. The effect of wind speed on the loss coefficient is strong. Small differences between laboratories in measurement location and wind conditions preceding the actual test can affect measured efficiency results.

The parameter $F_R(\tau\alpha)$ does not exhibit as strong an environmental dependence as $F_R U_L$ and should be a more repeatable measure of collector thermal performance. As a result, more emphasis is placed on investigating the changes in $F_R(\tau\alpha)$ with exposure as a characteristic index of performance. In a later section, the effect of variations in environmental conditions on both slope and intercept are investigated.

Considering series 1 and 2 results, only collectors F, G, and H show a distinct systematic decrease in the intercept parameter. These collectors all have plastic or glass fiber reinforced plastic (FRP) covers. Collector B, in fact, shows a general improvement in the intercept parameter with exposure. This collector with glass covers and a flat-black absorber is evidently quite stable. As expected, there are no general trends in the slope parameter $F_R U_L$ which is more sensitive to changes in environmental conditions.

An examination of figures 4.2.1 through 4.2.24 shows one other apparent trend in the intercept parameters. This parameter tends to peak between 30 and 60 exposure days and thereafter decrease

Table 4.2.1 Summary of all Reported $F_R(\tau\alpha)$ and F_RU_L Values

COLLECTOR	RETEST DAYS															
	0		3		15		30		60		120		240		480	
	FRTA	FRUL	FRTA	FRUL	FRTA	FRUL	FRTA	FRUL	FRTA	FRUL	FRTA	FRUL	FRTA	FRUL	FRTA	FRUL
A-1-1	0.602	4.562	0.593	4.308	N/A	N/A	0.599	4.023	0.606	3.978	0.590	4.060	0.591	4.381	0.583	4.366
A-1-2	N/A	N/A	0.596	4.440	N/A	N/A	0.605	4.092	0.628	4.318	0.613	3.960	0.596	4.505	0.600	4.440
A-1-3	0.622	4.549	N/A	N/A	0.623	3.910	0.636	4.244	0.623	4.987	0.598	3.766	0.596	4.585	N/A	N/A
A-1-4	0.601	4.429	N/A	N/A	0.610	4.148	0.603	4.307	0.591	5.107	N/A	N/A	N/A	N/A	N/A	N/A
A-2-1	0.609	5.250	0.609	4.850	0.610	4.610	0.623	4.280	0.602	4.550	0.607	4.870	0.617	4.392	0.623*	4.679
A-2-2	N/A	N/A	0.605	4.980	0.610	5.100	0.628	4.110	0.626	5.630	0.607	5.190	0.588	4.184	0.600*	4.394
A-2-3	0.612	4.490	N/A	N/A	0.637	5.120	0.622	4.560	0.610	5.150	0.610	5.020	0.604	4.305	N/A	N/A
A-2-4	0.581	4.427	N/A	N/A	0.629	4.967	0.617	4.893	0.608	5.113	N/A	N/A	N/A	N/A	N/A	N/A
A-3-1	0.627	3.910	0.633	3.810	0.605	3.600	0.628	4.310	0.629	4.120	0.641	3.980	0.641	4.360	0.646	3.901
A-3-2	N/A	N/A	0.612	3.660	0.636	4.450	0.612	4.390	0.614	4.250	0.629	4.030	0.626	4.420	0.607	3.544
A-4-1	0.611	4.349	0.660	5.167	0.614	4.389	0.601	4.583	0.598	3.805	N/A	N/A	0.617	4.024	0.643	3.974
A-4-2	N/A	N/A	0.655	5.445	0.595	4.571	0.604	4.702	0.598	4.350	N/A	N/A	0.607	4.430	0.654	4.505
B-1-1	0.654	5.460	0.654	5.437	N/A	N/A	0.649	5.001	0.670	5.078	0.670	5.490	0.630	5.022	0.659	5.479
B-1-2	N/A	N/A	0.640	5.428	N/A	N/A	0.661	5.306	0.668	5.074	0.669	5.170	0.656	5.594	0.651	5.440
B-1-3	0.652	5.476	N/A	N/A	0.652	5.350	0.688	5.420	0.656	5.624	0.647	5.173	0.648	5.610	N/A	N/A
B-1-4	0.666	5.459	N/A	N/A	0.669	5.536	0.681	5.539	0.636	5.038	N/A	N/A	N/A	N/A	N/A	N/A
B-2-1	0.654	5.380	0.640	5.384	0.665	6.105	0.648	5.648	0.673	5.705	0.666	5.780	0.668	5.254	0.683*	5.472
B-2-2	N/A	N/A	0.646	5.696	0.659	6.209	0.651	5.693	0.669	5.636	0.669	5.770	0.688	5.891	0.685*	5.349
B-2-3	0.648	5.588	N/A	N/A	0.666	5.852	0.668	6.011	0.662	5.364	0.668	5.320	0.671	5.608	N/A	N/A
B-2-4	0.648	5.730	N/A	N/A	0.651	5.737	0.655	5.869	0.653	5.824	N/A	N/A	N/A	N/A	N/A	N/A
B-3-1	0.652	5.433	0.653	5.390	0.683	5.460	0.656	5.174	0.663	5.417	0.674	4.990	0.686	5.540	0.689	5.200
B-3-2	N/A	N/A	0.636	5.180	0.654	5.150	0.653	5.159	0.668	5.520	0.675	5.060	0.694	5.750	0.690	5.349
B-4-1	0.672	5.212	0.696	5.865	0.709	5.746	0.719	5.723	0.662	4.616	0.651	4.719	0.688*	5.440	0.673	5.007
B-4-2	N/A	N/A	0.680	6.200	N/A	N/A	0.687	5.383	0.654	4.452	0.647	4.753	0.705*	5.881	0.665	4.984
C-1-1	0.545	4.377	0.528	4.076	N/A	N/A	0.528	3.889	0.534	3.627	0.531	4.059	0.511	3.834	0.492	3.838
C-1-2	N/A	N/A	0.520	3.969	N/A	N/A	0.538	3.915	0.529	3.717	0.527	4.172	0.512	3.591	0.493	3.929
C-1-3	0.538	3.908	N/A	N/A	0.524	4.105	0.522	3.566	0.530	4.283	0.524	3.714	0.510	4.457	N/A	N/A
C-1-4	0.540	4.465	N/A	N/A	0.496	3.765	0.485	3.345	0.465	3.828	N/A	N/A	N/A	N/A	N/A	N/A
C-2-1	0.524	4.531	0.522	4.324	0.541	4.578	0.542	4.488	0.539	4.098	0.541	4.294	0.537	3.942	0.529*	3.813
C-2-2	N/A	N/A	0.511	4.268	0.524	4.513	0.525	3.929	0.517	3.968	0.512	4.173	0.498	3.840	0.501*	3.983
C-2-3	0.557	4.739	N/A	N/A	0.552	4.105	0.549	4.586	0.546	4.456	0.552	4.131	0.557	4.420	N/A	N/A
C-2-4	0.541	4.802	N/A	N/A	0.540	4.604	0.540	4.549	0.521	4.022	N/A	N/A	N/A	N/A	N/A	N/A
C-3-1	0.549	4.228	0.530	3.919	0.540	3.889	0.531	3.867	0.528	3.799	0.541	3.747	0.536	3.776	0.556	3.907
C-3-2	N/A	N/A	0.517	4.044	0.531	3.782	0.530	4.026	0.523	3.725	0.543	3.600	0.538	3.839	N/A	N/A
C-4-1	0.552	4.151	0.573	4.849	0.540	3.975	0.546	4.713	0.532	3.833	0.524	3.311	0.507*	3.832	0.483	2.880
C-4-2	N/A	N/A	0.549	4.060	0.552	3.992	0.532	4.537	0.525	4.491	0.548	3.958	0.518*	3.811	0.540	3.389
D-1-1	0.648	3.468	0.629	3.152	N/A	N/A	0.632	2.654	0.642	2.648	0.644	3.180	0.620	2.969	0.617	3.060
D-1-2	N/A	N/A	0.633	3.179	N/A	N/A	0.639	3.059	0.649	2.790	0.666	3.220	0.635	2.781	0.622	3.015
D-1-3	0.626	2.833	N/A	N/A	0.613	2.982	0.637	3.174	0.618	3.090	0.634	2.902	0.619	3.229	N/A	N/A
D-1-4	0.640	3.200	N/A	N/A	0.623	2.968	0.632	2.790	0.605	3.013	N/A	N/A	N/A	N/A	N/A	N/A
D-2-1	0.640	3.410	0.650	3.200	0.647	3.490	0.634	3.250	0.637	3.300	0.651	3.820	0.610	3.789	0.657*	3.498
D-2-2	N/A	N/A	0.659	3.010	0.656	3.290	0.646	3.470	0.641	3.400	0.647	3.720	0.625	3.164	0.635*	3.578
D-2-3	0.655	3.450	N/A	N/A	0.660	3.400	0.663	3.280	0.640	2.950	0.662	3.280	0.636	3.564	N/A	N/A
D-2-4	0.636	3.385	N/A	N/A	0.658	3.434	0.645	3.364	0.643	3.485	N/A	N/A	N/A	N/A	N/A	N/A
D-3-1	0.647	2.555	0.641	2.410	0.619	2.610	0.639	2.940	0.648	3.040	0.632	2.425	0.634	2.740	0.650	3.140
D-3-2	N/A	N/A	0.635	3.640	0.629	2.620	0.652	3.100	0.657	3.110	0.646	2.487	0.645	2.870	0.661	3.134
D-4-1	0.636	3.055	0.657	3.276	0.688	3.946	0.691	3.583	0.642	2.953	0.616	3.021	0.656*	3.353	0.633	2.950
D-4-2	N/A	N/A	0.670	3.384	0.678	3.390	0.664	3.100	0.645	2.646	0.625	2.396	0.647*	3.281	0.634	2.822
E-1-1	0.613	7.465	0.605	5.997	N/A	N/A	0.624	5.866	0.625	6.260	0.600	5.770	0.585	6.158	0.571	6.479
E-1-2	N/A	N/A	0.598	6.443	N/A	N/A	0.624	6.269	0.619	6.129	0.605	5.480	0.596	6.645	0.569	6.359
E-1-3	0.599	6.801	N/A	N/A	0.595	6.063	0.609	6.222	0.616	6.470	0.604	6.680	0.578	6.032	N/A	N/A
E-1-4	0.590	6.149	N/A	N/A	0.619	5.805	0.618	5.574	0.595	7.101	N/A	N/A	N/A	N/A	N/A	N/A
E-2-1	0.588	6.488	0.576	5.816	0.605	6.700	0.602	6.233	0.595	6.679	0.590	6.750	0.612	6.185	0.600*	6.546
E-2-2	N/A	N/A	0.619	6.580	0.630	7.639	0.616	6.515	0.613	6.769	0.612	6.450	0.611	6.737	0.601*	6.633
E-2-3	0.602	7.027	N/A	N/A	0.614	6.963	0.610	5.970	0.609	6.780	0.605	6.810	0.620	6.330	N/A	N/A
E-2-4	0.603	6.045	N/A	N/A	0.595	6.448	0.588	6.234	0.569	6.653	N/A	N/A	N/A	N/A	N/A	N/A
E-3-1	0.621	6.306	0.596	5.630	0.602	6.600	0.616	6.547	0.621	5.820	0.625	6.820	0.642	5.945	0.657*	6.179
E-3-2	N/A	N/A	0.595	5.584	0.598	6.560	0.626	6.696	0.617	5.830	0.633	6.880	0.637	5.871	0.651*	6.332
E-4-1	0.619	6.257	0.598	5.990	0.597	6.331	0.594	6.172	0.618	6.451	N/A	N/A	0.611	5.837	0.619	6.050
E-4-2	N/A	N/A	0.602	6.217	0.583	5.996	0.585	5.792	0.614	6.451	N/A	N/A	0.610	6.016	0.618	4.937
F-1-1	0.665	6.504	0.648	5.152	N/A	N/A	0.668	5.152	0.664	5.859	0.633	5.590	0.616	5.655	0.631	6.433
F-1-2	N/A	N/A	0.638	6.728	N/A	N/A	0.659	5.798	0.644	5.528	0.642	5.627	0.615	5.291	0.621	6.200
F-1-3	0.646	5.802	N/A	N/A	0.632	5.927	0.672	5.680	0.653	6.473	0.651	5.837	0.620	6.289	N/A	N/A
F-1-4	0.644	6.093	N/A	N/A	0.639	5.682	0.631	5.401	0.617	6.312	N/A	N/A	N/A	N/A	N/A	N/A
F-2-1	0.652	6.799	0.666	6.280	0.678	5.895	0.675	6.101	0.661	6.167	0.651	5.921	0.624	6.068	0.648*	6.270
F-2-2	N/A	N/A	0.661	6.256	0.646	6.676	0.684	6.084	0.653	6.566	0.664	6.528	0.650	6.820	0.662*	6.496
F-2-3	0.668	6.068	N/A	N/A	0.656	6.081	0.687	6.100	0.665	6.143	0.664	6.376	0.650	6.319	N/A	N/A
F-2-4	0.653	6.141	N/A	N/A	0.652	6.171	0.658	6.047	0.626	5.746	N/A	N/A	N/A	N/A	N/A	N/A
F-3-1	0.679	5.350	0.674	4.936	0.651	5.916	0.663	6.058	0.657	5.479	0.653	5.394	0.668	5.570	0.666	5.405
F-3-2	N/A	N/A	0.660	4.967	0.627	5.922	0.642	6.172	0.655	5.826	0.646	5.388	0.652	5.684	0.653	5.530
F-4-1	0.657	5.860	0.631	5.337	0.651	5.769	0.637	5.383	0.655	5.798	N/A	N/A	0.651	5.370	0.648	5.354
F-4-2	N/A	N/A	0.623	5.655	0.627	5.740	0.616	5.451	0.634	6.651	N/A	N/A	0.622	5.136	0.690	7.331
G-1-1	0.572	5.905	0.548	5.322	N/A	N/A	0.563	5.438	0.584	5.025	0.567	5.672	0.548	5.276	0.528	5.877
G-1-2	N/A	N/A	0.567	5.429	N/A	N/A	0.568	5.431	0.566	5.010	0.565	5.066	0.514	5.305	0.537	5.899
G-1-3	0.553	5.480	N/A	N/A	0.539	5.347	0.581	5.039	0.552	5.538	0.546	4.550	N/A	N/A	N/A	N/A
G-1-4	0.563	5.463	N/A	N/A	0.549	4.948	0.503	4.933	0.538	5.884	N/A	N/A	N/A	N/A	N/A	N/A
G-2-1	0.550	5.540	0.556	5.253	0.553	5.238	0.559	5.168	0.560	5.455	0.560	5.928	0.516	5.325	N/A	N/A
G-2-2	N/A	N/A	0.534	5.201	0.541	5.110	0.514	4.590	0.541	5.543	0.547	5.638	N/A	N/A	N/A	N/A
G-2-3	0.546	5.397	N/A	N/A	0.566	5.052	0.587	4.968	0.563	5.539	0.564	5.458	0.521	5.578	N/A	N/A
G-2-4	0.529	5.367	N/A	N/A	0.569	5.528	0.563	4.824	0.555	5.645	N/A	N/A	N/A	N/A	N/A	N/A
G-3-1	0.586	5.329	0.548	4.614	0.557	5.281	0.573	5.241	0.572	4.906	0.569	5.599	0.572	4.974		
G-3-2	N/A	N/A	0.549	4.550	0.559	5.604	0.576	5.587	0.570	4.997	0.572	5.723	0.582	5.139		
G-4-1	0.588	5.587	0.601	5.865	0.572	5.258	0.569	5.429	0.571	4.952	N/A	N/A	0.550	4.438	0.558	5.204
G-4-2	N/A	N/A	0.595	5.894	0.557	5.002	0.553	5.281	0.559	4.975	N/A	N/A	0.539	4.824	0.554	5.429
H-1-1	0.636	5.776	0.615	5.672	0.627	5.380	0.613	4.907	0.656	5.230	0.633	4.790	0.608	5.522	0.594	5.286
H-1-2	N/A	N/A	0.641	5.483	0.618	5.338	0.638	5.177	0.648	5.068	0.638	4.590	0.594	5.423	0.581	5.229
H-1-3	0.632	5.770	N/A	N/A	0.624	5.180	0.654	5.455	0.643	5.990	0.627	5.821	0.628	5.575	N/A	N/A
H-1-4	0.643	5.505	N/A	N/A	0.617	4.405	0.628	4.901	0.584	5.444	N/A	N/A	N/A	N/A	N/A	N/A
H-2-1	0.625	6.014	0.618	5.654	0.630	5.902	0.638	5.575	0.618	5.540	0.615	5.350	0.618	5.851	0.575*	5.096
H-2-2	N/A	N/A	0.629	5.710	0.626	5.887	0.632	5.295	0.624	5.620	0.629	5.490	0.620	5.680	0.534*	4.356
H-2-3	0.623	6.108	N/A	N/A	0.659	6.344	0.663	5.904	0.624	5.790	0.643	5.670	0.628	5.208	N/A	N/A
H-2-4	0.607	5.930	N/A	N/A	0.637	6.049	0.622	5.258	0.597	5.677	N/A	N/A	N/A	N/A	N/A	N/A
H-3-1	0.638	5.620	0.647	5.590	0.665	5.630	0.634	5.293	0.629	5.440	0.638	5.040	0.628	5.510	0.616	4.941
H-3-2	N/A	N/A	0.627	5.571	0.653	5.450	0.639	5.599	0.630	5.650	0.639	5.010	0.645	5.740	0.636	5.117
H-4-1	0.640	5.144	0.648	5.218	0.635	5.190	0.652	6.212	0.585	5.655	0.605	4.072	0.593*	4.769	0.583	4.467
H-4-2	N/A	N/A	0.653	5.320	0.658	5.116	0.643	5.678	0.628	5.809	0.633	4.464	0.603*	4.993	0.620	5.072

* INDICATES THAT RETEST WAS PERFORMED AT EXPOSURE SOMEWHAT DIFFERENT FROM THAT SHOWN.

NOTES: 1) ALL COEFFICIENTS BASED ON COLLECTOR GROSS AREA.
2) UNITS OF FRUL ARE DEGREES(C)/W/SQ M .

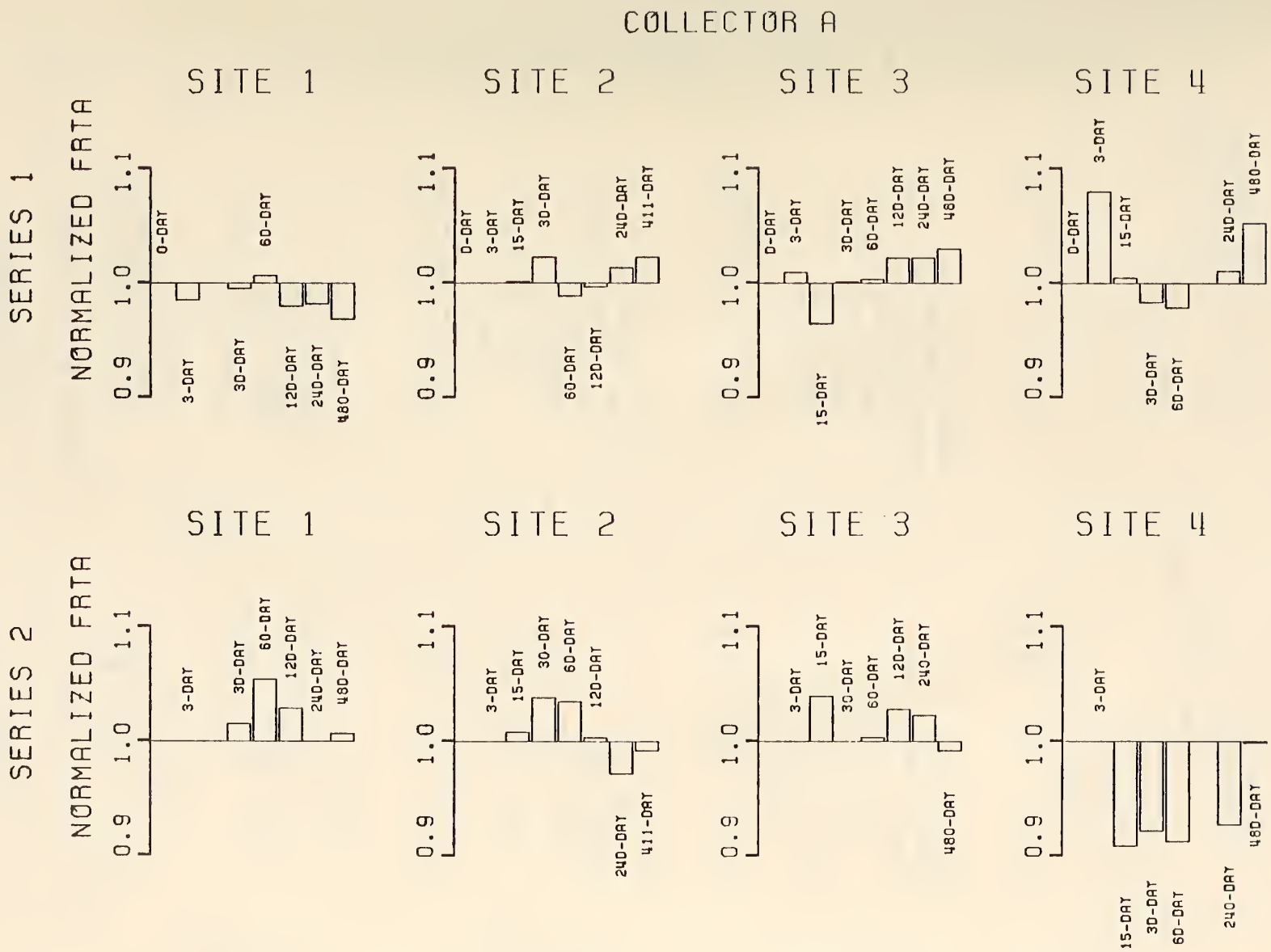

Figure 4.2.1. Collector A normalized $F_R(\tau\alpha)$ vs retests, series 1 & 2, all test sites

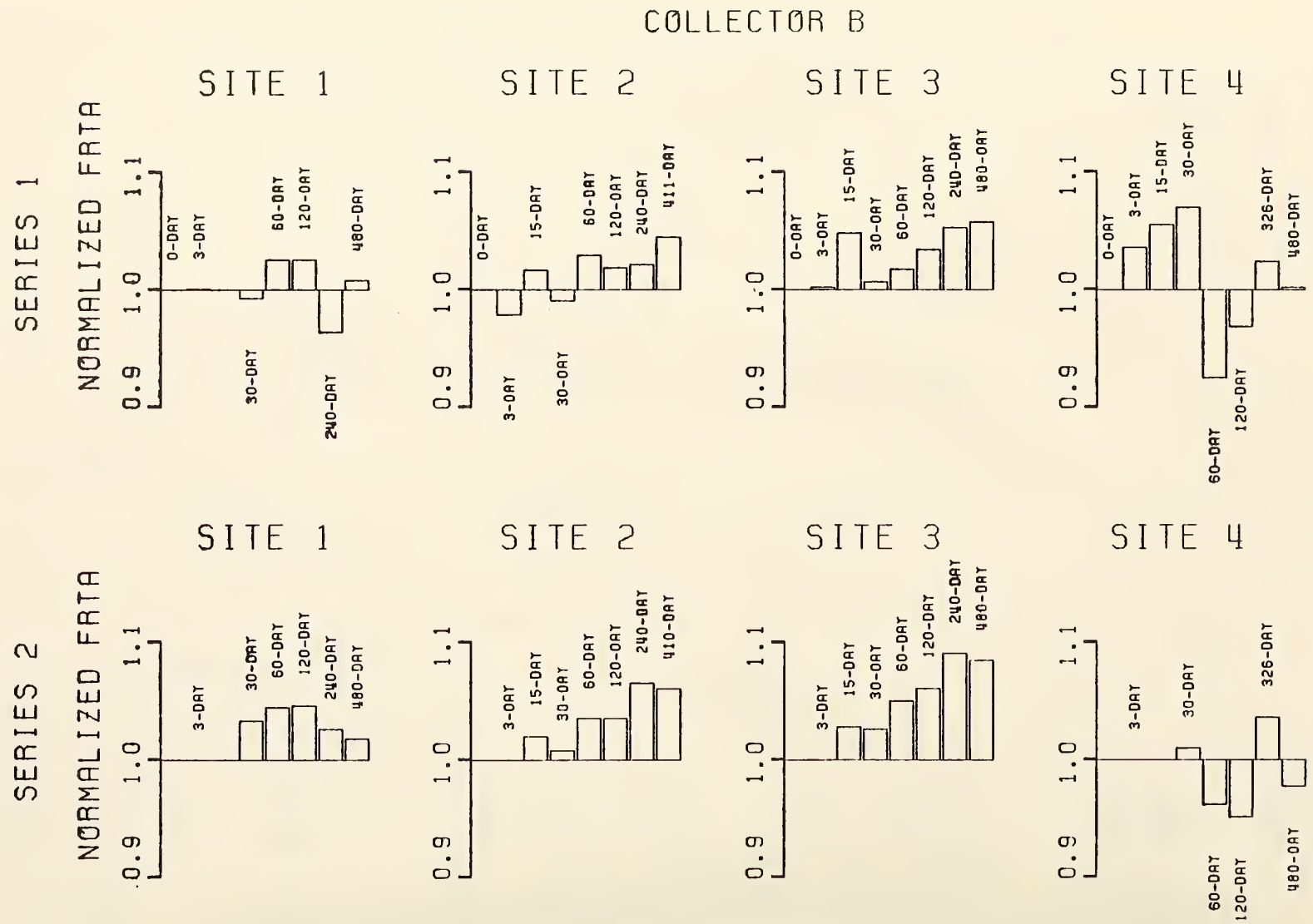

Figure 4.2.2. Collector B normalized $F_R(\tau\alpha)$ vs retests, series 1 & 2, all test sites

Figure 4.2.3. Collector C normalized $F_R(\tau\alpha)$ vs retests, series 1 & 2, all test sites

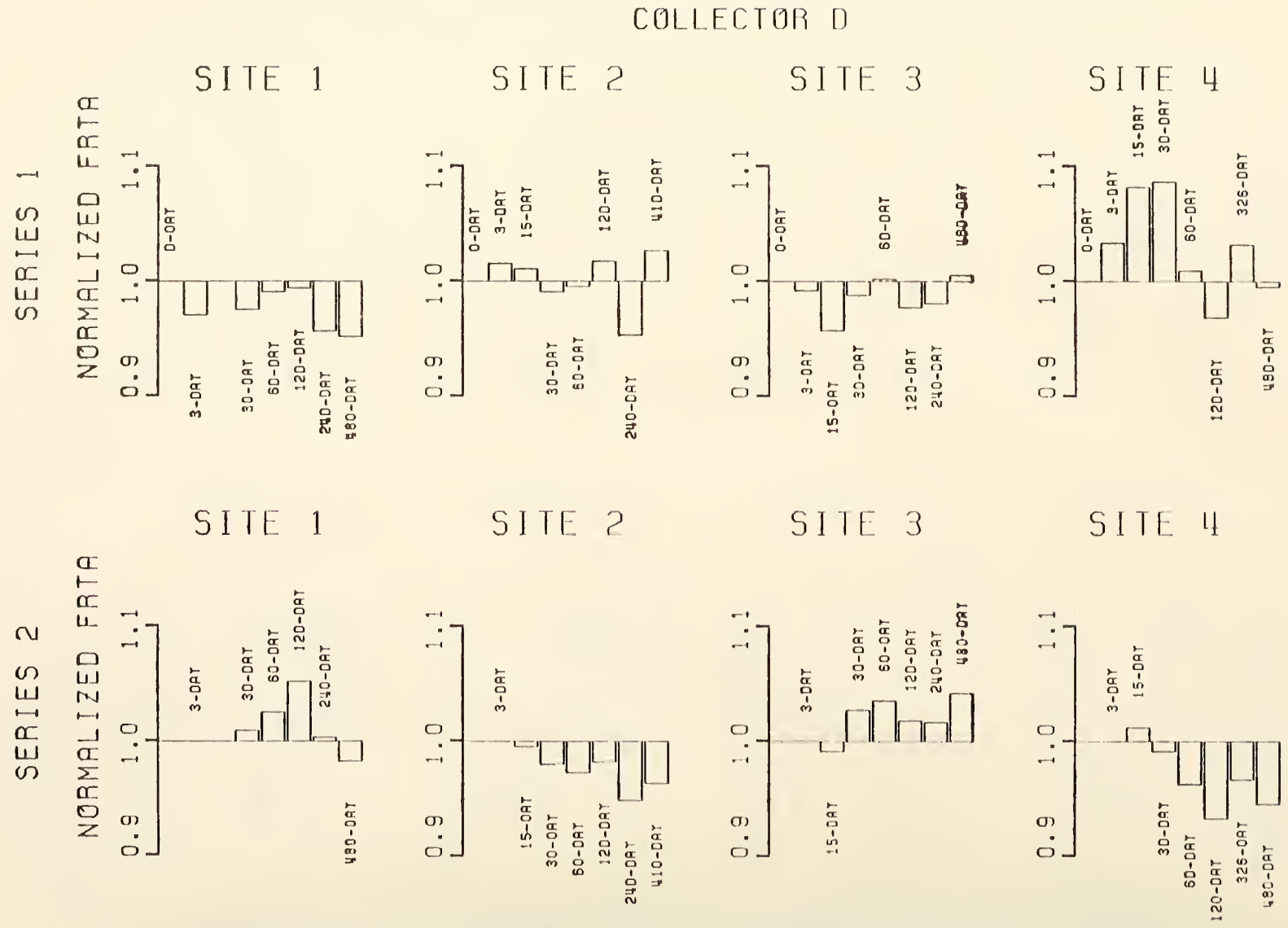

Figure 4.2.4. Collector D normalized $F_R(\tau\alpha)$ vs retests, series 1 & 2, all test sites

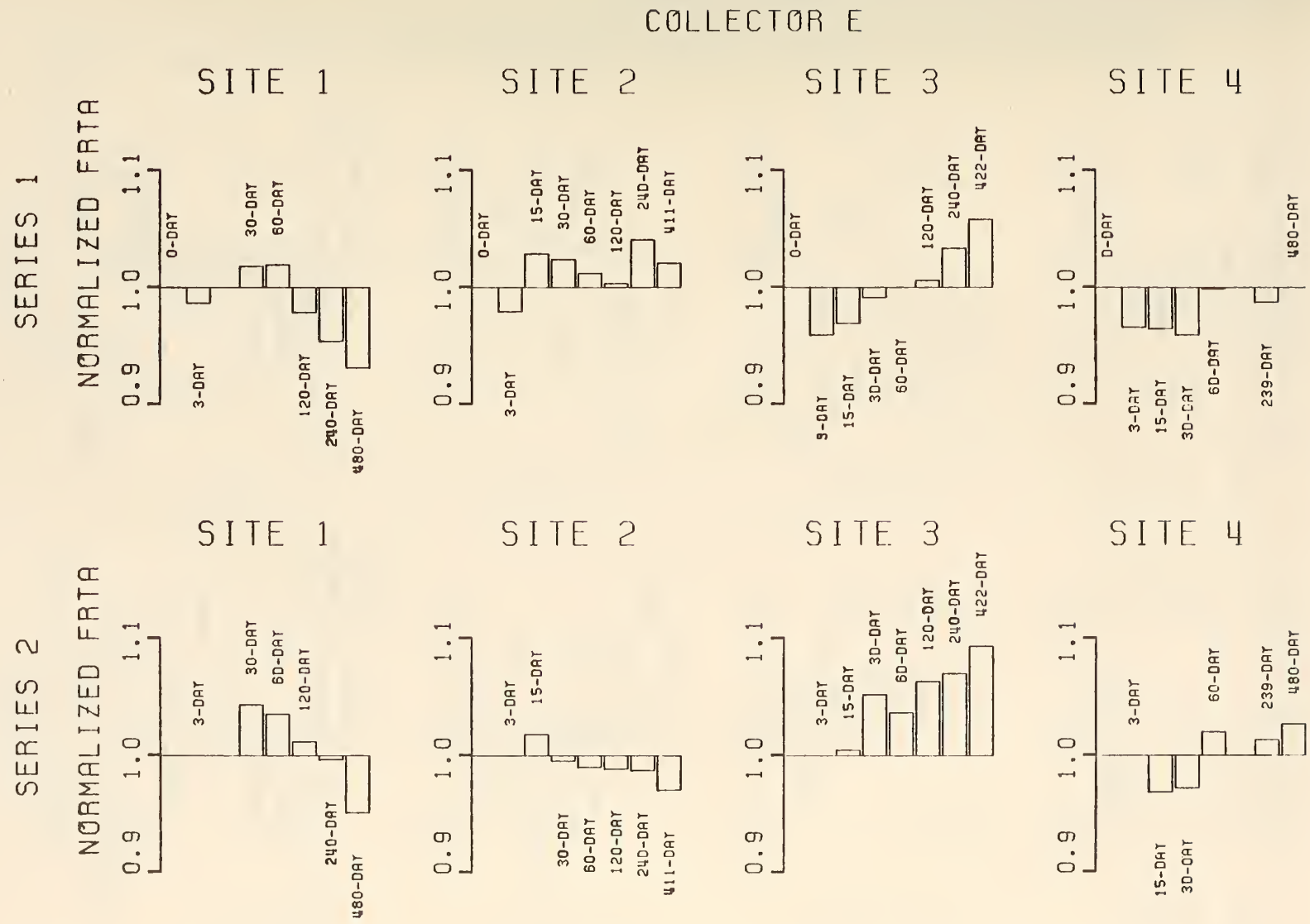

Figure 4.2.5. Collector E normalized $F_R(\tau\alpha)$ vs retests, series 1 & 2, all test sites

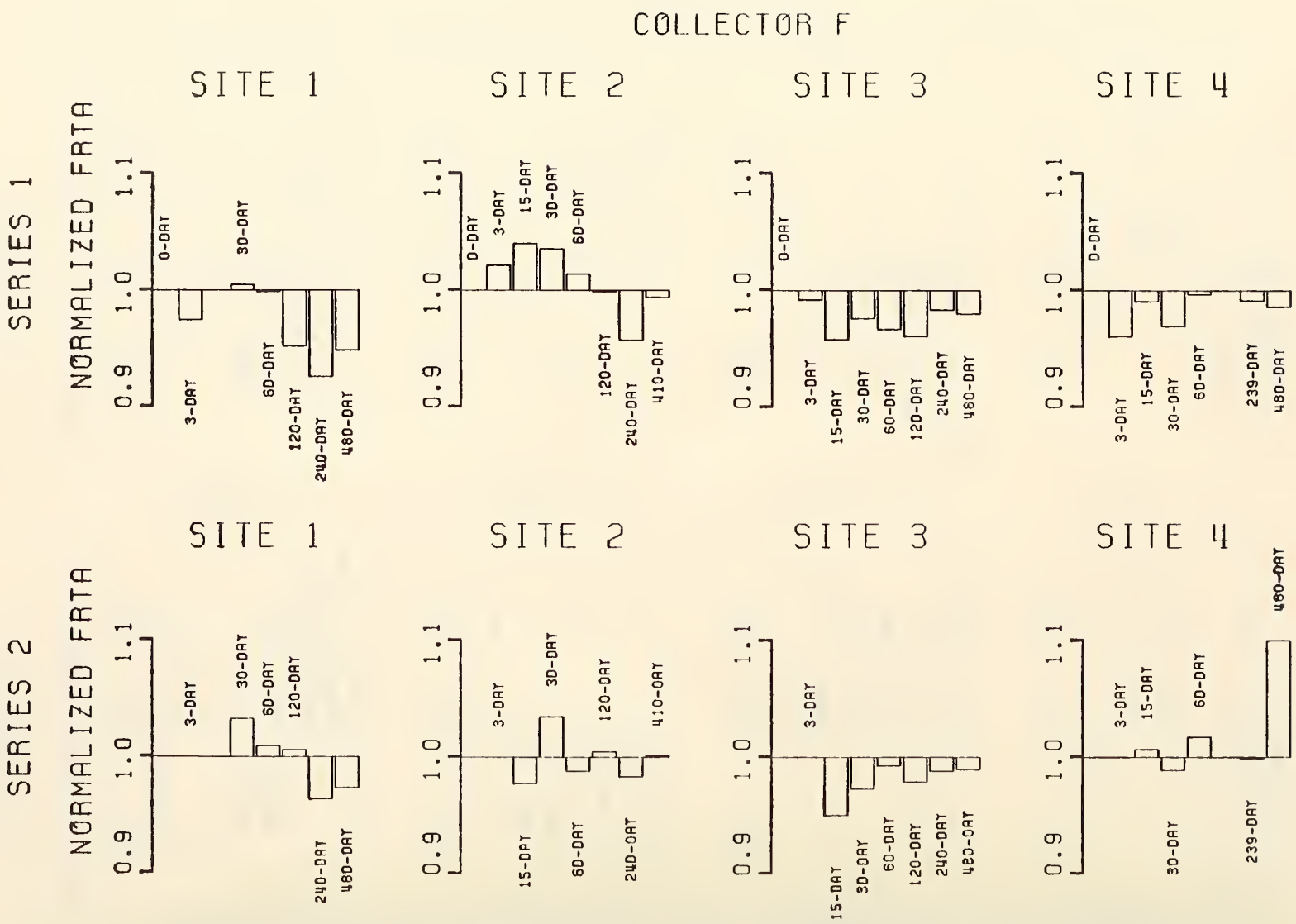

Figure 4.2.6. Collector F normalized $F_R(\tau\alpha)$ vs retests, series 1 & 2, all test sites

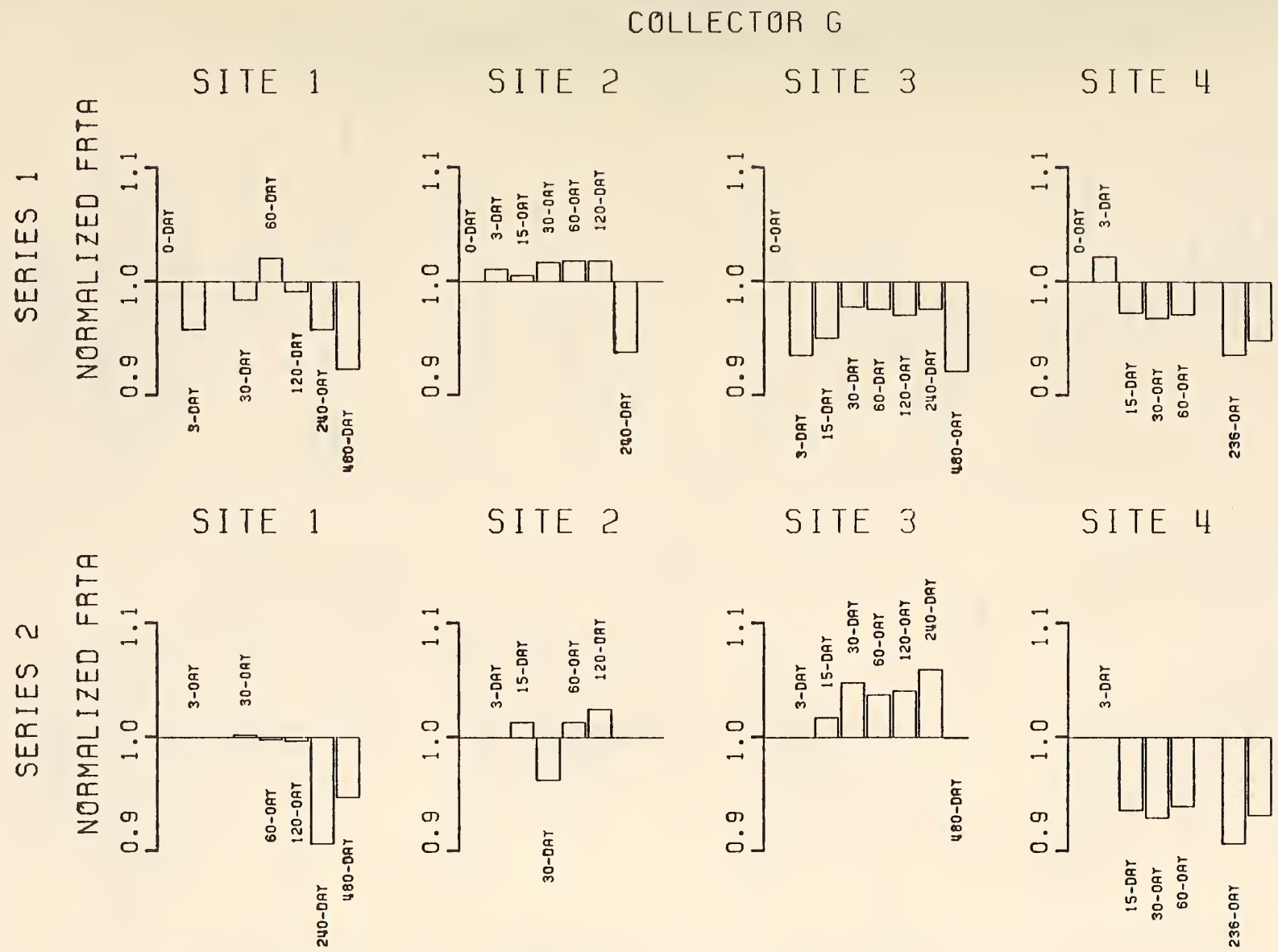

Figure 4.2.7. Collector G normalized $F_R(\tau\alpha)$ vs retests, series 1 & 2, all test sites

Figure 4.2.8. Collector H normalized $F_R(\tau\alpha)$ vs retests, series 1 & 2, all test sites

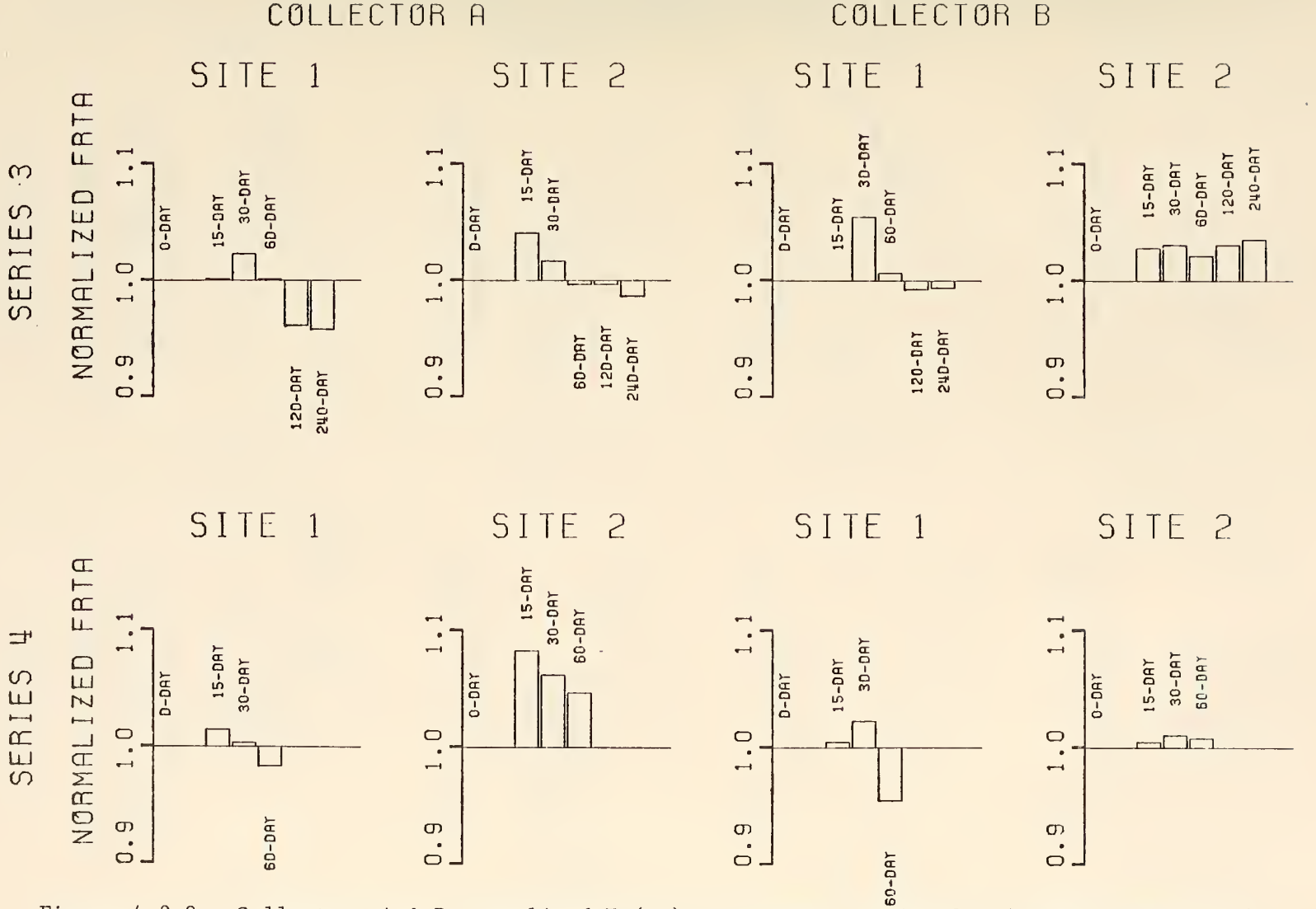

Figure 4.2.9. Collectors A & B normalized $F_R(\tau\alpha)$ vs retests, series 3 & 4, test sites 1 & 2

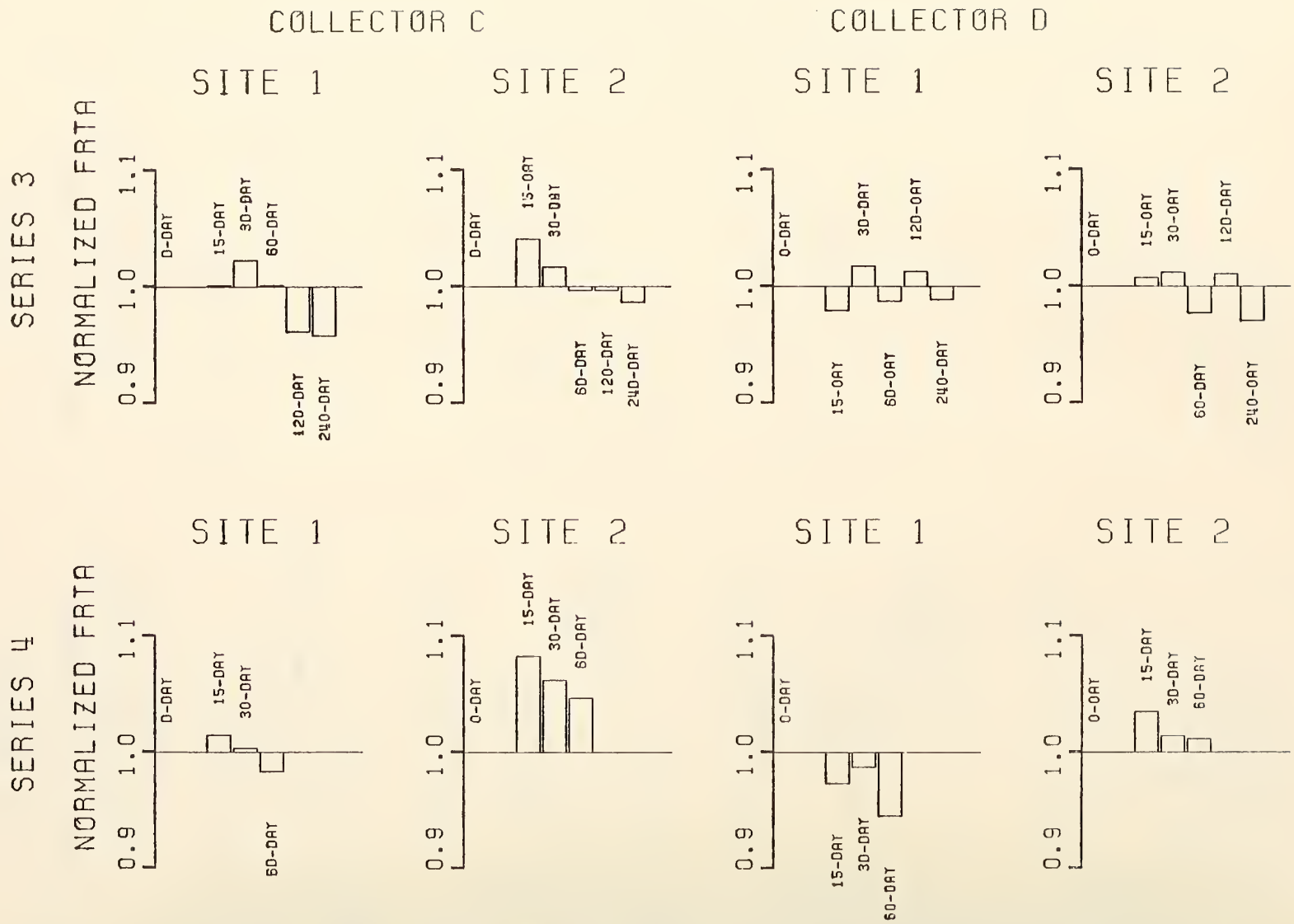

Figure 4.2.10. Collectors C & D normalized $F_R(\tau\alpha)$ vs retests, series 3 & 4, test sites 1 & 2

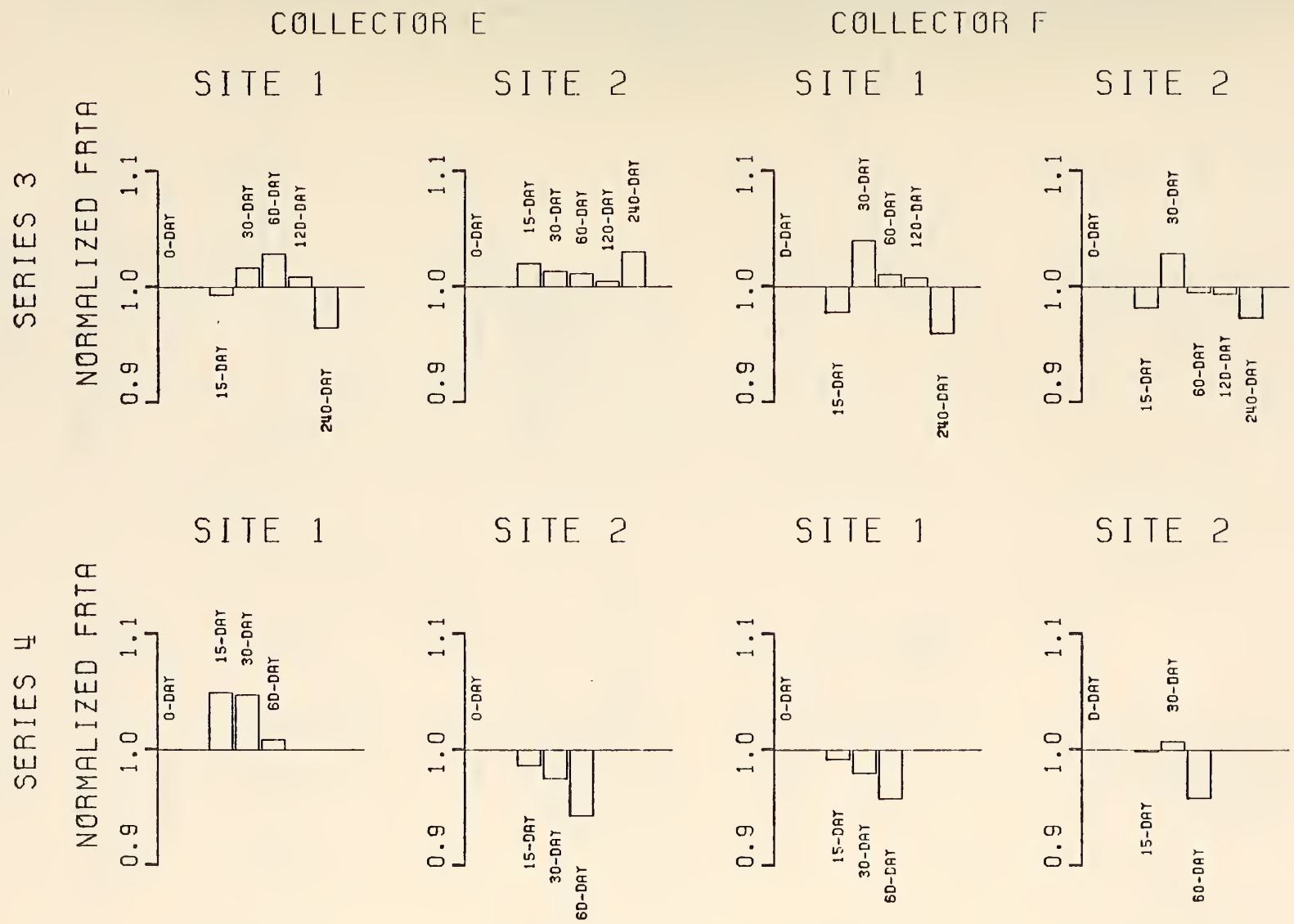

Figure 4.2.11. Collectors E & F normalized $F_R(\tau\alpha)$ vs retests, series 3 & 4, test sites 1 & 2

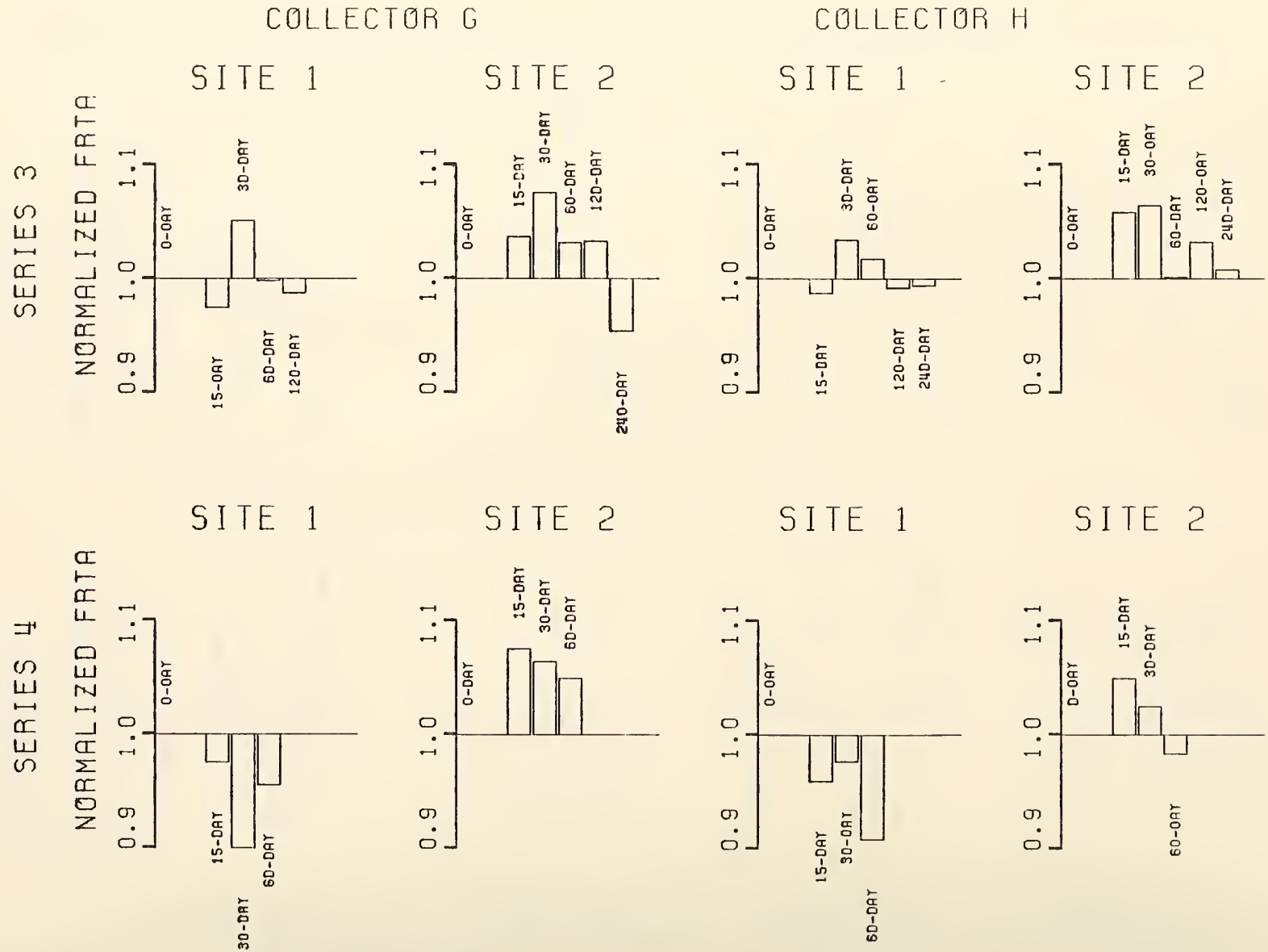

Figure 4.2.12. Collectors G & H normalized $F_R(\tau\alpha)$ vs retests, series 3 & 4, test sites 1 & 2

Figure 4.2.13. Collector A normalized $F_R U_L$ vs retests, series 1 & 2, all test sites

Figure 4.2.14. Collector B normalized $F_R^U{}_L$ vs retests, series 1 & 2, all test sites

Figure 4.2.15. Collector C normalized $F_R U_L$ vs retests, series 1 & 2, all test sites

Figure 4.2.16. Collector D normalized $F_{R}^{U}{}_{L}$ vs retests, series 1 & 2, all test sites

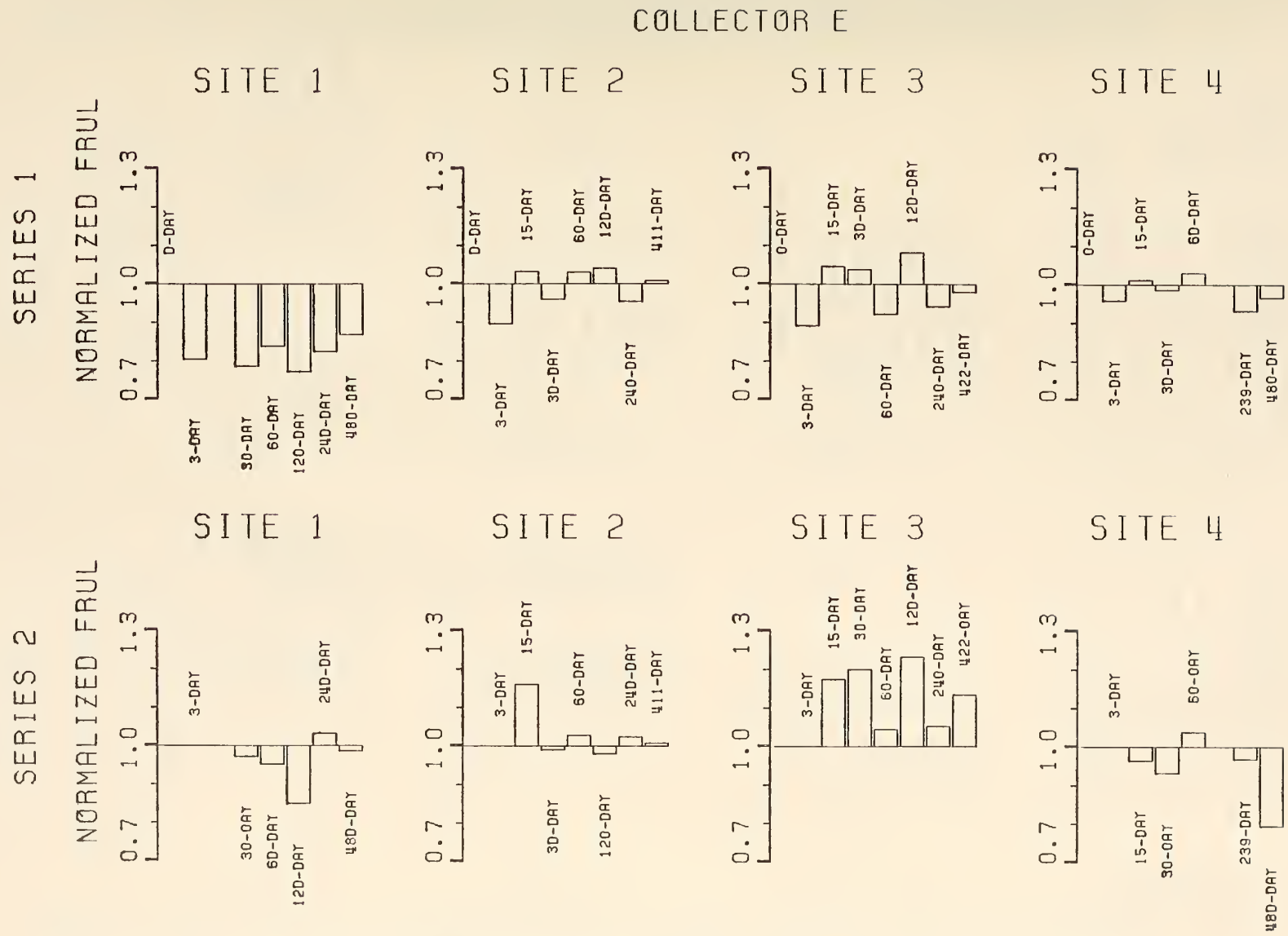

Figure 4.2.17. Collector E normalized $F_R U_L$ vs retests, series 1 & 2, all test sites

Figure 4.2.18. Collector F normalized $F_{R_L}^{U}$ vs retests, series 1 & 2, all test sites

Figure 4.2.19. Collector G normalized $F_{R}U_{L}$ vs retests, series 1 & 2, all test sites

Figure 4.2.20. Collector H normalized $F_R U_L$ vs retests, series 1 & 2, all test sites

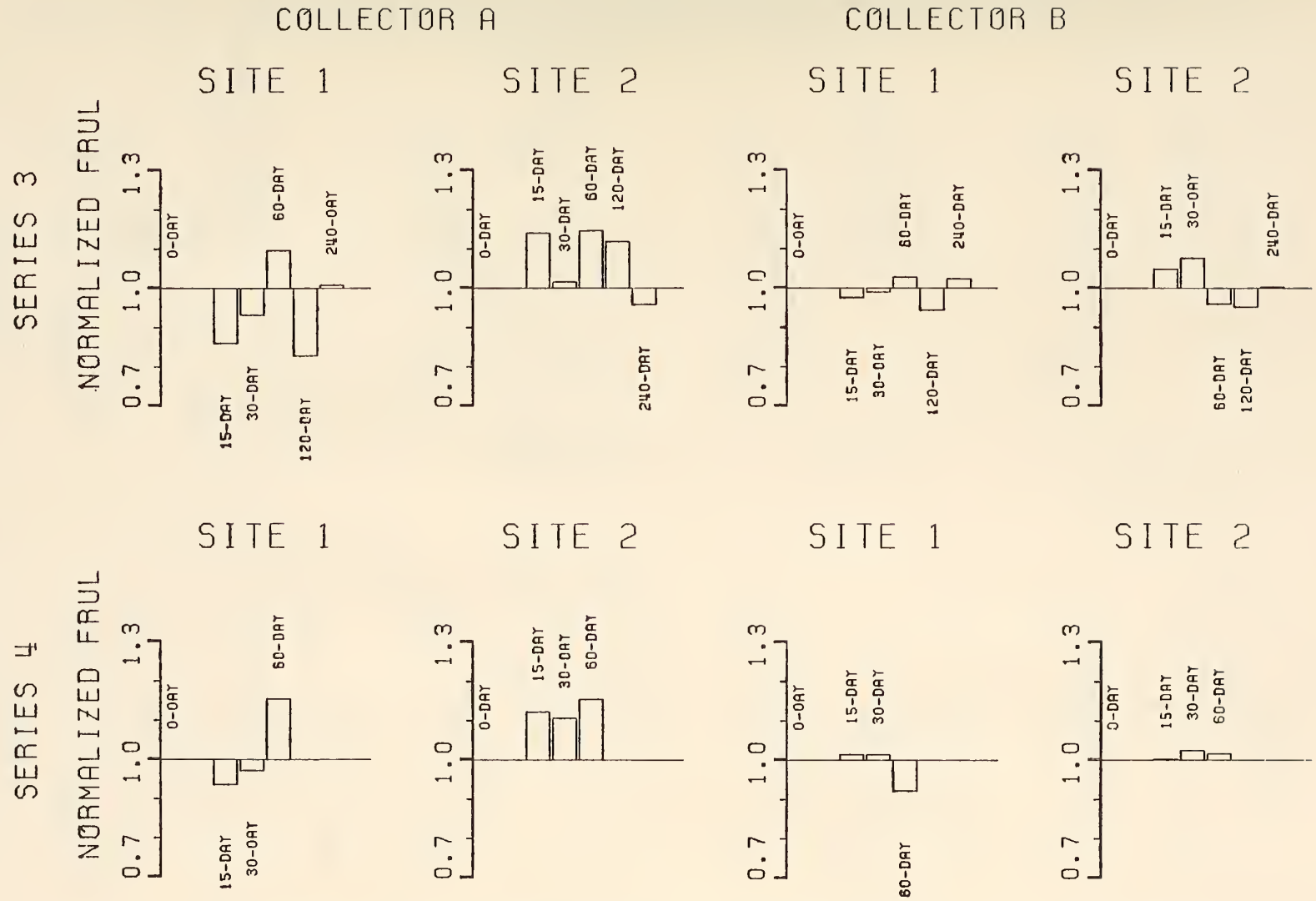

Figure 4.2.21. Collectors A & B normalized $F_R U_L$ vs retests, series 3 & 4, test sites 1 & 2

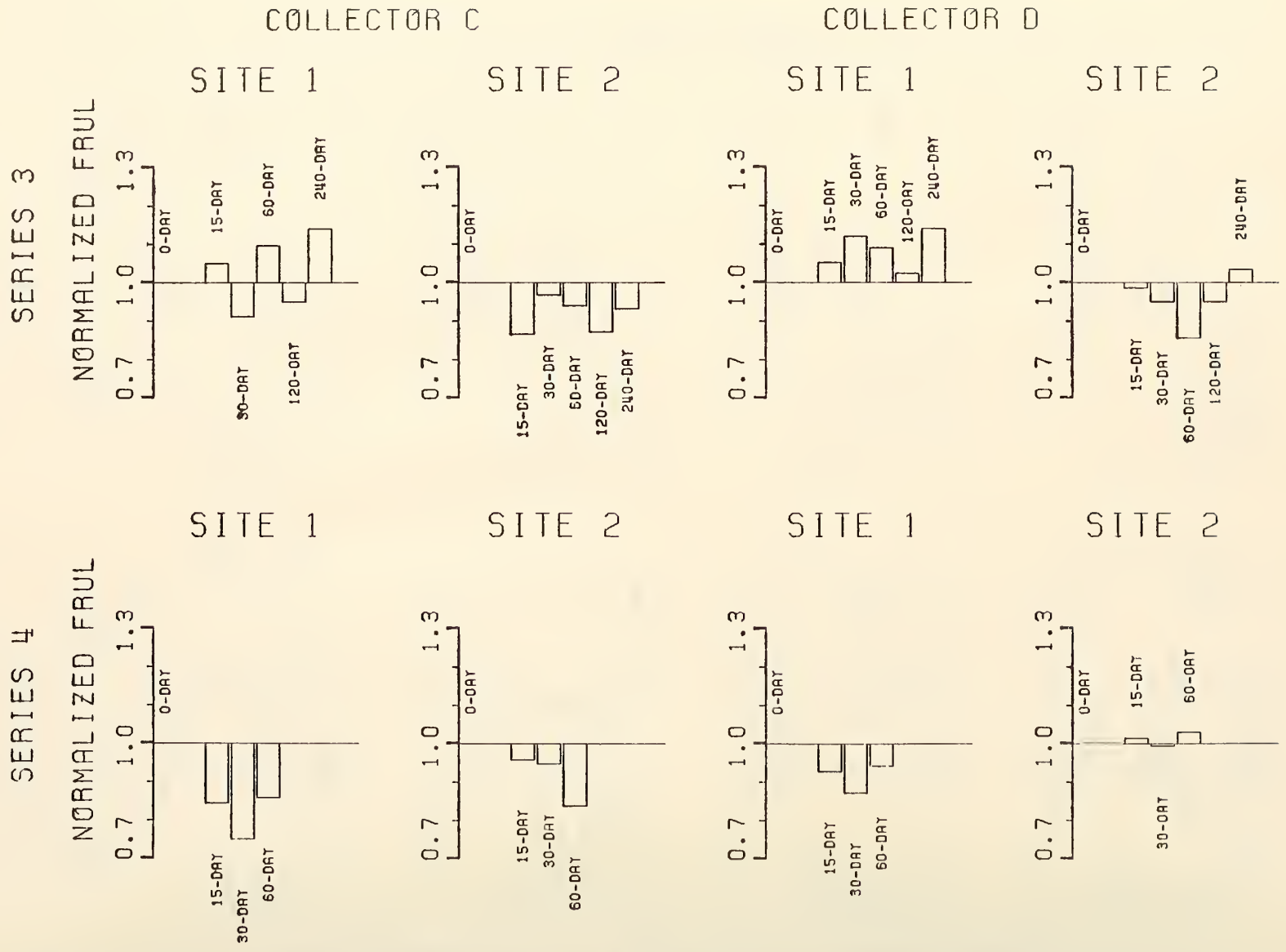

Figure 4.2.22. Collectors C & D normalized $F_R U_L$ vs retests, series 3 & 4, test sites 1 & 2

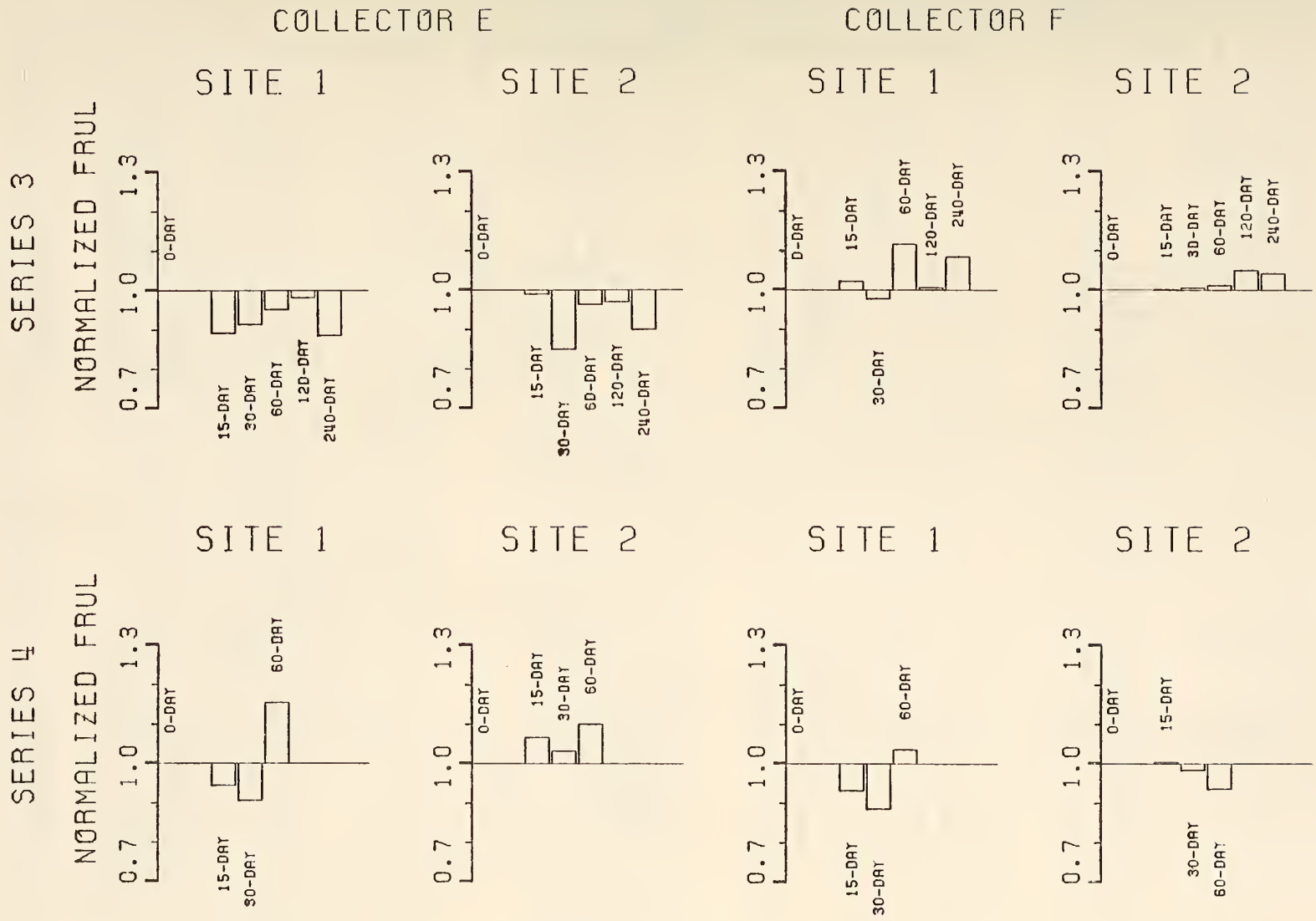

Figure 4.2.23. Collectors E & F normalized $F_R U_L$ vs retests, series 3 & 4, test sites 1 & 2

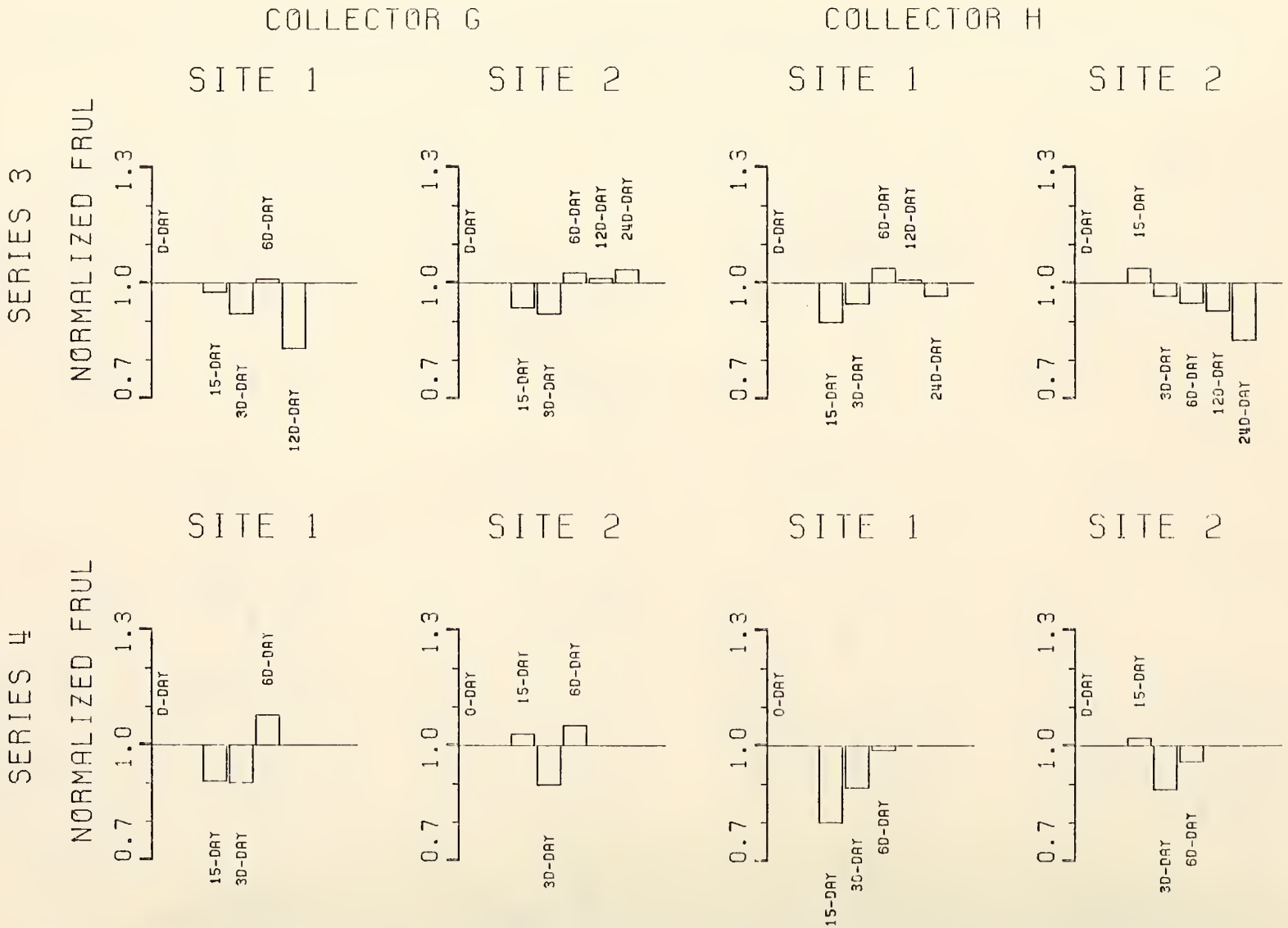

Figure 4.2.24. Collectors G & H normalized $F_R U_L$ vs retests, series 3 & 4, test sites 1 & 2

somewhat. This general trend is observed in more than one-half of the results shown. Attempts to correlate the 30 - 60 exposure day peak with particular collector materials were not successful. One possible factor, reported in recent literature [41], is that the transmittance values of polymer covers exhibit an initial increase followed by a monotonic decrease with exposure. However, the peak was observed for collectors with glass as well as polymer covers. It is also possible that the peak behavior could occur as a result of two or more compensating mechanisms [42]. It appears that further examination of the 30 - 60 exposure day peak behavior may be warranted since the mechanisms responsible for this pattern may be significant in investigating the long-term durability of collector materials.

Considering the series 3 and 4 tests, the intercept peaks are more distinct at 30 to 60 days except for the collectors G and H. Generally, the series 4 exposure procedure, which was discontinued after 60 days, appears to be much more severe than the other three series. Although there are many exceptions, the results obtained in series 4 after 60 days are approximately equal to the results obtained in the other three test series after 480 days. This observation suggests the possibility of designing accelerated exposure tests based on concentrated solar radiation.

Of the four test sites, the collectors exposed at site 1 show apparent degradation most frequently. As previously noted, this site is in a desert environment with a relatively high ambient temperature and with clear sky conditions common. This combination of environmental conditions results in higher collector stagnation temperatures than collectors tested at the other four sites. On the other hand, the cumulative solar irradiation received by collectors at this site in 480 days with a minimum of 17,000 kJ/m^2-day is less than the cumulative total received at the other sites. The reason is that this laboratory receives amounts of solar irradiation in excess of the qualifying 17,000 kJ/m^2-day nearly every day. These facts suggest that stagnation temperature may be the key parameter in inducing accelerated degradation.

The reported results from site 4 had greater variability than the results obtained at the other three sites. It is not apparent from the information available whether this trend resulted from differences in climatic conditions or test procedures.

The series 4 tests also provide further evidence that elevated stagnation temperature may give accelerated degradation. In series 4 tests, augmented exposure through the use of mirrors showed the most consistent pattern of performance degradation through the first 60 exposure days. The use of reflectors resulted in levels of solar irradiaton higher than would otherwise be experienced. As a consequence of augmentation, higher stagnation temperatures were achieved in collectors undergoing this series of tests. Unfortunately, difficulties in achieving uniform solar irradiation on the collectors arose from the use of reflectors. This problem along with other experimental difficulties resulted in the cancellation of this test series after 60 exposure days.

4.3 ANALYSIS OF SLOPE AND INTERCEPT DATA

As noted in the previous section, it is difficult to find obvious trends among the data from the test program. The measured values of $F_R(\tau\alpha)$ and F_RU_L exhibit considerable scatter and it does not appear justified to present and analyze all the collector results in depth. Therefore, collectors with typical results will be selected to analyze slope and intercept data statistically.

Figures 4.3.1 through 4.3.3 show typical efficiency curves for three collectors. Collector B is an extremely stable collector and the 0-day through 480-day efficiencies show a normal spread but no evidence of materials degradation. Collector E shows significant apparent degradation in thermal performance after an initial exposure period of approximately 30 days. Figure 4.3.2 shows that the 30-day retest curve represents the highest overall collector efficiency and that thermal performance decreased for subsequent exposure. (The reason that the 0-day curve is the lowest is unknown.) The results for collector F are shown in figure 4.3.3. A similar decline in thermal performance is evident in the figure. The absorber samples tested for this collector exhibited consistent degradation in absorptance and a slight improvement in emittance as shown elsewhere in the report. Correlations between materials sample degradation and collector efficiency results are analyzed in a later section.

The results in the previous section showed that generally changes in the two primary collector performance parameters were of about the same order of magnitude as the nearly random scatter in measured results. Consequently, it is in order to investigate further the accuracy associated with

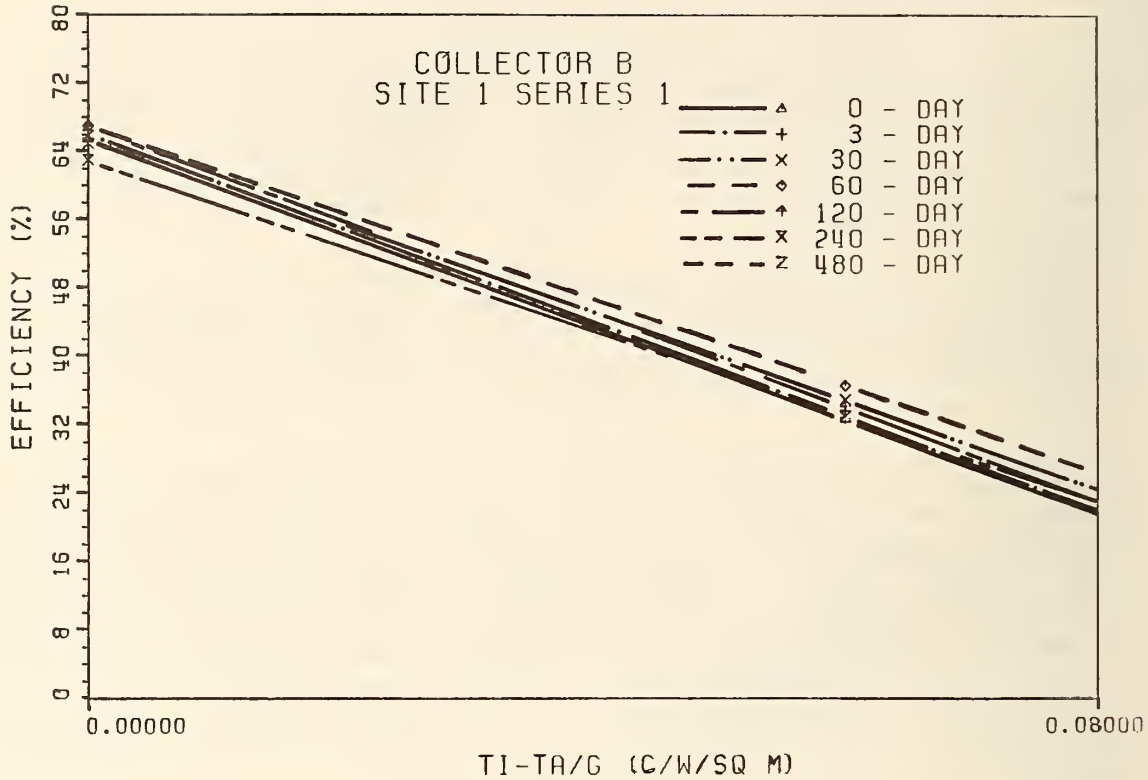

Figure 4.3.1. Collector B aggregate plot of measured efficiency, series 1, test site 1, all retests

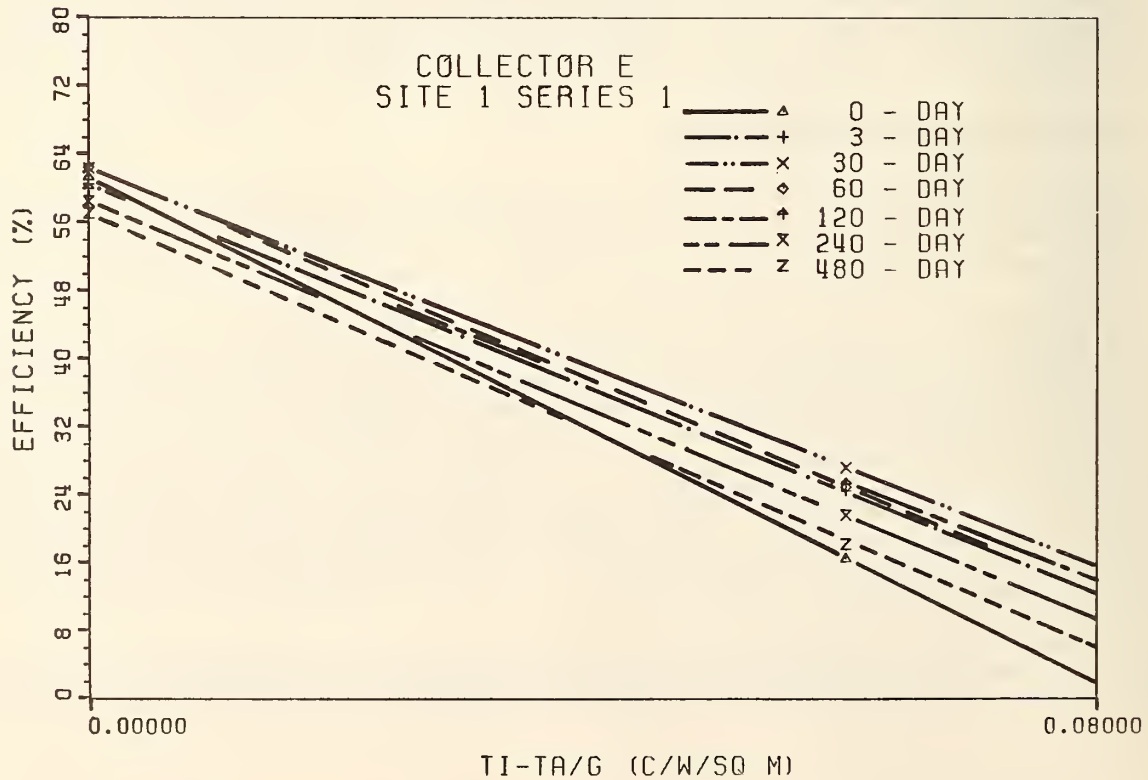

Figure 4.3.2 Collector E aggregate plot of measured efficiency, series 1, test site 1, all retests

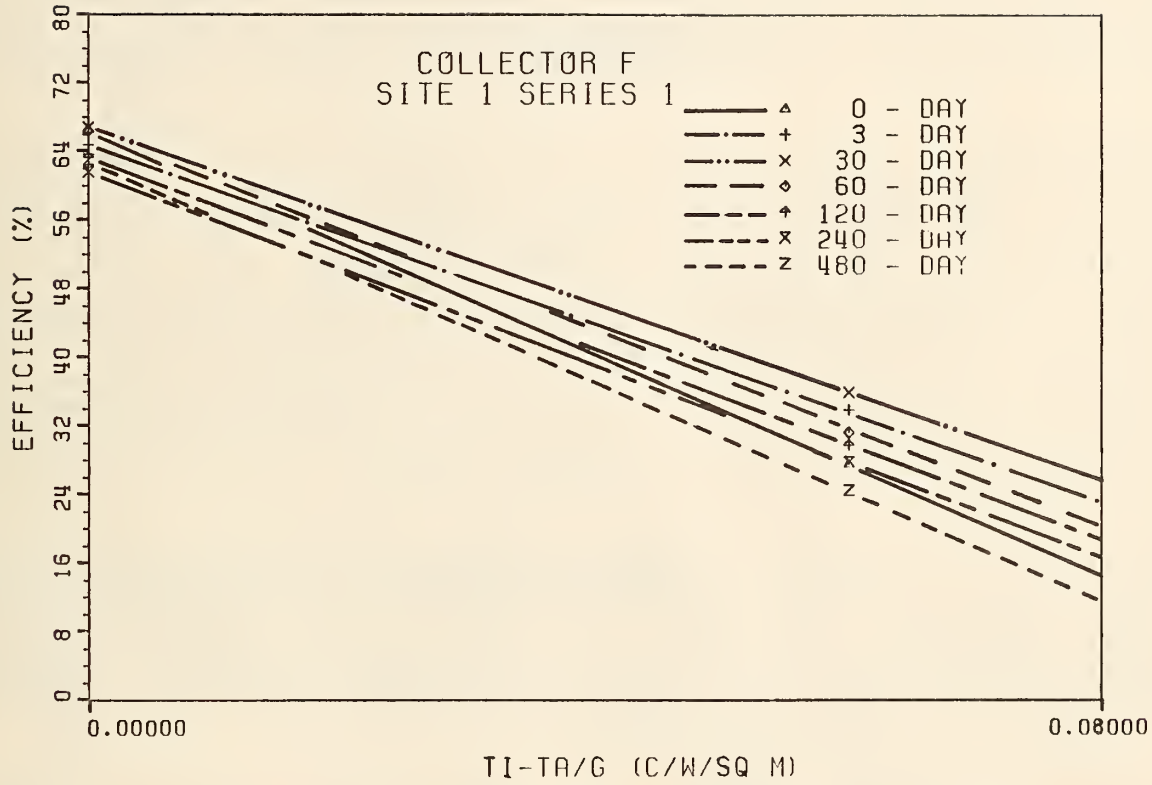

Figure 4.3.3 Collector F aggregate plot of measured efficiency, series 1, test site 1, all retests

the experimental facilities, variations in measured results within and between test sites, and the effects of environmental factors.

4.3.1 Variation Within and Between Test Sites

Variations in the reported values of the collector parameters result from experimental error in measuring collector energy output as well as from differences in collector material parameters. In order to emphasize differences associated with experimentation and test specimens of the same collector, results for an extremely stable collector (B) are investigated initially. Measurements of both collector efficiency and material properties, before and during exposure, showed that the performance of collector B was unchanged during the entire test program.

Figures 4.3.4 and 4.3.5 show typical variations of slope and intercept values within a given site for all four test series. The apparent peaking of $F_R(\tau\alpha)$ and other characteristics of these measured parameters follow the same general trends as noted earlier. Figures 4.3.6 and 4.3.7 show the primary collector performance parameters plotted versus time for test series 1 at all test sites. The results on these two plots are typical of between-site differences. As expected, the results are less consistent between sites with correspondingly higher standard deviations. Within a given test site, the standard deviation is about the same as estimated measurement uncertainty [24,25]. For a given collector and test series, the calculated standard deviations are higher for the results which include all four test sites. These two observations apply to stable collectors such as collector B.

Table 4.3.1 shows the results of a statistical analysis of the initial and final values of the two performance parameters. The results shown are based on test series 1 and 2 for each collector as reported by all four test sites. For series 2, the 3-day tests are used as the initial results. The final data are the 480-day results or the last test in those cases where the exposure period was shortened somewhat because of time limitations. Only collectors G and H, and possibly D, show a definite decrease in the mean value of the efficiency curve intercept. On the other hand, the loss coefficient parameter, F_RU_L generally shows a slight decrease for most of the collectors. The coefficient of variation for the intercept parameter generally increased for the collectors after exposure, but no clear trend is shown for the slope parameter variation. It should be noted that the above comparison includes unequal aging effects for the same model collector at different test sites. An increase in the coefficient of variation for the intercept parameter can be interpreted as meaning that the collector performance changes in a different manner at individual sites. Changes in the slope parameter, and to a lesser extent, the intercept parameter are undoubtedly masked by differences in test procedures, apparatus, and prevailing climatic conditions.

Table 4.3.2 shows that the scatter of measured efficiencies around the linear correlating curve was less for the final test as compared to the initial test for a typical stable collector. The table shows that the residual standard deviation decreased approximately 50 per cent for collector B under the series 1 test procedure. (The values of $F_R(\tau\alpha)$ and F_RU_L in table 4.3.2 included all reported data. These values may be somewhat different from those in table 4.2.1 based on results reported by the test laboratories who often used a subset of all efficiency values reported to generate an efficiency curve.) The results shown in table 4.3.2 indicate that the test laboratories improved their procedures with repetition and experience.

4.3.2 Influence of Experimental Apparatus

Generally, changes in the two primary performance parameters were of about the same order of magnitude as the random scatter in measured results for unexposed collectors. Consequently, the accuracy associated with the experimental facilities and possible site bias should be investigated.

There are no obvious degradation trends with exposure time observed in much of the reported data. Increases in $F_R(\tau\alpha)$ and decreases in F_RU_L were frequently observed. Several collectors, especially those tested at site 3, experienced a consistent increase in $F_R(\tau\alpha)$ or a decrease in F_RU_L throughout the entire exposure period. In other words, based on the reported results, after nearly three years of exposure the performance of several collectors was apparently better than the original performance. Physical reasoning dictates that such results be viewed with suspicion. Because of these anomalies, the experimental apparatus and procedures were investigated. An analysis of the effect of changes in pyranometer sensitivity with time was carried out. The temperature dependence of pyranometer performance was also examined. Finally, correlations were performed to determine whether excessive data scatter or suspicious results were associated more with particular pyranometers or test stands.

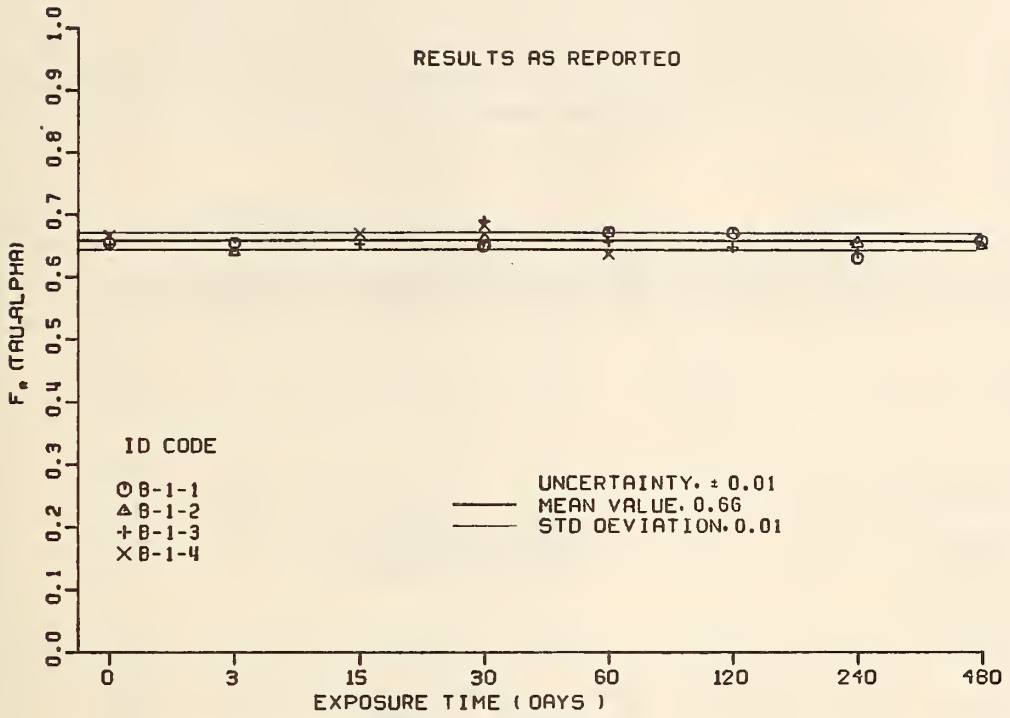

Figure 4.3.4 Collector B efficiency curve intercepts vs exposure time, test site 1, all series

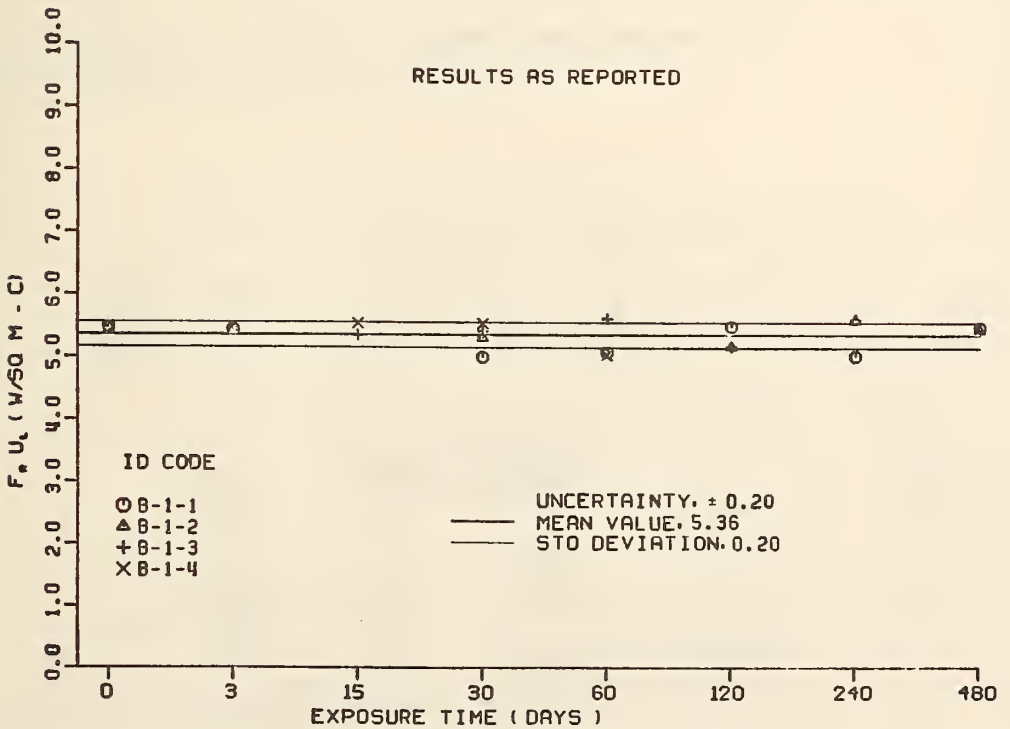

Figure 4.3.5 Collector B efficiency curve slope parameter vs exposure time, test site 1, all series

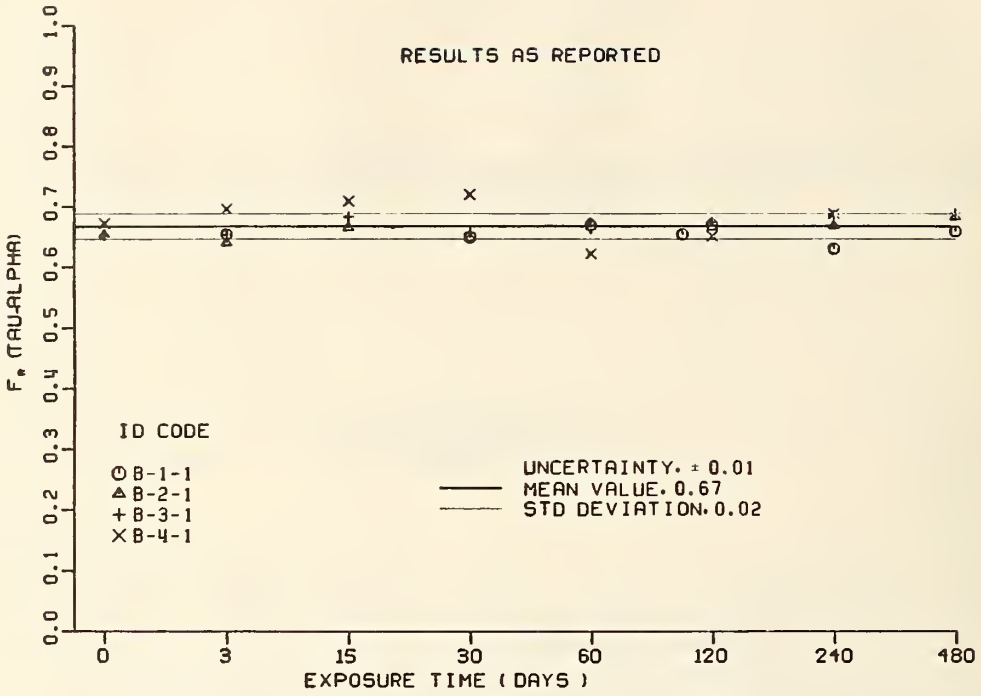

Figure 4.3.6. Collector B efficiency curve intercepts vs exposure time, all test sites, series 1

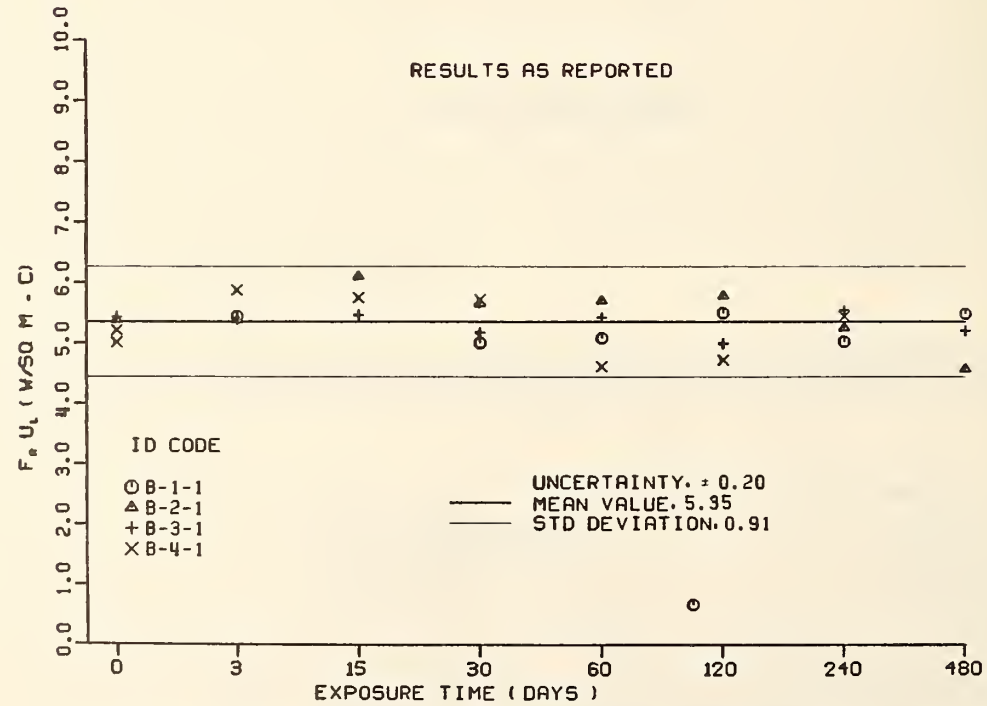

Figure 4.3.7. Collector B efficiency curve slope parameter vs exposure time, all test sites, series 1

Table 4.3.1. Statistical Analysis of Efficiency Curve Intercept and Slope Parameters Based on Initial and Final Tests, All Collectors and Test Sites, Series 1 and 2

Collector	Intercept $F_R(\tau\alpha)$				-Slope $(F_R U_L)$			
	Mean	Coef of Variation	Std Error of mean		Mean	Coef of Variation	Std Error of mean	
			Value	Per cent			Value	Per cent
A i*	0.615	3.034	0.00659	1.073	4.575	13.640	0.2206	4.823
f*	0.620	4.185	0.00917	1.480	4.225	8.994	0.1344	3.180
B i	0.654	2.302	0.00532	0.814	5.499	5.911	0.1149	2.090
f	0.674	2.184	0.00521	0.772	5.285	3.784	0.0707	1.338
C i	0.533	3.174	0.00598	1.122	4.204	4.459	0.0663	1.576
f	0.513	5.461	0.01060	2.064	3.677	10.950	0.1522	4.139
D i	0.646	2.006	0.00458	0.709	3.213	10.626	0.1207	3.757
f	0.639	2.495	0.00563	0.882	3.150	8.302	0.0924	2.935
E i	0.607	2.094	0.00449	0.740	6.418	8.123	0.1843	2.872
f	0.611	5.328	0.01151	1.884	6.189	8.733	0.1911	3.087
F i	0.654	2.621	0.00606	0.927	6.015	11.089	0.2358	3.921
f	0.652	3.264	0.00753	1.154	6.127	10.997	0.2382	3.888
G i	0.568	3.831	0.00769	1.354	5.429	7.982	0.1532	2.822
f**	0.544	2.600	0.00708	1.300	5.602	6.116	0.1713	3.058
H i	0.636	1.437	0.00323	0.508	5.580	4.849	0.0957	1.714
f	0.592	5.397	0.01130	1.908	4.946	7.008	0.1225	2.478

* i denotes initial test: 0-day for series 1, 3-day for series 2
f denotes final test: 480-day or somewhat less
** based on 4 data sets available

Table 4.3.2. Residual Standard Deviations for Collector B Test Series 1 Linear Efficiency Curve Correlations

Site	Test id	No. of data pairs	Intercept (percent)	(-)Slope (W/m^2-°C)	Residual std deviation
1	0-day	16	65.3	5.46	0.992
	480-day	16	65.9	5.49	0.544
2	0-day	16	65.5	5.49	1.904
	480-day	16	68.3	5.47	1.092
3	0-day	16	66.2	5.61	0.544
	480-day	16	70.0	5.46	0.659
4	3-day	12	69.9	5.86	1.107
	480-day	40	67.3	5.01	0.630

The investigation of possible interlab differences in reported results was conducted to determine whether any test site consistently reported values of efficiency curve intercepts or slope which were higher or lower than the mean of the results from the other laboratories. The approach taken was to plot the values of the parameters from each of the four sites on a common graph vs exposure using series 1 and 2 results. Table 4.3.3 shows the results as the percentage of times that a particular test site reported extreme values of $F_R(\tau\alpha)$. The table shows the times that a particular

Table 4.3.3. Comparison of Frequency of Extreme Values for $F_R(\tau\alpha)$ Reported by Test Sites

Site	Percentage of times a site reported values:		
	highest	lowest	highest or lowest
1	10.9	32.9	21.5
2	14.7	36.3	25.5
3	43.9	7.9	25.9
4	30.5	23.7	27.1

site reported either the highest, lowest, or highest or lowest values. The latter is a measure of the excess spread in reported results.

As shown in the table, sites 1 and 2 reported the lowest readings most often while sites 3 and 4 reported the highest readings more often. Caution is necessary in interpreting these results. The tabulation considers only the relative magnitudes of the reported values, i.e., the highest and lowest readings were tabulated but the quantitative amount by which a reading was the highest or lowest is not reflected in the tabulations. Also, the results presented may be affected by prevailing climatic conditions. The effects of environmental conditions on reported results are considered in a later section. Based on the last column in table 4.3.3, extreme readings, on the average, were essentially evenly distributed between the four test sites. This observation suggests relative consistency between the sites.

An analysis was made to determine if a particular pyranometer or test stand within a test site could be identified as a major source of the scatter in data. This evaluation was carried out by identifying values of $F_R(\tau\alpha)$ which fell outside the calculated experimental uncertainty limits as measured from linear curve fits of $F_R(\tau\alpha)$ as a function of exposure time for a particular collector - series combination. The experimental uncertainty in determining $F_R(\tau\alpha)$ resulting from instrumentation tolerances was taken to be 0.01 as calculated from a Kline-McClintock type analysis by Culkin [43]. Any values of $F_R(\tau\alpha)$ beyond this uncertainty from the linear fit were tabulated along with the pyranometer serial number and test stand number within the test site used for that result. The number of times each pyranometer and test stand were used was also tabulated in order to prevent an unjust bias of the data. For data falling outside the measurement uncertainty band, the percentage of times a particular pyranometer or test stand was used was then tabulated. Table 4.3.4 shows the results of this analysis through 120 exposure days.

The tabulated results show that no one pyranometer or test stand can be identified as a primary source of suspect data. It should be noted that of the points identified outside the permissible band, as many were found to be high as were found to be low. This results also held true for individual pyranometers. In other words, the points identified as suspect were randomly distributed. The pyranometers and test stands yielding such data were random as well.

An analysis was performed to examine the effect of pyranometer sensitivity changes on the reported results. From pyranometer calibration histories provided by two of the participating laboratories and the pyranometer manufacturers, it was observed that pyranometer sensitivity generally decreases with time and increasing ambient temperature. The net effect of a pyranometer sensitivity decrease is to charge the collector with less solar irradiance than it actually receives. Consequently, measured values of $F_R(\tau\alpha)$ would be greater than actual. On the other hand, pyranometer sensitivity

changes with time have no effect on measured values of $F_R U_L$ provided such changes are negligible during a given test.

The reported values of solar irradiance in the plane of the collector must be corrected in order to compensate for changes in pyranometer sensitivities. Generally, the pyranometers used in the test program were calibrated on an average of two times per year rather than at the time of each retest. Therefore, a method of interpolating calibration results was necessary to obtain an approximation for the sensitivity at the time of the test. A linear interpolation procedure was used.

Table 4.3.4. Correlations of Pyranometers and Test Stands with Experimental Results Outside Probable Measurement Uncertainty Ranges, Site 1, All Series through 120-day Retests

Pyranometer Serial No. or Test Stand	Times Used	Percentage of times used When values beyond Uncertainty Range
14317	16	18.75
14318	25	12.00
14319	13	38.46
14320	5	40.00
14321	21	9.52
14322	10	30.00
17349	25	20.00
18273	14	42.86
Stand 1	12	25.00
Stand 2	15	26.67
Stand 3	25	16.00
Stand 4	23	13.04
Stand 5	24	25.00
Stand 6	32	31.25

The reported values of $F_R(\tau\alpha)$ from site 2 were particularly appropriate for examining the effects of pyranometer sensitivity changes. This site used pyranometer calibration constants from calibrations performed at the beginning of the test program for data reduction throughout. The other participating laboratories generally used updated calibration constants from periodic recalibrations. Consequently, the values of the intercept parameter reported by site 2 represent a limiting worst case with regard to possible errors caused by pyranometer sensitivity changes.

Typical pyranometer sensitivity curves are presented in figure 4.3.8. Generally, maximum changes of from two to three percent in the reported values of $F_R(\tau\alpha)$ resulted from pyranometer sensitivity corrections. This correction had no significant effect on reducing the data scatter in the reported results. While the sensitivity changes introduced a minor consistent error in the reported results, this source of error was found to be too small to mask any significant degradation trends. After correction, the values of $F_R(\tau\alpha)$ still exhibited random fluctuations of at least the same order of magnitude as any general degradation trend.

A correction methodology was also applied to account for instrument sensitivity to ambient temperature. For a given solar irradiance, the voltage signal output of pyranometers decreases with increasing ambient temperature. The instrument sensitivity to operating temperature was assumed to be invariant with time and taken from the manufacturer's calibration information. It was found that temperature compensation did not result in any significant changes in the reported results. Generally, the effect of temperature dependence on pyranometer output was insignificant.

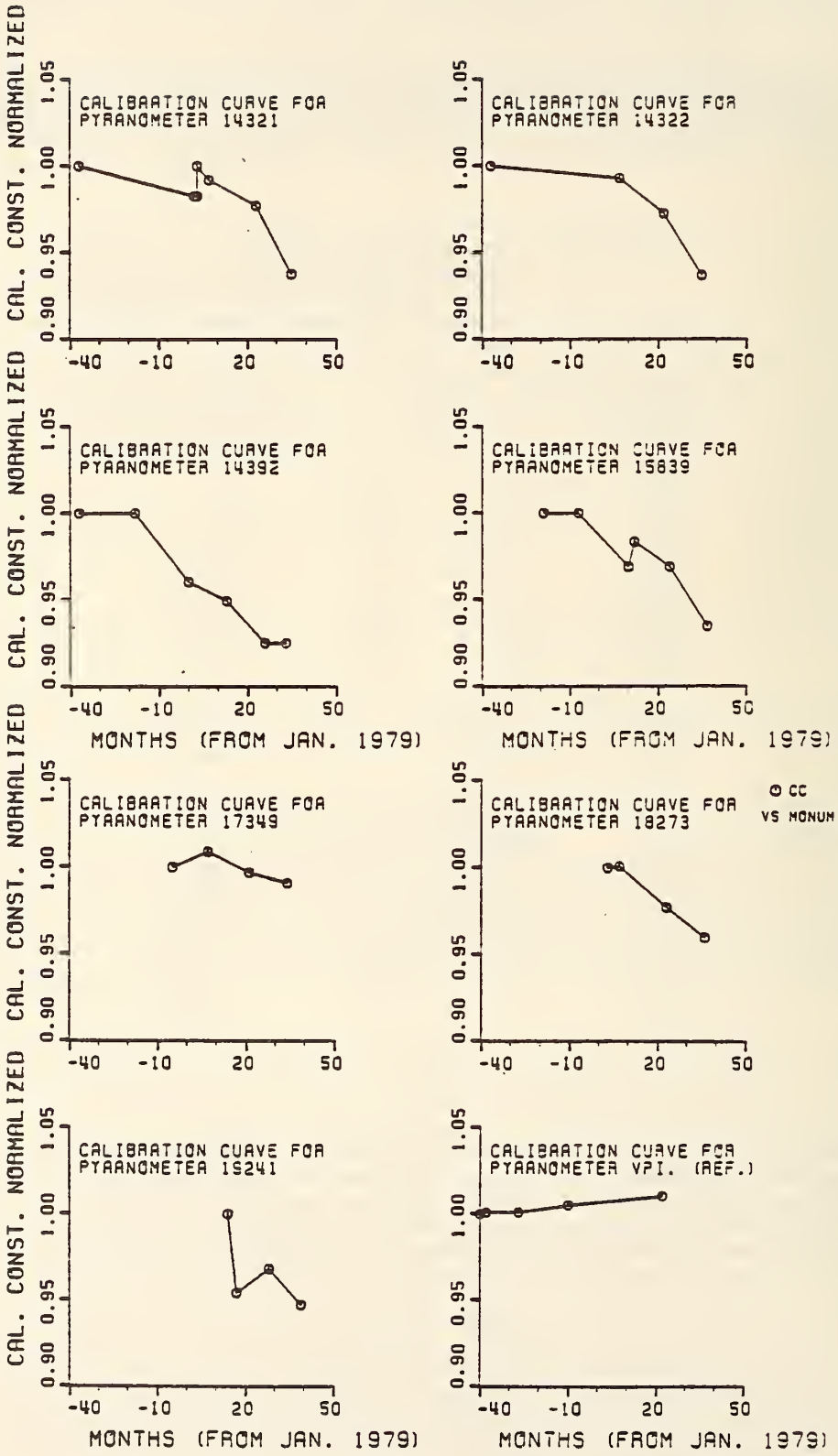

Figure 4.3.8. Typical Pyranometer calibrations vs time

4.3.3 Environmental Factors

The measurement of collector efficiency, which is the basis for investigating the thermal performance of collectors in the present study, may be affected by variations in test environments within and between the four test sites. The results of calculations to determine the expected effect on measured efficiency of different environmental parameters, such as wind speed, ambient temperature, total and scattered solar irradiance, and beam incident angle, are presented in this section. Such parameters can substantially affect both the heat transfer and optical characteristics of various collectors.

The parameter $F_R U_L$ is much more sensitive to variations in the test environment than is $F_R(\tau\alpha)$. The overall loss coefficient U_L represents the sum of the top, edge, and back loss conductions per unit aperture area. For well designed collectors including those used in the test program, most heat loss occurs through the top cover assembly. The top loss coefficient is a function of the convective heat transfer coefficient which, in turn, depends on wind speed, ambient temperature, and mean absorber plate temperature. The top loss coefficient also depends indirectly on the total and scattered solar irradiance since these parameters affect the mean absorber temperature. Consequently, U_L and $F_R U_L$ depend on the prevailing environmental conditions at the time of each efficiency test.

Since variations in the test environment were suspected to cause some of the random variations noted in the two collector parameters, an analytical procedure was used to adjust the results of efficiency tests under any particular set of test conditions. The motivation for correlating test results to a standard set of conditions was twofold. First, the spread in reported values of $F_R(\tau\alpha)$ and $F_R U_L$ which may be attributed to different environmental conditions should be reduced. Secondly, adjustment to a standard set of test conditions provides a common basis to compare results for the same model collector at different test sites. If the measured results correlate with test conditions, a correction of this type is necessary to determine whether interlaboratory differences in the testing procedures occurred.

An analytical procedure was developed earlier to effect correction of test data to a standard test condition. A detailed description of the correction procedure and mathematical model used is presented in Reference [40]. The correction is based on using an analytical model of the collector to calculate efficiencies at standard and at actual test conditions for a particular $[t_i - t_a]/G$. The difference between these calculated efficiencies is then added to the measured efficiency, i.e.,

$$\eta(X, \text{std}) = \eta_{\text{meas}}(X, \text{test}) + [\eta_{\text{calc}}(X, \text{std}) - \eta_{\text{calc}}(X, \text{test})]$$

where

$$X = [t_i - t_a]/G$$

is held constant. As shown in Reference [40], the experimental verification of this procedure has been reasonably successful provided the collector configuration fits the analytical model used.

The information required to apply the correction methodology includes pertinent weather parameters, operating conditions during testing, and physical dimensions of the collector. In addition, heat transfer and optical characteristics of the various collector components are necessary. The standard test environment used for the present investigation is shown in table 4.3.5. The values shown in this table represent approximately median weather conditions of the test conditions experienced throughout the test program.

The correction procedure as outlined was used on the reported test results for collectors B and E. These collectors were selected for analysis because they are typical of the most prevalent designs and employ construction materials that are commercially available. Both collectors have parallel flow through the absorber which is easier to model than the serpentine case. Collector E has a single FRP cover with a flat-black painted copper absorber. Collector B has a double, low-iron, glass cover assembly with a flat-black copper absorber. The double-covered collector was expected to be influenced less by variations in environmental conditions. The physical characteristics and heat transfer properties used in the correction were based on measurements obtained at the time of initial exposure. These values are tabulated in Reference [25].

Table 4.3.5. Reference Environment Used in Compensation for Environmental Dependence of Reported Results

Condition	Value
Ambient temperature	20°C
Solar: Irradiance	1000 W/m^2
Beam angle	15 deg
Diffuse fraction	0.15
Wind speed	3.0 m/s
Test fluid	water
Flow rate	0.02 $kg/s\text{-}m^2$
Collector slope	45.0 deg

Figure 4.3.9 shows a comparison between the calculated efficiency curve and an aggregate plot of all measured instantaneous efficiencies for collector B, series 1 at site 1 (B-1-1 0- through 480-day retests). This figure shows the typical agreement between the model and data which is judged to be satisfactory for calculating efficiency differences attributed to environmental variations. The correction procedure was then carried out to determine whether a significant amount of the scatter in the reported values of $F_R(\tau\alpha)$ and F_RU_L could be attributed to variations in environmental factors. Plots of the "corrected" values vs exposure time were prepared and comparisons of these were made to the plots of the "as reported" results. Figures 4.3.10 through 4.3.21, typical plots of this type, show that compensation for environmental differences at the time and location of the test does not significantly alter the reported results.

An analysis of the graphical results shows that no detectable changes in trends, or lack of trends, in the values of $F_R(\tau\alpha)$ and F_RU_L resulted from taking into account different environmental test conditions. The mean values of $F_R(\tau\alpha)$ generally remained within 0.01 efficiency per cent of the mean values of the reported results by individual sites or by series. The mean values of F_RU_L actually increased somewhat. This slight increase probably resulted from the standard value of wind speed being somewhat higher than the average wind speed experienced during testing. More importantly, the standard deviations about the mean values were not reduced significantly for either F_RU_L or $F_R(\tau\alpha)$. In fact, the standard deviation in $F_R(\tau\alpha)$ increased as a result of the analytical correction procedure. This unexpected result is attributed to a lack of responsiveness or precision in the test procedure. As shown in the tabulations of thermal performance data in appendix C of Reference [25], the measured efficiency trends do not always follow those expected when environmental parameters change. For example, there are cases where the wind speed increases somewhat while all the other operating conditions remain constant; however, the measured efficiency does not always decrease in these cases. It appears that the time response of the collectors along with inherent experimental uncertainties associated with the test method may be contributing to this anomaly.

While the plots of the corrected values of $F_R(\tau\alpha)$ and F_RU_L revealed no new trends, the weather compensation procedure did not affect the observed 30 - 60 exposure day peak behavior in $F_R(\tau\alpha)$ discussed earlier. This behavior, therefore, does not appear to be caused by environmental changes during the testing.

The analysis of variations in measured results caused by variations in environmental conditions show that such changes have no significant effect on the two primary efficiency curve parameters.

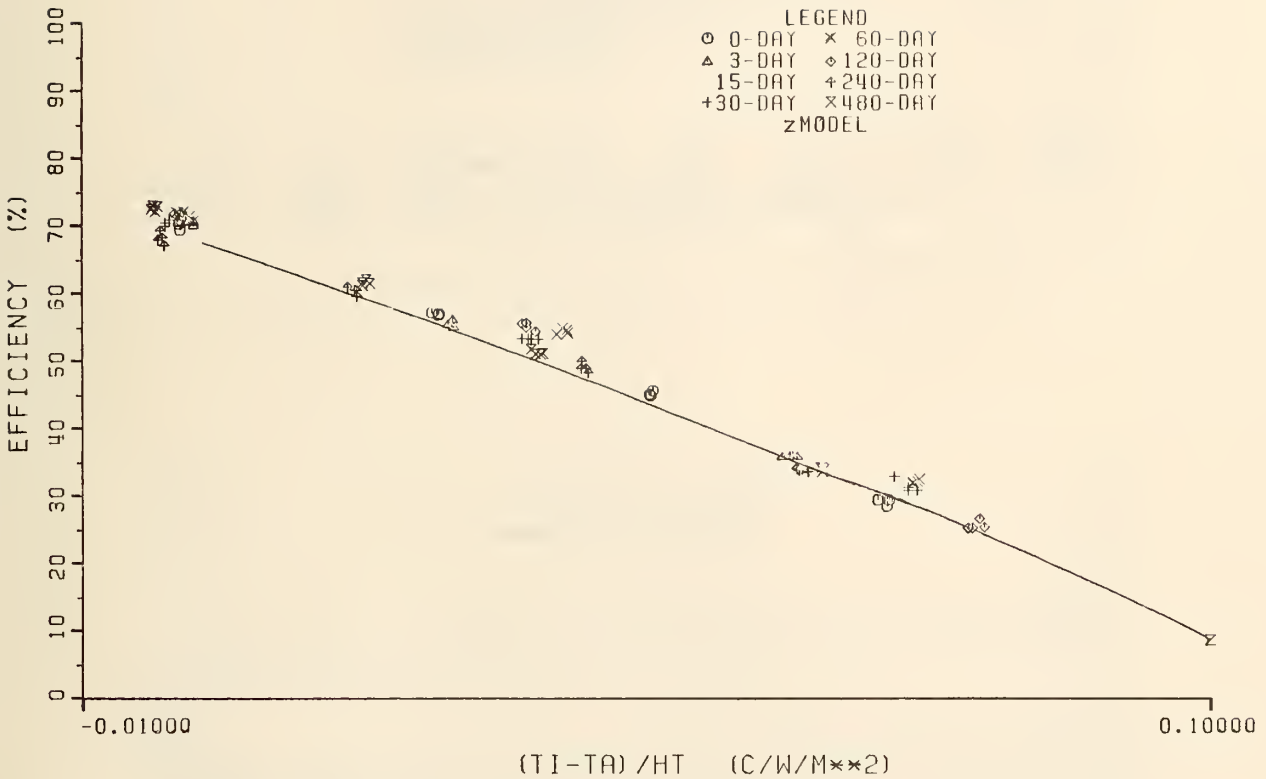

Figure 4.3.9. Comparison of calculated and measured efficiencies for collector B, site 1, test series 1, all retest data

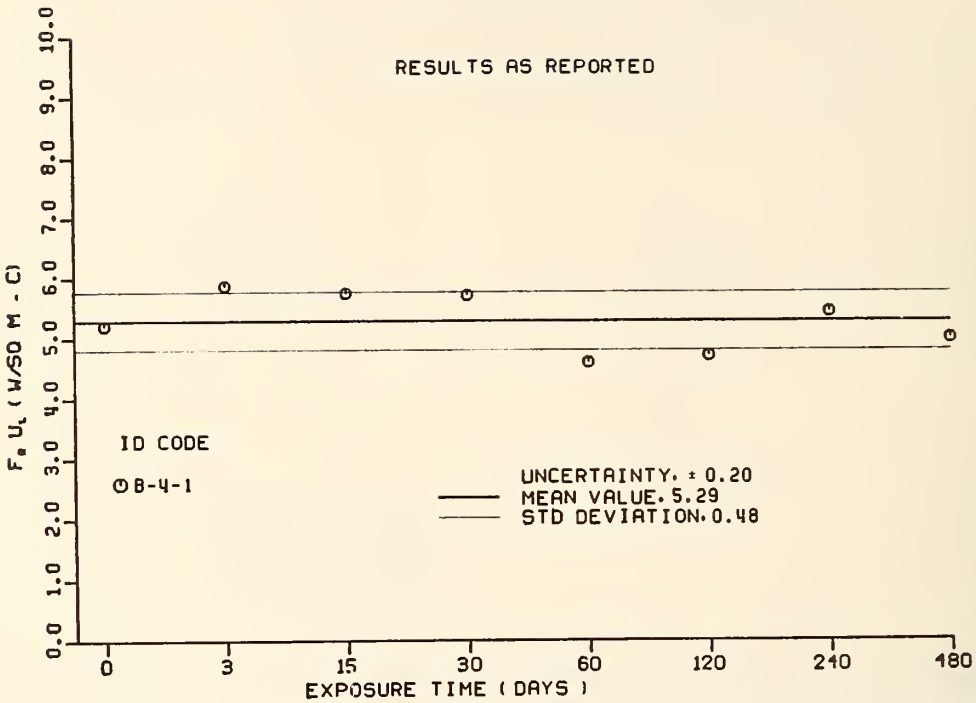

Figure 4.3.10. Reported values of $F_R U_L$ for collector B, site 4, test series 1 vs exposure time

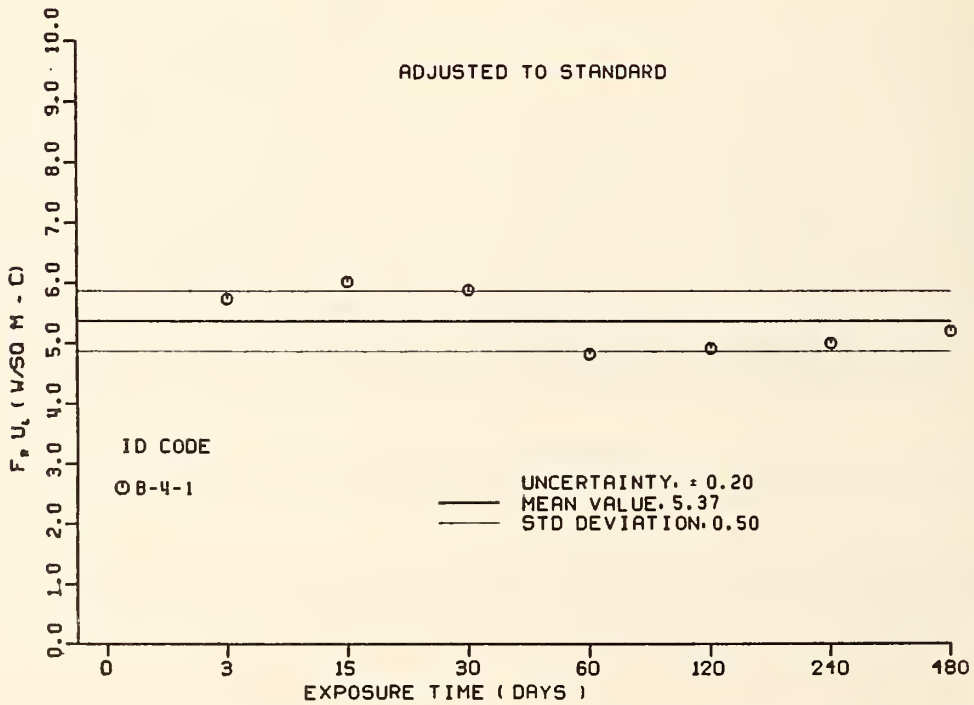

Figure 4.3.11. Values of $F_R U_L$ for collector B, site 4, test series 1 vs exposure time, adjusted to standard test conditions

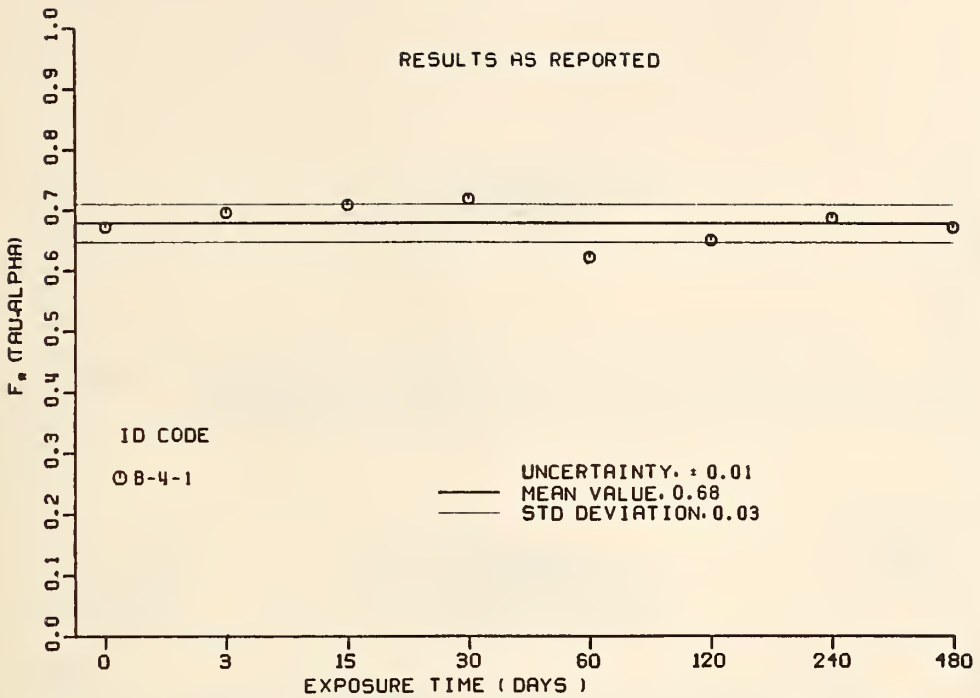

Figure 4.3.12. Reported values of $F_R(\tau\alpha)$ for collector B, site 4, test series 1 vs exposure time

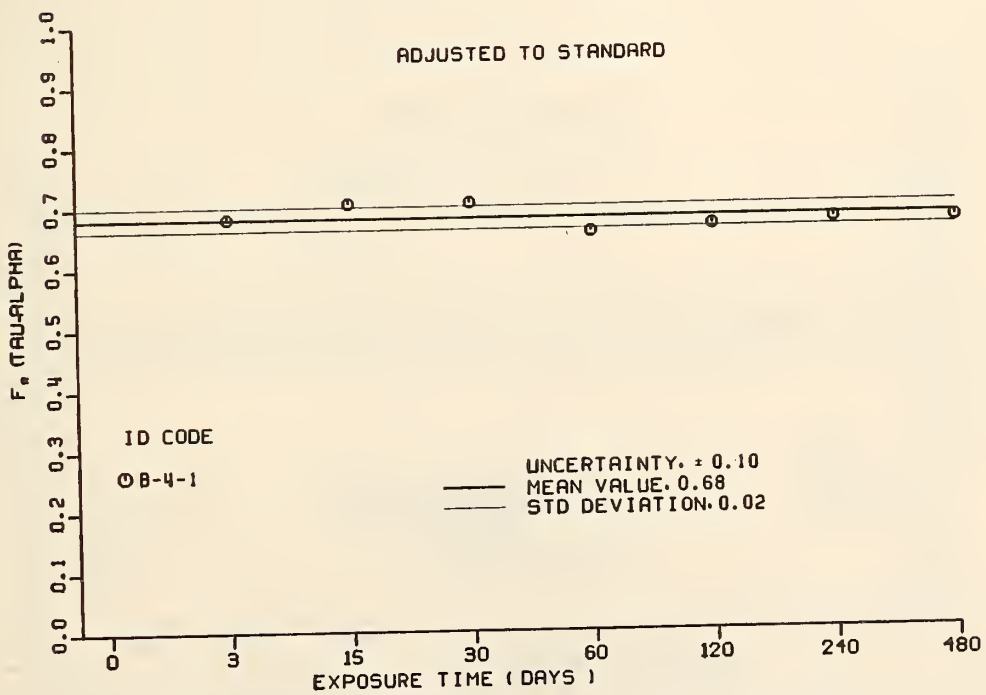

Figure 4.3.13. Values of $F_R(\tau\alpha)$ for collector B, site 4, test series 1 vs exposure time, adjusted to standard test conditions

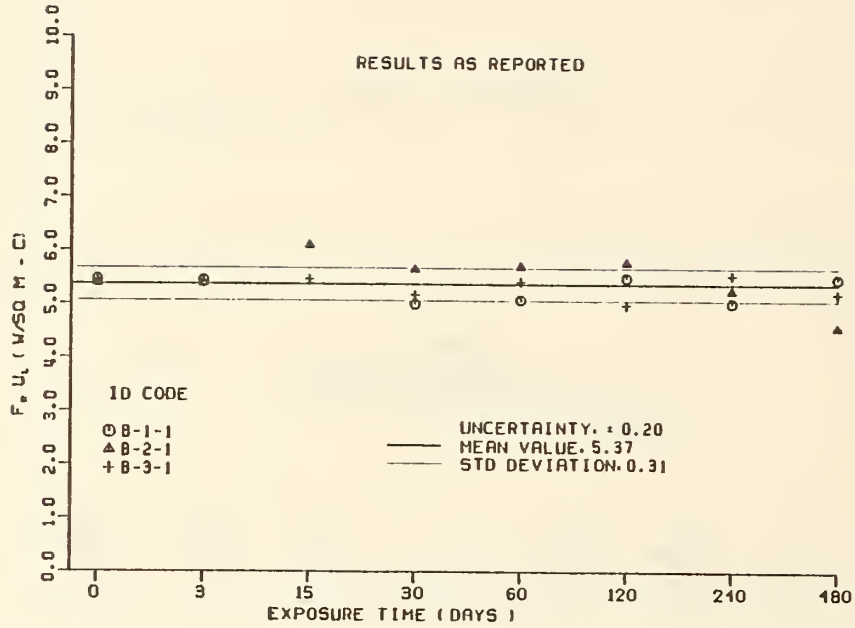

Figure 4.3.14. Reported values of $F_R U_L$ for collector B, site 1, 2, and 3, test series 1 vs exposure time

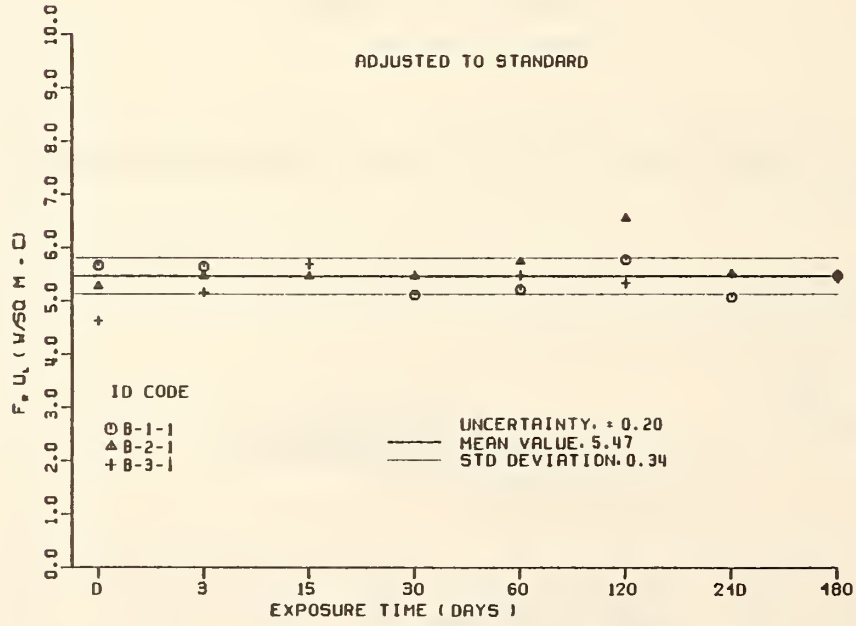

Figure 4.3.15. Values of $F_R U_L$ for collector B, sites 1, 2, and 3, test series 1 vs exposure time, adjusted to standard conditions

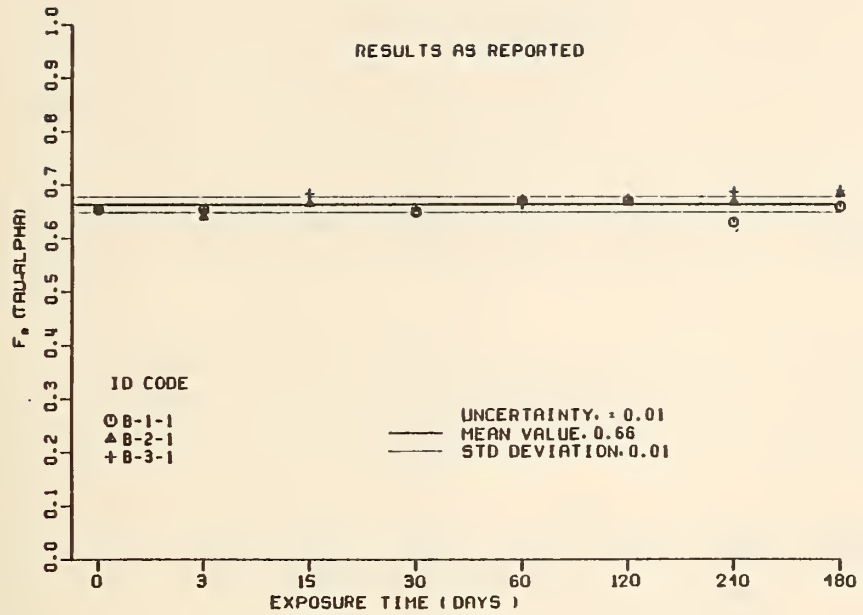

Figure 4.3.16. Reported values of $F_R(\tau\alpha)$ for collector B, sites 1, 2, and 3, test series 1 vs exposure time

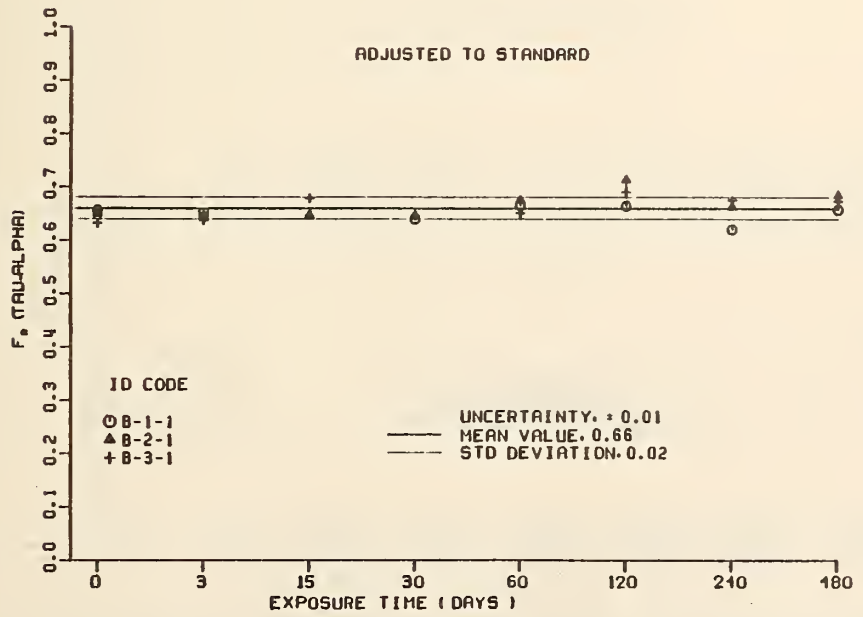

Figure 4.3.17. Values of $F_R(\tau\alpha)$ for collector B, sites 1, 2, and 3, test series 1 vs exposure time, adjusted to standard conditions

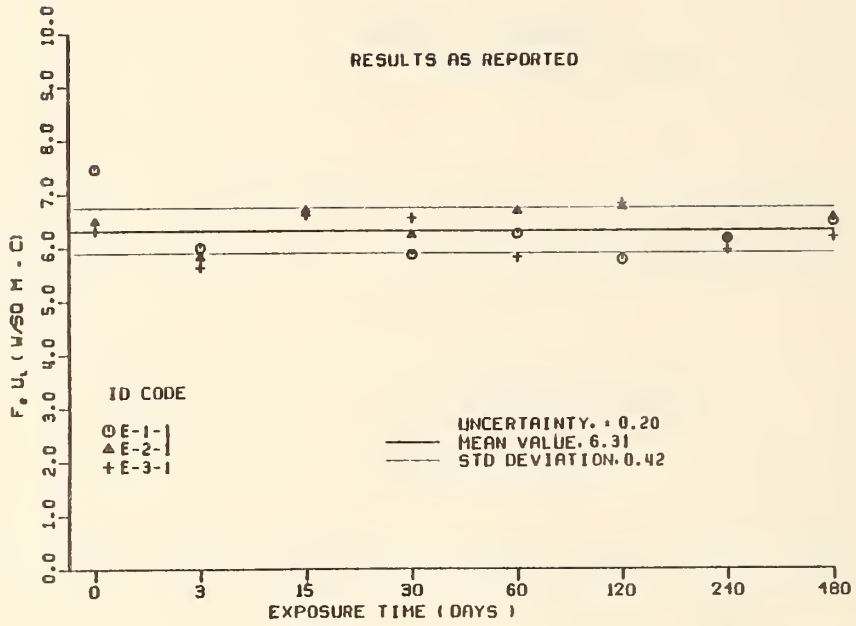

Figure 4.3.18. Reported values of $F_R U_L$ for collector E, sites 1, 2, and 3, test series 1 vs exposure time

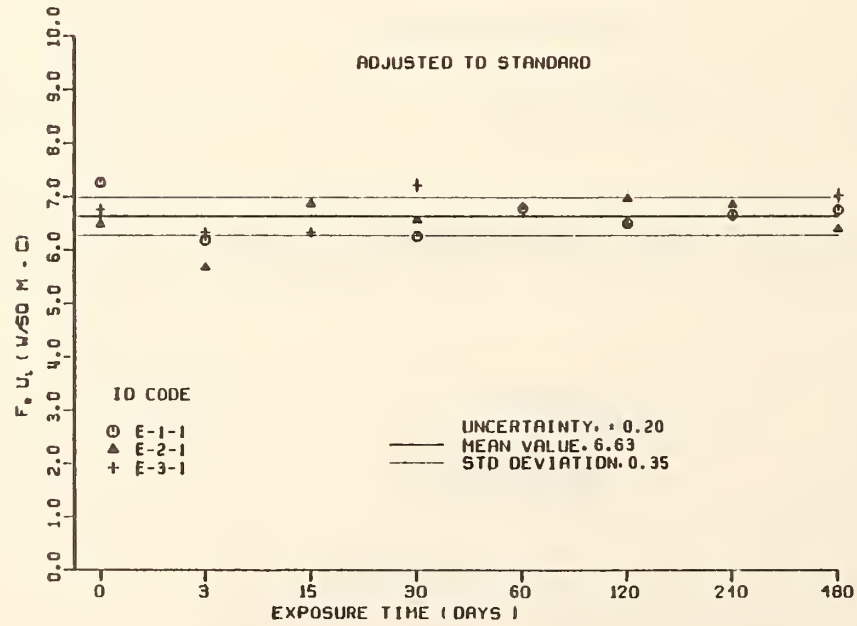

Figure 4.3.19. Values of $F_R U_L$ for collector E, sites 1, 2, and 3, test series 1 vs exposure time, adjusted to standard conditions

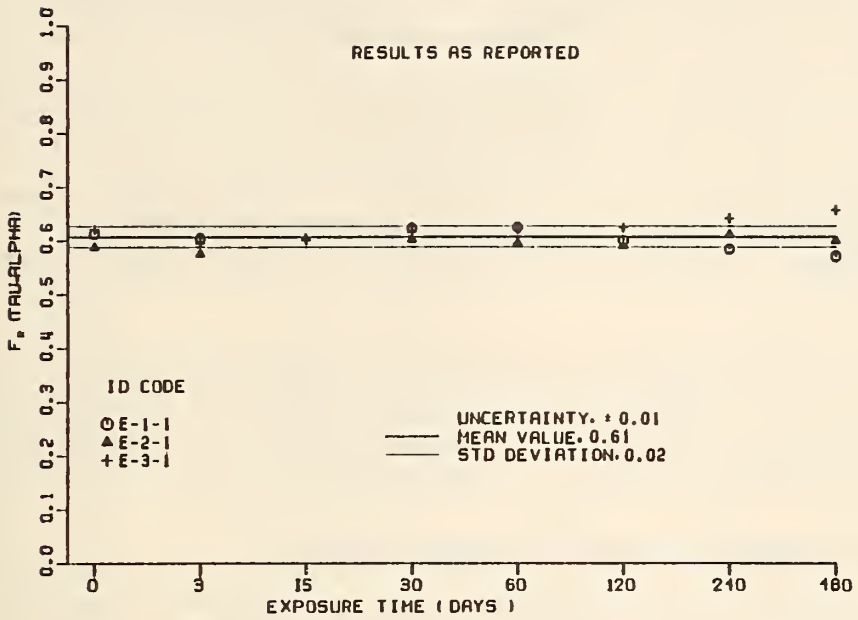

Figure 4.3.20. Reported values of $F_R(\tau\alpha)$ for collector E, sites 1, 2, and 3, test series 1 vs exposure time

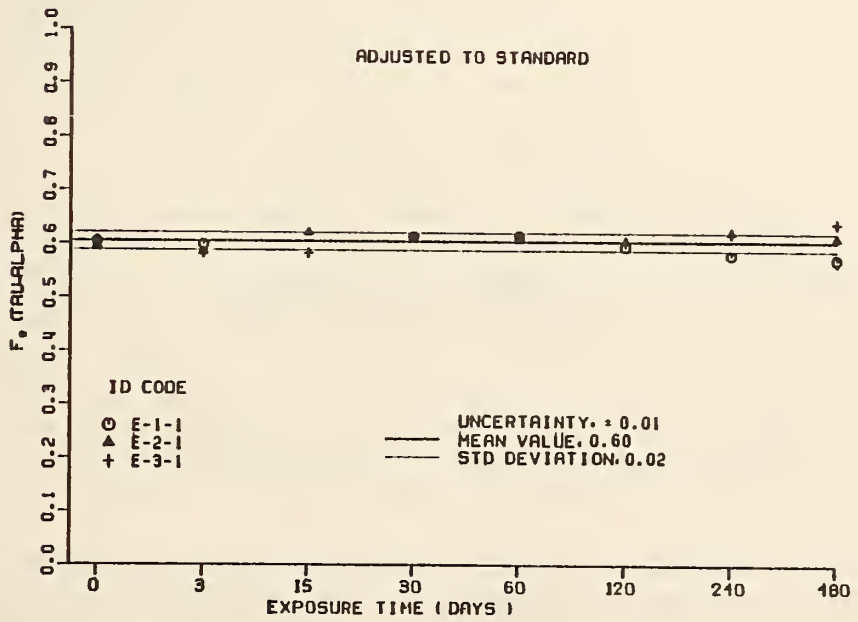

Figure 4.3.21. Values of $F_R(\tau\alpha)$ for collector E, sites 1, 2, and 3, test series 1 vs exposure time, adjusted to standard conditions

4.3.4 Effect on $F_R(\tau\alpha)$ of Linearized Efficiency Curves

The analysis of the reported values of the efficiency curve parameters is based on the assumption that efficiency can be adequately represented by a linear function of $[t_i - t_a]/G$. Actually, the slope of collector efficiency curves continually decreases with increasing temperature since the loss coefficient increases with absorber temperature. In this section, the validity of comparing values of $F_R(\tau\alpha)$ based on a linear efficiency curve as the characteristic parameter is established.

A comparison is made of the values of $F_R(\tau\alpha)$ extrapolated from the linearized model with those obtained by instantaneous efficiency measurements where the inlet temperature was equal to the ambient temperature. The "directly measured" values were taken to be all the instantaneous efficiencies obtained with $[t_i - t_a]/G$ less than or equal to $0.001^oC/Wm^2$. The measured values are shown in figure 4.3.22 as the abscissa with the extrapolated values shown as the ordinate. Perfect agreement would correspond to the case where the points would lie on the solid line. The extrapolated values are slightly and consistently higher than those measured directly. Each extrapolated value, however, is within 1.0 efficiency per cent of the measured value.

Based on figure 4.3.22, representing collector efficiency as a first-order function in $[t_i - t_a]/G$ introduces a small but consistent error in the values of $F_R(\tau\alpha)$ for collectors of the type used in the test program. Since this error is consistent and small, however, all efficiency curves may be assumed to be affected by about the same amount. Consequently, use of a linear efficiency correlation does not contribute to the scatter in reported values of $F_R(\tau\alpha)$ and has a negligible effect on the comparisons presented.

4.4 COLLECTOR THERMAL PERFORMANCE DEPENDENCE ON MATERIAL PROPERTIES

A mathematical model for collector thermal performance was used to calculate expected changes in efficiency curve parameters as a result of arbitrary and measured changes in several key material properties. The results are shown for changes in absorber plate emittance and absorptivity, cover normal beam transmittance, and conductivity of thermal insulation. The results calculated for typical changes in measured properties are then compared with measured changes of the collector efficiency curve parameters.

Collectors D and H were selected for the theoretical investigation. The efficiency curve parameters and material properties for these two collectors showed significant changes after exposure. Both collectors could be mathematically modeled in a straight-forward manner. Collector D has two glass covers and a selective absorber. Tests on actual samples of the absorber plate showed that the emittance changed appreciably during the exposure period for some of the collectors exposed. Collector H has an outer cover of poly(ethylene terephthalate)(PET) and an inner fluorinated (ethylene propylene) copolymer (FEP) cover with a flat-black absorber. Tests showed that significant changes had occurred in the solar transmittance of the two cover system primarily due to outgassing deposits.

The mathematical model used to calculate the thermal performance is based on the Hottel-Whillier-Bliss analysis with an extension to account for the serpentine flow configuration of collector H. A detailed description of the mathematical model is given in Reference [40]. Table 4.4.1 shows the base case parameters and dimensions required by the analytical model for the two collectors. Tables 4.4.2 and 4.4.3 show calculated efficiencies for the base case and arbitrary changes in properties. The calculations shown are for changing only one property with others held at the base case value for a range of $[t_i - t_a]/G$. In order to compare with measured results, a linear curve was fit to the calculated efficiency values shown. The abscissa values were selected in accordance with ASHRAE 93-77 [6] as approximately 0.1, 0.3, 0.5, and 0.7 of $[t_i - t_a]/G$ at stagnation conditions. The $F_R(\tau\alpha)$ and F_RU_L values shown in the tables are then the intercept and negative slope of the correlating curves. The mean residual errors for the curve fit based on these four sets of values are also included in the table. In the tables, τ_{sb} designates the solar beam transmittance of the inner cover (1) and outer cover (2). The results shown in the two tables are also depicted graphically in figure 4.4.1 where the parameters $F_R(\tau\alpha)$ and F_RU_L have been normalized by the case values.

Several observations follow from examining the effect on $F_RU_L(\tau\alpha)$ and F_RU_L of changes in the four materials. As would be expected, changes by 0.01 W/m-^{o}C in the thermal conductivity from the base case value have a strong effect on the slope parameter but a small effect on the intercept parameter. While conductivities were not measured before and after exposure, this property could change as a result of compaction, moisture entering fibrous insulation (Collector D), thermal damage, or moisture entry into open pores of organic foam insulation (Collector H).

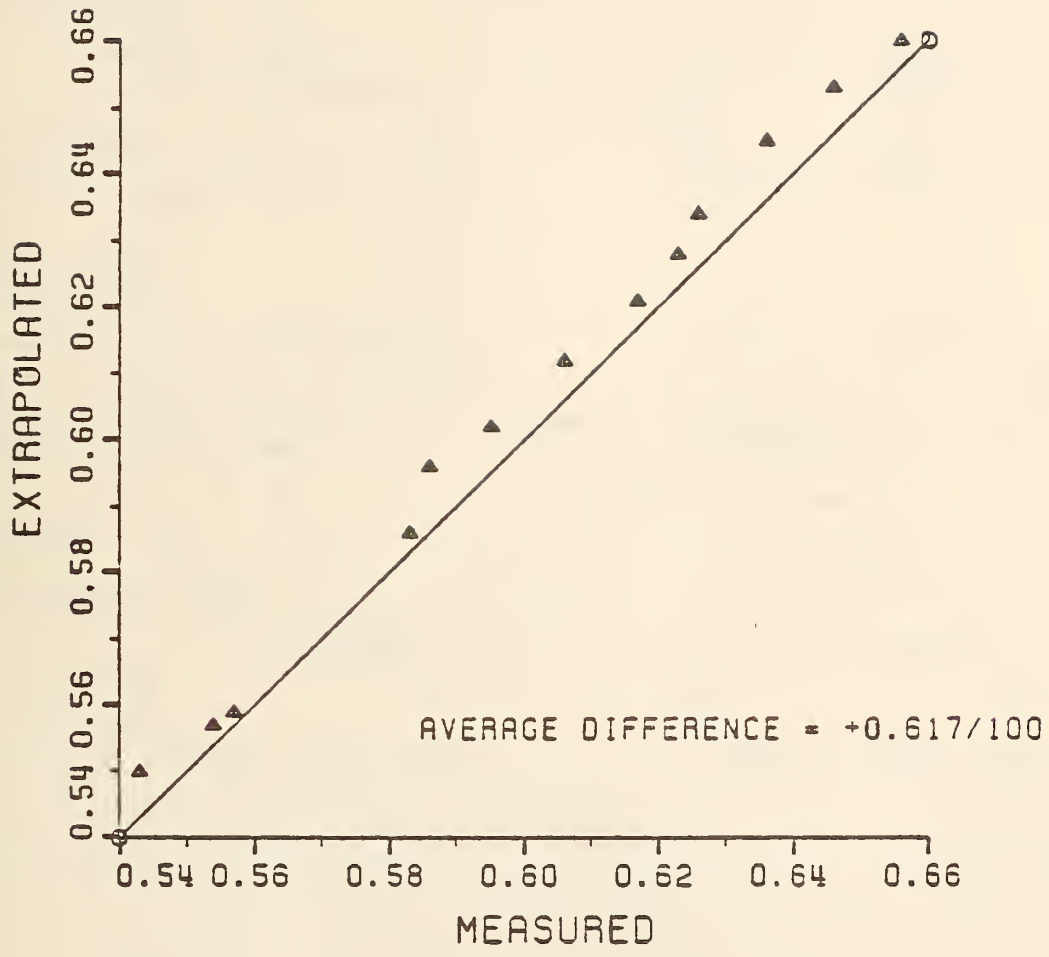

Figure 4.3.22. Comparison of measured $F_R(\tau\alpha)$ to values extrapolated from linearized efficiency curves

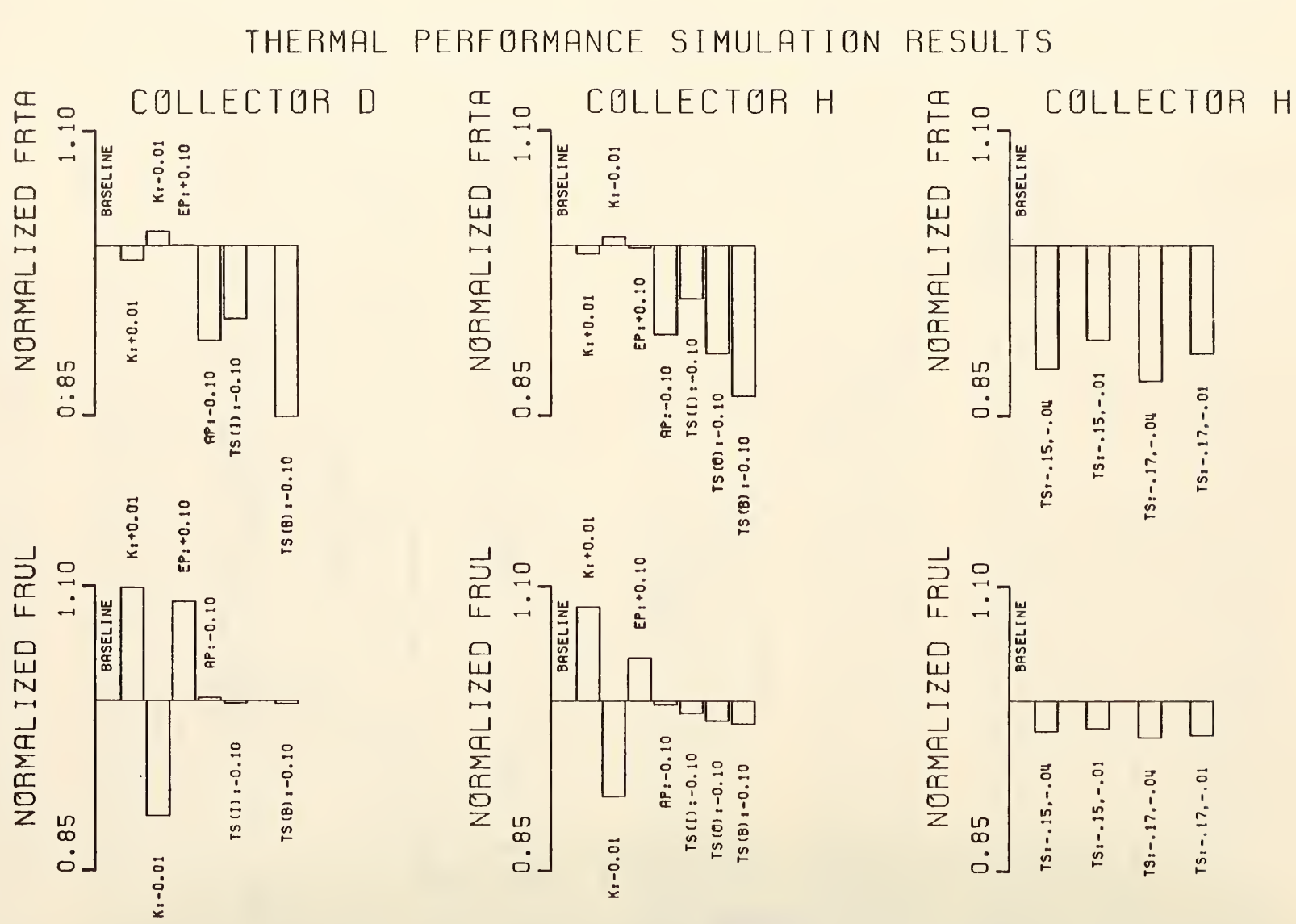

Figure 4.4.1. Calculated effects on thermal performance of material property changes for collectors D & H

Table 4.4.1 Base Case Collector Parameters for Calculating Thermal Performance Dependence on Material Properties

Dimension or Property	Units	Collector D	Collector H
Absorber			
Flow Configuration	-	parallel	serpentine
Effective Length	m	1.726	2.337
Effective Width	m	0.813	1.130
Flow Tubes: Number	-	10	8
O.D.	mm	8.1	15.88
Hydraulic Diameter	mm	4.93	12.70
Wetted Perimeter	mm	15.49	39.90
Thickness	mm	0.90	1.778
Thermal Conductivity	W/m°C	45.00	200.0
Emittance	-	0.07	0.89
Solar Absorptance	-	0.97	0.96
Cover Assembly			
Number of Covers	-	2	2
Air Space: under cover 1/under cover 2	mm	37.0/25.0	25.4/12.7
Infrared Emittance: cover 1/cover 2	-	0.84/0.84	0.33/0.76
Infrared Transmittance: cover 1/cover 2	-	0.02/0.02	0.60/0.12
Index of Refraction: cover 1/cover 2	-	1.30/1.30	1.33/1.68
Extinction Coefficient: cover 1/cover 2	mm	0.0021/0.0021	0.0275/0.1874
Thickness: cover 1/cover 2	mm	3.18/3.18	0.0254/0.1778
Insulation			
Thickness: Back	mm	88.9	25.4
Edge	mm	25.4	25.4
Conductivity: Back	W/m°C	0.04	0.02
Edge	W/m°C	0.04	0.02
Aperture Area	m^2	1.39	2.64
Gross Area	m^2	1.67	2.93

An increase in the absorber plate emittance would be expected to increase the loss coefficient U_L and have an insignificant effect on the optical parameter ($\tau\alpha$) as shown since this property controls long wavelength radiation from the absorber. The increase in ε_p by 0.1 increases $F_R U_L$ much more for collector D than for collector H since the former has a selective surface with a relatively low emittance value. Actual tests of collector D absorber plate samples showed in some cases that the plate emittance changed by approximately this amount in going from an initial value of 0.07 to 0.17 after exposure. The emittance of test samples from collector H decreased slightly after exposure from 0.89 and 0.86.

A decrease of 0.1 in the solar absorptance of the plate decreases the intercept parameters of both collectors by about 8 per cent and has a negligible effect on the efficiency curve slopes. Tests on absorber samples from both collectors showed the solar absorptance was essentially unchanged from the base case value after exposure.

The effect on $F_R(\tau\alpha)$ and $F_R U_L$ of changes in the solar transmittance of the cover system is consistent with expectations. The decreases in transmittance decrease $F_R(\tau\alpha)$ proportionately but decrease $F_R U_L$ very little. The calculations are based on the assumption that the cover reflectance is unchanged; a decrease in transmittance is assumed to increase the cover absorptance by the same amount. Consequently, the covers are somewhat warmer than in the base case and slightly reduce heat loss from the absorber. While the glass cover material of collector D would not degrade with exposure, the antireflective etching can lose its effectiveness, e.g., due to the buildup of outgassing condensation or dust. The cover system of collector H is more susceptible to degradation from exposure. Table 4.4.3 shows the effects of arbitrary decreases in solar beam transmittance of 0.10 from the base case value. The last four columns show additional results calculated for actual measured changes in transmittance for the two covers. Two samples of the outer cover, an ultraviolet-resistant PET film, experienced a decrease in transmittance from 0.85 to 0.84 and 0.81.

Table 4.4.2. Effects of Material Property Changes on $F_R(\tau\alpha)$ and F_RU_L for Collector D

	base case	k + 0.01 (W/m-°C)	k - 0.01 (Wm-°C)	ε_p + 0.10	α_p - 0.10	τ_{sbl} - 0.10 (inner)	τ_{sb} - 0.10 (both)
$\Delta t/G$ (°C-m^2/W)	Calculated efficiency (aperture area basis) (%)						
0.02	71.2	69.3	73.2	70.3	64.5	66.0	58.9
0.05	58.3	55.1	61.6	56.6	51.6	53.3	46.3
0.08	45.8	41.3	50.4	43.0	38.9	40.7	33.6
0.12	26.5	20.2	33.0	21.7	19.6	21.4	14.4
$F_R(\tau\alpha)$	0.806	0.796	0.816	0.806	0.738	0.754	0.683
F_RU_L (W/m^2-°C)	4.458	4.902	4.006	4.847	4.470	4.450	4.445
σ_η x 100 (%)	0.564	0.583	0.552	0.749	0.539	0.597	0.6032

σ_η is the mean residual error of the linear correlating curve

Base case stagnation $\Delta t/G$ rise = 0.17°C-m^2/W

Samples of the inner cover , FEP film, showed apparent changes from 0.96 to 0.81 and 0.79 after 480 days exposure. The transmittance changes in the inner cover resulted from an outgassing deposit on the inner surface which could be removed by washing. The results for the four degraded transmittance combinations are shown in the table.

Comparing calculated with the measured changes in the efficiency curve parameters (section 4.2), the observed variations in many cases for $F_R(\tau\alpha)$ are of approximately the same order. In many other cases, particularly for F_RU_L, the measured changes are not consistent with those expected solely from changes in collector material properties. Data scatter in the collector efficiency measurements most likely obscured the observation of these changes.

4.5 ABSORBER STAGNATION TEMPERATURE MEASUREMENT RESULTS

The stagnation, or no-flow, absorber plate temperature was routinely monitored with embedded thermocouples located in the center of the plate for the collectors used in the series 1 tests. Separate research was also carried out at VPI&SU to investigate the potential of alternative test procedures to detect thermal performance changes based on such temperature measurements. The data obtained were used to investigate the actual effects on collector components and to compare relative advantages of test methods based on energy output or stagnation temperature measurement.

4.5.1 General Considerations

Temperature (both ambient and collector component), solar radiation (flux and spectral distribution), and moisture availability are considered to be the significant environmental factors contributing to corrosion or degradation in optical properties of the key components of solar collectors. Therefore, the selection of exposure conditions (laboratory or field), the development of test procedures (real-time and accelerated), and the evaluation of material properties after exposure to test conditions must include characterization of these factors. Long-term average and weather tape climatic data for specific sites in the United States are available from the NOAA [44]. Local differences in conditions between the test site and the weather bureau instrumentation, variations in real weather from year-to-year and the need for supplemental information to correlate with the particular collector components resulted in the need to perform measurement of real-time conditions at each site, including irradiance simulators and laboratory tests.

Table 4.4.3. Effects of Material Property Changes on $F_R(\tau\alpha)$ and F_RU_L for Collector H

	base case	k+0.01 (W/m-°C)	k-0.01 (W/m-°C)	ε_p+0.10	α_p-0.10	τ_{sb1}-0.10 (inner)	τ_{sb2}-0.10 (outer)	τ_{sb}-0.10 (both)	$\tau_{sb1/2}$= 0.81/0.81	$\tau_{sb1/2}$= 0.81/0.84	$\tau_{sb1/2}$= 0.79/0.81	$\tau_{sb1/2}$= 0.79/0.84
$\Delta t/G$ (°C-m^2/W)	Calculated efficiency (aperture area basic) (%)											
0.01	66.8	65.6	67.9	66.3	60.9	63.4	59.8	57.0	58.9	60.7	58.1	59.9
0.03	54.6	52.3	56.9	53.7	48.8	51.3	47.9	45.2	47.2	49.0	46.4	48.2
0.05	40.6	37.1	44.0	39.1	34.8	37.5	34.2	31.4	33.5	35.3	32.9	34.6
0.07	25.1	20.5	29.7	23.1	19.4	22.1	18.8	16.2	18.3	20.0	17.7	19.4
$F_R(\tau\alpha)$	0.746	0.740	0.751	0.744	0.687	0.711	0.675	0.647	0.665	0.684	0.657	0.675
F_RU_L (W/m^2-°C)	6.953	7.527	6.370	7.217	6.929	6.880	6.834	6.812	6.766	6.784	6.730	6.746
σ_η x 100 (%)	0.824	0.814	0.832	0.858	0.830	0.830	0.876	0.855	0.888	0.892	0.878	0.882

Base case stagnation $\Delta t/G$ rise = 0.12°C-m^2/W

4.5.2 Temperature

The absorber plate is considered to be one of the components of the collector most susceptible to damage because of the magnitude and range of temperatures experienced during operational and nonoperational periods. The temperature of the absorber plates during a typical nonoperational exposure day at site 2 and site 4 are shown in figures 4.5.1 and 4.5.2, respectively. The influence of absorber material and other collector construction details on the peak temperature is illustrated in figure 4.5.1 by the range from about 120°C for collector B to about 210°C for collector D. Similar temperature profiles for collectors B and D at site 4 obtained under summer and winter conditions indicate the large variations with ambient temperature and wind conditions for a non-selective, double-glazed collector with relatively large heat loss coefficients as compared to the essentially identical plate temperature exhibited by a double-glazed, selective-coated absorber with a low loss coefficient.

A comparison of the absorber plate temperatures for collectors D when exposed at sites 1, 2, and 4 and to the xenon and tungsten simulators is shown in figure 4.5.3. The higher peak temperature obtained in the tungsten simulator is attributed to the deviation in spectral distribution from the sun (larger infrared portion) and the higher environmental temperature. The higher peak temperature obtained in the xenon simulator is partially the result of the higher peak flux of 1100 W/m^2 as compared to about 1000 W/m^2 experienced outdoors. The sharper rise and fall of the temperature in the simulator results from the abrupt turn-on and shut-off of the simulator lamps.

Absorber plate and cover material temperatures and degradation are dependent upon the solar radiation flux and spectral distribution. Measurements of the spectral distribution were beyond the scope of this program except for the radiometric measurement of solar radiation below 383 nm (ultra-violet) performed at site 1. Nonoperational exposure tests [33, 45-48] typically require exposures of at least 30 days at an irradiation level of 17,000 kJ/m^2 (1500 Btu/ft^2) per day or greater. Additionally, one period of 4 hours or more with an irradiance greater than 947 W/m^2 (300 $Btu/hr\text{-}ft^2$) is generally required. Continuous solar irradiance measurements were made at each site and the total number of accumulated days in which the total daily radiation exceeded various levels was calculated for a one-year period as shown in figure 4.5.4. This figure can be used to estimate the probability and length of exposure time required to meet exposure tests with a wide range of locations in the contiguous United States. The figure shows that site 4 (Gaithersburg, MD) has a considerably lower potential for such tests as compared to the other three locations. Complete data for the measured daily solar irradiance are included in the appendix for all four test sites throughout the duration of the reliability/durability test program.

4.5.3 Combined Irradiance and Ambient Temperature

The current nonoperational test procedure requires a number of hours of simultaneous exposure to solar irradiance and ambient temperature [7]. In order to evaluate the capability of the various sites to provide these minimum conditions and to obtain a data base for recommending modifications to current practice, measurements of irradiance and ambient temperature were analyzed over a one-year period for each site. The number of hours in which the exposure condition were less than the values of irradiance for 950, 1000, 1050, and 1100 W/m^2 and 15, 20, 25, and 30°C are shown for each site in tables 4.5.1 through 4.5.4. These data show that site 4 meets the ASTM E 823 exposure condition of an irradiance of 950 W/m^2 with an ambient temperature of 25°C only 9 hours per year.

4.5.4 Use of Stagnation Temperature for Monitoring Changes in Thermal Properties

An analytical and experimental investigation was carried out to evaluate an alternative to the energy output method for measuring thermal degradation of materials used in flat-plate collectors. The method, originally proposed by Birnbreier [49], is based on measuring the temperature of the absorber under a stagnation condition before and after prolonged exposure. For a given solar irradiance level, the measured absorber stagnation temperature depends on cover transmittance, solar absorptance and infrared emittance of the absorber, and the collector loss coefficient. The method, test procedures, and results are discussed in detail in References [30-32, 50]. References [30-31] are concerned with applying the stagnation temperature methods under nearly steady-state conditions while Reference [32] considers an averaging method to account for transients in the solar irradiance profile.

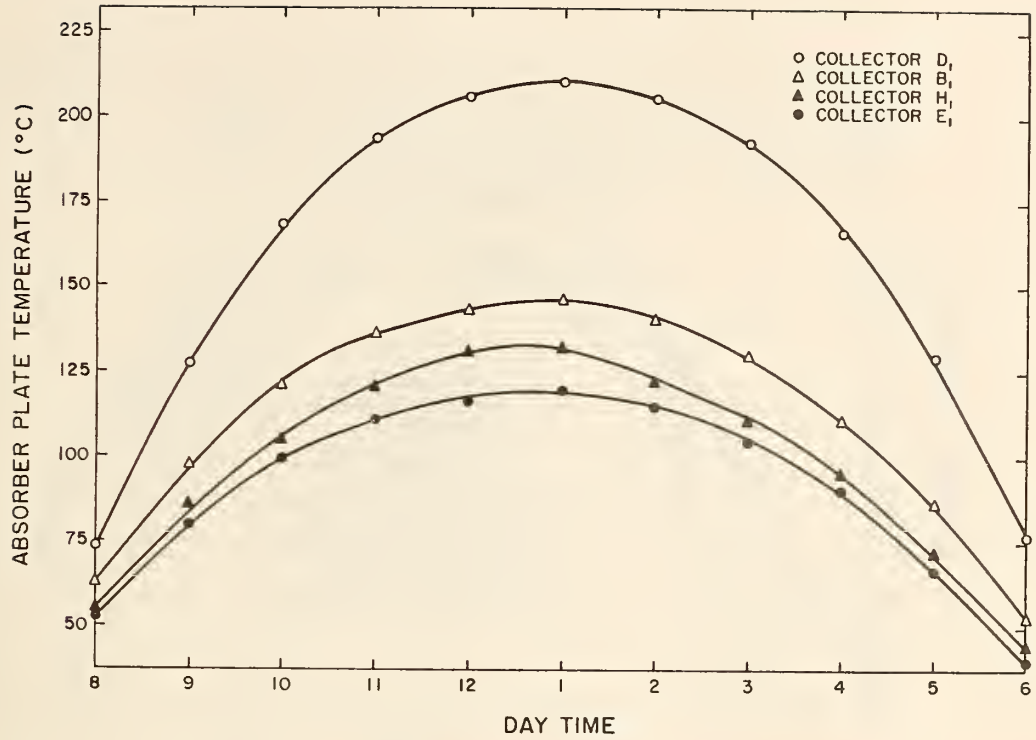

Figure 4.5.1. Typical absorber stagnation temperature profiles of exposed collectors, site 2, clear day

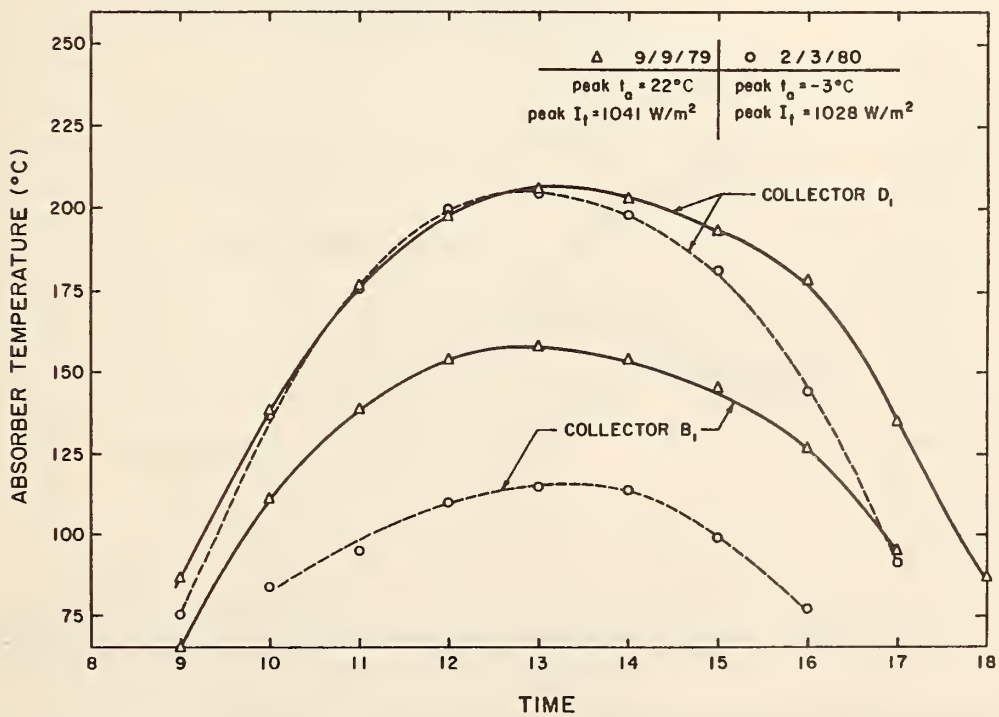

Figure 4.5.2. Daily absorber stagnation temperature profiles for double-glazed collectors B and D, site 4, clear day

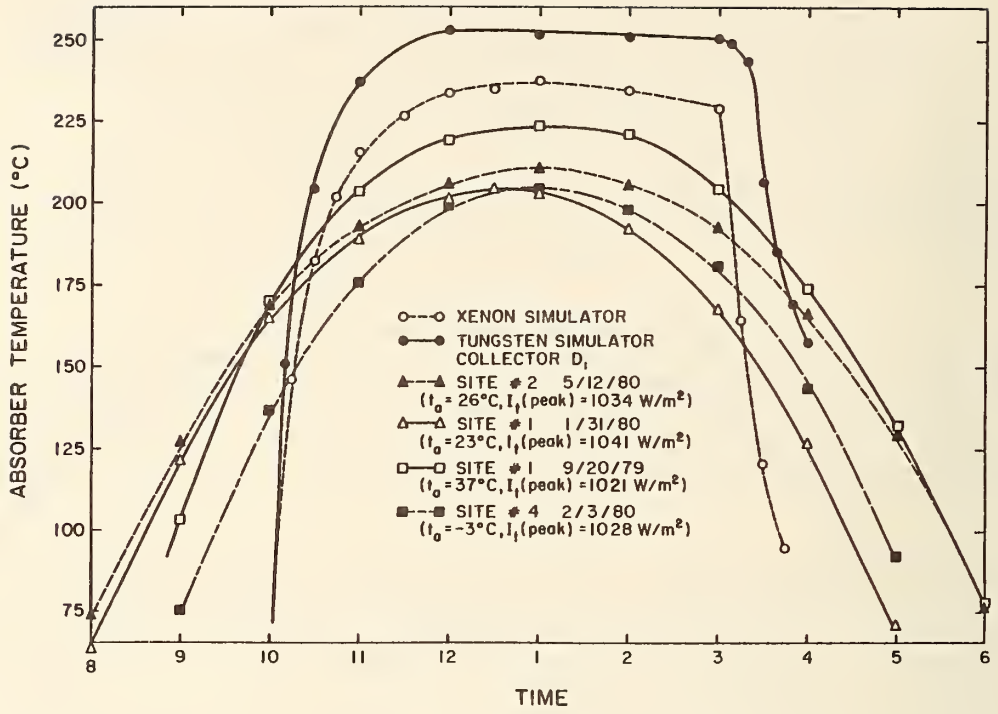

Figure 4.5.3. Comparison of absorber stagnation temperature profiles using solar irradiance simulators and outdoor exposure, collector D

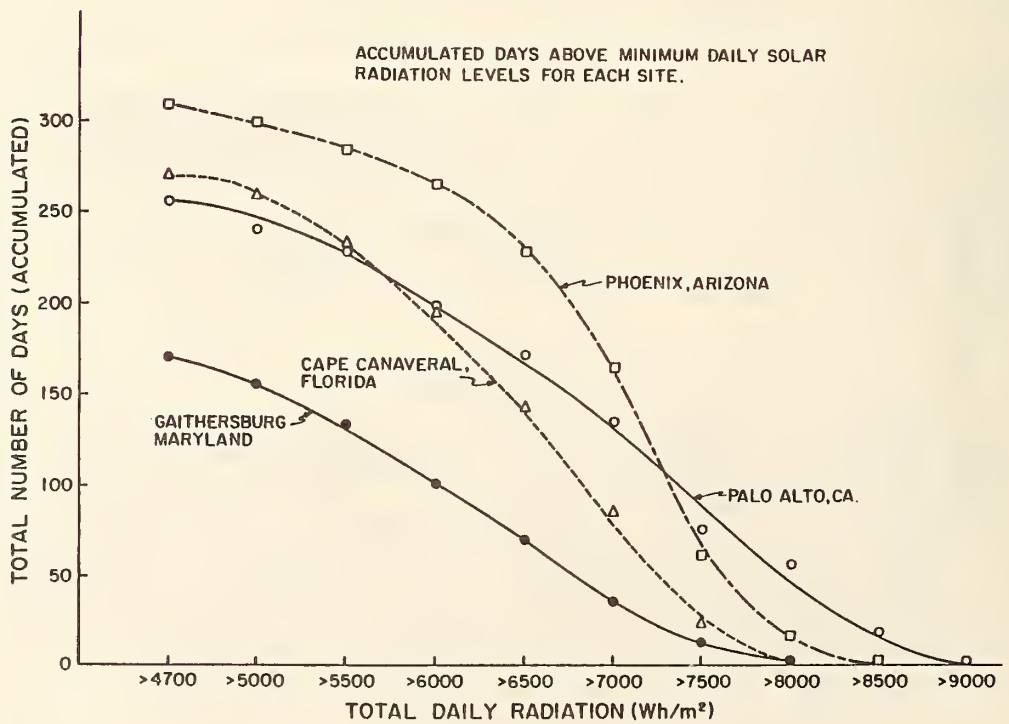

Figure 4.5.4. Days per year above minimum solar irradiance levels for each of the 4 test sites

Table 4.5.1 Hours of Exposure with Conditions Exceeding Corresponding Ambient Temperature and Irradiance Levels. Site 1, Phoenix, Arizona, July 1979 to June 1980.

	Irradiance (W/m^2)			
Ambient Temperature (°C)	950	1000	1050	1100
15	360.5	113.25	20.75	2.75
20	335	106.25	17.5	1.75
25	228.75	70.5	10.5	1.75
30	134.25	38.5	7.75	1.5

Table 4.5.2 Hours of Exposure with Conditions Exceeding Corresponding Ambient Temperature and Irradiance Levels, Site 2, Cape Canaveral, Florida, November 1979 to October 1980.

	Irradiance (W/m^2)			
Ambient Temperature (°C)	950	1000	1050	1100
15	389	177	42.5	14.0
20	324.5	136	27.5	12.0
25	230.5	77	12.0	7.5
30	94.5	19.5	3.0	0

Table 4.5.3 Hours of Exposure with Conditions Exceeding Corresponding Ambient Temperature and Irradiance Levels, Site 3, Palo Alto, California, July 1979 to June 1980.

	Irradiance (W/m^2)			
Ambient Temperature (°C)	950	1000	1050	1100
15	453	128	4.5	0
20	291	92	3.0	0
25	173	60	2.0	0
30	38	11.5	0	0

Table 4.5.4 Hours of Exposure with Conditions Exceeding Corresponding Ambient Temperature and Irradiance Levels, Site 4, Gaithersburg, Maryland, April 1979 to March 1980.

	Irradiance (W/m^2)			
Ambient Temperature (°C)	950	1000	1050	1100
15	56.25	22	1.5	0.25
20	35.5	13.5	1.0	0.25
25	9.0	4.0	--	--
30	2.5	1.0	--	--

The advantages and limitations of the proposed method are briefly summarized here; the reader is referred to the references for detailed information. The investigations showed that the proposed method is as sensitive to small changes in collector material properties as the currently used method based on measuring the energy output. Figure 4.5.5 shows the sensitivity of the new method to a range of property changes for typical collectors. In this figure, the abscissa is the stagnation temperature rise of the absorber above ambient normalized by the initial value. Property changes on the order of 0.1 in plate absorptance, cover solar transmittance, and plate emittance would be detectable using the new method with the exception of cover transmittance for collector E which would be only marginally detectable. While the measurements required in the stagnation temperature method are much simpler than those required to measure energy output, other factors, such as nonisothermal absorbers, variations in environmental conditions, and transient response, must be taken into account. Figure 4.5.5 assumes that the environmental conditions are essentially constant and that steady-state conditions exist. Figure 4.5.6 shows the variation of normalized stagnation temperature rise as a function of environmental parameters for collectors D and E. Clearly, wind speed, ambient temperature, and solar irradiance have the largest effect on measured stagnation temperature. These parameters, however, primarily affect U_L rather than $(\tau\alpha)$.

The investigation showed that even small transients in the solar irradiance profile greatly complicates the determination of small property changes. Reference [32] describes a method for reconciling problems arising from short-term transients in the solar irradiance profile as well as long-term variations in daily solar radiation. This method is based on measuring the absorber temperature continuously over a period of several days along with the total daily solar irradiation. The absorber temperature rise above ambient is then integrated to determine a daily value. The measurements provide data for a graph of the integrated absorber temperature parameter vs total daily irradiation in the collector aperture. Comparison of two such graphs, based respectively on data obtained over a period of several days before and after a prolonged durability exposure, show if the thermal properties of the collector have changed significantly. Using this approach, calculations showed that the effect of short-term transients in the daily irradiance profile is insignificant. Figure 4.5.7 shows expected results from using all-day integrated parameters for stagnation temperature and solar irradiation for a typical change in plate absorptivity.

The investigation showed that the all-day integration method is a viable approach for detecting changes in material properties that has advantages over alternative test methods based on steady-state measurements of either absorber stagnation temperature or collector energy output. Previously, the temperature measurement approach was limited to short time periods near solar noon on clear days outdoors or to using solar irradiance simulators indoors. Outdoor test data over a relatively short period of time was obtained to validate the calculated results and depict typical expected results using the test procedure. The principle limitation of both stagnation temperature methods, however, is the strong effect of other environmental conditions, particular wind speed, on the test results. It should also be noted that neither the temperature nor energy output measurement method can directly identify the particular material property that changed in a collector. With limitations on wind speed and for relatively clear days, the preliminary investigation suggests that stagnation temperature rise is a reproducible collector performance parameter which is at least as sensitive as the ASHRAE 93-77 method and much less expensive to measure. The method is applicable to a broad range of collector designs and can be extended to form the basis for simple comparative materials tests.

4.6 GENERAL OBSERVATIONS ON OUTDOOR TEST METHODS FOR MEASUREMENT OF COLLECTOR PERFORMANCE DEGRADATION

Except for catastrophic failures and some obvious problems with a few plastic glazing materials, the test program collectors, which are typical of modern commercial equipment, were quite durable in thermal performance and held up very well under unusually adverse nonoperational conditions over a period of approximately 3 years.

Neither the energy output measurement method or alternative methods based on measuring stagnation temperature are entirely satisfactory for determining the typically small property changes in materials that occurred during the test period. The stagnation temperature method involved simpler measurements and would be less expensive. However, this method has neither been validated extensively nor subjected to broad field experience. While the energy output measurement is widely used and accepted by the solar energy community for assessing solar collector thermal performance, variations in measured performance parameters are higher than is desirable for direct comparison of results to determine degradation in collector material properties.

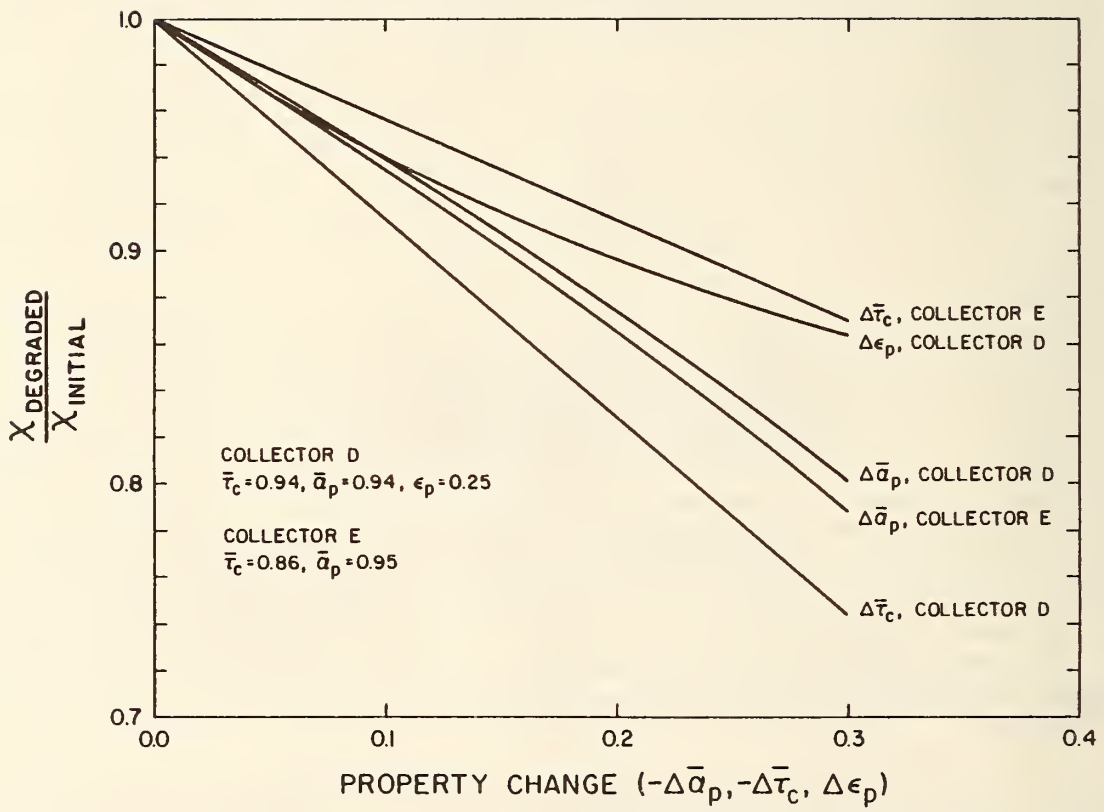

Figure 4.5.5. Sensitivity of normalized absorber stagnation temperature to changes in material properties

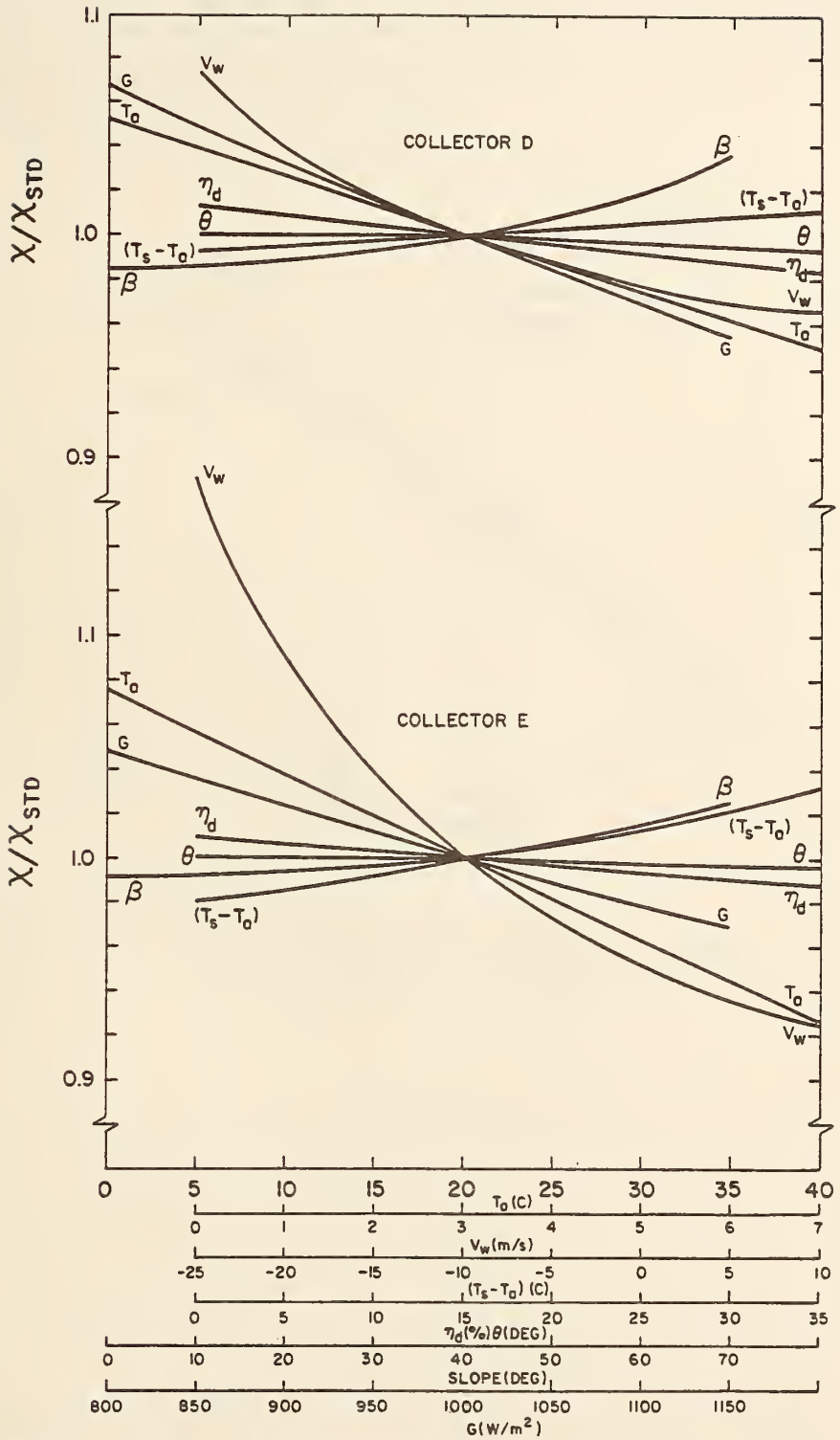

Figure 4.5.6. Effect of environmental test conditions on normalized absorber stagnation measurements

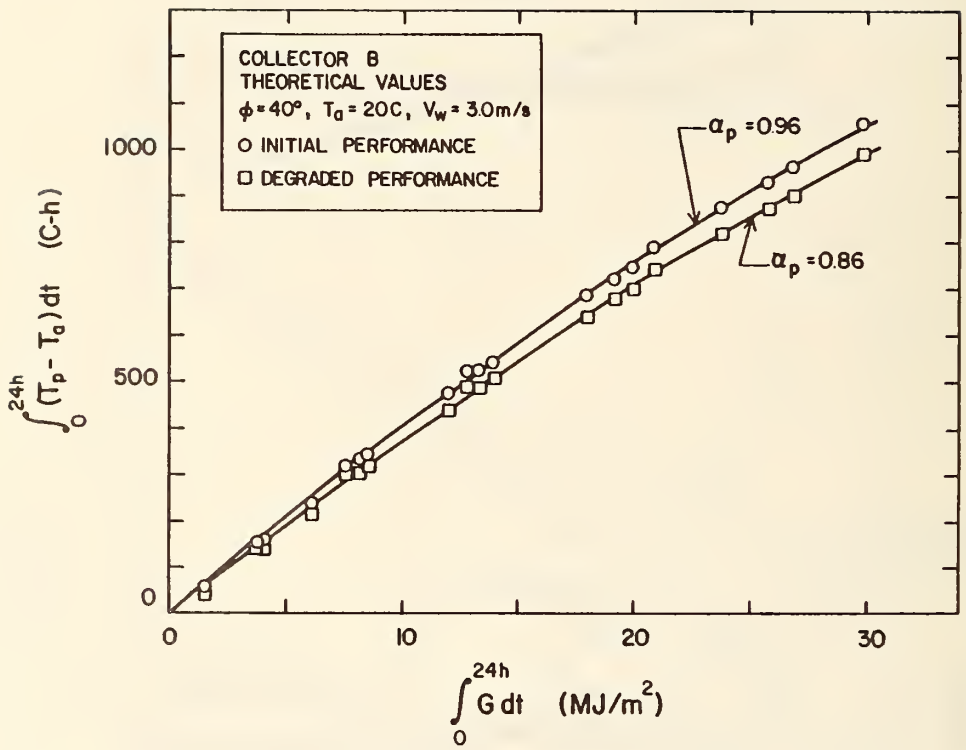

Figure 4.5.7. Sensitivity of the all-day integration method to a 0.10 change in plate absorptance for collector B

The precision of the measured thermal performance parameters, $F_R(\tau\alpha)$ and F_RU_L, obtained in this reliability/durability test program are consistent with the experimental error inherent in the current ASHRAE 93-77 test method [6]. For comparison, the variation in $F_R(\tau\alpha)$ and F_RU_L is somewhat better than in the original roundrobin test program [39] conducted by NBS. In that program, the coefficient of variation (standard deviation in percent of mean value) was 4.6 - 7.7 percent for $F_R(\tau\alpha)$ and 16 - 25 percent for F_RU_L. In a subsequent Department of Energy comparability test program [51], coefficients of variation for $F_R(\tau\alpha)$ ranged from 2.0 - 6.0 percent and ranged from 3.0 - 18 percent for F_RU_L. In the current test program, the coefficient of variation for the initial testing was 1.5 - 4.0 percent for $F_R(\tau\alpha)$ and 5 - 13 percent for F_RU_L. The data from these three test programs and the supporting analysis of the various factors which could affect the data show that the variations in the thermal performance results presented herein are within the precision limits of the current ASHRAE 93-77 test standard.

5. CONCLUSIONS AND RECOMMENDATIONS

In this section, the significant observations and recommendations resulting from this test program are summarized. These findings are primarily concerned with an evaluation of test methods for determining the thermal performance and durability of solar collectors and their materials. During the course of this investigation, significant research findings have been published in the open literature and presented to appropriate organizations concerned with the development of standards for solar collectors and their materials such as ASTM and ASHRAE.

5.1 COVER MATERIALS

- Outdoor exposure at sites having a combination of high prevailing humidity and high solar radiation generally produced more severe changes in polymeric cover materials than the other test sites. The most extensive microcracking and optical transmission losses occurred during the outdoor exposure of full-size solar collectors and cover mini-boxes at the test sites located in Cape Canaveral and Palo Alto. Next in order of severity were changes observed at the Gaithersburg site followed by those at the Phoenix site. This is consistent with the findings of Clark and Roberts [52] for cover specimens exposed in Florida and Arizona. It is most likely due to the combined effects of photodegradation and cyclic shrinking and swelling of the polymer surface due to moisture wetting and drying. It is essential that outdoor exposure testing include the combinations of environmental exposure parameters that will occur in normal use.

- Outdoor "real time" exposure on cover mini-boxes for 480 days ($\geq$ 17,000 kJ/m^2/day) is required for many polymeric materials in order to induce degradation that is detectable without sophisticated analysis. This is equivalent to two or more calendar years. Changes such as microcracking and embrittlement were not readily observable in shorter periods of time for many materials.

- Accelerated outdoor exposure of polymeric cover materials for 120 calendar days produced changes similar to those occurring in 480 days of "real time" exposure ($\geq$ 17,000 kJ/m^2/day). The cover specimens were mounted on the accelerated exposure cover mini-boxes shown in figure 2.2.2 of this report and exposed to concentrated sunlight ($\sim$ 6 suns) and an intermittent water spray using the apparatus described in ASTM E 838 [36].

- Outdoor exposure of cover materials at elevated temperatures representative of both operational and stagnation conditions is needed to assess the durability of polymeric covers of solar collectors. Elevated temperatures have an accelerating influence on the degradation of polymeric materials. In addition, exposure to stagnation temperatures resulted in the loss of ultraviolet radiation screening additives from several of the materials studied. Another consideration is that many polymers are more susceptible to degradation when heated above their glass transition temperature. The cover temperatures in stagnating solar collectors are higher than the glass transition temperatures of many polymers. The "real time" cover mini-boxes used in this test program produced cover temperatures representative of operational conditions in full-size flat-plate solar collectors. By controlling the cooling air flow in the accelerated outdoor test apparatus, it was possible to attain cover temperatures representative of stagnation conditions.

- Currently recognized indoor laboratory exposure tests are not capable of reproducing many of the changes observed in this program for polymeric materials exposed outdoors. The indoor laboratory exposure testing conducted in this test program, which used test procedures similar to those in ASTM E 765 [8], did not duplicate the extensive microcracking observed outdoors. Other testing for 1200 hours using a xenon arc weathering machine and an intermittent water spray, as specified in ASTM E 765, was also unsuccessful in duplicating this microcracking. In addition to causing light transmission losses, microcracking is of particular importance when thin film polymers are used as glazing because of its influence on mechanical properties. Yamasaki and Blaga [53] have had some success in using an indoor test to duplicate the surface degradation occurring outdoors on glass-fiber reinforced polyester sheets. However, several thousand hours of exposure in a weathering machine is required.

- Heat stability testing of cover materials at a temperature of 90°C in addition to the temperatures currently specified in ASTM E 765 [8] is desirable. ASTM E 765 currently specifies the use of two temperatures for screening purposes; 75°C for outer and single cover materials and 125°C for inner cover materials. Mathematical modelling has shown that the covers of single-glazed flat-plate solar collectors can reach 90°C under stagnation conditions with zero wind speed and solar radiation levels of 1000 W/m^2. Since the degradation of polymeric materials is accelerated by exposure to elevated temperatures, it is desirable to test covers for single-glazed collectors at 90°C.

- Accelerated aging of cover materials using xenon arc weathering machines should be performed at temperatures representative of stagnation conditions. Materials exposed to xenon arc radiation at 90°C, the temperature of single glazing in stagnating flat-plate solar collectors, had considerably more degradation than samples of the same materials exposed at 70°C. Another consideration is the loss or degradation of ultraviolet radiation screening additives at elevated temperatures.

- Exposure testing of polymeric glazings using elevated temperature and humidity conditions produced changes considerably different from those caused by outdoor exposure of samples of the same materials. The primary value of this type of long-term test would be for glazings of trickle down collectors and polymeric storage tanks where continuous exposure to moisture at elevated temperatures is likely. As was previously mentioned, there is a need for the development of an aging test which takes into account the synergistic effects of moisture, temperature, and sunlight. Cyclic moisture exposure to cause shrinking and swelling of the polymer should be considered as part of such a test.

- Normal and hemispherical spectral transmittance curves measured in the ultraviolet - visible spectral region are more sensitive indicators of cover materials degradation than integrated spectral transmittance values determined in accordance with ASTM E 424 [34]. Emphasis in current ASTM methods concerned with the durability of cover materials [8, 9, 11] has been placed on the use of integrated spectral transmittance values for measuring optical property changes in glazings. These integrated values are indicators of changes in the engineering properties of glazing materials and provide the type of data required by solar collector designers. However, they are not sensitive to spectral changes that occur in a limited part of the solar spectrum, i.e., at short wavelengths in many polymers. Since little or no energy is found in the solar spectrum in this short wavelength region, integrated spectral transmittance measurements are of little value in detecting these changes which are sensitive indicators of degradation in many polymers. More emphasis should be placed on the analysis of spectral curves.

- Normal ultraviolet-visible spectral transmittance measurements have greater sensitivity to chemical and/or physical changes in cover materials than hemispherical transmittance spectra. The normal measurements are a sensitive indicator of changes in light scattering.

- There is a need for data on the infrared spectral properties of organic materials; e.g. emittance and diffuse transmittance. These data are needed for the mathematical modelling of collector designs and the calculation of exposure temperatures.

5.2 ABSORBER MATERIALS

- Outdoor exposure of small-scale absorber samples mounted on the absorber of a simulated collector is an effective method for determining the thermal stability of large numbers of samples under stagnation conditions; however, it is not a valid test for determining the stability in the presence of moisture of these materials when used in solar collectors. In both ASTM E 781 [13] and this test program, care was taken to prevent moisture penetration at joints, seams, and seals. However as was observed in this test program, moisture penetration in full-size solar collectors appears to be a common occurrence. This moisture penetration resulted in corrosion and appearance changes not observed with small-scale specimens.

- Both the simulated solar collectors discussed above and the accelerated exposure mini-boxes used in this test program (see figure 2.2.5) are useful for exposing small absorber test specimens to stagnation temperatures; however, unlike the case with

cover materials, it is not clear that exposure to concentrated solar radiation accelerated the photolytic degradation of absorber materials. Similar changes were observed for test specimens exposed to concentrated sunlight in the mini-boxes and to "real time" conditions in the simulated collectors.

- Indoor laboratory exposure of absorber test specimens to temperatures characteristic of stagnating solar collectors is an effective method for determining their thermal stability. Temperature exposure produced thermal changes similar to those which occurred in the outdoor exposure of absorber test specimens.

- Exposure testing of absorber materials with continuous elevated temperature and humidity exposure conditions, such as those used in this test program, produced changes that are considerably more severe than those produced by the outdoor exposure of materials of the same composition in full-size solar collectors and exposure test boxes. The moisture exposure conditions specified in ASTM E 744 [12], 90°C and 95 percent relative humidity for 30 days, need to be reexamined since these conditions, which are similar to those used in this test program, may be unduly severe. Materials which are severely degraded as a result of exposure using these test conditions may still be capable of providing adequate service as absorbers in flat-plate solar collectors.

- Exposure to xenon arc radiation at elevated temperature produced significant optical property changes in several of the selective absorber materials studied. Exposure testing with xenon arc radiation should be performed at temperatures representative of solar collector operating conditions since degradation rates are generally accelerated by elevating the exposure temperature. The spectral transmission characteristics of the cover(s) used in a solar collector will control the amount, and spectral distribution, of the solar radiation reaching the absorber surface. For this reason, testing should be performed with the glazings to be used in the actual collector installed between the light source and the absorber surface, or with the worst-case configuration possible. The light source should be filtered to match the solar spectrum.

- The thermal cycling test most closely simulated the types of corrosion and other changes that were observed in full-size solar collectors. In this test, coupon specimens were removed from a chamber at -10°C and allowed to equilibrate at room temperature prior to being placed in an oven at 177°C. During this equilibration process, moisture condensed on the test specimen surfaces; this wetting most likely led to the corrosion observed. Because of the apparent importance of the condensed moisture, the humidity needs to be controlled during the equilibration process.

- Research needs to be conducted to define the extent to which the absorber materials in operational solar collectors are exposed to moisture. Factors such as wetting time, absorber temperature, diurnal breathing, and environmental exposure conditions need to be considered in this research. The problem of how to determine the proper test conditions for assessing the moisture stability of absorber materials is very complex, i.e., the presence of moisture on the inner surface of the glazing of a collector that is stagnating on a clear day does not mean that the relative humidity in the vicinity of the absorber is anywhere near as high as that in the vicinity of the glazing, since absorber temperatures are much higher than cover temperatures. In addition, the presence of porosity in many absorber coatings means that moisture can condense in these pores at humidities lower than 100 percent relative humidity. It is more likely that moisture would condense out on the absorber at night when it is cool rather than in the daytime. The problem is further exacerbated by the presence of moisture due to water leakage in many solar collectors, in addition to condensation caused by diurnal collector breathing.

- Spectral reflectance curves are a more sensitive indicator of absorber materials degradation than solar absorptance values determined by integrating over a standard solar energy distribution curve. Current ASTM standards concerned with the durability of absorber materials [12, 13] rely on the use of integrated values determined in accordance with ASTM E 424 [34]. Spectral reflectance changes in the near infrared region are a sensitive indicator of early degradation in many absorber materials. Since the solar spectrum contains very little energy in this region, integration tends to conceal these changes.

- Absorber materials generally exhibited larger changes in emittance than in integrated solar absorptance for both the outdoor exposure and indoor laboratory tests. Of the thirteen different types of absorber materials studied, the aluminum oxide conversion coating, material N, was the only exception to this trend.

- The absorber samples tested must duplicate the full-scale collector material in substrate, preparation, and coating application techniques to provide valid test results. The variability of black chrome performance with processing parameters is an example of this type of consideration.

5.3 SOLAR COLLECTORS

- Neither energy output measurements, based on ASHRAE Standard 93-77, nor stagnation temperature measurement methods are satisfactory for determining changes in material properties observed after outdoor exposure. Collector thermal performance measurements are not sufficiently sensitive and precise under typical test environments to detect the relatively small changes in efficiency curve slope and intercept resulting from changes in material properties (cover transmittance, absorber absorptance and emittance, and insulation thermal conductivity) caused by 480 days of outdoor exposure ($\geqslant$ 17,000 kJ/m^2/day).

- The absorber stagnation temperature methods evaluated during this investigation are at least as good an indicator of solar collector thermal performance changes, with the exception of bond conductance, as the ASHRAE 93-77 test method and are less expensive to implement.

- Initial reliability/durability screening tests for materials considered for use in solar collectors should be performed both in the laboratory and outdoors on small-scale samples using materials exposure tests such as those used in this program. These small-scale tests can be used to narrow down the choice of materials. Careful field measurement of peak stagnation temperatures for full-size collectors or extrapolation of thermal performance curves should be used as a basis for determining appropriate exposure test conditions.

- The final selection of materials for use in solar collectors should be based both on the results of small-scale materials tests and on an evaluation of the properties of materials samples taken from full-size solar collectors exposed outdoors. Materials should be capable of withstanding stagnation conditions without property changes greater than those allowed for in the collector design. Exposure testing of full-size collectors makes possible an evaluation of materials interactions that may not be obvious from small-scale materials tests. Additional consideration needs to be given to changes in the mechanical properties of solar collector materials; especially thin film glazings.

- The uncertainty in the measured efficiency curve intercept and slope parameters are as expected considering the inherent precision in the ASHRAE 93-77 test method. The coefficients of variation for the initial baseline tests of the eight collector types, from all test sites, were from 1.5 to 4.0 percent for the intercept parameter and 5 to 13 percent for the slope parameter. Statistical analyses of the test data showed no systematic trends, either higher or lower, with the site performing the testing or with individual collector test stands at a particular test site.

- Intercept values determined from linear first-order correlations of efficiency data provided good agreement with those obtained from second-order correlations. The effect on the intercept was less than one percent in all cases, with the linear curve always giving an intercept higher than the second-order curve.

- For flat-plate collectors of conventional design, calculation procedures are capable of giving results at least as good as those obtained with the ASHRAE 93-77 measurement procedure for the incident angle modifier. A coefficient of variation for the incident angle modifier parameter of 34 percent was found for measurements made on solar collectors of the same type at three test sites.

- A comparison of results obtained under natural outdoor test conditions with those obtained using tungsten-halogen and xenon arc simulators showed that higher

thermal performance results can be obtained with the solar irradiance simulators for collectors having polymeric covers. The highest results were obtained with the xenon arc simulator.

- Stagnation exposure testing of flat-plate solar collectors intended for use in systems with solar radiation augmentation reflectors should be conducted with these reflectors in place. Stagnation exposure testing of flat-plate solar collectors, in this program, for 60 days with reflectors ($\geq$ 17,000 kJ/m^2/day measured in the plane of the collector without reflectors) appeared to cause more severe thermal degradation than 480 days ($\geq$ 17,000 kJ/m^2/day) of stagnation exposure of the same types of collectors without the reflectors.

- The peak stagnation temperature for flat-plate solar collectors should be measured at a distance approximately one-fourth of the way below the top of the collector and with the collector tilted so that its aperture is normal to the sun. The magnitude of the peak temperature needs to be taken into account for both safety and durability considerations when selecting materials to withstand stagnation conditions. Measurements made as part of this test program [50] have shown that absorber and cover stagnation temperatures vary as a function of tilt angle and position on the absorber. This is most likely due to the combination of thermal stratification of air inside the collector and edge losses.

- Over a period of approximately three years, pyranometer sensitivity changes, if not calibrated out, could give rise to errors comparable to the uncertainty in the measured collector efficiency. These pyranometer calibration changes are not linear with respect to exposure time. Temperature dependence of the pyranometers, which had built-in temperature compensation circuits, was not found to be significant.

- There is a need for a water leakage test for flat-plate solar collectors similar to the test described in ASTM E 331 [54] for exterior windows, curtain walls, and doors. This method includes the use of a pressure differential, similar to that occurring with wind driven rain, to enhance the penetration of water into the assembly being tested. This test method could be simplified for flat-plate collectors by applying a negative pressure inside the collector case to induce the pressure differential.

  Several of the collectors used in this test program and others observed in the field showed signs of excessive internal moisture which appeared to result from leakage rather than condensation caused by diurnal collector breathing. The presence of moisture and resulting degradation of materials appears to be strongly dependent on both the design of collector joints and seams and the quality of workmanship in assembling the collectors. In several cases where two collectors of the same type were exposed side by side, only one of the two absorbers showed significant corrosion. Materials used in flat-plate collectors should be moisture resistant unless the collector is hermetically sealed.

- Outgassing deposits were observed on the glazings of virtually all of the solar collectors exposed in the test program. However, changes due to this outgassing could not be discerned by thermal performance measurements. The outgassing was especially severe in the case of collector H. All of the paint absorber coatings studied in this program caused a buildup of outgassing deposits on the glazing of absorber test box in which they were exposed. Other potential sources of outgassing include insulation materials, gaskets and sealants, and adhesives.

- The thermal shock/water spray test did not cause thermal shock problems in any of the solar collectors subjected to this test in this program.

6. REFERENCES

1. "Solar Heating and Cooling Demonstration Act of 1974," Public Law 93-409, September 3, 1974.

2. "Solar Energy Research, Development and Demonstration Act," Public Law 93-473, October 26, 1974.

3. "National Program for Solar Heating and Cooling of Buildings," Report No. ERDA 76-6, Energy Research and Development Administration (now Department of Energy), Washington, DC 20545, November 1976.

4. "Methods of Testing to Determine the Thermal Performance of Solar Domestic Water Heating Systems," ASHRAE Standard 95-1981, American Society for Heating, Refrigerating, and Air-Conditioning Engineers, Inc., 1791 Tullie Circle, N.E., Atlanta, GA, December 1981.

5. "Methods of Testing Thermal Storage Devices Based on Thermal Performance," ASHRAE Standard 94-77, ibid., February 1977.

6. "Methods of Testing to Determine the Thermal Performance of Solar Collectors," ASHRAE Standard 93-77, ibid., February 1977.

7. "Practice for Nonoperational Exposure and Inspection of a Solar Collector," ASTM E 823-81, American Society for Testing and Materials, 1916 Race St., Philadelphia, PA 19103.

8. "Practice for Evaluation of Cover Materials for Flat-Plate Solar Collectors," ASTM E 765-80, ibid.

9. "Practice for Exposure of Cover Materials for Solar Collectors to Natural Weathering Under Conditions Simulating Operational Mode," ASTM E 782-81, ibid.

10. "Practice for Determining Resistance of Solar Collector Covers to Hail by Impact with Propelled Ice Balls," ASTM E 822-81, ibid.

11. "Practice for Exposure of Solar Collector Cover Materials to Natural Weathering Under Conditions Simulating Stagnation Mode," ASTM E 881-82, ibid.

12. "Practice for Evaluating Solar Absorptive Materials for Thermal Applications," ASTM E 744-80, ibid.

13. "Practice for Evaluating Absorptive Solar Receiver Materials When Exposed to Conditions Simulating Stagnation in Solar Collectors with Cover Plates," ASTM E 781-81, ibid.

14. "Specification for Rubber Seals Used in Flat-Plate Solar Collectors," ASTM D 3667-78, ibid.

15. "Specification for Rubber Seals Used in Concentrating Solar Collectors," ASTM D 3771-79, ibid.

16. "Specification for Rubber Seals Contacting Liquids in Solar Energy Systems," ASTM D 3832-79, ibid.

17. "Specification for Rubber Seals Used in Air-Heat Transport of Solar Energy Systems," ASTM D 3903-80, ibid.

18. "Specification for Rubber Hose Used in Solar Energy Systems," ASTM D 3952-80, ibid.

19. "Practice for Laboratory Screening of Metallic Containment Materials for Use with Liquids in Solar Heating and Cooling Systems," ASTM E 712-80, ibid.

20. "Practice for Simulated Service Testing for Corrosion of Metallic Containment Materials for Use with Heat Transfer Fluids in Solar Heating and Cooling Systems," ASTM E 745-80, ibid.

21. "Practice for Screening Polymeric Containment Materials for the Effects of Heat and Heat Transfer Fluids in Solar Heating and Cooling Systems," ASTM E 862-82, ibid.

22. Waksman, D., Streed, E. R., and J. Seiler, "NBS Solar Collector Durability/Reliability Test Program Plan," NBS Technical Note 1136, National Bureau of Standards, Washington, DC 20234, January 1981.

23. Streed E. R. and Waksman, D., "NBS Solar Collector Durability/Reliability Program," Durability of Building Materials and Components, ASTM STP 691, P. J. Sereda and G. G. Litvan, Eds., American Society for Testing and Materials, 1980, pp. 239-249.

24. Streed E. R., and Waksman, D., "Uncertainty in Determining Thermal Performance of Liquid-Heating Flat-Plate Solar Collectors," Journal of Solar Energy Engineering, ASME, Vol. 103, May 1981, pp. 126-134.

25. Streed E. R. and Waksman, D., "Uncertainty in Determining Thermal Performance of Liquid-Heating Flat-Plate Solar Collectors," NBS Technical Note 1140, National Bureau of Standards, Washington, DC 20234, March 1981.

26. Thomas, W. C., Dawson, A. G., III, Waksman, D., and Streed, E. R., "Incident Angle Modifiers for Flat-Plate Solar Collectors: Analysis of Measurement and Calculation Procedures," Journal of Solar Energy Engineering, ASME, Vol. 104, November 1982, pp. 349-357.

27. Thomas, W. C., Dawson, A. G., III, Waksman, D., and Streed, E. R., "Determination of Incident Angle Modifiers for Flat-Plate Solar Collectors," Proceedings of ASME Solar Energy Division: Fourth Annual Conference, April 1982, pp. 501-510.

28. Streed, E. R., Waksman, D., Dawson, A. G., III, and Lunde, A., "Comparison of Solar Simulator and Outdoor ASHRAE Standard 93 Thermal Performance Tests," Proceedings of 1980 Annual Meeting, American Section of the International Solar Energy Society, June 1980, pp. 405-409.

29. Waksman, D., Streed, E. R., and Dawson, A. G., III, "The Influence of Environmental Exposure on Solar Collectors and Their Materials," Proceedings of 1980 Annual Meeting, American Section of the International Solar Energy Society, June 1980, pp. 415-419.

30. Dawson, A. G., III, Thomas, W. C., and Waksman, D., "Evaluation of Absorber Stagnation Temperature as a Characteristic Performance Parameter of Flat-Plate Solar Collectors," ASME Paper 82-WA/Sol-5, American Society of Mechanical Engineers, New York, NY 10017, November 1982.

31. Dawson, A. G., III, Thomas, W. C., and Waksman, D.. "Solar Collector Durability Evaluation by Stagnation Temperature Measurements," Journal of Solar Energy Engineering, ASME, Vol. 105, August 1983, pp. 259-267.

32. Thomas, W. C., Dawson, A. G., III, and Waksman, D., "Testing Solar Collector Materials Durability by Integrated Day-Long Stagnation Temperature Measurements," Proceedings of ASME Solar Energy Division: Fifth Annual Technical Conference, April 1983, pp. 301-307.

33. Waksman, D., Streed, E. R., Reichard, T. W., and Cattaneo, L. E., "Provisional Flat-Plate Solar Collector Testing Procedures: First Revision," NBS Interagency Report 78-1305A, National Bureau of Standards, Washington, DC 20234, June 1978.

34. "Test for Solar Energy Transmittance and Reflectance (Terrestrial) of Sheet Materials," ASTM E 424-71, op. cit. 7.

35. "Test for Total Normal Emittance of Surfaces Using Inspection-Meter Techniques," ASTM E 408-71, op. cit. 7.

36. "Practice for Performing Accelerated Outdoor Weathering Using Concentrated Natural Sunlight," ASTM E 838-81, op. cit. 7.

37. Newland G. C. and Tamblyn, J. W., " Mechanism of Ultraviolet Stabilization of Polymers by Aromatic Salicylates," Journal of Applied Polymer Science, 8, 1964, pp. 1949-1956.

38. Moore, S. W., "Los Alamos Optical Materials Reliability, Maintainability, and Exposure Testing Program," Report No. LA 9735 MS, Los Alamos National Laboratory, Los Alamos, New Mexico, 1983.

39. Streed, E. R., Thomas, W. C., Dawson, A. G., III, Wood, B. D., and Hill, J. E., "Results and Analysis of a Round-Robin Test Program for Liquid-Heating Flat-Plate Solar Collectors," NBS Technical Note 975, National Bureau of Standards, Washington, DC 20234, August 1978.

40. Thomas, W. C., "Solar Collector Test Procedures: Development of a Method to Refer Measured Efficiencies to Standardized Test Conditions," Report VPI-E-80.23, Virginia Polytechnic Institute and State University, Blacksburg, VA 24061, November 1980.

41. Cheng, H. and Bannerot, R. B., "On the Weathering of Thin Plastic Films," ASME Paper 81-WA/Sol-6, American Society of Mechanical Engineers, New York, NY 10017, November 1981.

42. Douro, D. D., "Investigation of Performance Degradation and Test Methods for Flat-Plate Solar Collectors," M.S. Thesis, Mechanical Engineering Department, Virginia Polytechnic Institute and State University, Blacksburg, VA 24061, June 1982.

43. Culkin, D. S., "Analysis of Flat-Plate Solar Collector Durability Test Data," M.S. Thesis, Mechanical Engineering Department, Virginia Polytechnic Institute and State University, Blacksburg, VA 24061, June 1982.

44. "Hourly Solar Radiation Surface Meteorological Observations," TD-9724, SOLMET, National Oceanic and Atmospheric Administration (NOAA), Asheville, NC, 1979.

45. "Test Methods and Minimum Standards for Certifying Solar Collectors," ISCC Document 80-1, Interstate Solar Coordination Council, December 1980.

46. "Test Methods and Minimum Standards for Certifying Solar Collectors," SRCC Standard 100-81, Solar Rating and Certification Corporation, 1001 Connecticut Avenue, NW, Washington, DC, March 1982.

47. "Standard for Solar Collectors," ARI Standard 910-81, Air-Conditioning and Refrigeration Institute, 1815 North Fort Myer Drive, Arlington, VA 22209, 1981.

48. "Intermediate Minimum Property Standards Supplement - Solar Heating and Domestic Hot Water Systems," 1977 Edition, prepared for HUD by NBS. Available from GPO, Order No. SN 023-000-90161-7.

49. Birnbreier, H., "Durability Tests by Stagnation Temperature Measurements," International Energy Agency Task III meeting, Heidelberg, West Germany, December 1978.

50. Dawson, A. G., III, "Stagnation Temperature Test Methods for Determining Solar Collector Thermal Performance," Ph.D Dissertation, Mechanical Engineering Department, Virginia Polytechnic Institute and State University, Blacksburg, VA 24061, June 1981.

51. Kirkpatrick, D. L., "Flat-Plate Solar Collector Performance Data Base and User's Manual," Report No. SERI/STR-254-1515, Solar Energy Research Institute, Golden, CO 80401, July 1983.

52. Clark, E. J. and Roberts W. E., "Weathering Performance of Cover Materials for Flat Plate Solar Collectors," NBS Technical Note 1170, National Bureau of Standards, Washington, DC, 20234, November 1982.

53. Yamasaki, R. S. and Blaga,, A., "Accelerated Weathering Test for Glass Fiber Reinforced Polyester (GRP) Sheets," Durability of Building Materials and Components, ASTM STP 691, P. J. Sereda and G. G. Litvan, Eds., American Society for Testing and Materials, 1980, pp. 874-889.

54. "Standard Test Method for Water Penetration of Exterior Windows, Curtain Walls, and Doors by Uniform Static Air Pressure Difference," ASTM E 331-70, American Society for Testing and Materials, 1916 Race Street, Philadelphia, PA 19103.

APPENDIX A: SOLAR RADIATION EXPOSURE SUMMATIONS

Table A.1. Exposure Summation for all Collectors (MJ/sq m)

Collector ID	Exposure Days* 3	15	30	60	120	240	480	Total Days*	Total Exposure
A-1-1	82	414	775	1527	3293	6594	13118	485	13251
A-1-2	82	414	770	1525	3293	6592	13118	485	13250
A-1-3	86	411	774	1678	3244	6524	0	250	6805
A-1-4	80	399	775	1570	0	0	0	63	1639
B-1-1	81	412	772	1575	3305	6626	13151	488	13363
B-1-2	78	407	755	1563	3303	6624	13149	485	13282
B-1-3	86	411	774	1678	3244	6524	0	250	6805
B-1-4	80	399	775	1570	0	0	0	63	1639
C-1-1	81	412	769	1525	3263	6591	13139	487	13324
C-1-2	78	406	756	1511	3277	6614	13129	484	13243
C-1-3	86	411	774	1678	3244	0	0	120	3244
C-1-4	80	399	775	0	0	0	0	31	800
D-1-1	81	408	772	1546	3314	6616	13141	485	13274
D-1-2	66	350	727	1628	3285	6559	0	468	12806
D-1-3	86	411	774	1678	3244	6524	0	250	6805
D-1-4	80	399	775	1570	0	0	0	63	1639
E-1-1	84	418	775	1579	3320	6638	13163	486	13322
E-1-2	84	418	775	1625	3328	6628	0	470	12904
E-1-3	86	411	774	1678	3244	6524	0	250	6805
E-1-4	80	399	775	1570	0	0	0	63	1639
F-1-1	84	418	778	1553	3288	6479	0	395	10787
F-1-2	84	418	778	1553	3288	6606	13131	485	13250
F-1-3	86	411	774	1678	3244	6524	0	250	6805
F-1-4	80	399	775	1570	0	0	0	63	1639
G-1-1	84	418	778	1531	3300	6598	13122	486	13267
G-1-2	84	418	778	1535	3301	6602	13126	485	13245
G-1-3	86	411	774	1678	3244	6524	0	250	6805
G-1-4	80	399	775	1570	0	0	0	63	1639
H-1-1	81	413	774	1525	3221	6528	13054	486	13198
H-1-2	85	409	758	1520	3219	6525	13043	483	13117
H-1-3	86	411	774	1678	3244	6524	0	250	6805
H-1-4	80	399	775	1570	0	0	0	63	1639
A-2-1	77	414	841	1693	3336	6499	0	424	11313
A-2-2	77	414	801	1656	3299	6451	0	423	11249
A-2-3	72	356	743	1598	3241	6393	0	247	6581
A-2-4	81	413	799	0	0	0	0	59	1627
B-2-1	77	414	841	1700	3322	6423	0	415	11101
B-2-2	77	414	801	1658	3284	6379	0	415	11057
B-2-3	72	356	783	1642	3264	6348	0	250	6654
B-2-4	81	413	799	0	0	0	0	59	1635
C-2-1	77	414	840	1702	3379	6512	0	419	11214
C-2-2	77	414	840	1705	3292	6441	0	396	10527
C-2-3	72	356	783	1644	3318	6419	0	247	6650
C-2-4	86	412	831	0	0	0	0	57	1620
D-2-1	77	414	841	1676	3318	6455	0	420	11191
D-2-2	77	414	801	1638	3281	6416	0	419	11127
D-2-3	72	356	743	1581	3223	6358	0	247	6584
D-2-4	81	413	799	0	0	0	0	59	1610
E-2-1	77	414	841	1712	3322	6489	0	426	11369
E-2-2	77	414	801	1677	3283	6454	0	426	11322
E-2-3	72	356	743	1619	3225	0	0	120	3225
E-2-4	81	413	799	0	0	0	0	59	1655
F-2-1	77	414	841	1677	3317	0	0	234	6268
F-2-2	77	414	801	1639	3277	6381	0	405	10689
F-2-3	72	356	743	1581	3219	0	0	233	6146
F-2-4	81	413	799	0	0	0	0	59	1612
G-2-1	77	414	850	1728	3407	6563	0	423	11364
G-2-2	77	414	829	1701	3374	6534	0	422	11308
G-2-3	72	356	772	1643	3316	6476	0	248	6687
G-2-4	81	413	849	0	0	0	0	59	1698
H-2-1	77	414	841	1677	3303	6401	0	414	11055
H-2-2	77	414	801	1637	3265	6386	0	417	11088
H-2-3	72	356	743	1580	3209	0	0	234	6160
H-2-4	81	413	799	0	0	0	0	59	1612
A-3-1	65	435	867	1692	3537	6937	0	479	13680
A-3-2	65	435	867	1692	3537	6937	0	479	13680
B-3-1	78	362	708	1573	3147	6724	0	468	13137
B-3-2	72	356	702	1566	3140	6718	0	468	13131
C-3-1	78	362	708	1578	3184	6733	0	478	13419
C-3-2	72	356	702	1555	3129	6707	0	351	9564
D-3-1	65	435	873	1698	3544	6943	0	479	13687
D-3-2	65	435	873	1698					
E-3-1	83	426	836	1707	3583	6668	0	422	10782
E-3-2	83	426	836	1707	3583	6668	0	422	10782
F-3-1	65	435	873	1698	3544	6943	0	479	13687
F-3-2	65	435	873	1698	3544	6943	0	479	13687
G-3-1	83	426	836	1707	3583	6668	0	430	12995
G-3-2	83	426	836	1707	3583	6668	0	430	12995
H-3-1	78	362	708	1573	3147	6724	0	468	13137
H-3-2	72	356	702	1566	3140	6718	0	468	13131
A-4-1	108	388	864	1702	3665	7049	0	361	11103
A-4-2	108	388	864	1702	3665	7049	0	361	11103
B-4-1	66	360	823	1694	3510	7458	0	460	14172
B-4-2	66	360	823	1694	3510	7458	0	460	14172
C-4-1	64	371	842	1802	3558	7375	0	425	13146
C-4-2	64	371	842	1802	3558	7375	0	425	13146
D-4-1	66	360	823	1694	3510	7458	0	460	14172
D-4-2	66	360	823	1694	3510	7458	0	460	14172
E-4-1	96	534	958	1875	3817	7193	0	361	11246
E-4-2	96	534	958	1875	3817	7193	0	361	11246
F-4-1	96	534	958	1875	3817	7193	0	361	11246
F-4-2	96	534	958	1875	3817	7193	0	361	11246
G-4-1	108	388	864	1702	3665	7049	0	361	11103
G-4-2	108	388	864	1702	3665	7049	0	361	11103
H-4-1	64	371	842	1802	3558	7375	0	425	13146
H-4-2	64	371	842	1802	3558	7375	0	425	13146

* Days with a Minimum Solar Radiation Level of 17,000 kJ/sq m

Table A.1. Exposure Summation for all Collectors (Btu/sq ft)

Collector ID	Exposure Days* 3	15	30	60	120	240	480	Total Days	Total Exposure
A-1-1	7288	36495	68259	134509	289982	580668	1155180	485	1166860
A-1-2	7288	36495	67886	134369	290000	580488	1155107	485	1166787
A-1-3	7612	36264	68183	147772	285675	574503	0	250	599264
A-1-4	7122	35169	68319	138256	0	0	0	63	144389
B-1-1	7159	36366	68012	138754	291059	583514	1158071	488	1176745
B-1-2	6893	35860	66520	137654	290871	583322	1157906	485	1169586
B-1-3	7612	36264	68183	147772	285675	574503	0	250	599264
B-1-4	7122	35169	68319	138256	0	0	0	63	144389
C-1-1	7159	36366	67757	134369	287362	580429	1157029	487	1173271
C-1-2	6893	35834	66627	133107	288562	582411	1156098	484	1166112
C-1-3	7612	36264	68183	147772	285675	0	0	120	285675
C-1-4	7122	35169	68319	0	0	0	0	31	70467
O-1-1	7159	35989	68015	136159	291823	582609	1157193	485	1168873
O-1-2	5823	30874	64081	143390	289324	577597	0	468	1127655
O-1-3	7612	36264	68183	147772	285675	574503	0	250	599264
D-1-4	7122	35169	68319	138256	0	0	0	63	144389
E-1-1	7443	36886	68277	139086	292403	584559	1159098	486	1173081
E-1-2	7443	36886	68277	143126	293104	583677	0	470	1136334
E-1-3	7612	36264	68183	147772	285675	574503	0	250	599264
E-1-4	7122	35169	68319	138256	0	0	0	63	144389
F-1-1	7443	36886	68532	136761	289587	570586	0	395	949858
F-1-2	7443	36886	68532	136761	289587	581743	1156282	485	1166745
F-1-3	7612	36264	68183	147772	285675	574503	0	250	599264
F-1-4	7122	35169	68319	138256	0	0	0	63	144389
G-1-1	7443	36886	68532	134815	290602	581017	1155501	486	1168223
G-1-2	7443	36886	68532	135229	290702	581388	1155871	485	1166334
G-1-3	7612	36264	68183	147772	285675	574503	0	250	599264
G-1-4	7122	35169	68319	138256	0	0	0	63	144389
H-1-1	7159	36381	68241	134322	283658	574898	1149503	486	1162225
H-1-2	7498	36089	66749	133857	283484	574573	1148572	483	1155066
H-1-3	7612	36264	68183	147772	285675	574503	0	250	599264
H-1-4	7122	35169	68319	138256	0	0	0	63	144389
A-2-1	6857	36487	74097	149119	293778	572275	0	424	996209
A-2-2	6861	36491	70535	145847	290526	568098	0	423	990531
A-2-3	6371	31402	65446	140758	285437	563009	0	247	579571
A-2-4	7174	36388	70432	0	0	0	0	59	143338
B-2-1	6857	36487	74097	149758	292546	565638	0	415	977500
B-2-2	6861	36491	70535	146077	289204	561784	0	415	973646
B-2-3	6371	31402	69012	144673	287461	559044	0	250	585994
B-2-4	7174	36388	70432	0	0	0	0	59	143977
C-2-1	6857	36487	74034	149898	297570	573490	0	419	987451
C-2-2	6861	36491	74038	150154	289945	567197	0	396	926953
C-2-3	6371	31402	68949	144813	292209	565304	0	247	585647
C-2-4	7612	36299	73223	0	0	0	0	57	142663
O-2-1	6857	36487	74097	147587	292246	568447	0	420	985492
O-2-2	6861	36491	70535	144315	288960	564973	0	419	979814
O-2-3	6371	31402	65446	139226	283871	559884	0	247	579808
D-2-4	7174	36388	70432	0	0	0	0	59	141806
E-2-1	6857	36487	74097	150763	292590	571414	0	426	1001165
E-2-2	6861	36491	70535	147689	289120	568372	0	426	996961
E-2-3	6371	31402	65446	142600	284031	0	0	120	284031
E-2-4	7174	36388	70432	0	0	0	0	59	145792
F-2-1	6857	36487	74097	147731	292123	0	0	234	552013
F-2-2	6861	36491	70535	144332	288574	561924	0	405	941252
F-2-3	6371	31402	65446	139243	283485	0	0	233	541246
F-2-4	7174	36388	70432	0	0	0	0	59	141950
G-2-1	6857	36487	74906	152180	300018	577986	0	423	1000657
G-2-2	6861	36491	73076	149817	297130	575364	0	422	995793
G-2-3	6371	31402	67987	144728	292041	570275	0	248	588872
G-2-4	7174	36388	74807	0	0	0	0	59	149583
H-2-1	6857	36487	74097	147731	290910	563694	0	414	973528
H-2-2	6861	36491	70535	144230	287580	562396	0	417	976371
H-2-3	6371	31402	65446	139141	282569	0	0	234	542459
H-2-4	7174	36388	70432	0	0	0	0	59	141950
A-3-1	5794	38379	76371	148998	311492	610851	0	479	1204670
A-3-2	5794	38379	76371	148998	311492	610851	0	479	1204670
B-3-1	6954	31958	62374	138523	277122	592133	0	468	1156794
B-3-2	6411	31415	61831	137980	276579	591590	0	468	1156251
C-3-1	6954	31958	62374	138980	280432	592933	0	478	1181613
C-3-2	6411	31415	61831	137007	275606	590617	0	351	842229
O-3-1	5794	38379	76951	149578	312072	611431	0	479	1205250
O-3-2	5794	38379	76951	149578	312072	611431	0	479	1205250
E-3-1	7392	37517	73633	150336	315580	587199	0	422	949447
E-3-2	7392	37517	73633	150336	315580	587199	0	422	949447
F-3-1	5794	38379	76951	149578	312072	611431	0	479	1205250
F-3-2	5794	38379	76951	149578	312072	611431	0	479	1205250
G-3-1	7392	37517	73633	150336	315580	587199	0	430	1144325
G-3-2	7392	37517	73633	150336	315580	587199	0	430	1144325
H-3-1	6954	31958	62374	138523	277122	592133	0	468	1156794
H-3-2	6411	31415	61831	137980	276579	591590	0	468	1156251
A-4-1	9524	34227	76130	149950	322755	620736	0	361	977752
A-4-2	9524	34227	76130	149950	322755	620736	0	361	977752
B-4-1	5820	31735	72488	149222	309135	656724	0	460	1247989
B-4-2	5820	31735	72488	149222	309135	656724	0	460	1247989
C-4-1	5713	32752	74214	158700	313355	649423	0	425	1157650
C-4-2	5713	32752	74214	158700	313355	649423	0	425	1157650
D-4-1	5820	31735	72488	149222	309135	656724	0	460	1247989
O-4-2	5820	31735	72488	149222	309135	656724	0	460	1247989
E-4-1	8493	47059	84388	165130	336187	633416	0	361	990331
E-4-2	8493	47059	84388	165130	336187	633416	0	361	990331
F-4-1	8493	47059	84388	165130	336187	633416	0	361	990331
F-4-2	8493	47059	84388	165130	336187	633416	0	361	990331
G-4-1	9524	34227	76130	149950	322755	620736	0	361	977752
G-4-2	9524	34227	76130	149950	322755	620736	0	361	977752
H-4-1	5713	32752	74214	158700	313355	649423	0	425	1157650
H-4-2	5713	32752	74214	158700	313355	649423	0	425	1157650

* Days with a Minimum Solar Radiation Level of 1,500 Btu/sq ft

Table A.2. Exposure Summation for Material Samples at Phoenix

A. Cover Samples Miniboxes

Exposure Schedule: Started 5- 8-79 Ended 11-18-80

(2-12-80 through 3- 3-80 Excluded)

Calendar Days	Exposure Days*	Date	Total Solar Radiation Btu/sq ft	MJ/sq m
85	80	7-30-79	194587	2209
170	160	10-23-79	371472	4218
283	240	3- 5-80	565881	6426
372	320	6- 2-80	759847	8629
454	400	8-23-80	953122	10823
540	479	11-17-80	1127756	12807

B. Absorber Sample Coupons AC12 - AH12, AJ12, AL12, & AP12

Exposure Schedule: Started 6- 4-79 Ended 6-14-81

(3-24-80 through 8-28-80 Excluded)

Calendar Days	Exposure Days	Date	Total Solar Radiation Btu/sq ft	MJ/sq m
82	80	8-24-79	188493	2140
170	160	11-20-79	367469	4173
292	240	3-21-80	565438	6421
381	320	11-23-80	743729	8446
487	400	3- 9-81	934281	10609
576	480	6- 6-81	1133008	12866
584	488	6-14-81	1153849	13103

C. Absorber Sample Coupons AI11, AA12, AM12, AN12, AN13, & AA15 - AAP15

Exposure Schedule: Started 6- 4-79 Ended 6-14-81

(3-24-80 through 1- 3-81 Excluded)

Calendar Days	Exposure Days	Date	Total Solar Radiation Btu/sq ft	MJ/sq m
82	80	8-24-79	188493	2140
170	160	11-20-79	367469	4173
292	240	3-21-80	565438	6421
397	320	4-16-81	764755	8684
456	376	6-14-81	902626	10250

* Days with a Minimum Solar Radiation Level of 17,000 kJ/sq m

Table A.3. Exposure Summation for Material Samples at Cape Canaveral

A. Cover Sample Miniboxes

Exposure Schedule: Started 4- 6-79 Ended 2-10-81

Calendar Days	Exposure Days*	Date	Total Solar Radiation Btu/sq ft	MJ/sq m
97	80	7-11-79	188013	2135
199	160	10-21-79	373420	4240
328	240	2-27-80	571479	6489
435	320	6-13-80	770512	8750
528	400	9-14-80	951532	10805
645	480	1- 9-81	1141726	12965
677	500	2-10-81	1194989	13570

B. Absorber Sample Coupons

Exposure Schedule: Started 5- 2-79 Ended 10-24-81

(4-14-80 through 12-20-80 Excluded)

Calendar Days	Exposure Days	Date	Total Solar Radiation Btu/sq ft	MJ/sq m
93	80	8- 2-79	182811	2076
203	160	11-20-79	372875	4234
330	240	3-26-80	571779	6493
455	320	4- 6-81	781735	8877
541	400	7- 1-81	967635	10988
638	480	10- 6-81	1149935	13059
656	494	10-24-81	1182464	13428

* Days with a Minimum Solar Radiation Level of 17,000 kJ/sq m

Table A.4. Exposure Summation for Material Samples at Palo Alto

A. Cover Sample Miniboxes

Exposure Schedule: Started 4- 6-79 Ended 7-28-81

Calendar Days	Exposure Days*	Date	Total Solar Radiation Btu/sq ft	MJ/sq m
88	80	7- 2-79	200822	2280
172	160	9-24-79	390452	4434
342	240	3-12-80	612243	6952
437	320	6-15-80	803841	9128
519	400	9- 5-80	989828	11240
666	480	1-30-81	1196403	13586
782	560	5-26-81	1399242	15890
845	623	7-28-81	1549724	17599

B. Absorber Sample Coupons

Exposure Schedule: Started 5- 2-79 Ended 7-28-81

(5-22-80 through 5-29-80 Excluded)

Calendar Days	Exposure Days	Date	Total Solar Radiation Btu/sq ft	MJ/sq m
83	80	7-23-79	199394	2264
178	160	10-26-79	391549	4446
341	240	4- 6-80	609729	6924
433	320	7-15-80	803517	9124
517	400	10- 7-80	981376	11144
690	480	3-29-81	1207844	13716
776	560	6-23-81	1398119	15877
811	595	7-28-81	1481065	16819

* Days with a Minimum Solar Radiation Level of 17,00 kJ/sq m

Table A.5 Exposure Summation for Material Samples at Gaithersburg

A. Cover Sample Miniboxes

Exposure Schedule: Started 5- 5-79 Ended 6- 8-81

Calendar Days	Exposure Days*	Date	Total Solar Radiation Btu/sq ft	MJ/sq m
130	80	9-11-79	213024	2419
320	160	3-19-80	443133	5032
443	240	7-20-80	645341	7328
575	320	11-29-80	848138	9631
766	397	6- 8-81	1083173	12300

B. Absorber Sample Coupons

Exposure Schedule: Started 5- 5-79 Ended 6- 8-81

(8-15-80 through 12- 5-80 Excluded)

Calendar Days	Exposure Days	Date	Total Solar Radiation Btu/sq ft	MJ/sq m
130	80	9-11-79	213024	2419
320	160	3-19-80	443133	5032
443	240	7-20-80	645341	7328
622	320	5- 8-81	875453	9941
653	336	6- 8-81	918297	10428

* Days with a Minimum Solar Radiation Level of 17,000 kJ/sq m

NBS-114A (REV. 2-8C)

U.S. DEPT. OF COMM. BIBLIOGRAPHIC DATA SHEET (See instructions)	1. PUBLICATION OR REPORT NO. NBS/TN-1196	2. Performing Organ. Report No.	3. Publication Date September 1984

4. TITLE AND SUBTITLE

NBS Solar Collector Durability/Reliability Test Program: Final Report

5. AUTHOR(S)

David Waksman, William C. Thomas, Elmer R. Streed

6. PERFORMING ORGANIZATION (If joint or other than NBS, see instructions)

NATIONAL BUREAU OF STANDARDS
DEPARTMENT OF COMMERCE
GAITHERSBURG, MD 20899

7. Contract/Grant No.

8. Type of Report & Period Covered

Final

9. SPONSORING ORGANIZATION NAME AND COMPLETE ADDRESS (Street, City, State, ZIP)

Office of Solar Heat Technologies
U.S. Department of Energy
Washington, DC 20585

10. SUPPLEMENTARY NOTES

☐ Document describes a computer program; SF-185, FIPS Software Summary, is attached.

11. ABSTRACT (A 200-word or less factual summary of most significant information. If document includes a significant bibliography or literature survey, mention it here)

Efforts in the development of reliability/durability tests for solar collectors and their materials have been hampered by the lack of real time and accelerated degradation data that can be correlated with in use conditions. The focus of this report is on research undertaken at the National Bureau of Standards (NBS) to help generate the data required to develop methods for predicting the long term durability and reliability of flat-plate solar collectors and their materials.

In this research, eight different types of flat-plate solar collectors were exposed outdoors at four sites located in different climatic regions. Small scale cover and absorber materials coupon specimens consisting of samples taken from a collector of each of the eight types used and a number of additional materials were exposed concurrently with the full-size collectors. Periodic measurements were made of collector and materials performance as a function of outdoor exposure time. Indoor laboratory aging tests were conducted concurrently on specimens of the same materials to provide a basis for comparison with the outdoor exposure tests.

This report presents the results obtained in this test program. Recommendations are made regarding the use and limitations of performance measurements and environmental exposure tests for assessing the durability of solar collectors and absorber and cover materials.

12. KEY WORDS (Six to twelve entries; alphabetical order; capitalize only proper names; and separate key words by semicolons)

absorber materials; accelerated aging; cover materials; durability; environmental exposure; solar collectors; solar materials, stagnation testing, thermal performance.

13. AVAILABILITY

☒ Unlimited

☐ For Official Distribution. Do Not Release to NTIS

☒ Order From Superintendent of Documents, U.S. Government Printing Office, Washington, D.C. 20402.

☐ Order From National Technical Information Service (NTIS), Springfield, VA. 22161

14. NO. OF PRINTED PAGES

148

15. Price

USCOMM-DC 6043-P80

*U.S. GOVERNMENT PRINTING OFFICE : 1984 0-420-997/10038

NBS Technical Publications

Periodicals

Journal of Research—The Journal of Research of the National Bureau of Standards reports NBS research and development in those disciplines of the physical and engineering sciences in which the Bureau is active. These include physics, chemistry, engineering, mathematics, and computer sciences. Papers cover a broad range of subjects, with major emphasis on measurement methodology and the basic technology underlying standardization. Also included from time to time are survey articles on topics closely related to the Bureau's technical and scientific programs. As a special service to subscribers each issue contains complete citations to all recent Bureau publications in both NBS and non-NBS media. Issued six times a year.

Nonperiodicals

Monographs—Major contributions to the technical literature on various subjects related to the Bureau's scientific and technical activities.

Handbooks—Recommended codes of engineering and industrial practice (including safety codes) developed in cooperation with interested industries, professional organizations, and regulatory bodies.

Special Publications—Include proceedings of conferences sponsored by NBS, NBS annual reports, and other special publications appropriate to this grouping such as wall charts, pocket cards, and bibliographies.

Applied Mathematics Series—Mathematical tables, manuals, and studies of special interest to physicists, engineers, chemists, biologists, mathematicians, computer programmers, and others engaged in scientific and technical work.

National Standard Reference Data Series—Provides quantitative data on the physical and chemical properties of materials, compiled from the world's literature and critically evaluated. Developed under a worldwide program coordinated by NBS under the authority of the National Standard Data Act (Public Law 90-396). NOTE: The Journal of Physical and Chemical Reference Data (JPCRD) is published quarterly for NBS by the American Chemical Society (ACS) and the American Institute of Physics (AIP). Subscriptions, reprints, and supplements are available from ACS, 1155 Sixteenth St., NW, Washington, DC 20056.

Building Science Series—Disseminates technical information developed at the Bureau on building materials, components, systems, and whole structures. The series presents research results, test methods, and performance criteria related to the structural and environmental functions and the durability and safety characteristics of building elements and systems.

Technical Notes—Studies or reports which are complete in themselves but restrictive in their treatment of a subject. Analogous to monographs but not so comprehensive in scope or definitive in treatment of the subject area. Often serve as a vehicle for final reports of work performed at NBS under the sponsorship of other government agencies.

Voluntary Product Standards—Developed under procedures published by the Department of Commerce in Part 10, Title 15, of the Code of Federal Regulations. The standards establish nationally recognized requirements for products, and provide all concerned interests with a basis for common understanding of the characteristics of the products. NBS administers this program as a supplement to the activities of the private sector standardizing organizations.

Consumer Information Series—Practical information, based on NBS research and experience, covering areas of interest to the consumer. Easily understandable language and illustrations provide useful background knowledge for shopping in today's technological marketplace.
Order the **above** *NBS publications from: Superintendent of Documents, Government Printing Office, Washington, DC 20402.*
Order the **following** *NBS publications—FIPS and NBSIR's—from the National Technical Information Service, Springfield, VA 22161.*

Federal Information Processing Standards Publications (FIPS PUB)—Publications in this series collectively constitute the Federal Information Processing Standards Register. The Register serves as the official source of information in the Federal Government regarding standards issued by NBS pursuant to the Federal Property and Administrative Services Act of 1949 as amended, Public Law 89-306 (79 Stat. 1127), and as implemented by Executive Order 11717 (38 FR 12315, dated May 11, 1973) and Part 6 of Title 15 CFR (Code of Federal Regulations).

NBS Interagency Reports (NBSIR)—A special series of interim or final reports on work performed by NBS for outside sponsors (both government and non-government). In general, initial distribution is handled by the sponsor; public distribution is by the National Technical Information Service, Springfield, VA 22161, in paper copy or microfiche form.

U.S. Department of Commerce
National Bureau of Standards
Gaithersburg, MD 20899